United States Environmental Protection Agency

# Using Repeated LIDAR to Characterize Topographic Change in Riparian Areas and Stream Channel Morphology in Areas Undergoing Urban Development: An Accuracy Assessment Guide for Local Watershed Managers

## APM 286

RESEARCH AND DEVELOPMENT

EPA/600/R-10/120
October 2010
www.epa.gov

# Using Repeated LIDAR to Characterize Topographic Change in Riparian Areas and Stream Channel Morphology in Areas Undergoing Urban Development: An Accuracy Assessment Guide for Local Watershed Managers

# APM 286

Prepared by

S. Taylor Jarnagin, Ph.D.

U.S. Environmental Protection Agency
National Exposure Research Laboratory
Environmental Sciences Division
Landscape Ecology Branch
Research Triangle Park, NC



U.S. Environmental Protection Agency
Office of Research and Development
Washington, DC 20460

Disclaimers:

The United States Environmental Protection Agency through its Office of Research and Development funded and managed the research described here. Some of the information in this document has been funded wholly by the United States Environmental Protection Agency under Contract number EP-D-05-088 to Lockheed Martin. It has been subjected to the Agency's peer and administrative review and has been approved for publication as an EPA document. Mention of trade names or commercial products does not constitute endorsement or recommendation by EPA for use.

## Table of Contents

**List of Figures and Tables**

**Appendices**

## Abstract/Executive Summary

Urban development and the corresponding increases in impervious surfaces associated with that development have long been known to have adverse impacts upon urban riparian systems, water quality and quantity, groundwater recharge, streamflow, and aquatic ecosystem integrity. The ability of Best Management Practices (BMPs) to mitigate the impact of urban development is an emerging area of research and a central component of the Clean Water science mission of the US EPA. The ability to monitor and characterize urban development and corresponding stream channel changes due to urban development with remote sensing, high spatial and temporal resolution mapping, and Geographic Information Systems (GIS) technology is an area of research focus in the geospatial sciences and the US EPA Landscape Ecology Branch.

A key component in the geospatial assessment of urban development is the analysis of changes in ground surface topography, contributing watershed area, and stream channel geomorphology using Digital Elevation Models (DEMs). LiDAR (Light Detection And Ranging) is an active remote sensing technology that uses light pulses to measure distance and other characteristics (texture, hardness, etc.) of terrain and objects. LiDAR can be used to construct DEMs that are much finer in spatial scale over much larger areas than have been previously possible. Repeated LiDAR-derived DEMs can be used to characterize the changes over time associated with urban development.

This study is an attempt to categorize and characterize the accuracy and precision of repeated LiDAR-derived DEMs. This study used ground truth measurements in conjunction with repeated airborne LiDAR coverages to assess LiDAR accuracy and assess the precision of LiDAR over different land use/land cover (LULC) types. This study is a portion of a larger research program, the Clarksburg Monitoring Project, which combines remotely sensed imagery, GIS, and LIDAR to map and monitor urban development and ground-based measurements of streamflow, precipitation, aquatic biota, and water quality to measure stream response to urban development and BMP effectiveness.

This study used a ground survey and repeated LiDAR overflights to assess overall LiDAR accuracy, LiDAR accuracy by ground cover type and slope, and the precision (repeatability) of LiDAR-derived DEMs and elevation measurements. The surveyed ground control network consisted of 604 surveyed locations acting as ground-truth for the LiDAR-derived measurements. We found significant differences in the absolute accuracy of LiDAR by vegetation and surface condition class, with a decline in accuracy with increased interference from vegetation, surface condition, and increasing slope. The precision of repeated LiDAR-derived elevations across vegetation cover classes and slope also was significantly different among vegetation cover classes and with increased slope; with declining precision found for both increasing slope and interference intensity of vegetation cover classes.

We also looked at larger study areas to measure the precision of LiDAR-Derived DEM differences by LULC. Each comparison yielded significantly different means for each group with Forest showing the greatest mean difference and the Agricultural LULC class showing the least. We compared stream transect ground-truth measurements to LiDAR-derived stream

transects and found that the LiDAR-derived inter-annual transect differences measured were from 2 to 12 times larger than the ground-truth-derived differences. The relationship between the ground-truth transect measurements and the LiDAR-derived transects was noisy and the ability of repeated LiDAR to reveal stream channel morphology changes at a 1-foot spatial scale appears to be quite poor. The ability to use LULC to generally predict the precision of repeat LiDAR-derived DEMs and elevation estimates also was weak. Changes in vegetation condition and slope that adversely affect LiDAR accuracy and precision occur at a spatial scale much less than that captured by the LULC variable. The use of repeat LiDAR to extract stream channel paths and predict watershed boundaries was also found to be highly variable between LiDAR coverages.

The results of this study should be taken as a warning to watershed modelers and managers that LiDAR-derived stream channels, stream transects and morphology, elevation changes, and watershed boundaries and areas may not be nearly so certain as one might otherwise assume from the fine spatial scale of the LiDAR output maps. The final conclusion of this study is that a user of LiDAR who attempts to delineate changes at or near to the spatial level of resolution of the base data (about 1 meter or 3 feet in our study) cannot rely on LiDAR alone to assess those changes. Ground truth is needed to verify changes predicted by repeat LiDAR measurements. The loose relationship seen by the LiDAR transects and ground-truth transects should act as a warning to the LiDAR user: use LiDAR to identify where change appears to have occurred and then use ground-truth to verify.

Acknowledgements

I thank my EPA reviewers Dave Williams and Maliha Nash for their ides and suggestions.  I also thank Rick Van Remortel and Ed Evanson of Lockheed Martin for their ideas and discussions regarding LiDAR processing and land use/land cover classification/compilation.  Their ideas, suggestions, and assistance went beyond the call of duty called for by their contract.  I would also like to thank Mark S. Murphy (CSC ArcGIS Support Staff) and Tim Wade (EPA LEB-RTP) for their ArcGIS suggestions, tools, and patient advice.  Their counsel proved invaluable (and much better than the on-line support at esri.com).  I also would like to thank Asa Eckert-Erdheim, a high school student volunteer from the Durham School of Arts, Durham, NC.  Asa spent many hours heads-up digitizing while compiling land use/land cover change.  Hopefully, he learned something from his volunteer internship other than how boring science is.  I also would like to thank Dr. Kaye Brubaker and her Intro to GIS class who also labored in the heads-up digitizing mines.  Again I hope the learning experience was as valuable to them as the data were to me.  Finally I would like to thank Eric Naibert, Keith Van Ness, and the other folks at the Montgomery County Maryland Department of Environmental Protection for their invaluable assistance in the gathering of ground truth data for the accuracy assessment of the County-supplied stream transect data.

## Introduction

Changes in topography, impervious surfaces, and land use and land cover associated with urban development have been shown to alter streamflow and stream geomorphology and topography (Schueler, 1994; USEPA, 1994; Arnold and Gibbons, 1996; Caraco et al., 1998; Jennings and Jarnagin, 2002; Jarnagin, 2004; Jarnagin, 2007). Measuring these changes in streams is a difficult and labor-intensive task (Gardina, 2008). If LiDAR could reliably measure these changes over a wide area over time, this would be a great benefit to watershed manages and interested stakeholders and help to evaluate the effectiveness of Best Management Practices (BMPS) in mitigating the adverse effects of urban development. .

LiDAR (Light Detection And Ranging) is a remote sensing technology that uses light pulses to measure distance and other characteristics (texture, hardness, etc.) of terrain and objects. LiDAR is an active remote sensing technique where the light pulse is sent from the system and the length of time for the return signal is recorded, allowing for the distance between the sensor and the object imaged to be calculated. LiDAR systems can be either mobile (such as airborne LiDAR) or stationary. Both the position and orientation of the LiDAR sensor must be known in order to accurately measure distance. GPS (Global Positioning System) receivers are used to accurately determine the position of the aircraft and the environmental surface sensed with LiDAR. One of the final results of airborne LiDAR is a very accurate and high-resolution Digital Elevation Model (DEM) of the environmental surfaces remotely sensed with LiDAR. See Figure 1 for a schematic drawing of an airborne LiDAR system.

Aerial topographic LiDAR is obtained in a series of flightlines that collect overlapping data points. These are merged by complex software into the LiDAR All-Points data cloud. Typically, what is delivered to the user is a computer-algorithm filtered Ground-Points dataset converted into a DEM. The user may also request and receive First Return and Last Return Data (the first and last set of pulses returned to the sensor, respectively). Intensity data may also be provided. The computer algorithms and software used to create these data sets are proprietary and exist as a black box with respect to the user. The typical user of LiDAR data will only be using the end products of the LiDAR overflights, LiDAR-derived DEMs, not the raw data used to create those products.

This study is an attempt to categorize and characterize the accuracy and precision of LiDAR-derived DEMs. This study used ground truth measurements in conjunction with an airborne LiDAR coverage to assess LiDAR accuracy and repeat airborne LiDAR coverages to assess the precision of LiDAR over different land use/land cover (LULC) types. This study is a portion of a larger research program, the Clarksburg Monitoring Project, that combines remotely sensed imagery, GIS (Geographic Information Systems), and LIDAR to map and monitor urban development and stream response to urban development. For further information about the Clarksburg Monitoring Project see:
< http://www.epa.gov/esd/land-sci/epic/clarksburg01-05.htm >;
< http://www.montgomerycountymd.gov/dectmpl.asp?url=/content/dep/water/spaclarksburg.asp >; < http://egsc.usgs.gov/currentscienceprojects.html >: "Best Management Practices Designed to Improve Developing Landscapes"; and < http://egsc.usgs.gov/clarksburghighlights.html > (all links last accessed 9/21/2010).

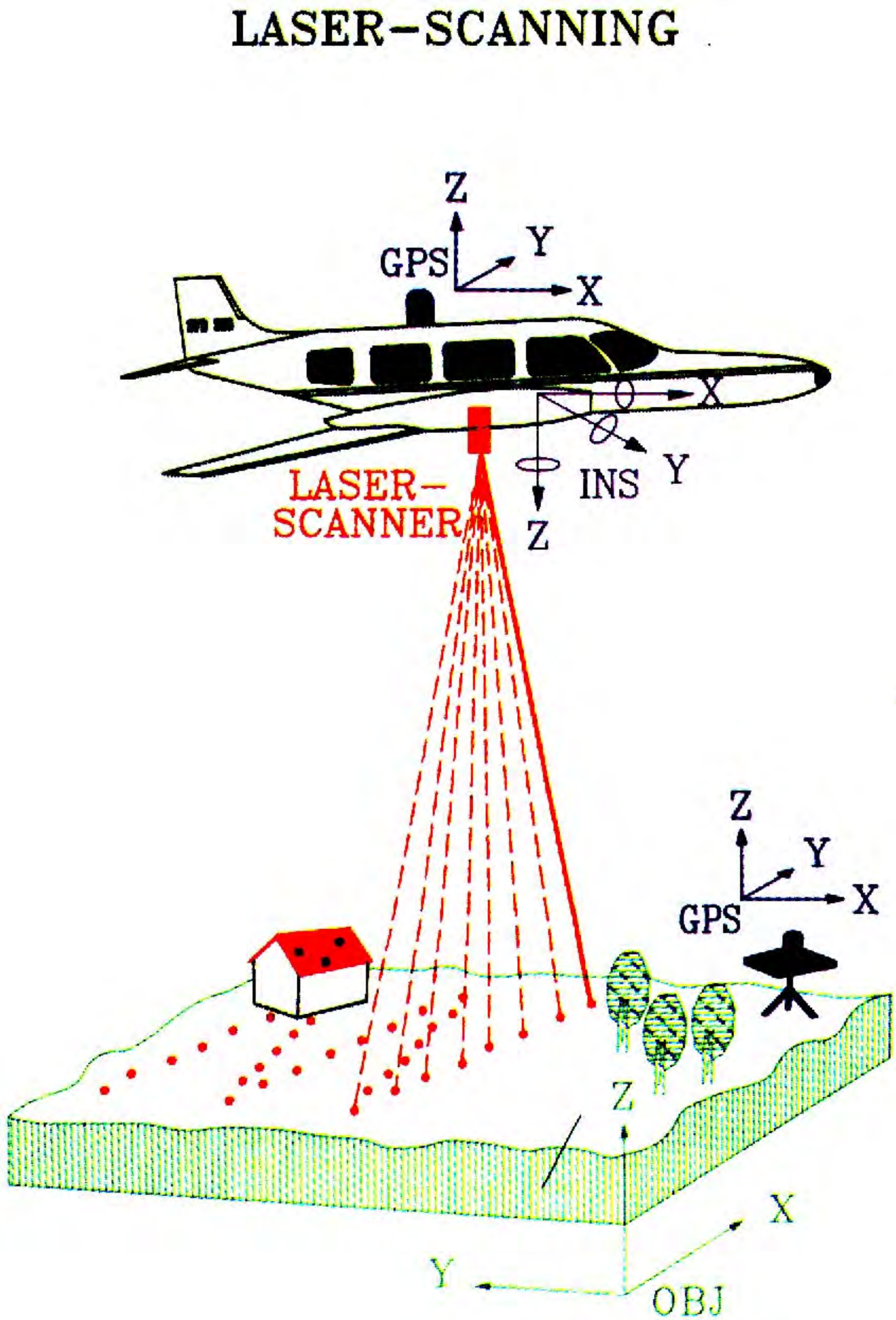


Figure 1: LiDAR schematic.  Image Source: Spencer B. Gross Inc., Portland OR.

## Accuracy and Precision

The *accuracy* of a set of measurements describes how close they are to the true or actual value of the measured quantity. The *precision* of a set of measurements is the degree to which the measurements agree with each other. Reproducibility, replicability, and repeatability are synonyms for measurement *precision*. Figure 2 is an excellent graphic from an online Math Skills Review at the Texas A&M Department of Chemistry Website that visually illustrates *Accuracy* versus *Precision*:

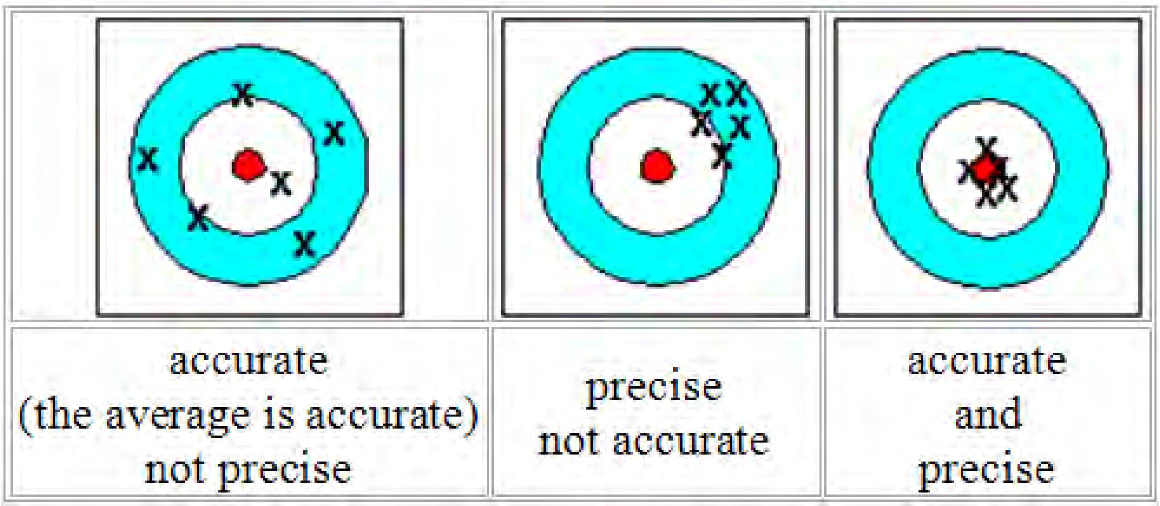


**Accuracy** refers to how closely a measured value agrees with the correct value.
**Precision** refers to how closely individual measurements agree with each other.

Figure 2: *Accuracy* versus *Precision*: from Texas A&M website < http://www.chem.tamu.edu/class/fyp/mathrev/mr-sigfg.html >. Last accessed 09/08/2010.

## Study Area and LiDAR Coverages

The study area for this project is the Clarksburg Special Protection Area (CSPA) in Montgomery County Maryland. Repeat LiDAR coverages were obtained as a part of the ongoing research project: "Collaborative Research: Streamflow, Urban Riparian Zones, BMPs, and Impervious Surfaces" (see: < http://www.epa.gov/esd/land-sci/epic/clarksburg01-05.htm > for an overview. Last accessed 09/08/2010. Figure 3 shows the location of the CSPA in relation to the state of Maryland and the Washington DC metro area.

Five airborne LiDAR coverages were obtained in the CSPA in the 2002-2008 time period. The vendors, instruments, mean LiDAR raw point spacing, and reported accuracies for those overflights are listed in Table 1.

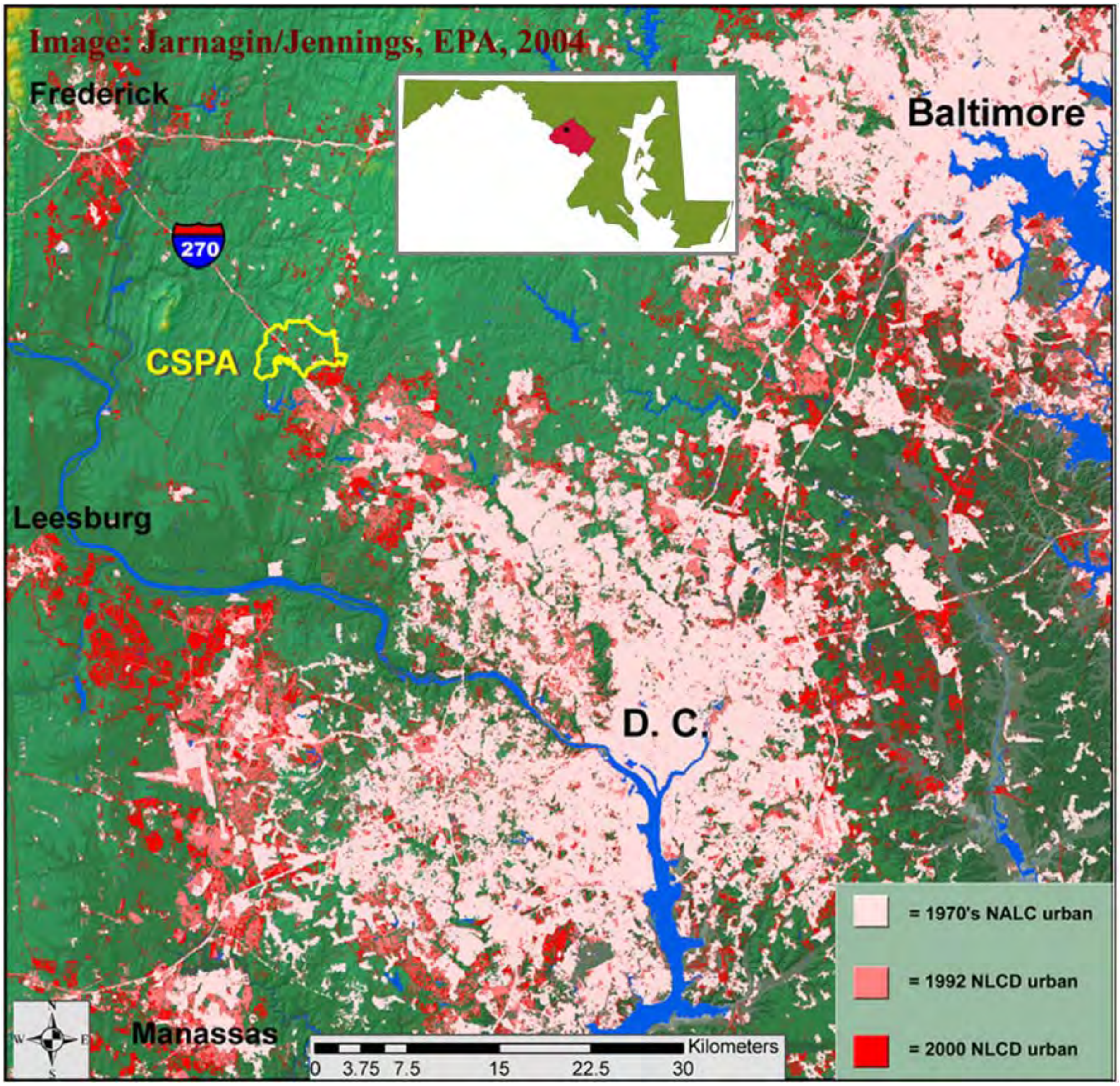


Figure 3: Location of the Clarksburg Special Protection Area (CSPA).

Year: 2002
Month: December
Vendor: Airborne 1
Instrument: Optech ALTM-2025
Mean LIDAR raw point spacing: sub 0.8 meter
Reported Accuracy:
  Average vertical difference: 0.07 meter (0.23 foot)
  Average horizontal difference: 0.04 meter (0.13 foot)
  Max vertical difference: 0.12 meter (0.39 foot)
  Max horizontal difference: 0.07 meter (0.23 foot)

Year: 2004
Month: March
Vendor: Laser Mapping Specialists Inc.
Instrument: Optech ALTM-2033
Mean LIDAR raw point spacing: sub 0.8 meter
Reported Accuracy:
  Vertical RMSE: 0.05 meter (0.15 foot)
  Average horizontal difference: < 0.30 meter (< 1 foot)
  Max vertical difference: 0.08 meter (0.28 foot)
  Max horizontal difference: not reported

Year: 2006
Month: March
Vendor: Canaan Valley Institute (CVI)
Instrument: Optech ALTM-3100
Mean LIDAR raw point spacing: sub 0.1 meter
Reported Accuracy:
  Vertical RMSE: 0.04 meter (0.15 foot)
  Average horizontal difference: 0.13 meter (0.43 foot)
  Max vertical difference: 0.08 meter (0.28 foot)
  Max horizontal difference: not reported

Year: 2007
Month: March
Vendor: Canaan Valley Institute (CVI)
Instrument: Optech ALTM-3100
Mean LIDAR raw point spacing: sub 0.15 meter
Reported Accuracy:
  Vertical RMSE: 0.03 meter (0.10 foot)
  Average horizontal difference: 0.05 meter (0.16 foot)
  Max vertical and horizontal differences: not reported

Year: 2008
Month: March
Vendor: Sanborn
Instrument: Leica ALS-50
Mean LIDAR raw point spacing: 1.4 meters
Reported Accuracy: (not reported - specifications below were met):
  Vertical RMSE (Bare Earth): 0.15 meter (0.49 foot)
  Horizontal RMSE: 1 meter (3.29 feet)
  Max vertical and horizontal differences: not reported

Table 1: LiDAR Overflights information: Vendors, instruments, mean LiDAR raw point spacing, and reported accuracies for the five LiDAR overflights used in this study.

### Absolute versus Averaged Error

Typically, LiDAR vendors express vertical error using an averaged estimate of error: root mean square error (RMSE). For an unbiased estimator, the RMSE is the square root of the variance, known as the standard error. If you want to know the confidence in an overall estimate of an elevation value for a flat surface, the RMSE provides a good estimate of precision.

However, what we are often interested in is the error associated with a single point measurement or a limited set of measured points (as in a stream transect). Calculating the mean value of the error of a set of points yields a smaller number since positive and negative error values tend to cancel each other out for an unbiased estimator. For this study, I have used the absolute value of the error unless otherwise stated. This tends to maximize the reported value but yields a better accuracy estimate for a single point or limited set of points.

## Part 1: LiDAR Accuracy and Precision Assessment: Ground Truth Measurements.

### 2006 Ground Survey: Overall LiDAR Accuracy and LiDAR Accuracy by Ground Cover Type

In March of 2006, students and faculty from the University of Maryland, College Park joined EPA and USGS scientists, Montgomery County Maryland Department of Environmental Protection scientists and staff, and employees from Johnson Mirmiran & Thompson PA, Sparks Maryland in surveying a set of ground control locations near the Sopers Branch stream gauge in the Clarksburg Special Protection Area (CSPA), near Clarksburg Maryland. EPA funded the placement of a highly accurate geodetic ground survey monument network and the ground survey crew used Total Stations (an electronic transit integrated with an electronic distance meter) to read slope distances from the monuments to the ground control network. EPA also funded a LiDAR overflight concurrent with the ground survey to allow a direct comparison of LiDAR-derived locations with a high-accuracy ground survey. The ground control network consisted of 604 surveyed locations (Figure 4)

The overall accuracy of the LiDAR-derived elevations is found in Table 2. Both mean and absolute elevation differences are given. Using a mean value yields an accuracy estimate of 0.07 feet (2.1 cm) while the absolute value is an order of magnitude larger at 0.46 feet (14.1 cm).

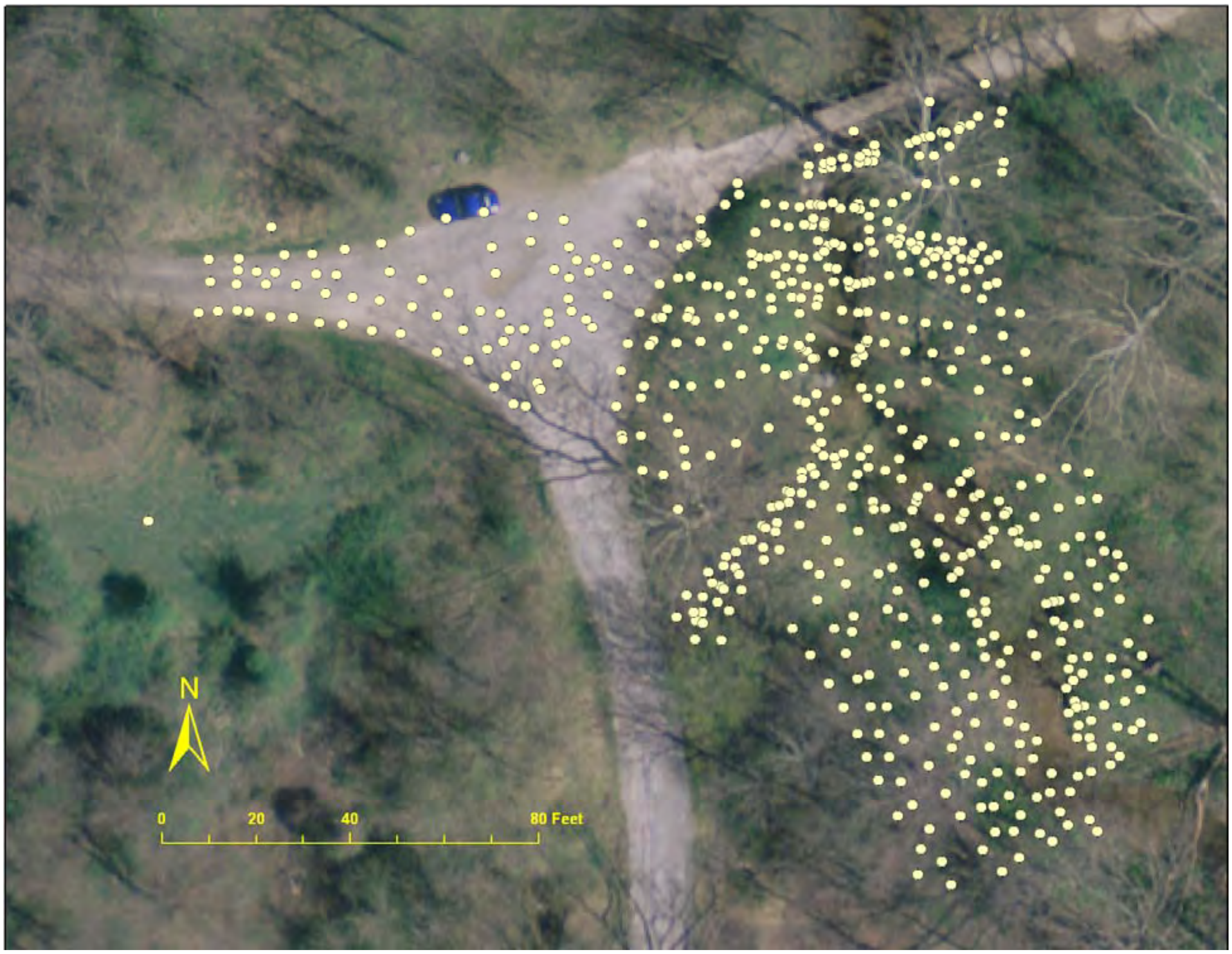

Figure 4: Ground survey points (n = 604).

Actual Values, All Points: n = 604
Mean elevation difference = 0.069
Std Dev = 0.706
± 95% C.I. = 0.056
Maximum elevation difference = 3.863
Minimum elevation difference = -2.396

Absolute Values, All Points: n = 604
Mean (Abs) elevation difference = 0.461
Std Dev = 0.539
± 95% C.I. = 0.043
Max (Abs) elevation difference = 3.863

Table 2: 2006 Ground Survey Results - LiDAR Accuracy for all ground control points. All distances are in feet. Actual (±) values and absolute values of differences between LiDAR-derived and ground truth elevations.

I classified the ground control points according to the amount of overhanging branches and ground litter and vegetation (Figure 5). Three vegetation condition classes were used: "Good" (near-stream ground conditions have open, level, and firm-to-hard surfaces with few or no overhanging branches), "OK" (near-stream vegetative conditions have relatively little ground vegetation with relatively more overhanging branches and ground litter), and "Bad" (near-stream vegetative conditions have more irregular and softer ground conditions with moderate-to-heavy amounts of ground litter and dense underbrush and relatively dense overhanging branches).

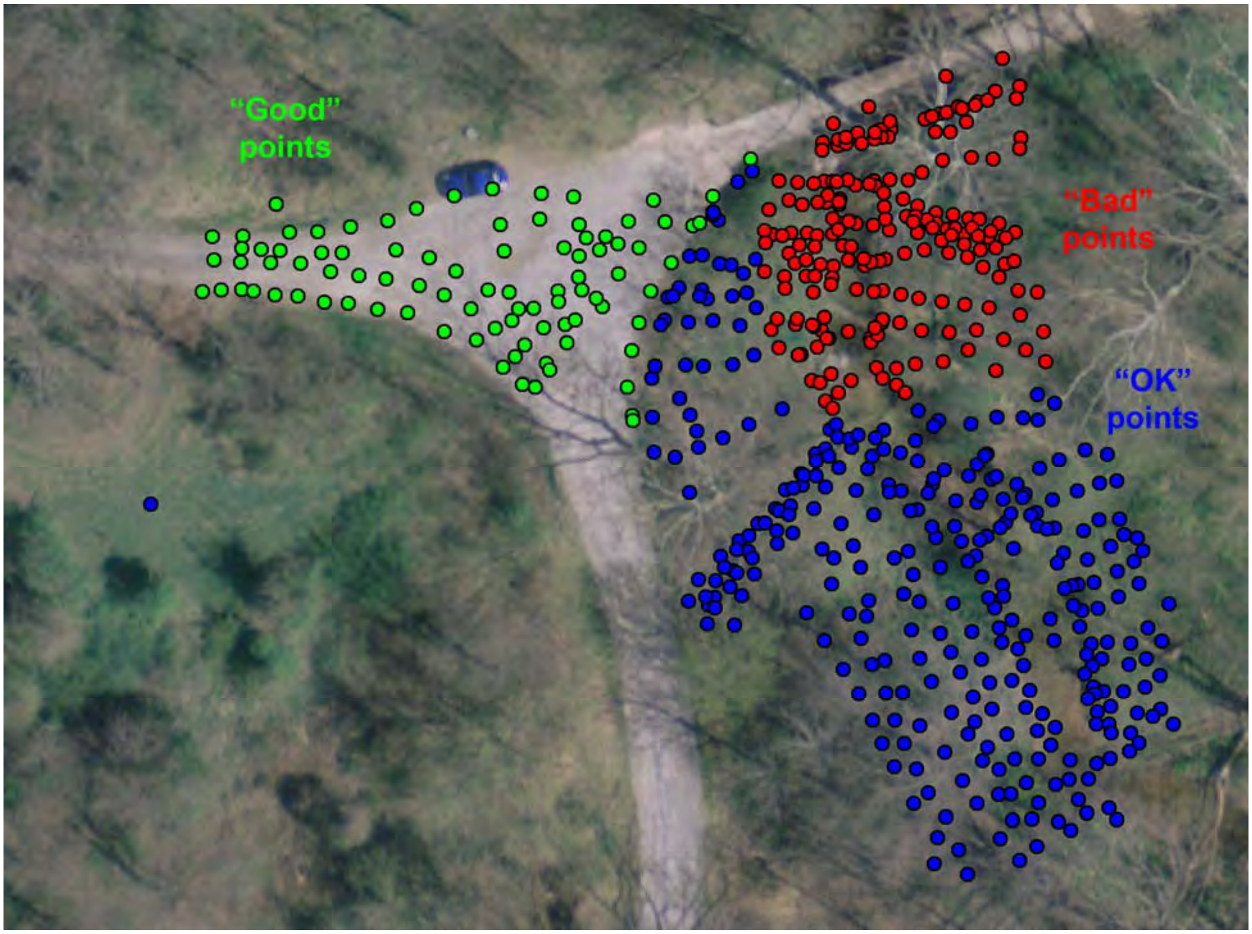


Figure 5: "Good", "OK", and "Bad" vegetative and surface condition classes (represented by green, blue. and red symbols respectively).

Comparison of the absolute accuracy by vegetation and surface condition class yields significant differences with a decline in accuracy with increased interference with vegetation and surface condition (Figure 6). See Appendix Nine for a visual depiction of the vegetation classes.

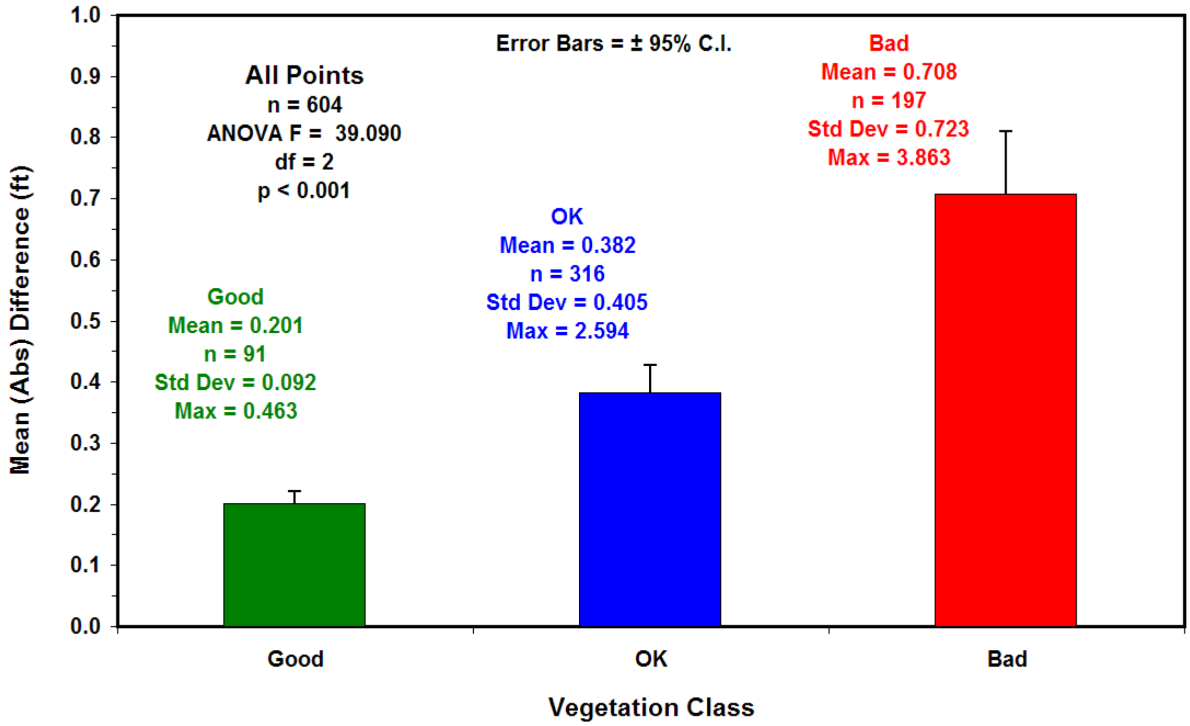


**Mean (Abs) Difference (ft) Between Vegetation Cover Classes**

Figure 6: Differences in absolute accuracy between Vegetation Cover Classes. Good ground conditions yield significantly better accuracy.

**2006 Ground Survey: LiDAR Precision: Accuracy at Ground Survey Elevations for Repeated LiDAR Coverages by Vegetation Cover Class**

The accuracy of repeat LiDAR-derived elevations were calculated at the 604 surveyed ground control truth elevation points for the LiDAR coverages for 2002, 2004, 2006, 2007, and 2008. The mean absolute difference between the ground truth elevation and the LiDAR-derived elevation for each year was significantly different among years (ANOVA F = 23.381, df = 4, p < 0.001) but that was more a measure of the large sample size (n = 3020) than large differences between mean elevations, which ranged from 0.4 - 0.7 feet (Table 3). The relationship of significantly better accuracy for the "Good" vs. "OK" vs. "Bad" vegetation cover classes held for all five years of LiDAR coverages. The precision of repeat LiDAR-derived elevations across vegetation cover classes was measured by using the sum of differences for each ground truth elevation point as the metric. A smaller sum of differences implies a greater precision. Figure 7 displays the significant differences found among vegetation cover classes, with increasing difference found for the "Good" vs. "OK" vs. "Bad" vegetation cover classes.

| Year | Mean_Abs_Diff | n | Std Dev | ± 95% C.I. | Minimum | Maximum |
|---|---|---|---|---|---|---|
| 2002 | 0.598 | 604 | 0.644 | 0.051 | 0.001 | 3.383 |
| 2004 | 0.633 | 604 | 0.678 | 0.054 | 0.001 | 4.005 |
| 2006 | 0.427 | 604 | 0.505 | 0.040 | 0.000 | 3.996 |
| 2007 | 0.410 | 604 | 0.448 | 0.036 | 0.000 | 2.563 |
| 2008 | 0.682 | 604 | 0.806 | 0.064 | 0.001 | 4.350 |

| Year | 2002 | 2004 | 2006 | 2007 | 2008 |
|---|---|---|---|---|---|
| 2002 | 0.000 | | | | |
| 2004 | 0.035 | 0.000 | | | |
| 2006 | -0.171 | -0.206 | 0.000 | | |
| 2007 | -0.189 | -0.223 | -0.017 | 0.000 | |
| 2008 | 0.083 | 0.049 | 0.255 | 0.272 | 0.000 |

| Year | 2002 | 2004 | 2006 | 2007 | 2008 |
|---|---|---|---|---|---|
| 2002 | 1.000 | | | | |
| 2004 | 1.000 | 1.000 | | | |
| 2006 | 0.000 | 0.000 | 1.000 | | |
| 2007 | 0.000 | 0.000 | 1.000 | 1.000 | |
| 2008 | 0.213 | 1.000 | 0.000 | 0.000 | 1.000 |

Table 3: Mean Absolute Difference between Ground Truth Elevation and LiDAR-Derived Elevation for 2002, 2004, 2006, 2007, and 2008 coverages. Matrix of pairwise mean differences using least squares means: Post Hoc test of ABS_DIFF; using model MSE of 0.396 with 3015 df. Bonferroni Adjustment: Matrix of pairwise comparison probabilities.

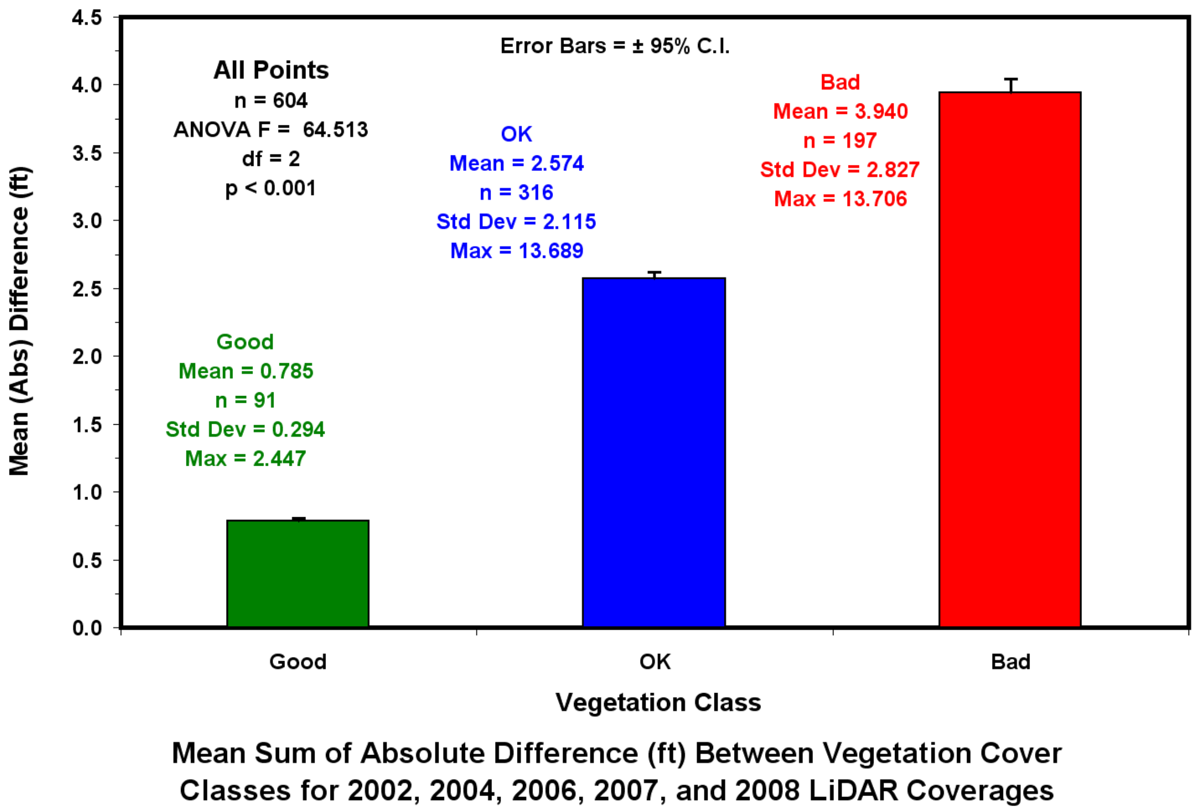


Figure 7: Sum of absolute year-to-year differences between ground truth elevation and LiDAR-derived elevations (n = 604) for repeat LiDAR coverages: 2002, 2004, 2006, 2007, and 2008.

**Multi-Year LiDAR Coverages: LiDAR Accuracy by Slope Percent**

Slope has been shown to account for differences in LiDAR accuracy, with increasing error found in areas of increasing slope. Our repeat LiDAR and ground truth elevation dataset offered an excellent opportunity to test this relationship. The 2007 LiDAR data over the ground survey area was used as the 'best' data and processed to a 3-foot DEM (the 'best' spatial resolution based upon the point spacing and the DEM rules stated in Maune, 2001). The ArcInfo Grid 'slope' function was used to generate a %slope gradient and 'Slope Quintiles' were created by using a combination of equal sample sizes and natural breaks in the data (Figure 8).

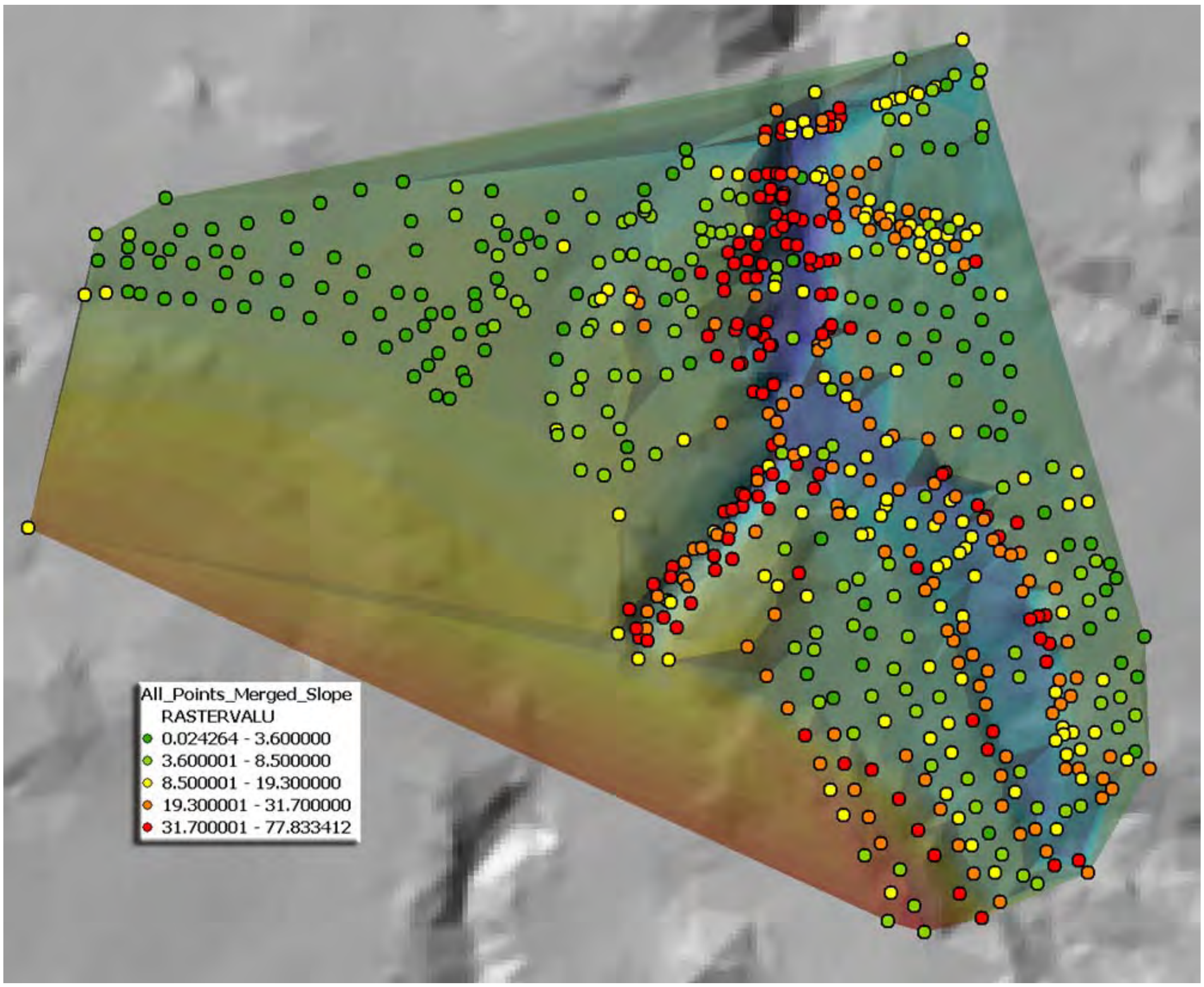


Figure 8: Slope quintiles created from slope derived from the 2007 LiDAR-derived 3-foot DEM calculated at the 604 ground-truth survey points.

For this exercise, the accuracy value is calculated as the absolute value of the difference between the survey ground truth points and the LiDAR-derived elevation values. 'Mean Sum Accuracy' (Figure 9 and Table 4) is the mean of the sum for 2002, 2004, 2006, 2007, and 2008 for each point in the quintile. 'MeanDiff' is the absolute value of the difference between the LiDAR-derived elevation values for 2002-2004, 2004-2006, 2006-2007, and 2007-2008.

'MeanDiff All Years' is the absolute value of the difference between the LiDAR-derived elevation values for all four between-year pairs. The accuracy of the LiDAR-derived elevation at the surveyed ground truth points significantly declined with increasing percent slope.

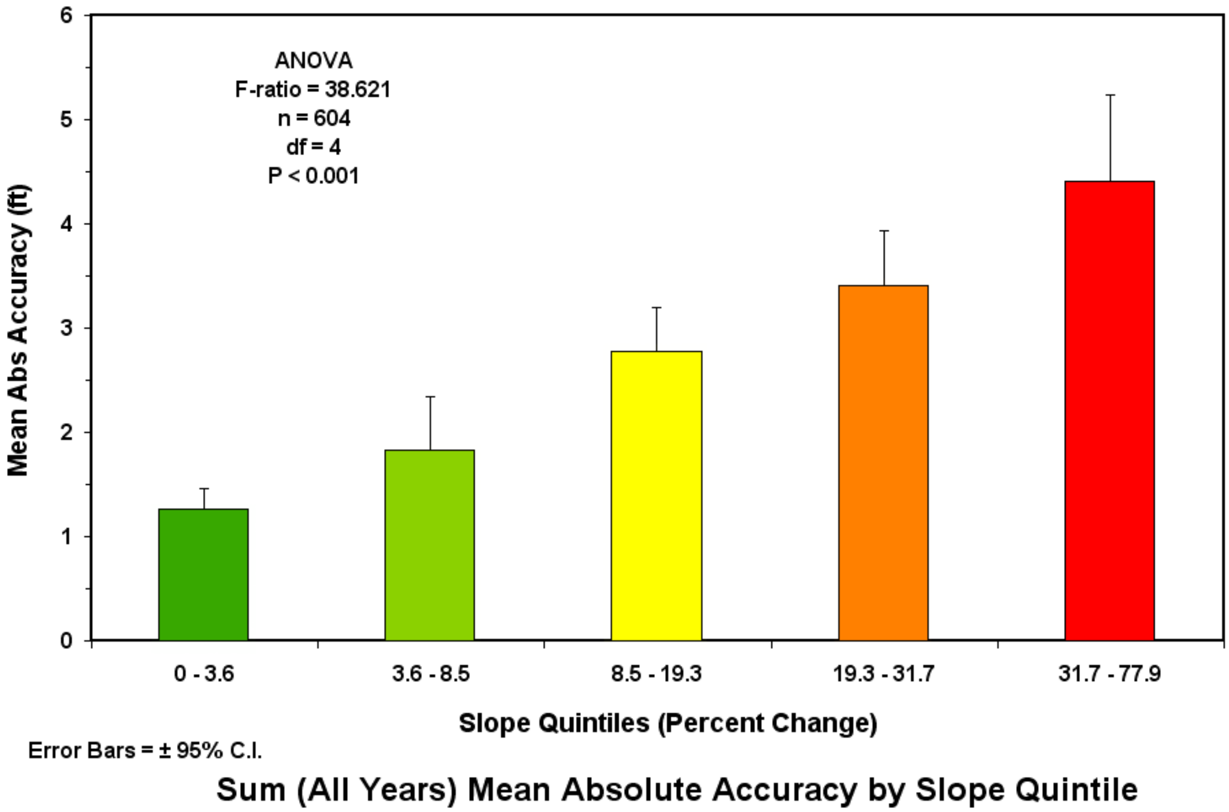


Figure 9: Sum (All Years) Mean Absolute Accuracy by Slope Quintile.

| **Slope Quintiles** | **Mean Sum Accuracy** | **n** | **stdev** | **± 95% C.I.** |
|---|---|---|---|---|
| **0 - 3.6** | **1.26** | **116** | **1.08** | **0.20** |
| **3.6 - 8.5** | **1.84** | **123** | **1.81** | **0.51** |
| **8.5 - 19.3** | **2.77** | **121** | **2.48** | **0.42** |
| **19.3 - 31.7** | **3.41** | **122** | **2.10** | **0.53** |
| **31.7 - 77.9** | **4.41** | **122** | **2.97** | **0.83** |

Table 4: Sum (All Years) Mean Absolute Accuracy by Slope Quintile.

Year-by-year mean absolute accuracy by slope quintile is shown in Appendix One. These data are noisier than the sum of years but show the same general trend: increasing accuracy with lower slope.

**LiDAR Precision Assessment: Differences in LiDAR-Derived Elevations at Surveyed Ground-Truth Points between Subsequent Sets of Multi-Year LiDAR Coverages.**

Another method of assessing precision (without respect to how accurate the measurements are) is to compare year-to-year differences between the LiDAR-derived elevations for subsequent coverages in the multi-year LiDAR coverage dataset.

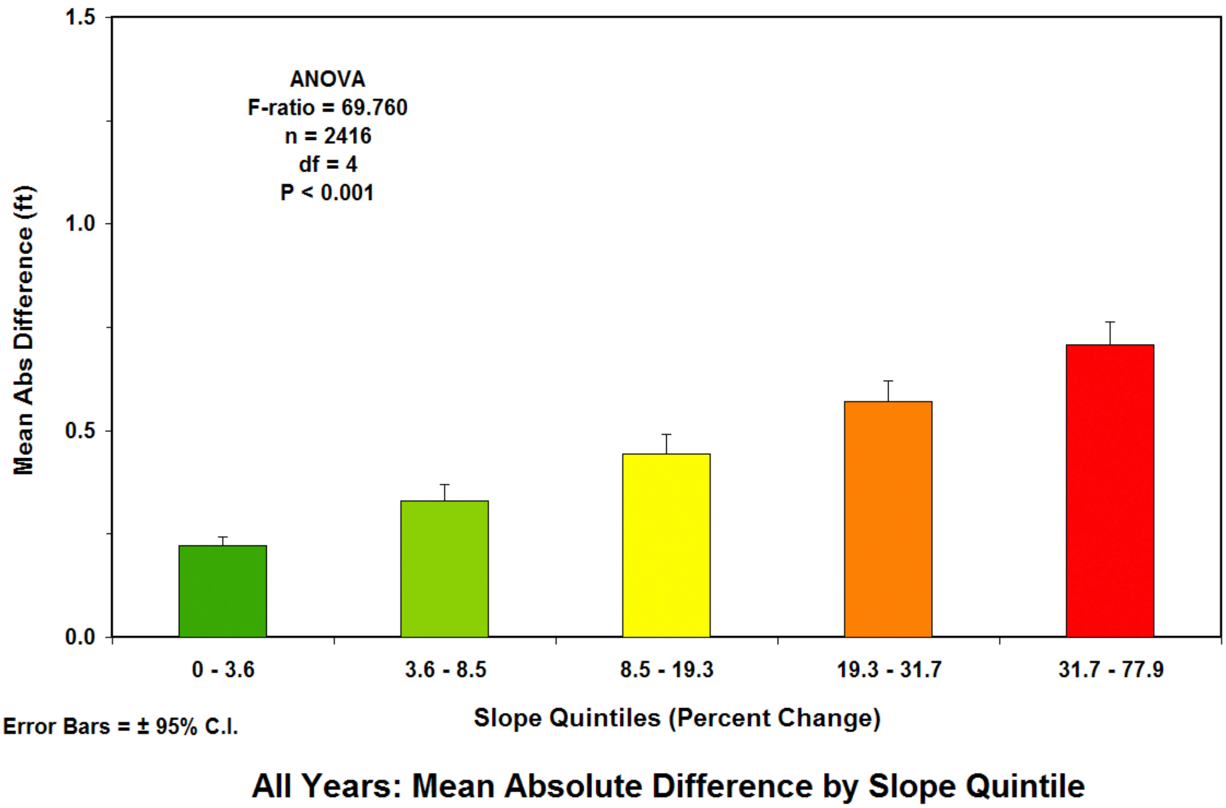


Figure 10: All Years Mean Absolute Year-to-Year Differences Between LiDAR-Derived Elevations at Ground-Truth Points by Slope Quintile.

| Slope Quintiles | MeanDiff All Years | n | stdev | ± 95% C.I. |
|---|---|---|---|---|
| 0 - 3.6 | 0.22 | 464 | 0.25 | 0.02 |
| 3.6 - 8.5 | 0.33 | 500 | 0.43 | 0.04 |
| 8.5 - 19.3 | 0.44 | 476 | 0.52 | 0.05 |
| 19.3 - 31.7 | 0.57 | 488 | 0.56 | 0.05 |
| 31.7 - 77.9 | 0.71 | 488 | 0.65 | 0.06 |

Table 5: All Years Mean Absolute Year-to-Year Differences Between LiDAR-Derived Elevations at Ground-Truth Points by Slope Quintile.

Figure 10 shows the means of differences by slope quintile and the ANOVA statistics between groups. There was a significant difference between groups with increasing differences (less precision) as the percent slope increased. Table 5 displays the resulting numeric values.

Year-by-year mean absolute difference by slope quintile is shown in Appendix Two. These data are noisier than the sum of years but show the same general trend: increasing precision with lower slope.

**LiDAR Precision Assessment: Multi-Year LiDAR Coverages by Land Use/Land Cover (LULC)**

In most real-life applications of LiDAR-derived elevations, DEMs, and topography, there are few or no ground-truth elevations other than those used to calibrate the LiDAR overflight. The multi-year LiDAR coverage dataset offered an opportunity to indirectly assess LiDAR precision by using those multiple measurements sorted by Land Use/Land Cover (LULC) classes and slope. We first needed to determine which areas did not undergo development and change in LULC over the time period covered. Modified Anderson Level One and Level Two classification of LULC was done for the study watersheds for the 1998, 2002, 2004, 2006, 2007, and 2008 periods. Table 6 shows the modified Anderson Level One classification used.

| LULC Code | LULC Class |
|---|---|
| 1 | Agricultural |
| 2 | Barren |
| 3 | Forest |
| 4 | Impervious Surface (Urban) |
| 5 | Natural Clearing |
| 6 | Urban Grasses Cultivated |
| 7 | Urban Grasses Fallow |
| 8 | Water |
| 9 | Wetland |

Table 6: Modified Anderson Level One Land Cover Classes used in the study.

Appendix Three: Sequence of modified Anderson Level One LULC classes mapped from 1-foot (or better) digital orthoimages (used as the ground-truth for LULC mapping) from the 1998, 2002, 2004, 2006, and 2008 aerial overflights by Montgomery County in the Clarksburg Special Protection Area. 1998 was used as the base year. LULC coverages were done for the Sopers Branch, Tributary 104 (T104), and Tributary 109 (T109) watershed areas, with the LULC mapped to a 500-foot buffer and the County-mapped stream channels overlaid. For comparisons of LiDAR precision (repeatability of LiDAR-derived elevation), only areas with no LULC change over time were used as comparison locations.

### Stream Transects

The Montgomery County, Maryland Department of Environmental Protection (DEP) does yearly measurements of streams in the CSPA as a part of their geomorphology assessments of stream health. These repeated measurements are taken annually at a linear spatial scale of one foot or less across stream transects chosen to yield information about changes in stream morphology as a result of the urban development in the CSPA. I used a Trimble GeoXT2003 handheld Global Positioning System (GPS) to find the geographic locations of the DEP transects and compared LiDAR-derived DEM transects at the same locations over time. I used a 1-foot LiDAR-derived DEM to match the spatial scale of analysis used by the DEP and interpolated both results to a uniform 1-foot spatial scale. Due to positional uncertainty (location error) in the GPS locations and the temporal disconnect between stream transect dates and LiDAR overflight dates, no attempt was made to directly compare ground-truth transects with LiDAR-derived transects (a measure of accuracy). Instead, as a measurement of precision, year-to-year differences between interpolated stream transect depths and LiDAR-derived transect elevations were compared. The metric used for comparison was the "Sum Inter-Annual Delta Difference". This was calculated by the taking the sum of the absolute values of the differences in inches between interpolated depths along the respective ground-truth and LiDAR-derived transects, divided by the linear distance measured and the number of years in the series of measurements. This yields a normalized value that expresses the inches per year per linear foot of measured difference per measurement method for each stream transect location. Table 7 and Figure 11 show the ground-truth vs. LiDAR-Derived Sum Inter-Annual Delta Differences measured. Appendix Four shows a sequence of images that display the ground-truth stream transect measurements and LiDAR-derived stream transect elevation values.

| Sample Location | Ground-Truth | LiDAR-Derived |
|---|---|---|
| LSSB101 A1 X1 | 0.4047 | 2.8104 |
| LSLS104 A1 X1 | 0.4148 | 1.3688 |
| LSLS104 A1 X2 | 0.5269 | 1.6167 |
| LSLS104 A2 X1 | 0.4579 | 2.6024 |
| LSLS104 A2 X2 | 0.3445 | 1.7940 |
| LSLS104 A3 X1 | 0.9265 | 2.2474 |
| LSLS104 A3 X2 | 0.7639 | 1.7919 |
| LSLS104 A3 X3 | 0.9083 | 2.3634 |
| LSLS104 A3 X4 | 0.8778 | 3.3982 |
| LSLS109 A1 X1 | 0.1250 | 1.3024 |
| LSLS109 A1 X2 | 0.2492 | 0.8203 |
| LSLS109 A2 X1 | 0.2785 | 3.3259 |
| LSLS109 A2 X2 | 0.6027 | 3.5540 |
| LSLS109 A3 X1 | 0.1793 | 1.4810 |

Table 7: Ground-Truth vs. LiDAR-Derived Sum Inter-Annual Delta Differences (inches/foot/year).

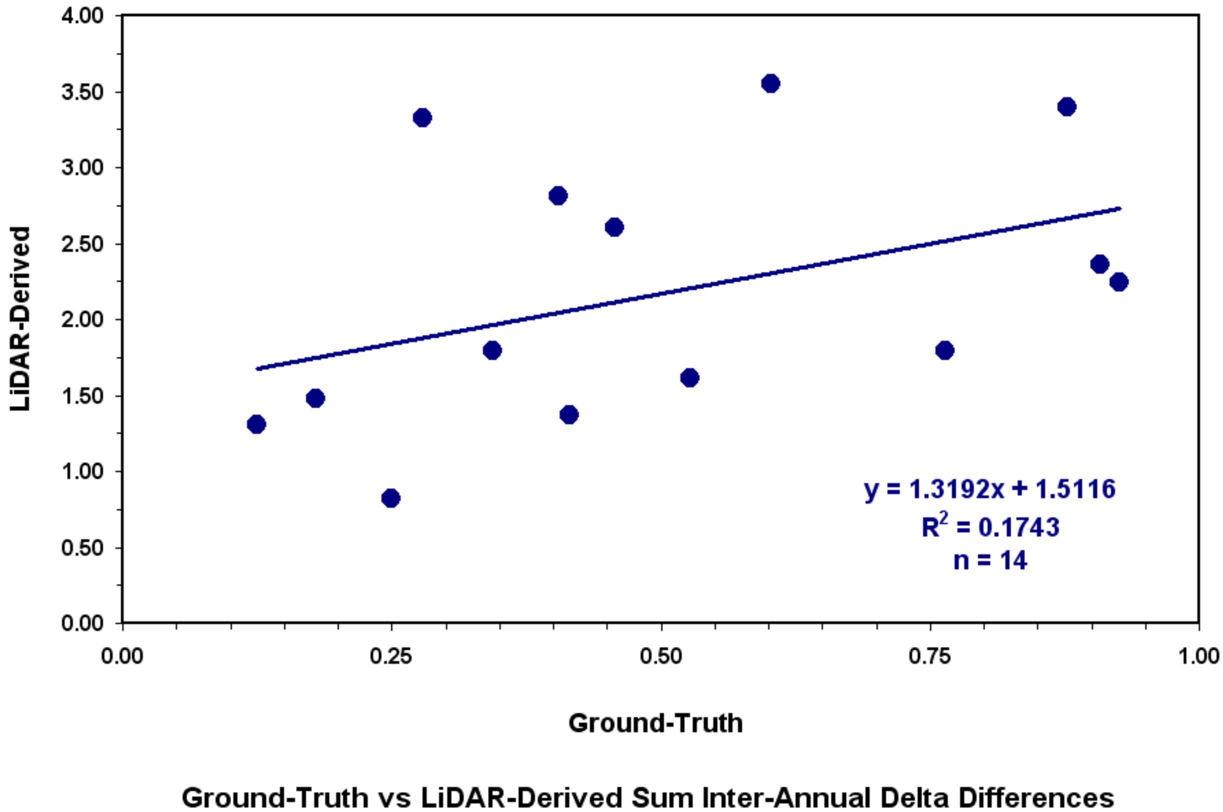


Figure 11: Stream Transects: Ground Truth vs. LiDAR-Derived Transect Elevations.

The LiDAR-derived Sum Inter-Annual Delta Differences measured were from 2 to 12 times larger than the ground-truth-derived differences. Additionally, the year-to-year difference seen between some LiDAR transects was extreme. The relationship between the two variables was noisy ($R^2$ = 0.17) and the ability of repeat LiDAR to reveal stream channel morphology changes at a 1-foot spatial scale appears to be quite poor.

### Part 2: LiDAR Precision Assessment Using Multi-Year LiDAR Coverages Where No Ground Truth Measurements Exist.

#### Large-Scale Elevation Changes Shown in LiDAR

Appendix Five shows a sequence of images that display the year-to-year LiDAR-derived elevation differences between 3-foot DEMs for the 500-foot buffered areas around the Sopers Branch, Tributary 104 (T104), and Tributary 109 (T109) watersheds in the CSPA. Year-to-year differences in 3-foot LiDAR-derived DEMs are shown for sequential years 2002-2004, 2004-2006, 2006-2007, and 2007-2008. All elevation differences have been scaled to the same metric, with the difference between the later year minus the earlier year shown; increasing red (negative) values indicate that the elevation was greater in the prior year (elevation has decreased over time) while increasing blue (positive) values indicate that the elevation was less in the prior year (elevation has increased over time). Sopers Branch is a control watershed, not currently undergoing urban development. As expected, year-to-year differences are largely minor (within ± 1 foot) or largely confined to the outer edges of the DEMs where edge effects are present and some development activities have occurred in the 500-foot buffer outside the watershed boundary. T104 and T109 are areas undergoing development and large-scale cut-and-fill operations associated with urban development can be detected using the sequential LiDAR coverages. For comparisons of LiDAR precision (repeatability of LiDAR-derived elevation), only areas with no elevation change ± 2 feet over time were used as comparison locations.

#### LiDAR-Derived DEM Differences by LULC

To look at the precision of LiDAR-derived 3-foot DEM elevations by LULC class, areas of no elevation change (± 2 feet) over time and no LULC change over time were compared for the 2002-2004, 2004-2006, 2006-2007, and 2007-2008 LiDAR derived elevation differences for the Sopers Branch, T104, and T109 watersheds.. A random sample of 60 points was selected from the coverages for the Agricultural, Forest, Impervious Surfaces, and Urban Grasses Cultivated LULC classes. A mean was calculated for the absolute values of the differences for the four coverage pairs for each watershed for each of the four LULC classes considered. Each comparison yielded significantly different means for each group with Forest showing the greatest mean difference and the Agricultural LULC class showing the least. Due to the very large sample sizes, these significant differences between LULC classes must be taken with a grain of salt. Smaller within-LULC samples (n = 30) showed a high degree of internal variation of the mean. Figures 11-13 and Tables 8-10 show the mean differences found.

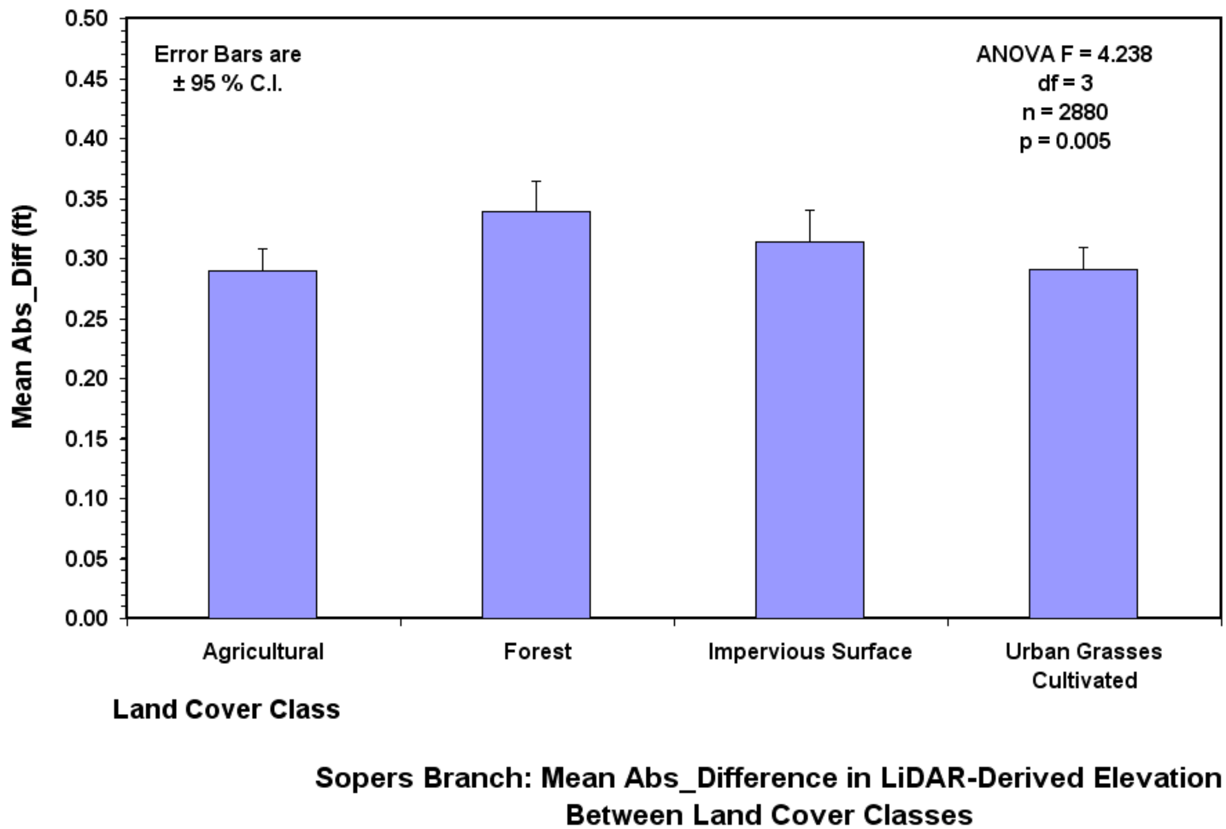


Figure 12: LiDAR-Derived DEM Differences by LULC Class for Sopers Branch.

| Land Cover Class (Sopers Branch) | Sample | Mean Abs_Diff (ft) | n | Std Dev | ± 95 % C.I. |
|---|---|---|---|---|---|
| Agricultural | All | 0.289 | 720 | 0.256 | 0.019 |
| Forest | All | 0.339 | 720 | 0.334 | 0.024 |
| Impervious Surface | All | 0.314 | 720 | 0.372 | 0.027 |
| Urban Grasses Cultivated | All | 0.291 | 720 | 0.249 | 0.018 |

Table 8: LiDAR-Derived DEM Differences by LULC Class for Sopers Branch.

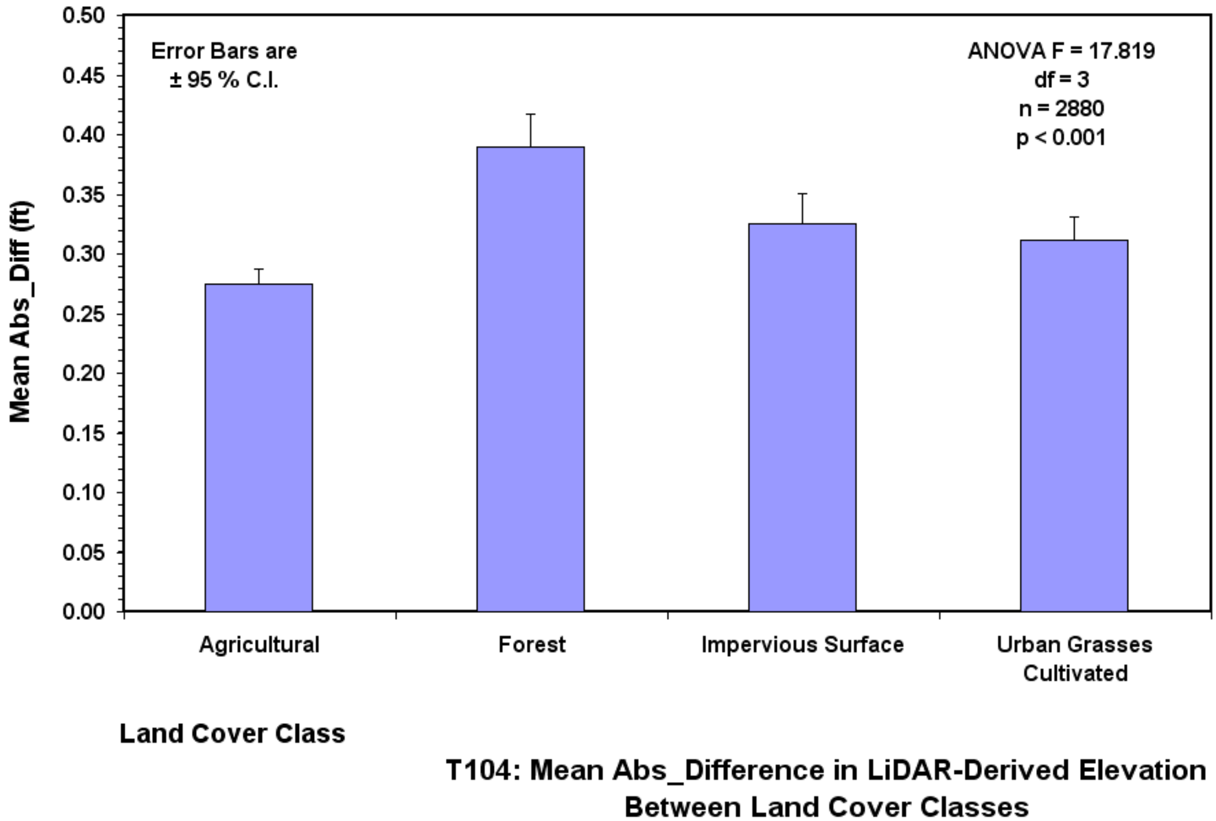


Figure 13: LiDAR-Derived DEM Differences by LULC Class for T104.

| Land Cover Class (T104) | Sample | Mean Abs_Diff (ft) | n | Std Dev | ± 95 % C.I. |
|---|---|---|---|---|---|
| Agricultural | All | 0.275 | 720 | 0.177 | 0.013 |
| Forest | All | 0.389 | 720 | 0.382 | 0.028 |
| Impervious Surface | All | 0.326 | 720 | 0.348 | 0.025 |
| Urban Grasses Cultivated | All | 0.312 | 720 | 0.261 | 0.019 |

Table 9: LiDAR-Derived DEM Differences by LULC Class for T104.

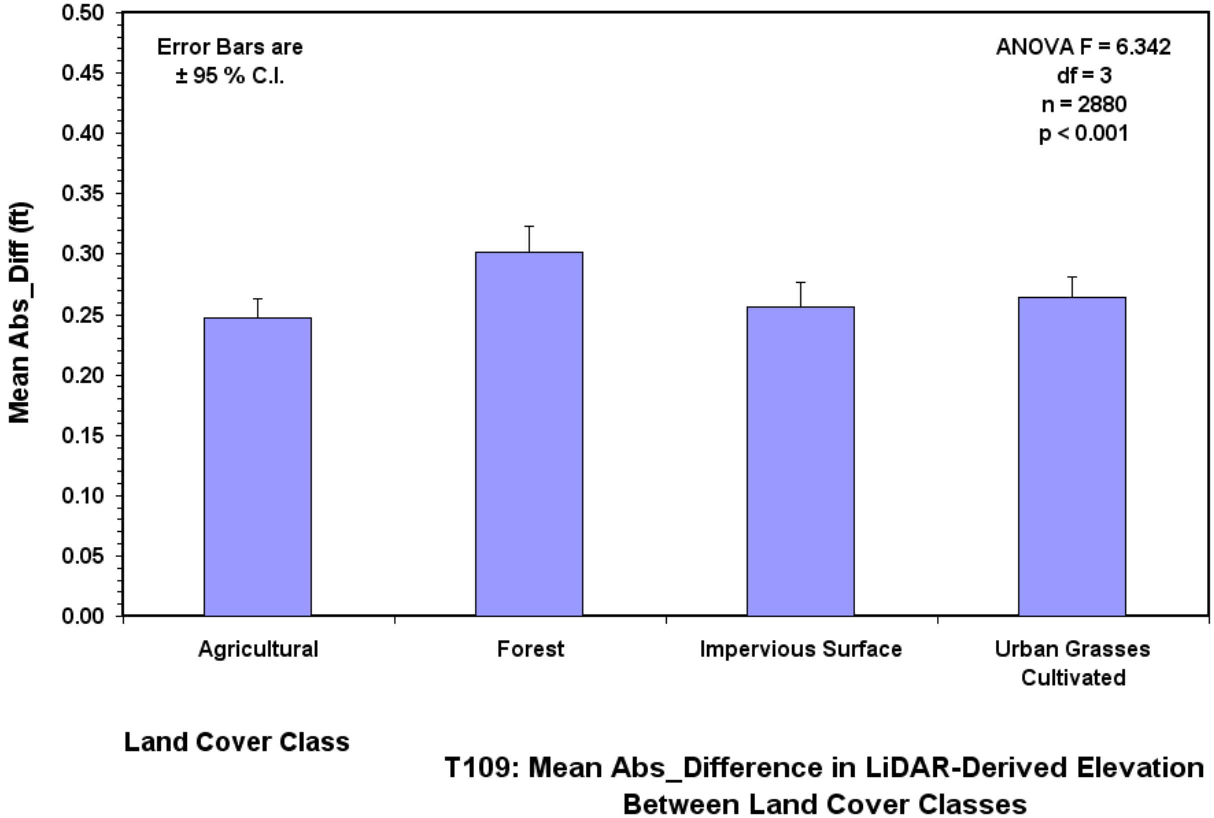


Figure 14: LiDAR-Derived DEM Differences by LULC Class for T109.

| Land Cover Class (T109) | Sample | Mean Abs_Diff (ft) | n | Std Dev | ± 95 % C.I. |
|---|---|---|---|---|---|
| Agricultural | All | 0.247 | 720 | 0.222 | 0.016 |
| Forest | All | 0.302 | 720 | 0.286 | 0.021 |
| Impervious Surface | All | 0.257 | 720 | 0.269 | 0.020 |
| Urban Grasses Cultivated | All | 0.264 | 720 | 0.237 | 0.017 |

Table 10: LiDAR-Derived DEM Differences by LULC Class for T109.

### LiDAR-Derived DEM Precision by Slope Gradient by LULC

To investigate the effect of slope on LiDAR-derived elevations by LULC class, a percent slope gradient was calculated for the Forest and Impervious Surfaces LULC classes for Sopers Branch, T104, and T109 using the 3-foot DEM derived from the 2007 LiDAR coverage. To avoid edge effects, an interior 3-foot buffer was used and only no-LULCC-change and no-elevation-change areas were used. The slope percentages at 3-ft DEM resolution were derived by year and rounded to whole integer percentages; the few cells of gradient > 30% were rolled into the 30% category; the five years' class and cell count distributions were combined across years and the mean average value (MAV) of the absolute differences between subsequent years calculated for each slope percentage. Quintiles were formed by using the closest equal-number technique from the slope percentage classes and the MAVs averaged for each quintile. Figures 15-17 and Tables 11-13 display the all-years values computed for the Forest LULC class and Figures 18-20 and Tables 14-16 display the all-years values computed for the Impervious Surfaces LULC class. Individual between-year differences are shown in Appendix Six for both LULC classes.

There was little change in between-year elevation differences computed until the largest slope-percent quintile was considered. In the Forest LULC class, Sopers Branch showed the least difference in elevation between slope-percent quintiles while T104 and T109 showed an increased difference in elevation with the largest slope-percent quintile. For the Impervious Surfaces LULC class, the largest slope-percent quintile showed the largest difference in elevation in all three watersheds. See the Discussion section for speculation as to why this may have occurred.

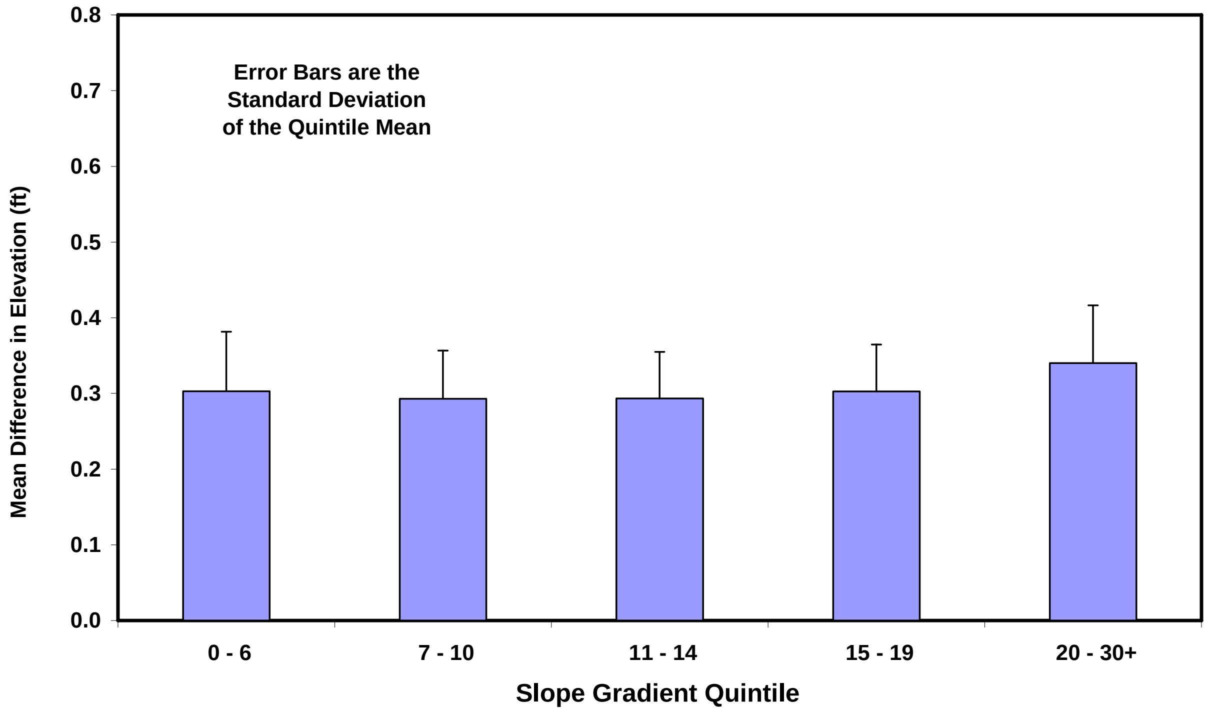


**All Years Forest No-Change Land Cover, Sopers Branch:
Mean Difference in Elevation by Slope Gradient Quintile**

Figure 15: No-Change Land Cover, Mean Differences in Elevation by Slope Gradient Quintiles - Sopers Branch, Forest LULC Class

| Quintile Slope Groups | Quintile n | Mean Diff All Years | Std Dev |
|---|---|---|---|
| 0 - 6 | 2902604 | 0.303 | 0.079 |
| 7 - 10 | 3482788 | 0.293 | 0.064 |
| 11 - 14 | 3533244 | 0.294 | 0.061 |
| 15 - 19 | 3244784 | 0.303 | 0.062 |
| 20 - 30+ | 3427552 | 0.340 | 0.076 |

Table 11: No-Change Land Cover, Mean Differences in Elevation by Slope Gradient Quintiles - Sopers Branch, Forest LULC Class.

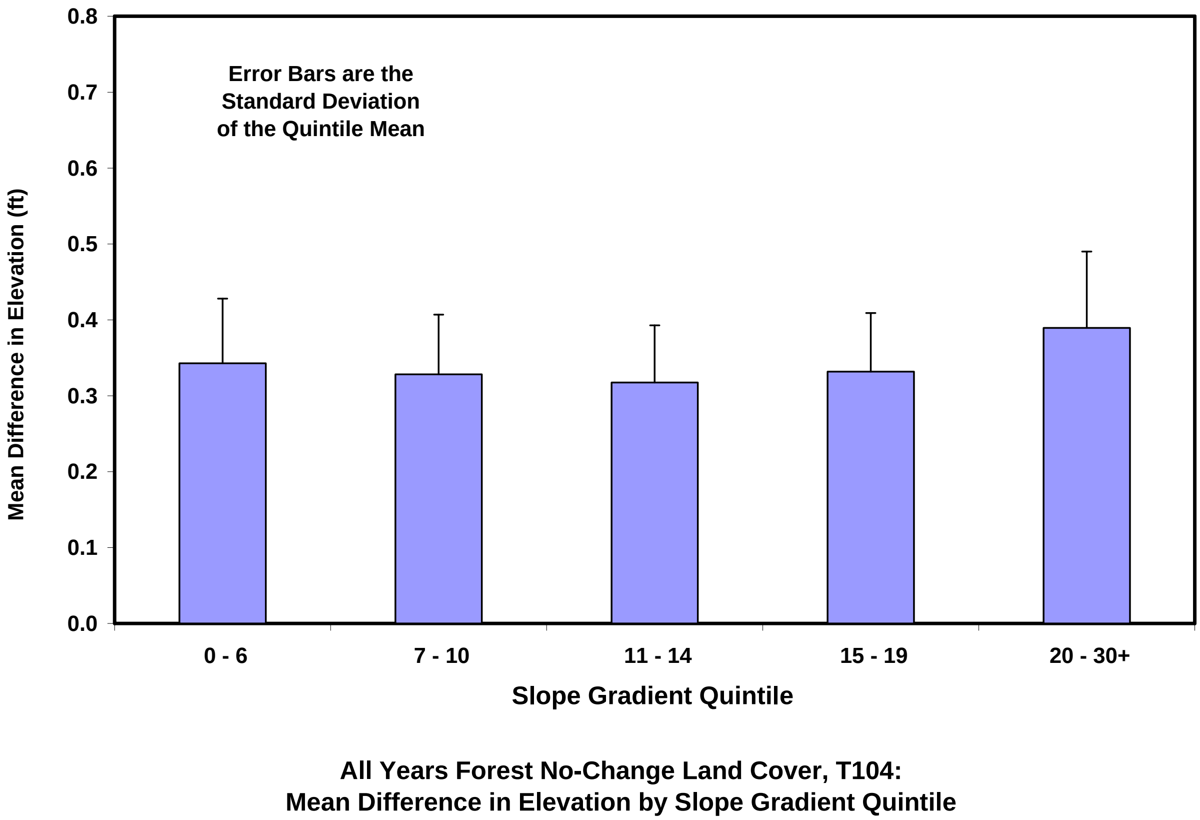


Figure 16: No-Change Land Cover, Mean Differences in Elevation by Slope Gradient Quintiles - T104, Forest LULC Class.

| **Quintile Slope Groups** | **Quintile n** | **Mean Diff All Years** | **Std Dev** |
|---|---|---|---|
| **0 - 6** | **282464** | **0.343** | **0.085** |
| **7 - 10** | **273672** | **0.328** | **0.079** |
| **11 - 14** | **286812** | **0.317** | **0.075** |
| **15 - 19** | **287704** | **0.332** | **0.077** |
| **20 - 30+** | **398008** | **0.389** | **0.101** |

Table 12: No-Change Land Cover, Mean Differences in Elevation by Slope Gradient Quintiles - T104, Forest LULC Class.

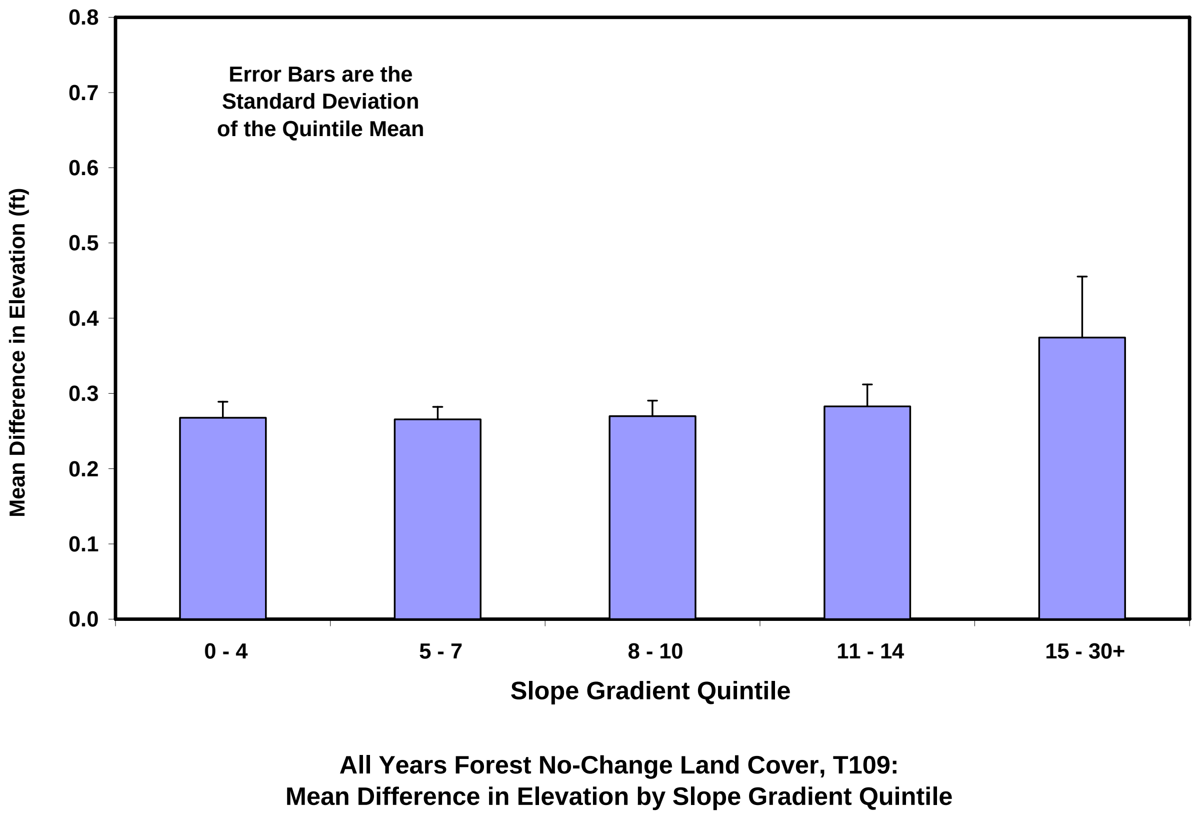


Figure 17: No-Change Land Cover, Mean Differences in Elevation by Slope Gradient Quintiles - T109, Forest LULC Class.

| Quintile Slope Groups | Quintile n | Mean Diff All Years | Std Dev |
|---|---|---|---|
| 0 - 4 | 320104 | 0.268 | 0.021 |
| 5 - 7 | 425816 | 0.265 | 0.017 |
| 8 - 10 | 395800 | 0.270 | 0.021 |
| 11 - 14 | 349564 | 0.283 | 0.029 |
| 15 - 30+ | 355772 | 0.374 | 0.081 |

Table 13: No-Change Land Cover, Mean Differences in Elevation by Slope Gradient Quintiles - T109, Forest LULC Class.

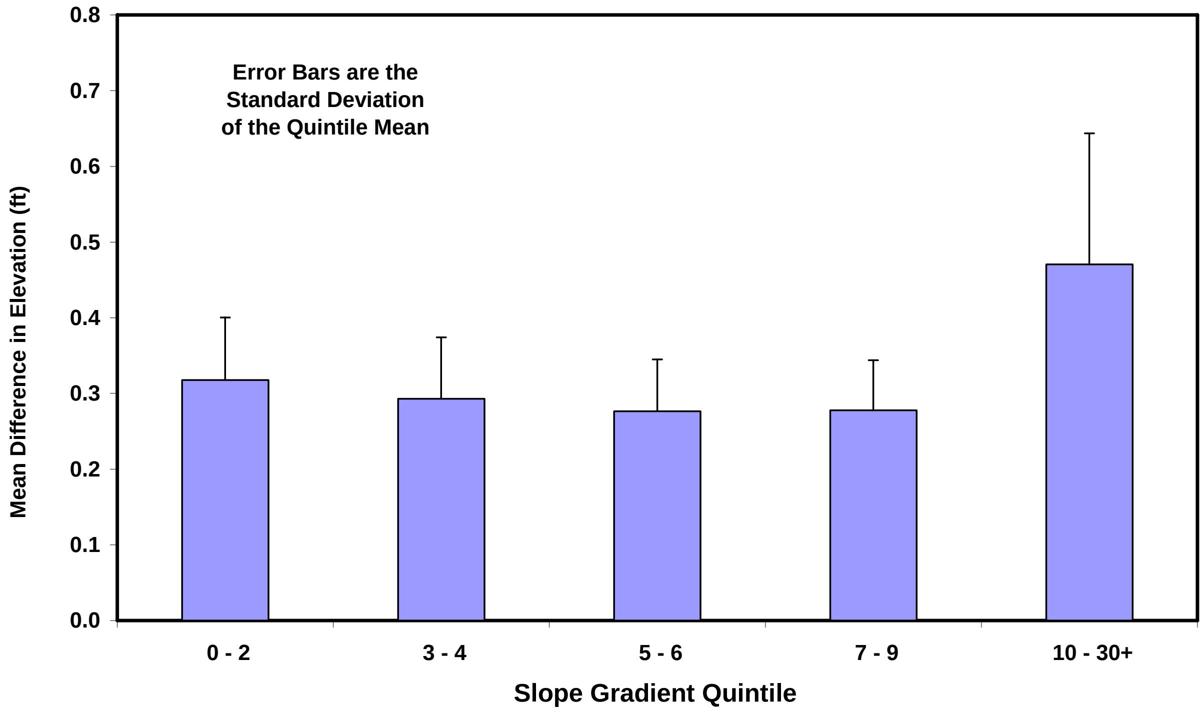


**All Years Impervious Surface No-Change Land Cover, Sopers Branch:**
**Mean Difference in Elevation by Slope Gradient Quintile**

Figure 18: No-Change Land Cover, Mean Differences in Elevation by Slope Gradient Quintiles - Sopers Branch, Impervious Surfaces LULC class.

| Quintile Slope Groups | Quintile n | Mean Diff All Years | Std Dev |
|---|---|---|---|
| 0 - 2 | 144972 | 0.318 | 0.083 |
| 3 - 4 | 216864 | 0.293 | 0.081 |
| 5 - 6 | 181252 | 0.276 | 0.069 |
| 7 - 9 | 144952 | 0.277 | 0.066 |
| 10 - 30+ | 104676 | 0.471 | 0.173 |

Table 14: No-Change Land Cover, Mean Differences in Elevation by Slope Gradient Quintiles - Sopers Branch, Impervious Surfaces LULC class.

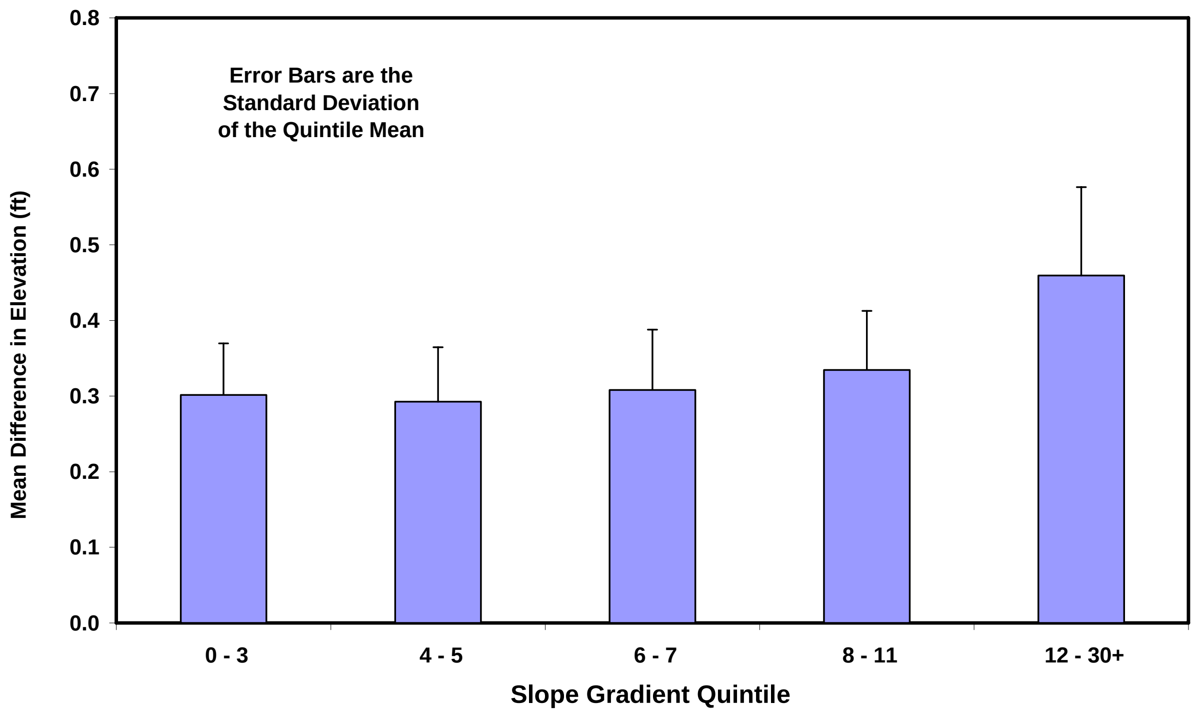


**All Years Impervious Surface No-Change Land Cover, T104:**
**Mean Difference in Elevation by Slope Gradient Quintile**

Figure 19: No-Change Land Cover, Mean Differences in Elevation by Slope Gradient Quintiles - T104, Impervious Surfaces LULC class.

| Quintile Slope Groups | Quintile n | Mean Diff All Years | Std Dev |
|---|---|---|---|
| 0 - 3 | 68188 | 0.301 | 0.068 |
| 4 - 5 | 68924 | 0.293 | 0.072 |
| 6 - 7 | 62696 | 0.308 | 0.080 |
| 8 - 11 | 75984 | 0.335 | 0.078 |
| 12 - 30+ | 91480 | 0.459 | 0.117 |

Table 15: No-Change Land Cover, Mean Differences in Elevation by Slope Gradient Quintiles - T104, Impervious Surfaces LULC class.

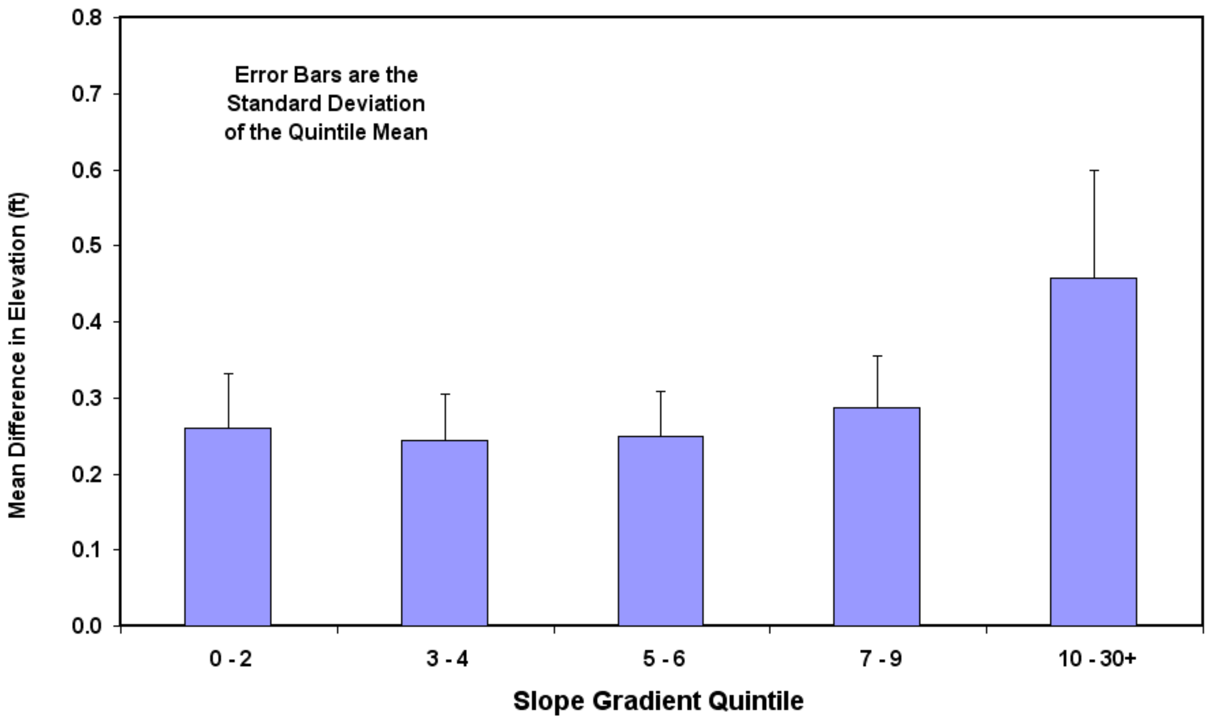


Figure 20: No-Change Land Cover, Mean Differences in Elevation by Slope Gradient Quintiles - T109, Impervious Surfaces LULC class.

| Quintile Slope Groups | Quintile n | Mean Diff All Years | Std Dev |
|---|---|---|---|
| 0 - 2 | 41196 | 0.260 | 0.071 |
| 3 - 4 | 62208 | 0.244 | 0.061 |
| 5 - 6 | 55788 | 0.249 | 0.061 |
| 7 - 9 | 48028 | 0.287 | 0.069 |
| 10 - 30+ | 50648 | 0.457 | 0.141 |

Table 16: No-Change Land Cover, Mean Differences in Elevation by Slope Gradient Quintiles - T109, Impervious Surfaces LULC class.

### Stream Channels

One of the primary goals of this research was to assess the ability of repeat LiDAR coverages to accurately assess changes in stream channels over time in areas undergoing urban development. LiDAR-derived 3-foot DEMs were used to calculate flow accumulation and delineate stream channels in ArcGIS. Figure 21 shows the three study watershed and the stream channels derived from the 2002, 2004, 2006, 2007, and 2008 LiDAR coverages.

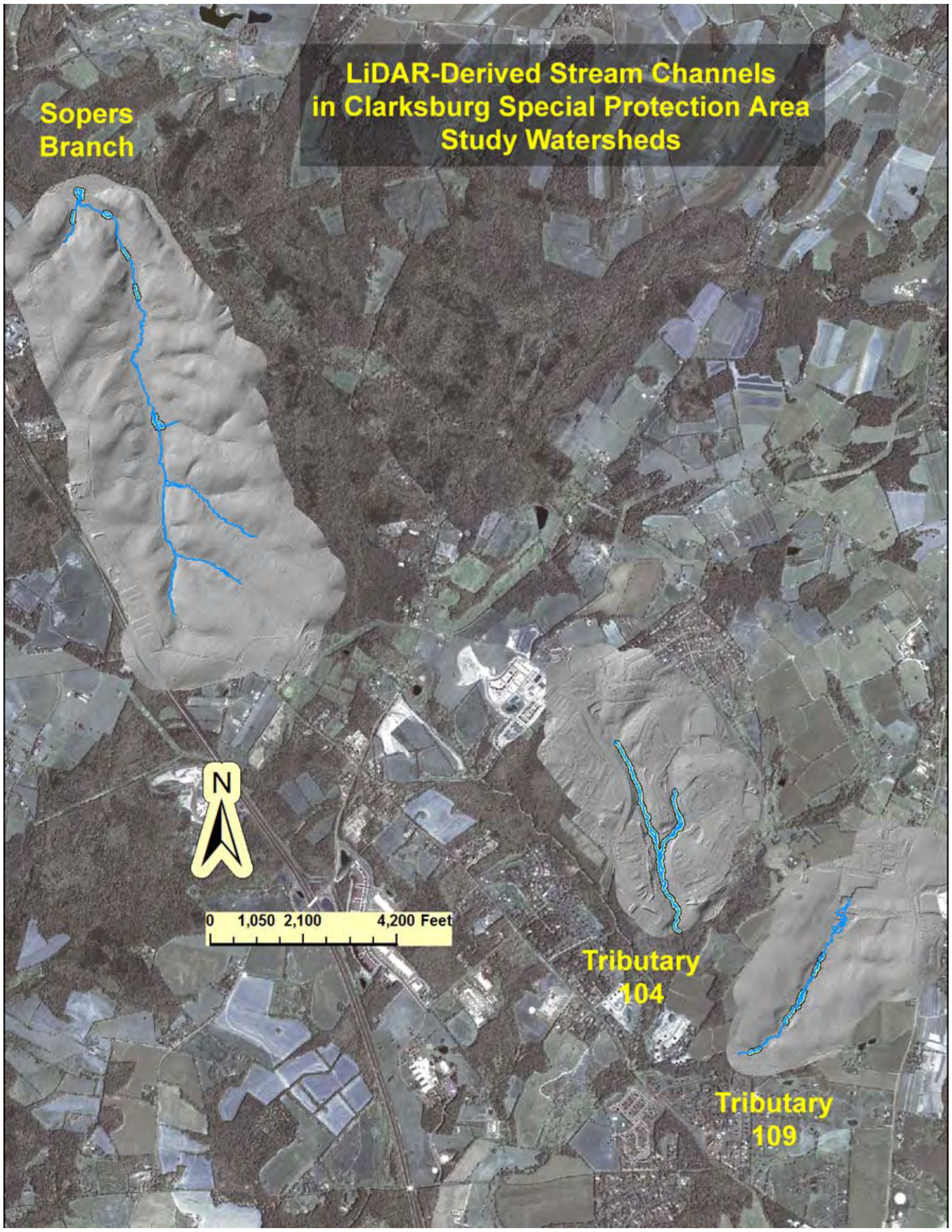


Figure 21: ArcGIS-Derived Stream Channels from LiDAR-Derived 3-foot DEMs from the 2002, 2004, 2006, 2007, and 2008 LiDAR coverages. The stream channels for Sopers Branch, T104, and T109 are shown overlaid on a shaded-relief image derived from the 2007 LiDAR-derived DEM and the three watersheds are overlaid on 2002 IKONOS imagery of the CSPA.

Areas where multiple LiDAR-derived stream channels closely overlaid each other were classified as 'low-variance' channels and areas where the channels did not overlay closely were classified as 'high-variance' channels. Three areas were identified for each of the channel-variance groups for each of the three watersheds (Figures 22-24).

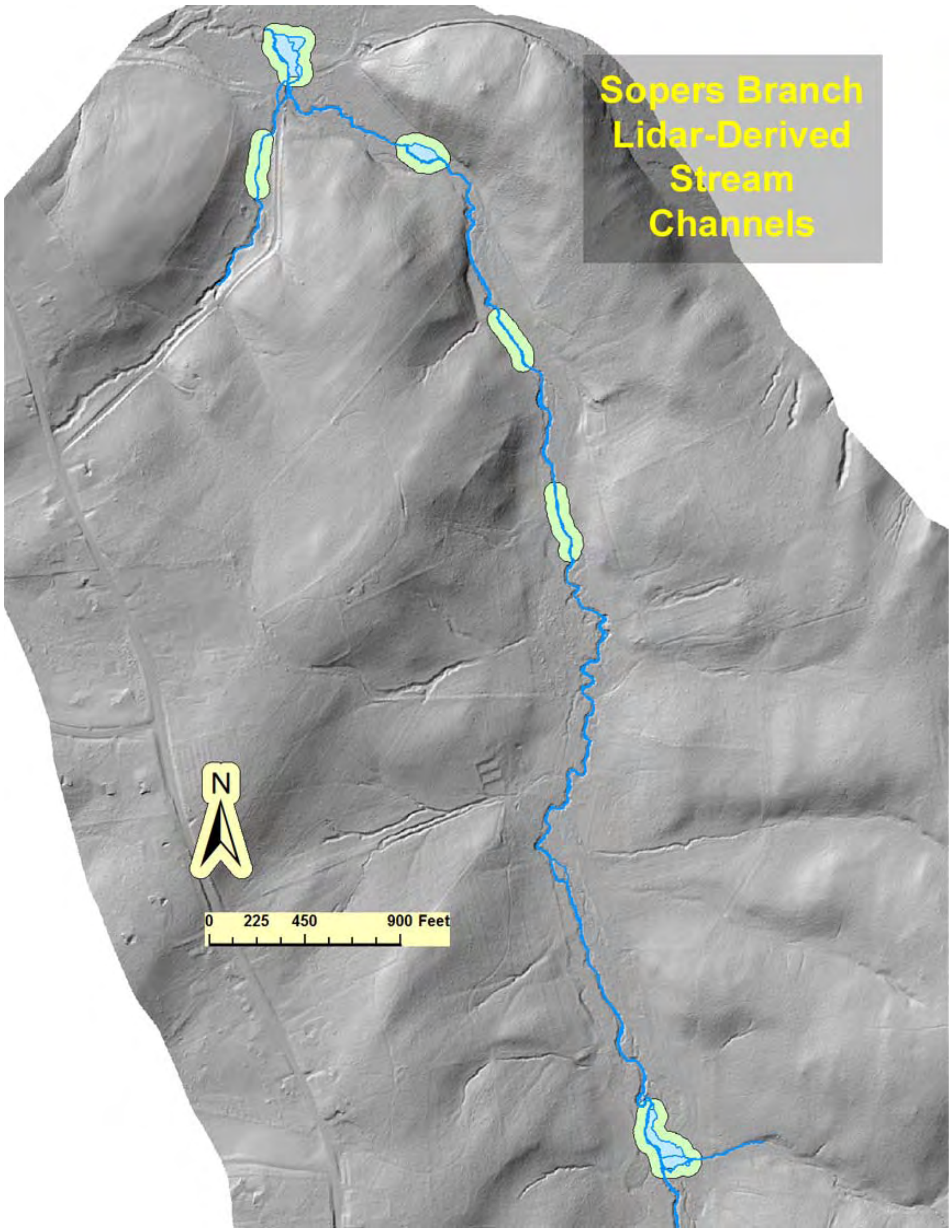


Figure 22: High-Variance and Low-Variance LiDAR-Derived Stream Channel Areas derived from the 2002, 2004, 2006, 2007, and 2008 LiDAR coverages at a 3-foot DEM spatial scale for the Sopers Branch watershed. Channels are overlaid on a shaded-relief image derived from the 2007 3-foot LiDAR-derived DEM.

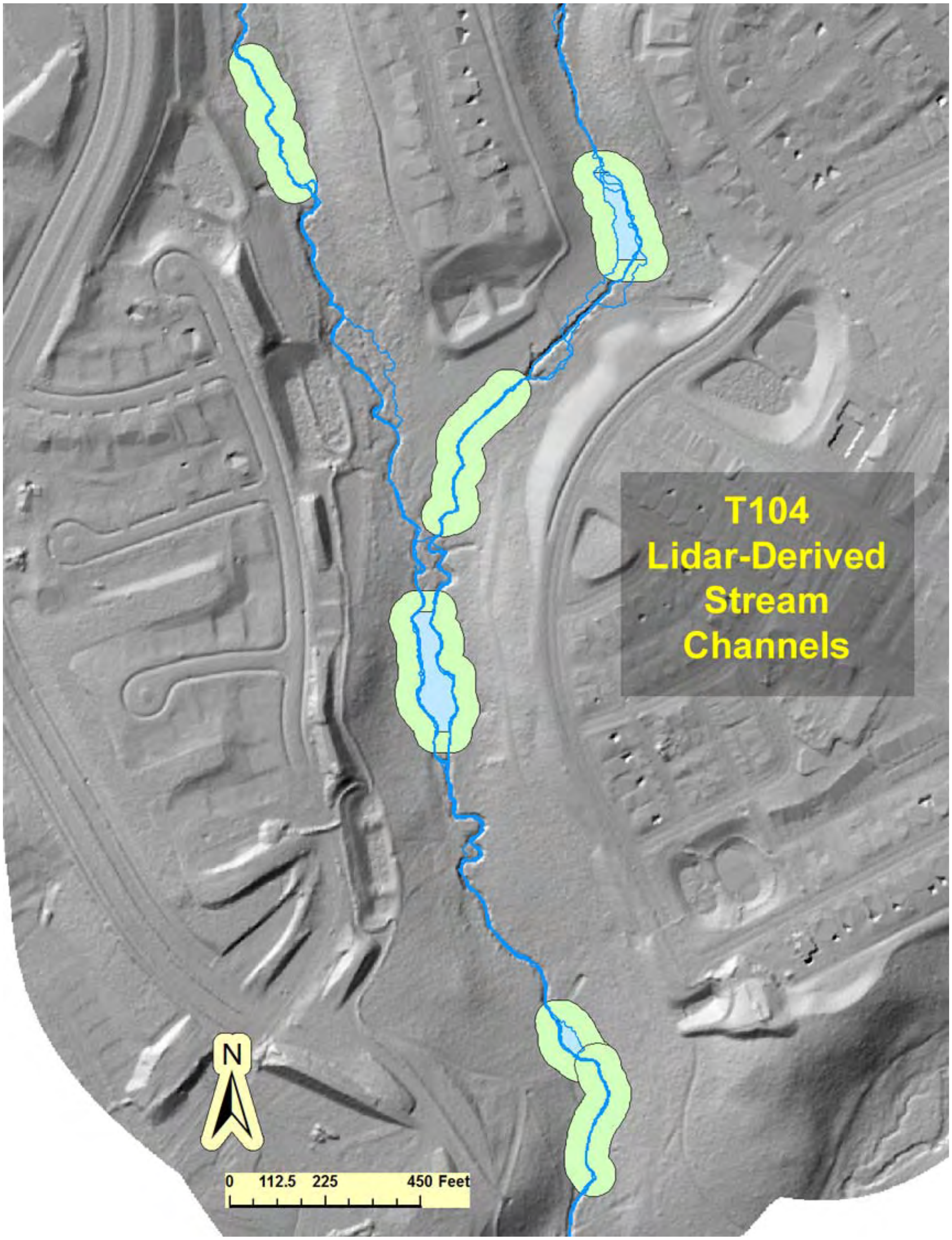


Figure 23: High-Variance and Low-Variance LiDAR-Derived Stream Channel Areas derived from the 2002, 2004, 2006, 2007, and 2008 LiDAR coverages at a 3-foot DEM spatial scale for the T104 watershed. Channels are overlaid on a shaded-relief image derived from the 2007 3-foot LiDAR-derived DEM.

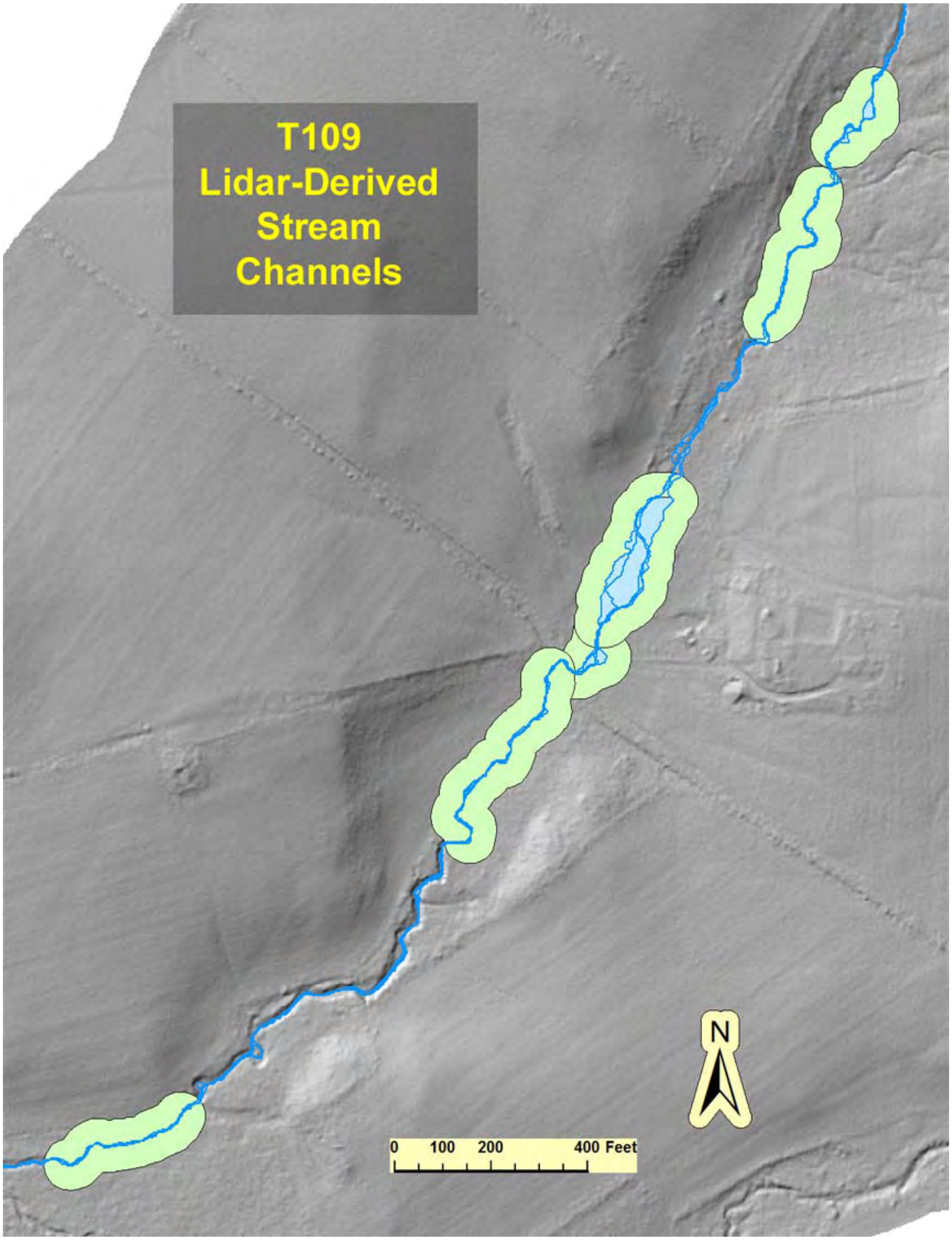

Figure 24: High-Variance and Low-Variance LiDAR-Derived Stream Channel Areas derived from the 2002, 2004, 2006, 2007, and 2008 LiDAR coverages at a 3-foot DEM spatial scale for the T109 watershed. Channels are overlaid on a shaded-relief image derived from the 2007 3-foot LiDAR-derived DEM.

Review of the LiDAR-derived DEMs for the High vs. Low-Variance Stream Channel Areas shows that in High-Variance Areas, the stream channel was not readily visible in the shaded relief imagery (see Figures 25-28 for High vs. Low-Variance Stream Channel Areas in T104).

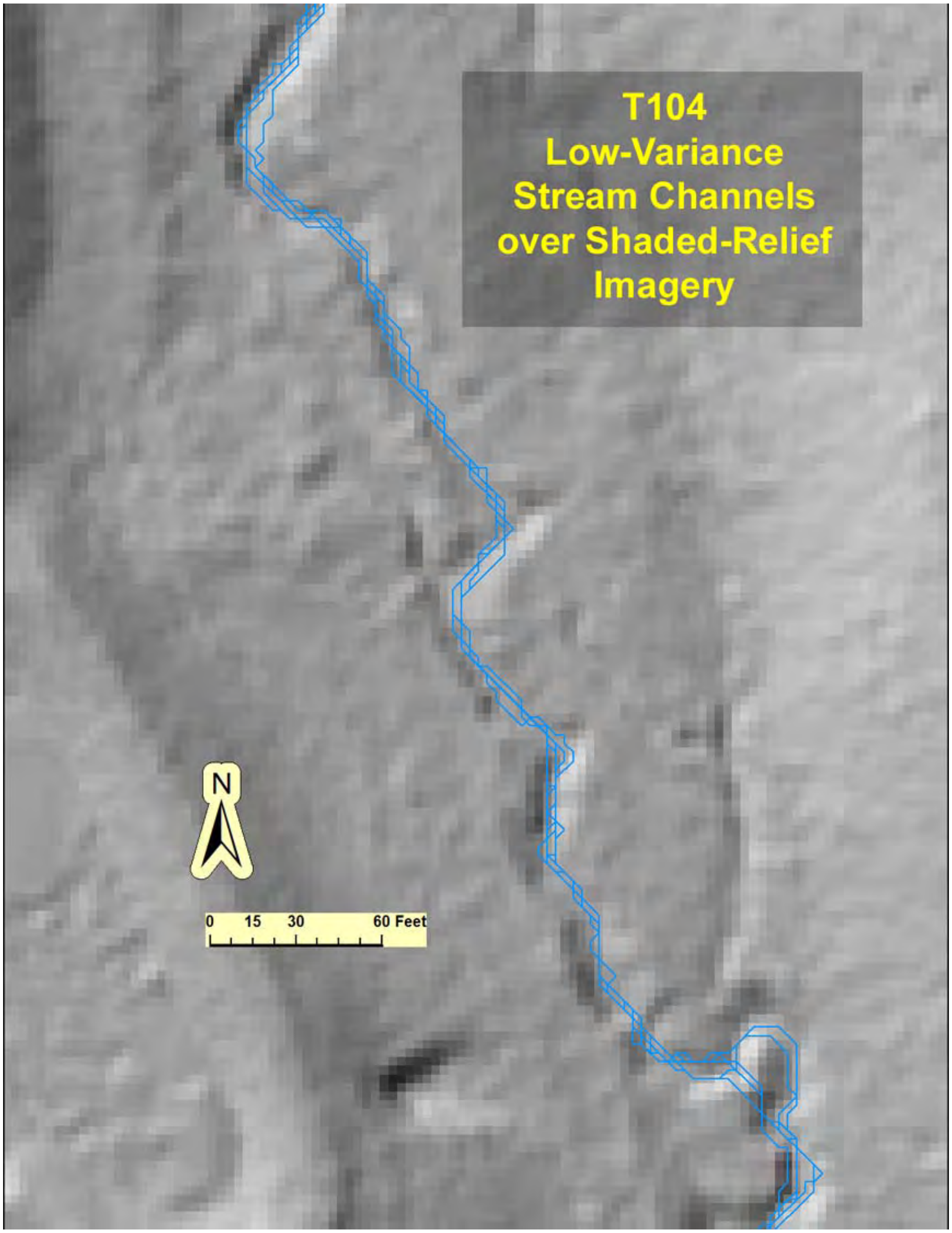


Figure 25: T104 Low-Variance Stream Channel Area Example: LiDAR-Derived Stream Channels Overlaid on 2007 Shaded Relief Imagery.

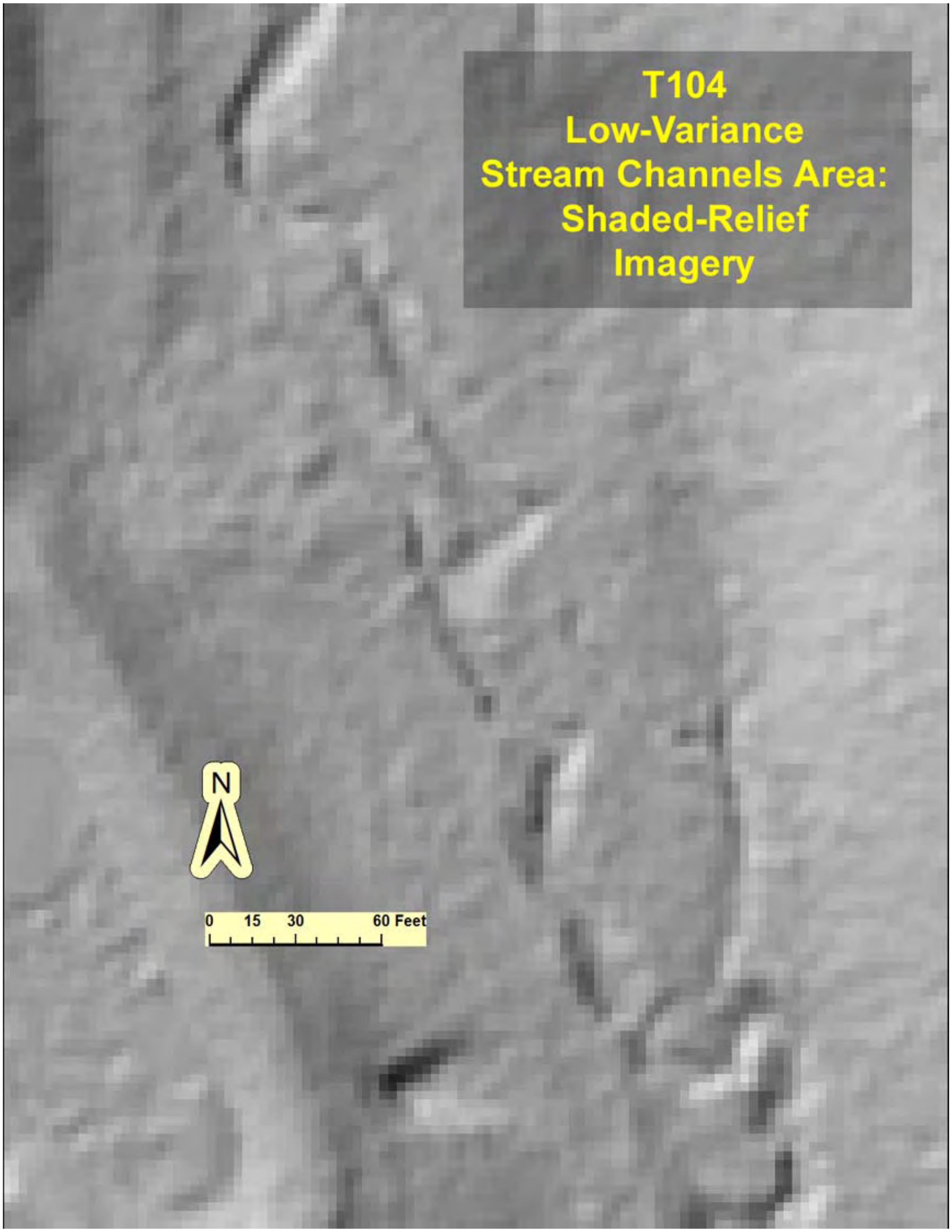

Figure 26: T104 Low-Variance Stream Channel Area Example: 2007 Shaded Relief Imagery - the stream channel is relatively well delineated.

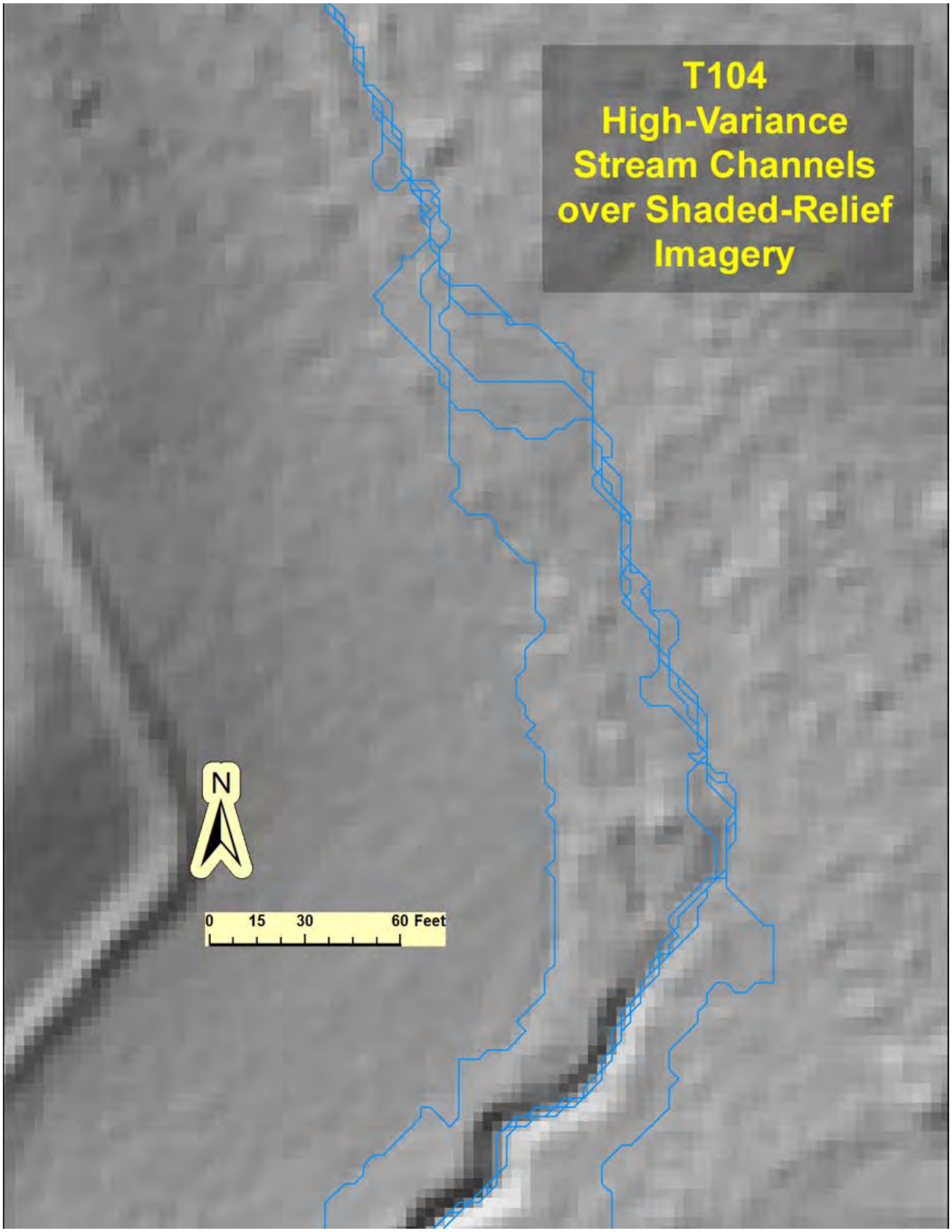

Figure 27: T104 High-Variance Stream Channel Area Example: LiDAR-Derived Stream Channels Overlaid on 2007 Shaded Relief Imagery.

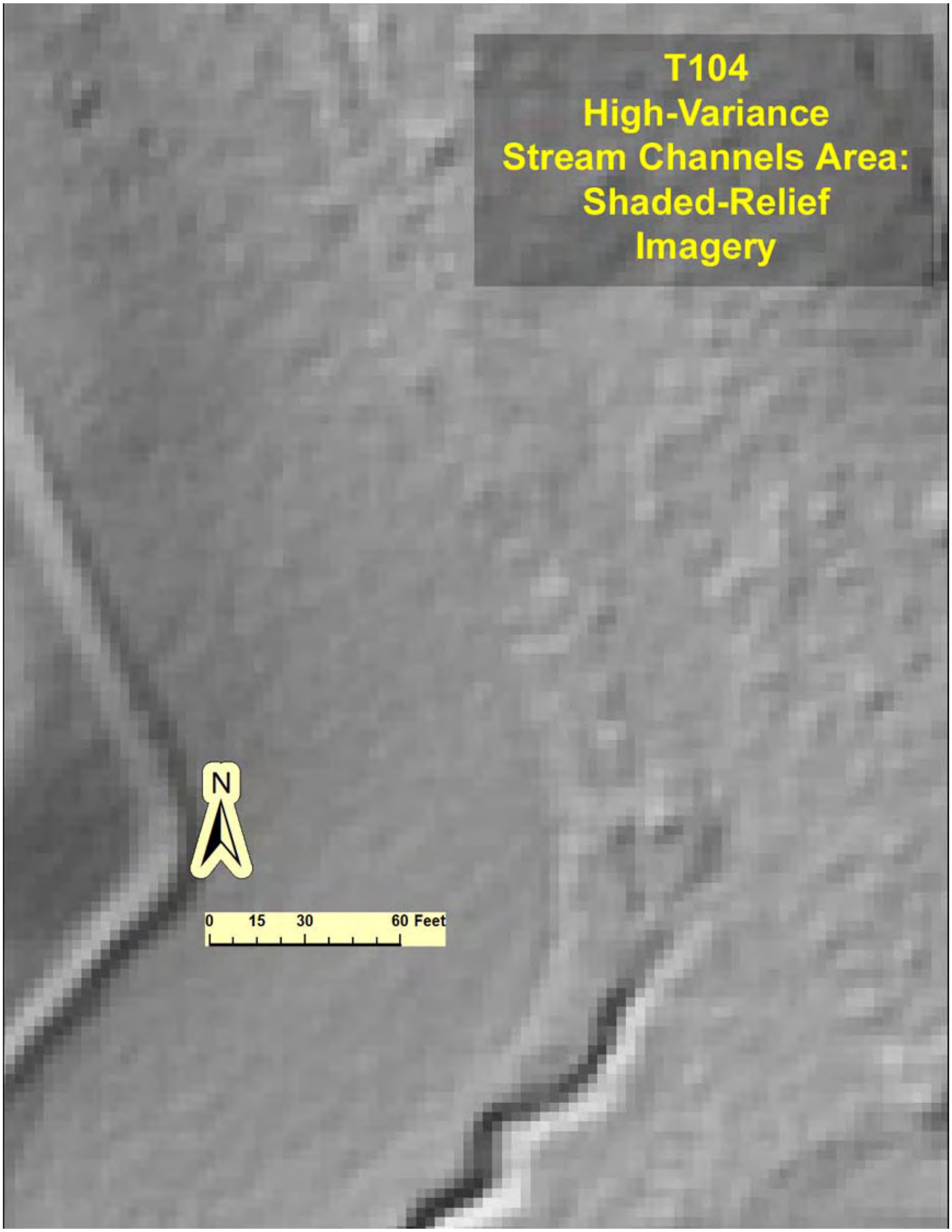

Figure 28: T104 High-Variance Stream Channel Area Example: 2007 Shaded Relief Imagery - the stream channel is relatively not apparent.

The reason for the difference between High vs. Low-Variance Stream Channel Areas is not readily apparent. I tested a number of variables to compare metrics on High vs. Low-Variance Stream Channel Areas (LiDAR Ground Point Density, ratio of LiDAR All Points to Ground Point Density, LiDAR-Derived Elevation Differences, etc.). No general metric provided a significant explanation for the difference between High vs. Low-Variance Stream Channel Areas. LiDAR Ground Point Density appeared to explain the most variance but not to a significant level (Figure 29). Appendix Seven displays some of the metrics calculated.

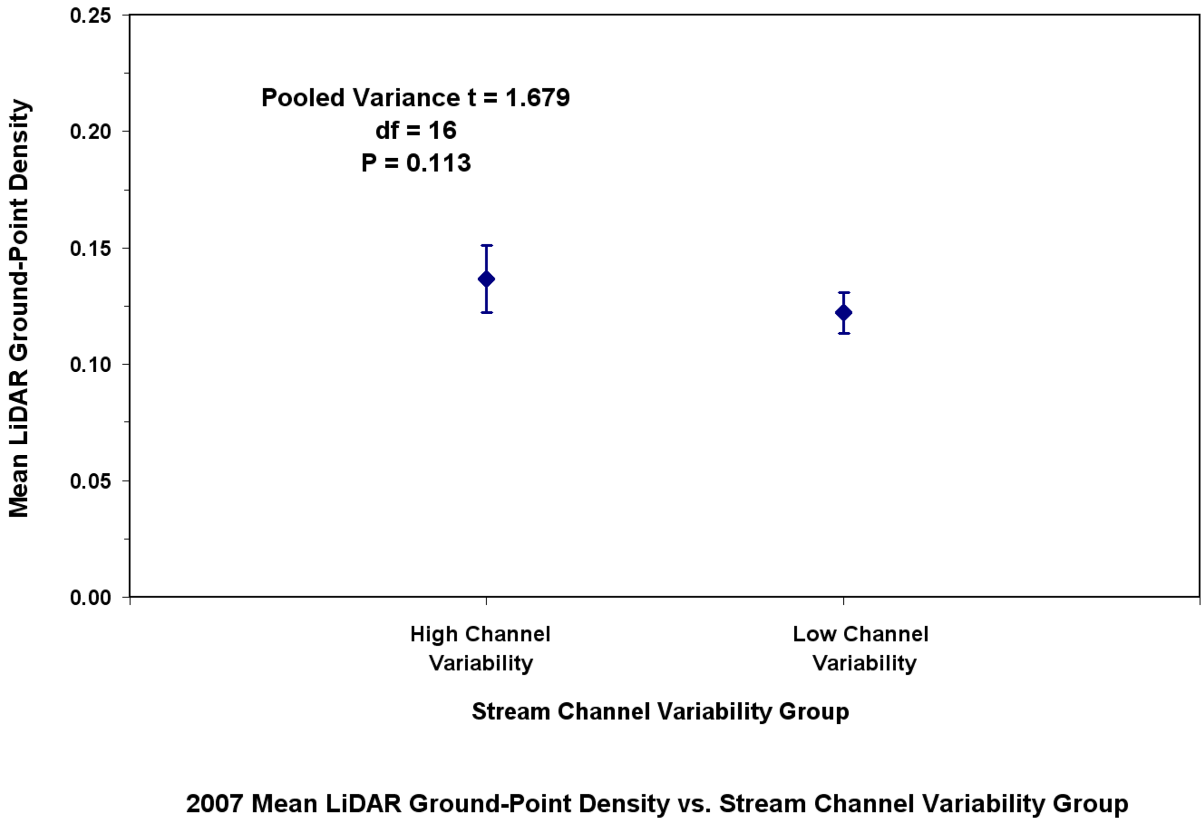


Figure 29: Mean LiDAR Ground Point Density for High vs. Low-Variance Stream Channel Areas.

**Stream Sinuosity**

Stream sinuosity is a measurement of the actual path length of a stream compared to the shortest path length along a given distance. A higher degree of sinuosity measured means a greater degree of meandering along a given distance of stream length. Changes in sinuosity over time can be indicative of changes due to urbanization and using LiDAR to calculate changes in sinuosity could be a useful tool to track streams over time. Rosgen sinuosity measurements (Rosgen, 1994, 1996) were applied to the LiDAR-derived DEM-based flow accumulation stream channels derived from ArcHydro (Maidment, 2002) for the 2002, 2004, 2006, 2007, and 2008 LiDAR coverages. The stream channels were masked to focus on reaches without Barren or Impervious Surfaces within the buffers and stratified by Strahler stream order (tributary networks, Strahler, 1957). The weighted mean average Rosgen sinuosity was measured for Strahler stream orders 1 and 2 for the LiDAR coverages. No clear trend was apparent when comparing T104 and T109 over time (where development had occurred) to Sopers Branch (where no development had occurred). Figure 30 and Table 17 show the Sinuosity over Time.

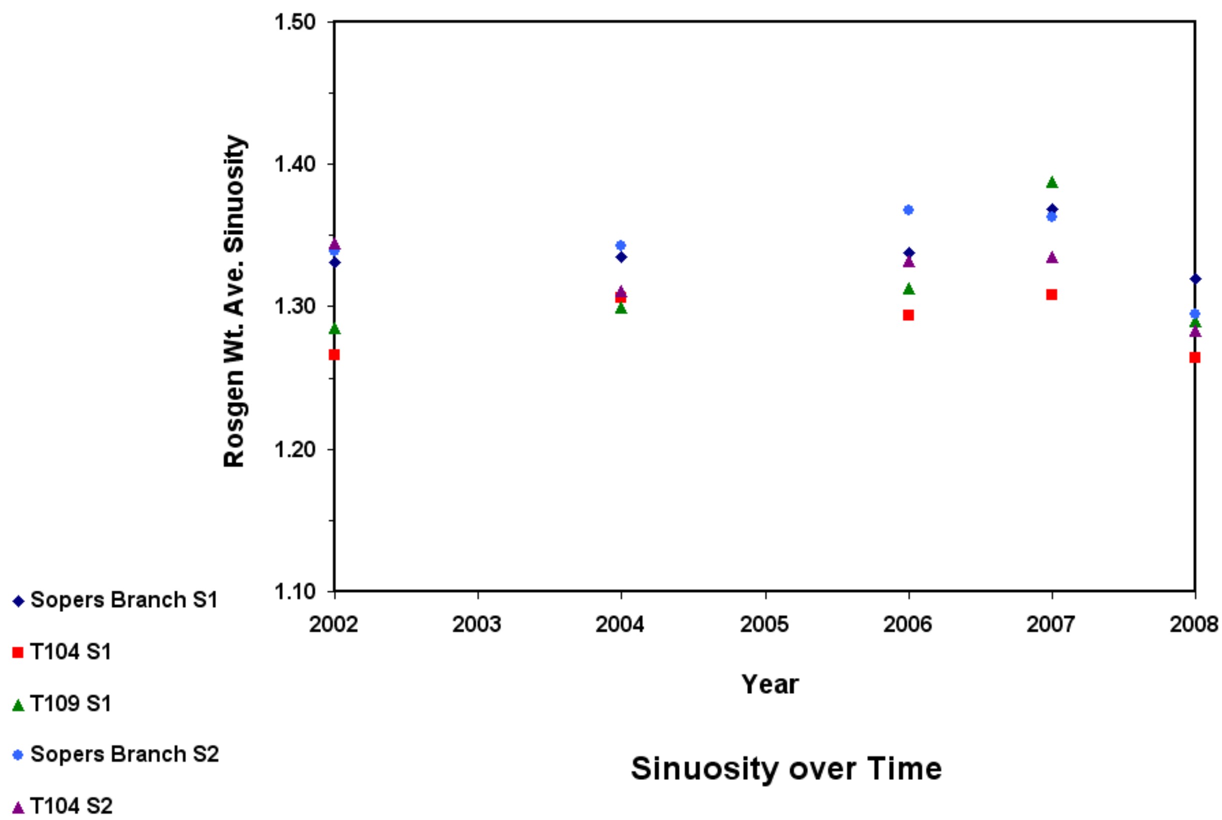


Figure 30: Weighted Mean Average Rosgen Sinuosity over Time for Sopers Branch, T104, and T109 for 2002, 2004, 2006, 2007, and 2008.

| Watershed | Strahler Order | Year | Wt. Avg. Rosgen Sinuosity |
|---|---|---|---|
| Sopers Branch | 1 | 2002 | 1.33 |
| Sopers Branch | 1 | 2004 | 1.34 |
| Sopers Branch | 1 | 2006 | 1.34 |
| Sopers Branch | 1 | 2007 | 1.37 |
| Sopers Branch | 1 | 2008 | 1.32 |
| T104 | 1 | 2002 | 1.27 |
| T104 | 1 | 2004 | 1.31 |
| T104 | 1 | 2006 | 1.29 |
| T104 | 1 | 2007 | 1.31 |
| T109 | 1 | 2008 | 1.26 |
| T109 | 1 | 2002 | 1.28 |
| T109 | 1 | 2004 | 1.30 |
| T109 | 1 | 2006 | 1.31 |
| T109 | 1 | 2007 | 1.39 |
| T109 | 1 | 2008 | 1.29 |
| Sopers Branch | 2 | 2002 | 1.34 |
| Sopers Branch | 2 | 2004 | 1.34 |
| Sopers Branch | 2 | 2006 | 1.37 |
| Sopers Branch | 2 | 2007 | 1.36 |
| Sopers Branch | 2 | 2008 | 1.29 |
| T104 | 2 | 2002 | 1.34 |
| T104 | 2 | 2004 | 1.31 |
| T104 | 2 | 2006 | 1.33 |
| T104 | 2 | 2007 | 1.34 |
| T104 | 2 | 2008 | 1.28 |

Table 17: Weighted Mean Average Rosgen Sinuosity over Time for Sopers Branch, T104, and T109 for 2002, 2004, 2006, 2007, and 2008.

Figures 31 and 32 display the lack of general relationship between the LiDAR-derived sinuosity measurements and increasing flow magnitude (calculated via flow accumulation values) and percent slope gradient.

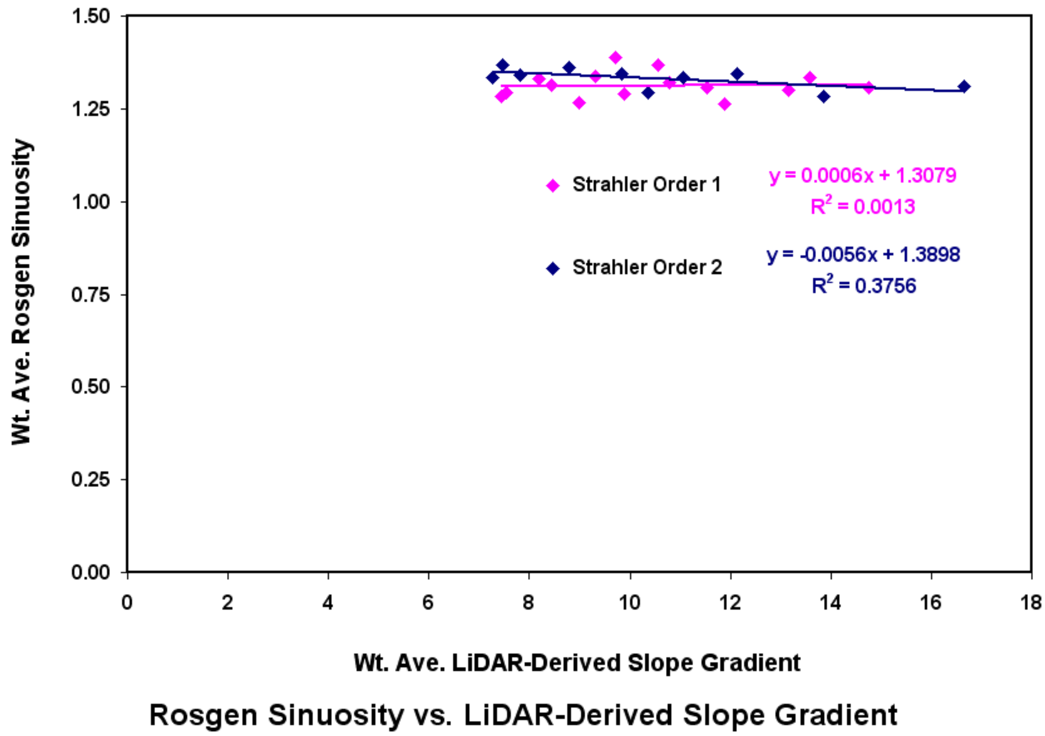


Figure 31: LiDAR-Derived Rosgen Sinuosity vs. LiDAR-Derived Slope Gradient. For 2nd order stream segments, we see a weak declining sinuosity with increasing slope, which would be expected. This relationship did not appear with 1st order stream segments.

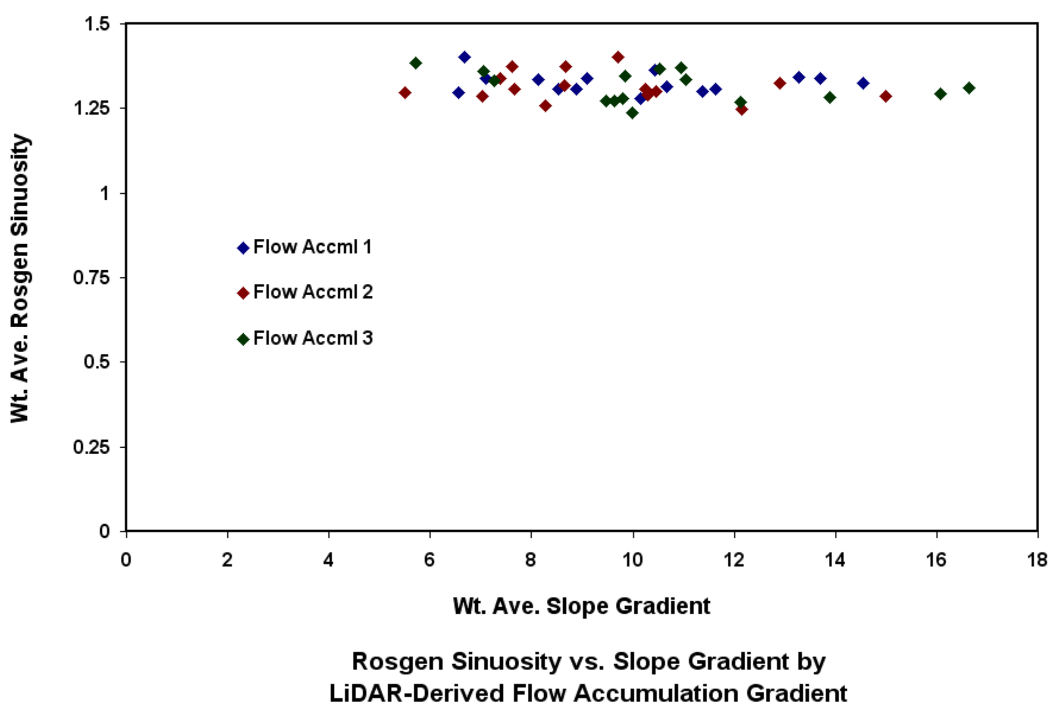


Figure 32: LiDAR-Derived Rosgen Sinuosity vs. LiDAR-Derived Flow Accumulation Gradient.

### LiDAR-Derived DEM Watershed Boundaries Precision

We used the repeat LiDAR-derived 3-foot DEMs for 2002, 2004, 2006, 2007, and 2008 to calculate flow accumulation and place stream channels within the topographic landscape. Using the stream channel pixel closest to the stream gauge location determined via GPS, we calculated the contributing watershed at the gauge pour point. As might be expected from the year-to-year variations in LiDAR-derived stream channels, the pour points used to calculate the catchments in ArcHydro varied somewhat from year-to-year as well. Figures 33-35 display the variations seen in pour point placement for the five years of LiDAR data.

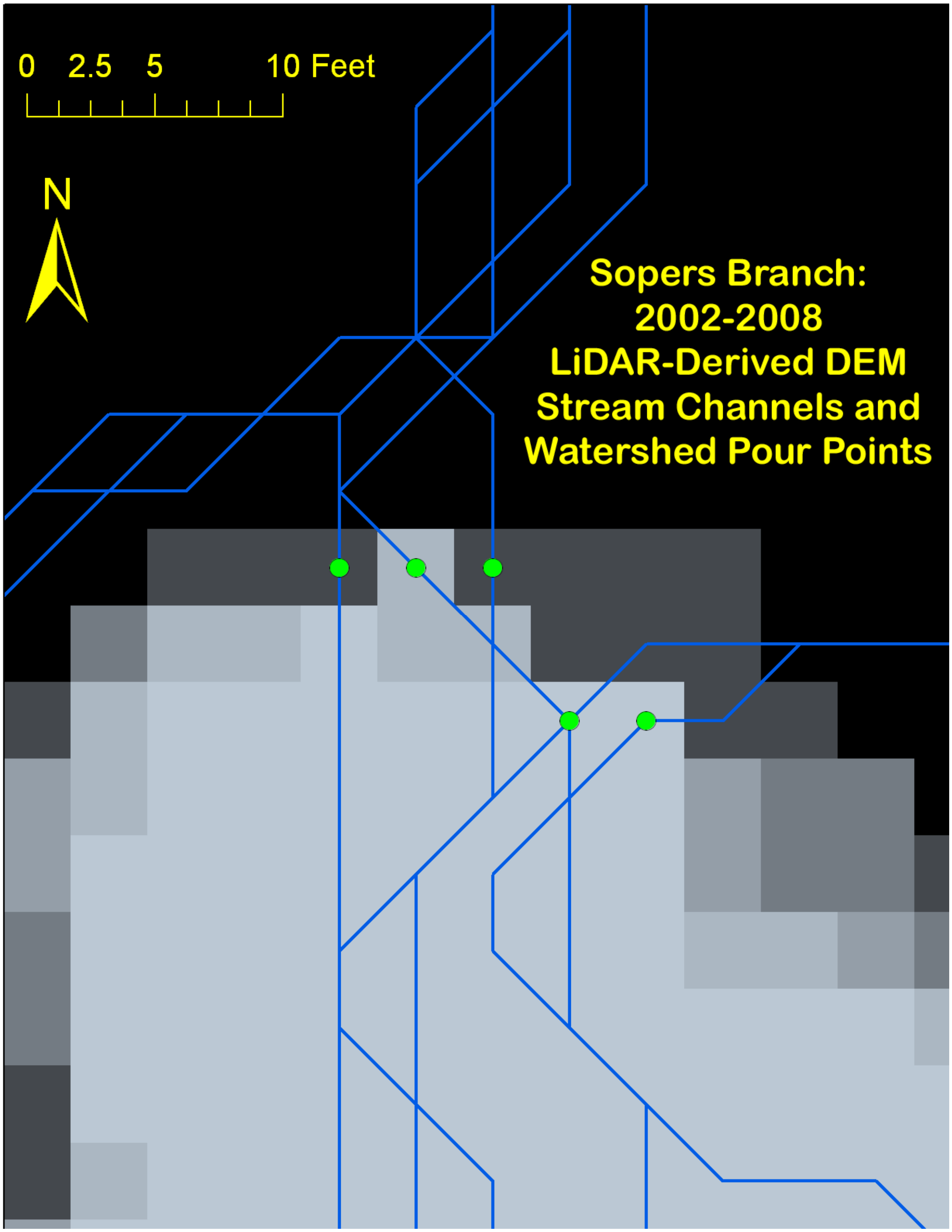

Figure 33: LiDAR-Derived 3-foot DEM Stream Channels and Watershed Pour Points for 2002, 2004, 2006, 2007, and 2008 for Sopers Branch. The gray shaded pixels reveal the number of years a particular pixel was included in the watershed defined by the DEM pour point: lighter gray = more included.

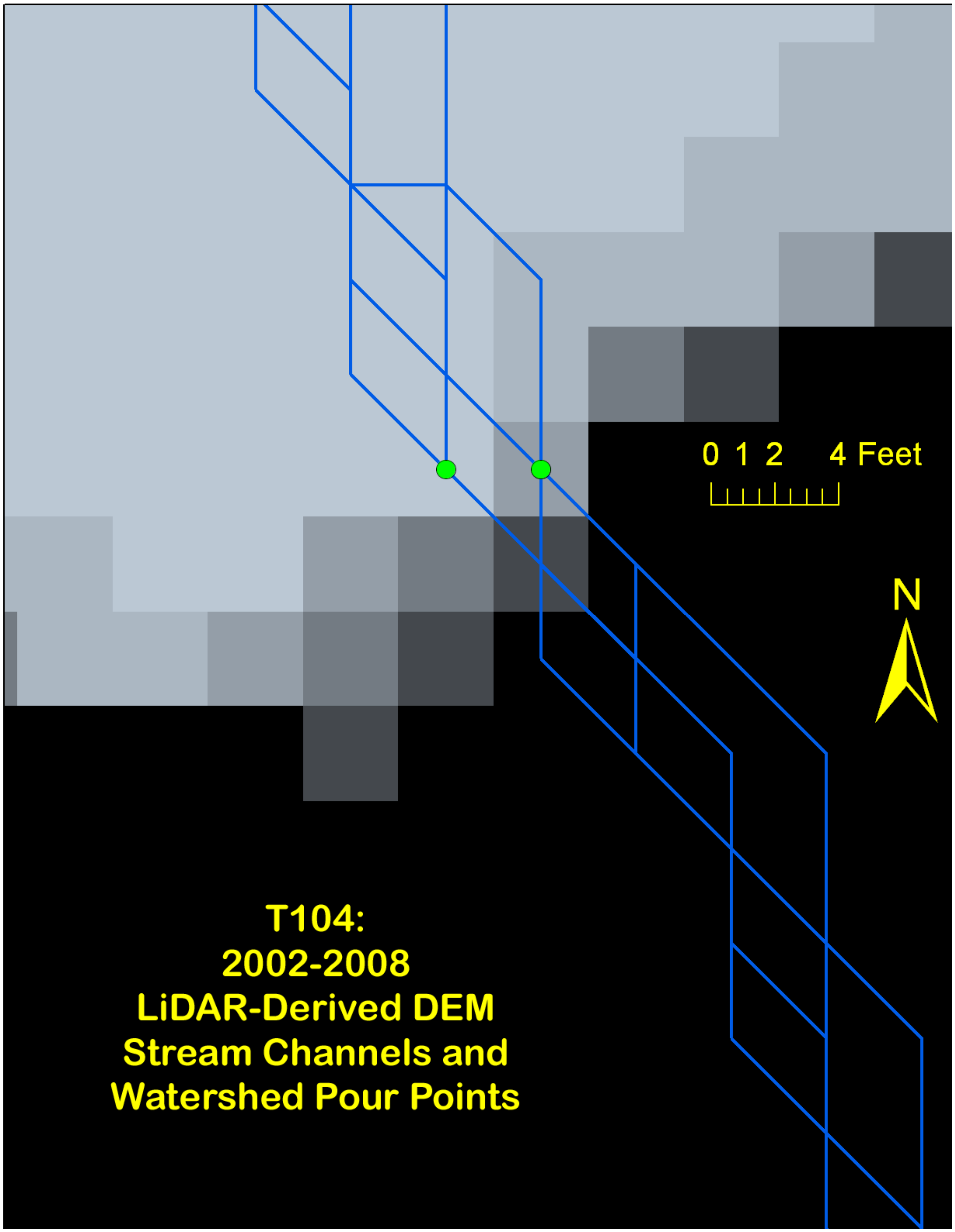

Figure 34: LiDAR-Derived 3-foot DEM Stream Channels and Watershed Pour Points for 2002, 2004, 2006, 2007, and 2008 for T104. The gray shaded pixels reveal the number of years a particular pixel was included in the watershed defined by the DEM pour point: lighter gray = more included.

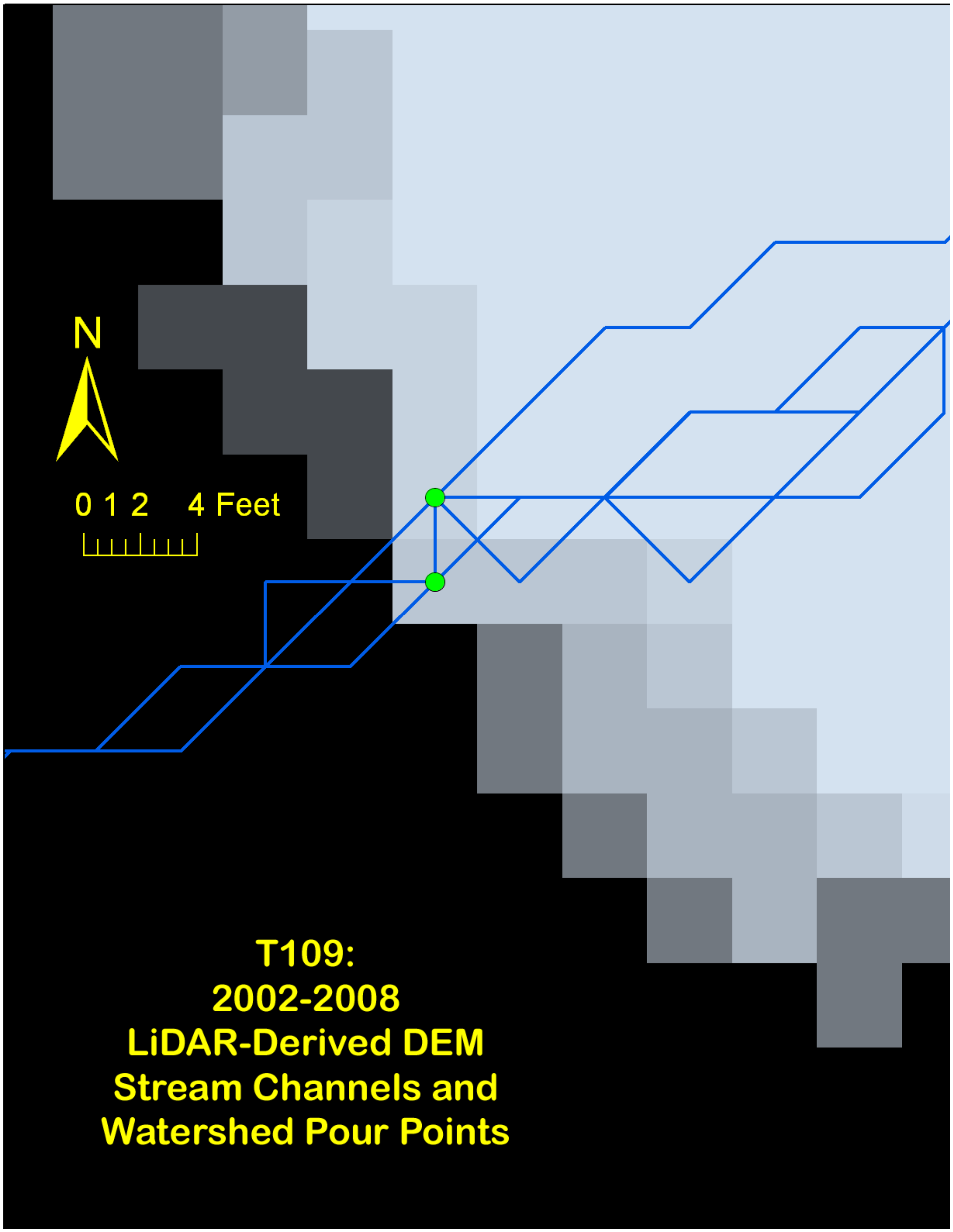


Figure 35: LiDAR-Derived 3-foot DEM Stream Channels and Watershed Pour Points for 2002, 2004, 2006, 2007, and 2008 for T109. The gray shaded pixels reveal the number of years a particular pixel was included in the watershed defined by the DEM pour point: lighter gray = more included.

The differences in the LiDAR-derived DEM pour points combine with the differences in LiDAR derived elevations across the landscape to produce LiDAR-derived watersheds that vary from year-to-year.  Figures 36-38 display the watersheds derived from the LiDAR coverages.

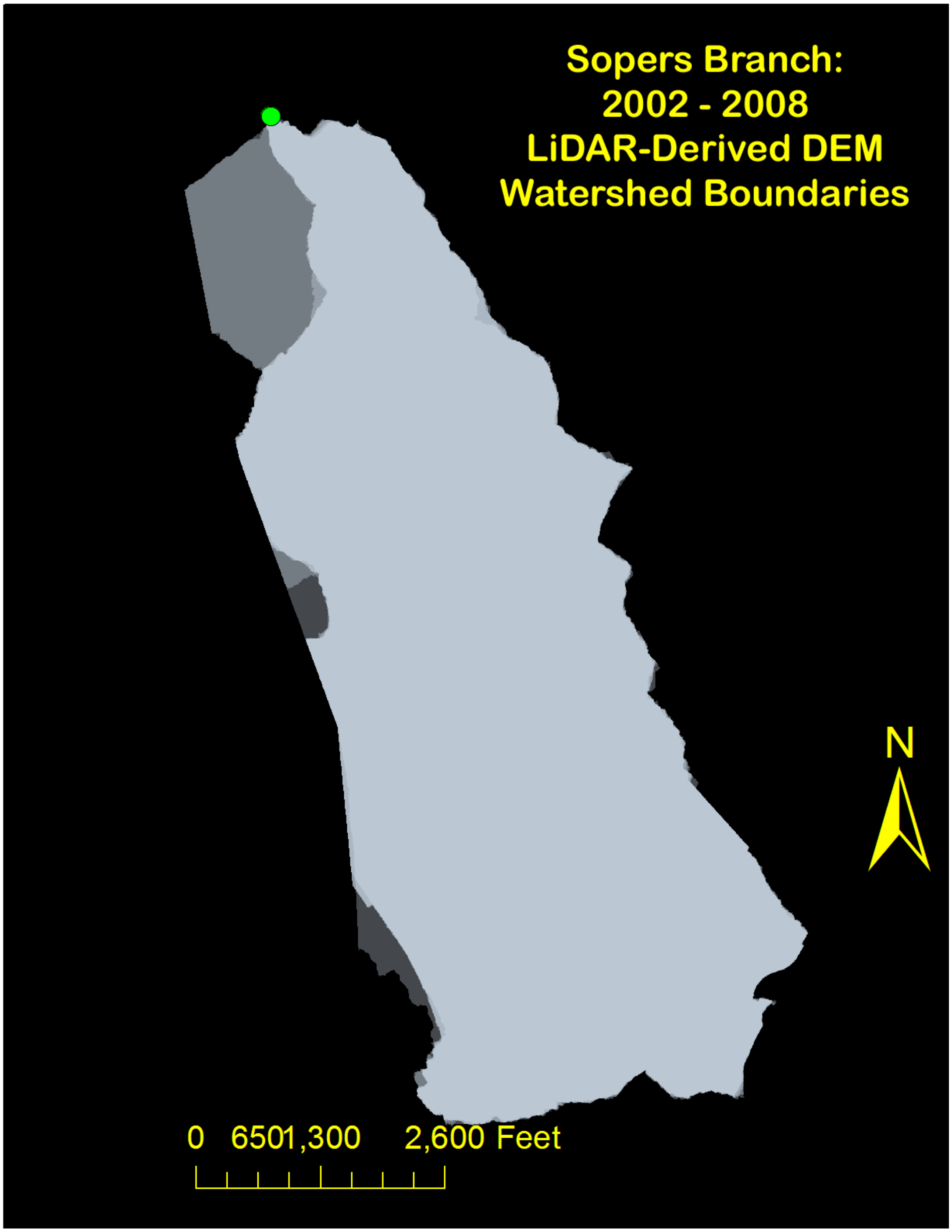


Figure 36: 2002, 2004, 2006, 2007, and 2008 LiDAR-Derived DEM Watershed Boundaries for Sopers Branch.  The gray shaded pixels reveal the number of years a particular pixel was included in the watershed defined by the DEM pour point: lighter gray = more included.

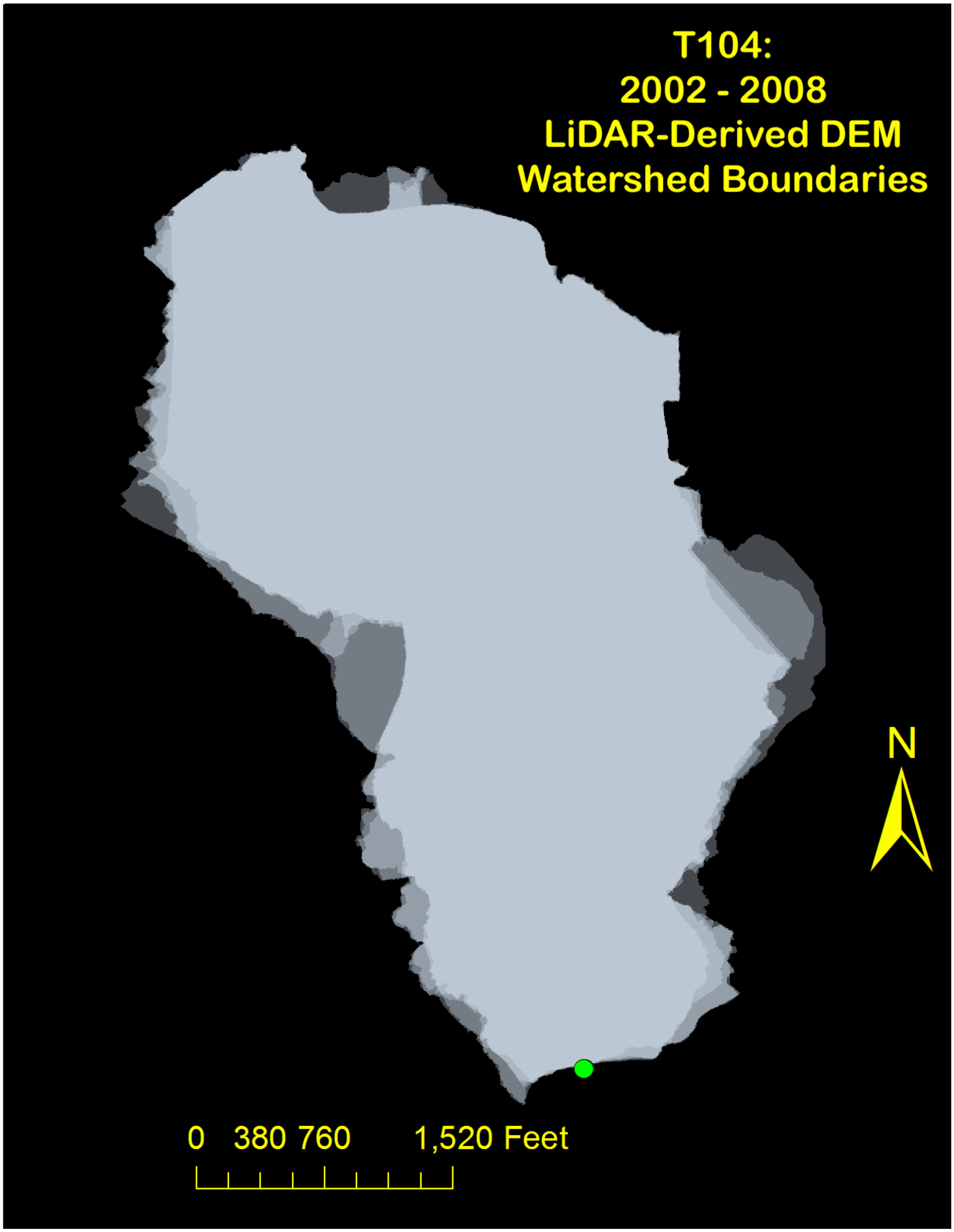

Figure 37: 2002, 2004, 2006, 2007, and 2008 LiDAR-Derived DEM Watershed Boundaries for T104. The gray shaded pixels reveal the number of years a particular pixel was included in the watershed defined by the DEM pour point: lighter gray = more included.

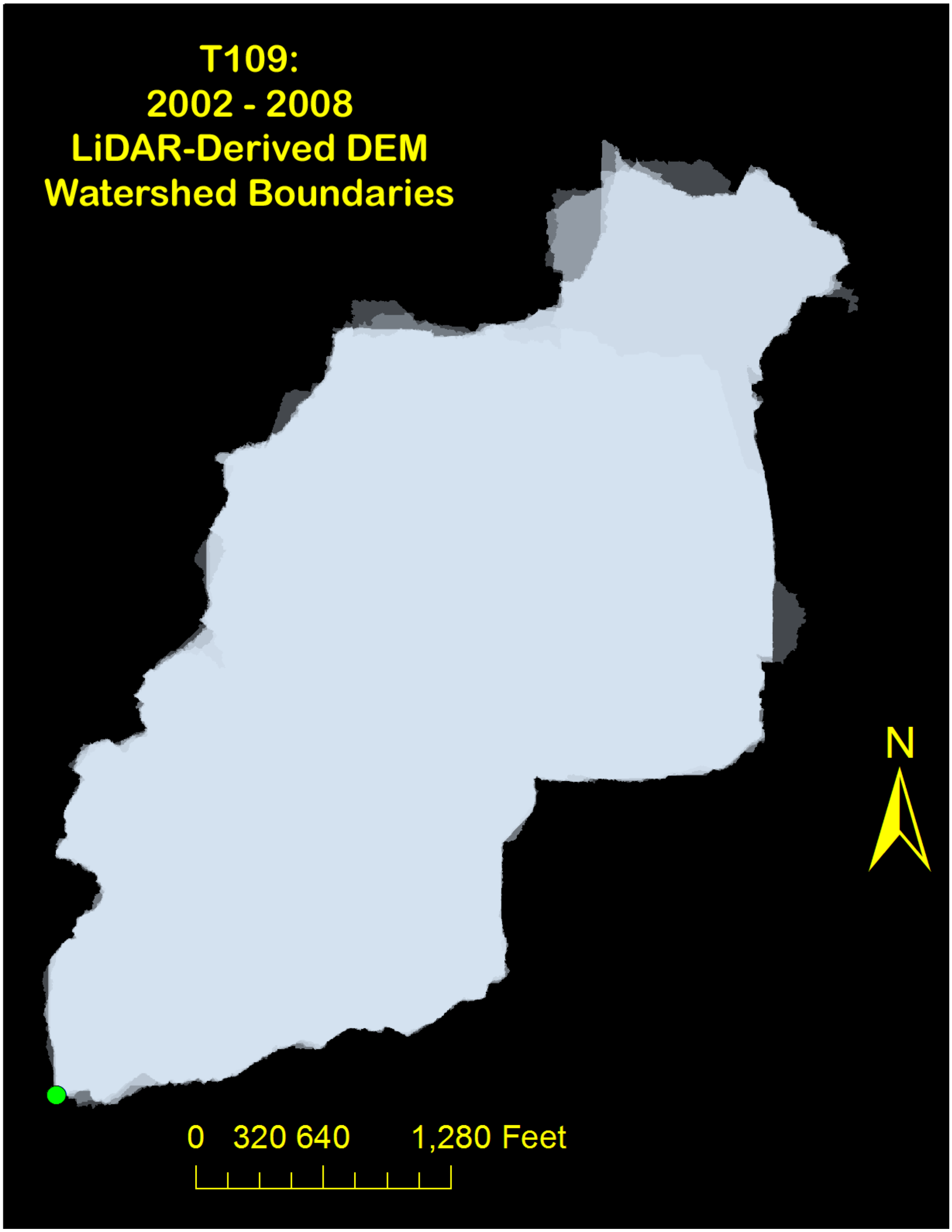


Figure 38: 2002, 2004, 2006, 2007, and 2008 LiDAR-Derived DEM Watershed Boundaries for T109. The gray shaded pixels reveal the number of years a particular pixel was included in the watershed defined by the DEM pour point: lighter gray = more included.

The LiDAR-derived elevation differences are largely restricted to edge-effects in the year-to-year watershed boundaries. The large section in the NW of Sopers Branch is an anomaly produced in part by the lack of sufficient LiDAR coverage in the 2002 and 2004 LiDAR overflights on the west side of the watershed and the 2006 LiDAR coverage had some quality control issues (dropouts) in the NW corner that also affected the area included in the watershed or not. In both T104 and T109, urban development also affected the area included in the watershed or not. Table 17 shows the absolute percentage difference between subsequent years in LiDAR coverages. Figure 39 shows the 2007-2008 watershed difference in T109, with the section of the watershed in red being present in the contributing DEM-shed in 2007 but not in 2008. This occurred as a result of construction in the upper watershed and an east-west road (and elevated grade associated with the road) that cuts off that portion of the watershed from the pour point. In reality, culverts and the anthropogenic drainage patterns associated with the road construction may still hydraulically link the upper portion of the watershed to the remainder but this cannot be determined from the LiDAR coverages.

| Watershed | Years Compared | Relative Percent Change Area |
|---|---|---|
| T104 | 2002-2004 | 1.35 |
| T104 | 2004-2006 | 2.41 |
| T104 | 2006-2007 | 0.74 |
| T104 | 2007-2008 | 2.37 |
| T109 | 2002-2004 | 0.09 |
| T109 | 2004-2006 | 1.05 |
| T109 | 2006-2007 | 1.43 |
| T109 | 2007-2008 | 12.06 |

Table 18: Watershed Area Percent Differences based on LiDAR-Derived DEMs for 2002, 2004, 2006, 2007, and 2008 in T104 and T109.

Appendix Eight shows the year-to-year differences in watersheds calculated from subsequent years of LiDAR coverages.

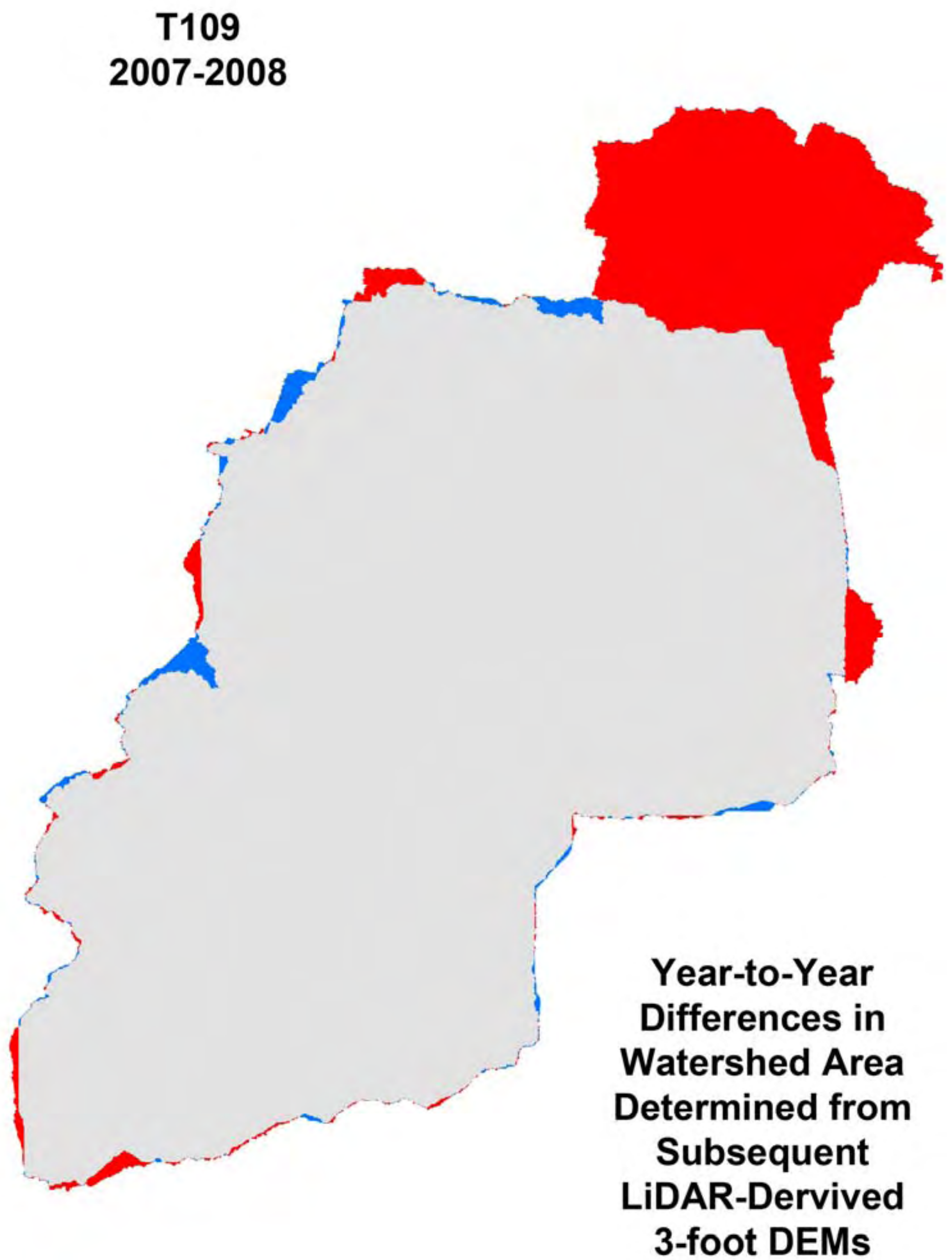


Figure 39: 2007-2008 watershed difference in T109, with the section of the watershed in red being present in the contributing DEM-shed in 2007 but not in 2008. Gray = Area Present in both coverages; Red = Area Present in Year 1 but not Year 2; Blue = Area Present in Year 2 but not Year 1.

**Discussion**

Previous studies of LiDAR accuracy (Hodgson and Bresnahan, 2004; Hodgson et al., 2005; Gardina, 2008) have shown that there are several factors that affect the accuracy of LiDAR-derived elevations: internal errors within the LiDAR system, processing errors within the LiDAR algorithms (determining which points in the All-Data cloud are Ground and which are not), interpolation errors between LiDAR points, error in placement of ground control points (ground-truth), LiDAR point variation, slope of the surface being measured, and vegetation (land cover). Fowler (2000, 2001) stressed that there are physical limits on the ability of airborne LiDAR pulses to capture data based upon aircraft flying height, LiDAR impulse wavelength, GPS limitations, etc. There is therefore a physical limit beyond which airborne LiDAR cannot resolve. Fowler determined that the best you could achieve with airborne LiDAR under optimal conditions was about ± 0.5 foot. Additional errors due to system processing error compounded by vegetative conditions, slope, land cover, etc. all would cause actual accuracy to be less than optimal.

Internal errors within the LiDAR system and data processing errors are beyond the ability of the typical LiDAR user to know or control but knowledge and quantification of the ground-based sources of error in LiDAR-derived elevations could help the typical LiDAR user understand the abilities and limitations of the data. Gardina (2008) looked at the 2002 and 2006 LiDAR coverages in the CSPA and used the same ground truth data as used in this project. He determined that up to 75% of the overall error in LiDAR-derived elevations was due to internal system error in the LiDAR data.

In our study, the results obtained in Part 1 (LiDAR accuracy and precision assessment using ground truth measurements) confirmed the previously reported sources of LiDAR error. Both increasing slope of the surface being imaged and increasing density of surface and overhanging vegetation had a negative effect on the accuracy of the LiDAR data. The year-to-year precision of LiDAR-derived stream transects was surprisingly poor considering the overall measured accuracy of individual LiDAR points. The user of LiDAR needs to remember that comparing multi-year LiDAR coverages in streambeds combines the worst of all error conditions. The near-stream and in-stream conditions of high slope, narrow streambeds (which increase the difficulty in resolving topography with a limited LiDAR point density), and increased near-stream and in-stream vegetation all combine to create an uncertain LiDAR-derived elevation surface used to delineate stream channels. Comparing multiple years of these coverages increases the error when computing changes. Given the limitations of LiDAR-derived DEM-based stream channels revealed in this study, the LiDAR user is advised to use LiDAR-indicated areas of stream channel change with a grain of salt and a dash of skepticism. LiDAR did show a weak association with the stream transects ground truth (Figure 11 and Table 7). Airborne LiDAR may be useful to identify areas where ground surveys should be conducted to verify the LiDAR-derived results. Hand-held, ground-based LiDAR may be a good method of measuring stream channel change and the use of raw LiDAR data (rather than the LiDAR-derived DEMs) may also improve year-to-year comparative accuracy and precision.

The results in Part 2 (LiDAR precision assessment using multi-year LiDAR coverages where no ground truth measurements exist) were also less clear than I had hoped. LiDAR is clearly useful in mapping large-scale changes in topography that result along with urban development. LiDAR-derived elevations in forested areas appear to have less accuracy/precision that those in more open areas studied (agricultural, impervious surfaces, and urban cultivated grasses).

When looking at LiDAR-derived DEM precision by slope gradient by LULC, the results were also less than clear. The largest slope-percent quintile typically displayed increased error but the first few quintiles typically did not. The Forest LULC class, particularly in Sopers Branch, showed the least difference in elevation between slope-percent quintiles. Sopers Branch is the largest watershed and the most forested and would have the greatest range of forested slope gradients compared to T104 and T109 where the forested areas were typically found in the riparian areas. I believe that within-group vegetation variability within the Forested land cover class is so high that it overwhelms the slope gradient/LiDAR accuracy relationship. Both of the "OK" and "Bad" vegetation classes delineated in the ground-truth portion of the study (Appendix Nine) would be included in the general land cover class of "Forest". I believe that the near-ground impact of vegetation condition is larger than the general LULC impact on predicting LiDAR accuracy/precision. This limits the use of LULC as a filter for predicting LiDAR accuracy/precision to a first-order estimator. For the LULC classes representing more open areas (Agricultural, Impervious Surfaces, and Cultivated Urban Grasses), using LULC as a filter to predict relative LiDAR accuracy/precision appears more justified.

The variability in stream channel placement using LiDAR-derived DEMs to predict stream channels using ArcHydro flow accumulation algorithms led to highly variable stream channel locations and these impacted the watershed boundaries and areas computed to a much greater extent that I would have predicted at the start of this study. Particularly disturbing to people attempting to model watershed hydrology was the variability in watershed area derived from year-to-year LiDAR coverages. The results of this study should be taken as a warning to watershed modelers and managers that watershed boundaries and areas may not be nearly so certain as one might otherwise assume. The final conclusion of this study is that a user of LiDAR who attempts to delineate changes at or near to the spatial level of resolution of the base data (about 1 meter or 3 feet in our study) cannot rely on LiDAR alone to assess those changes. Ground truth is needed to verify changes predicted by repeat LiDAR measurements. The loose relationship seen by the LiDAR transects and ground-truth transects (Figure 11) should act as a warning to the LiDAR user: Use LiDAR to identify where change appears to have occurred and then use ground -truth to verify.

Further research would be useful to determine if the use of raw data LiDAR-derived surfaces to look for stream channel change would improve the accuracy and utility of year-to-year geomorphologic assessments of stream channel change compare to the DEM-based comparisons studied in this report.

## References


Caraco, D., R. Claytor, P. Hinkel, H. Y. Kwon, T. Schueler, C. Swann, S. Vysotsky, and J. Zielinske. 1998. Rapid Watershed Planning Handbook. Center for Watershed Protection, Ellicott City, Maryland.

Fowler, R. A. 2000. The Lowdown on Lidar. Earth Observation Magazine (EOM) 9(3): 27–30.

Fowler, R. A. 2001. The thorny problem of LIDAR Specifications. Earth Observation Magazine (EOM) 10(4): 25-28.

Gardina, V. J. 2008. Analysis Of Lidar Data For Fluvial Geomorphic Change Detection At A Small Maryland Stream. Master of Science Thesis, University of Maryland, College Park MD.

Hodgson, M. E. and P. Bresnahan. 2004. Accuracy of Airborne Lidar-Derived Elevation: Empirical Assessment and Error Budget. Photogrammetric Engineering & Remote Sensing 70(3): 331-339.

Hodgson, M. E., J. Jensen, G. Raber, J. Tullis, B. A. Davis, G. Thompson, and K. Schuckman. 2005. An evaluation of Lidar-derived elevation and terrain slope in leaf-off conditions. Photogrammetric Engineering & Remote Sensing 71(7): 817-824.

Jarnagin, S. T. 2007. Historical analysis of the relationship of streamflow flashiness with population density, imperviousness, and percent urban land cover in the Mid-Atlantic region. Internal Report APM 408. United States Environmental Protection Agency, Office of Research and Development, Environmental Photographic Interpretation Center (EPIC), Reston VA, September 2007, EPA/600/X-07/021, 100p.

Jarnagin, S. T. 2004. Regional and Global Patterns of Population, Land Use, and Land Cover Change: An Overview of Stressors and Impacts. GIScience & Remote Sensing 41(3): 207-227.

Jennings, D. B. and S. T. Jarnagin. 2002. Changes in anthropogenic impervious surfaces, precipitation and daily streamflow discharge: a historical perspective in a mid-Atlantic subwatershed. Landscape Ecology 17(5): 471-489.

Maidment, D. R. (Editor) 2002. Arc Hydro: GIS for Water Resources. ESRI Press, Redlands CA.

Maune, D. F. (Editor) 2001. Digital Elevation Model Technologies and Applications: The Dem Users Manual. ASPRS Publications, Bethesda, MD. ISBN: 1570830649 / 978-1-5708306-4-8 / 1-57083-064-9.

Rosgen, D. L. 1994. A Stream Classification System. Catena, 22 169199. Elsevier Science, Amsterdam, Netherlands.

Rosgen, D. L.  1996.  Applied River Morphology. 2nd ed.  Wildland Hydrology, Fort Collins, CO.  ISBN: 978-0-9653289-0-6.

Schueler T. R.  1994.  The Importance of Imperviousness.  Watershed Protection Techniques 1(3): 100-111.

Strahler, A. N.  1957.  Quantitative analysis of watershed geomorphology.  Transactions of the American Geophysical Union 8(6): 913–920.

USEPA.  1994.  The Quality of Our Nation's Water: 1992.  United States Environmental Protection Agency, EPA-841-S-94-002, Washington, D.C., USEPA, Office of Water.

## Appendices

Appendix One: Year-by-year mean absolute accuracy by slope quintile for ground control survey points (n = 604). These data are noisier than the sum of years but show the same general trend: increasing accuracy with lower slope.

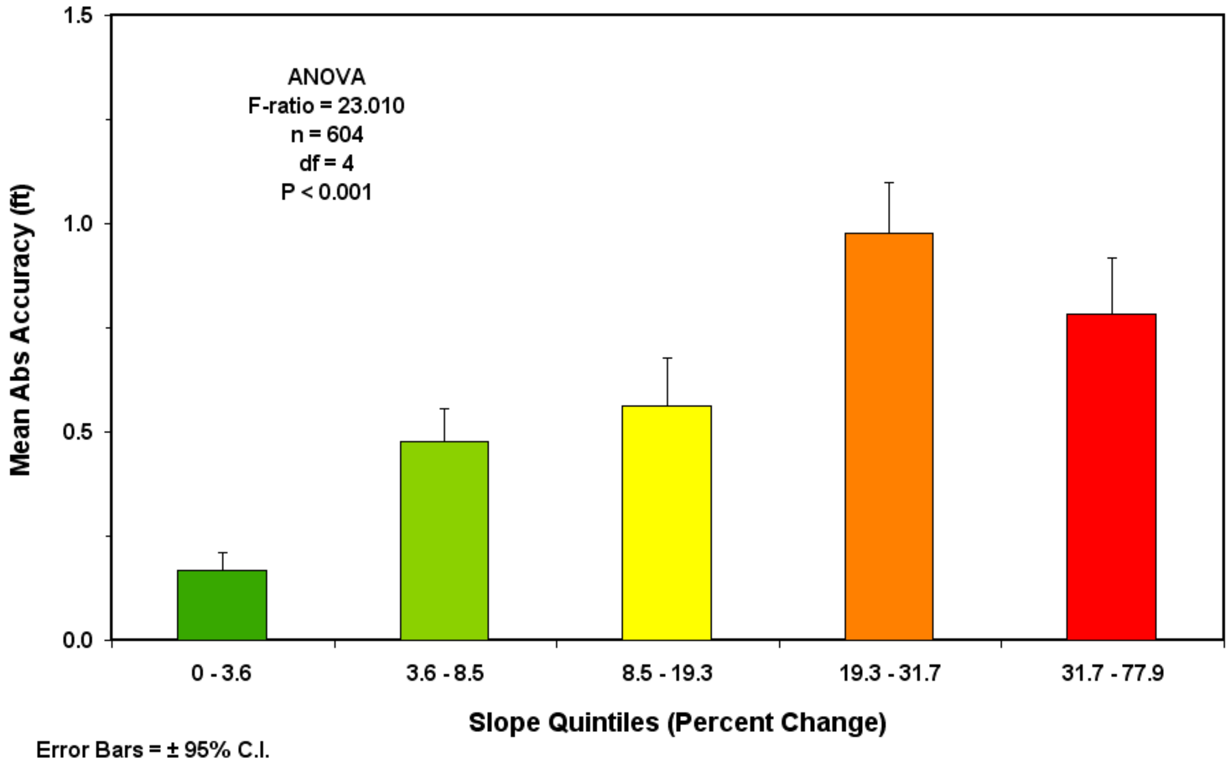

2002 Mean Absolute Accuracy by Slope Quintile

| Slope Quintiles | Mean 2002 Accuracy | n | stdev | ± 95% C.I. |
|---|---|---|---|---|
| 0 - 3.6 | 0.17 | 116 | 0.23 | 0.04 |
| 3.6 - 8.5 | 0.48 | 123 | 0.44 | 0.08 |
| 8.5 - 19.3 | 0.56 | 121 | 0.65 | 0.12 |
| 19.3 - 31.7 | 0.98 | 122 | 0.68 | 0.12 |
| 31.7 - 77.9 | 0.78 | 122 | 0.76 | 0.13 |

I

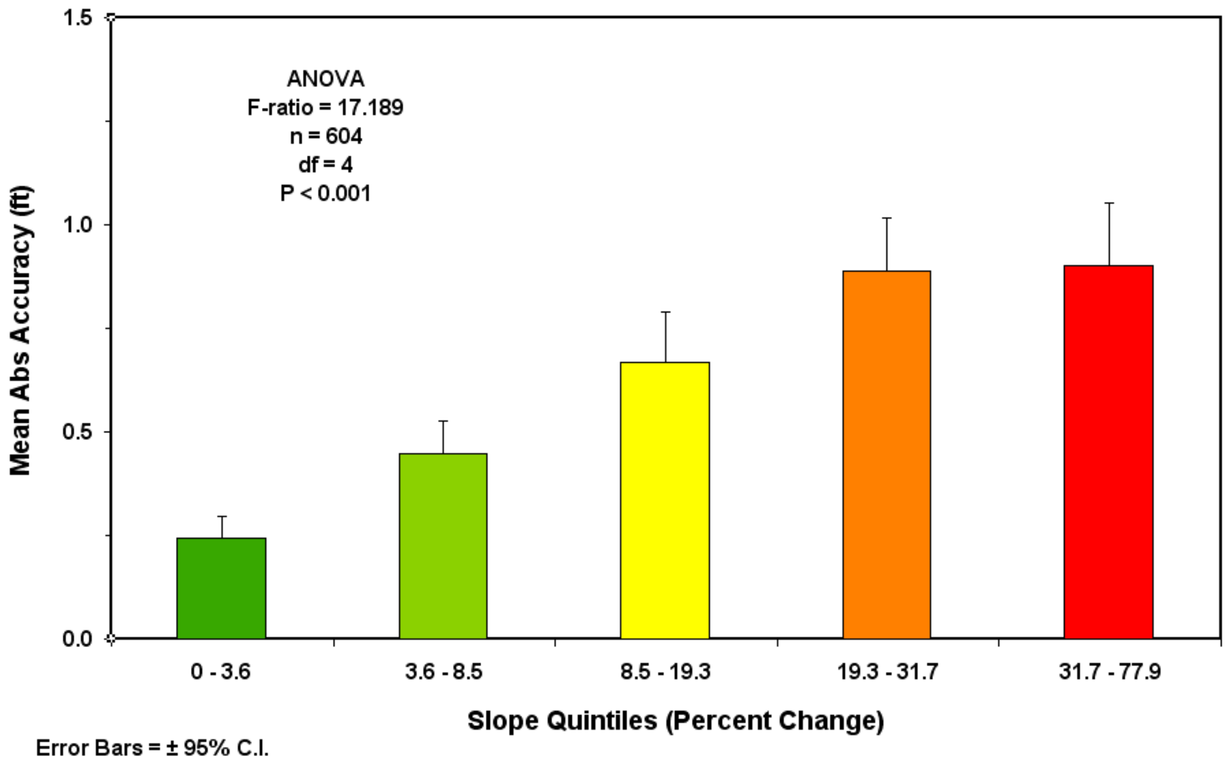


**2004 Mean Absolute Accuracy by Slope Quintile**

| Slope Quintiles | Mean 2004 Accuracy | n | stdev | ± 95% C.I. |
|---|---|---|---|---|
| **0 - 3.6** | **0.24** | **116** | **0.29** | **0.05** |
| **3.6 - 8.5** | **0.45** | **123** | **0.44** | **0.08** |
| **8.5 - 19.3** | **0.67** | **121** | **0.69** | **0.12** |
| **19.3 - 31.7** | **0.89** | **122** | **0.72** | **0.13** |
| **31.7 - 77.9** | **0.90** | **122** | **0.84** | **0.15** |

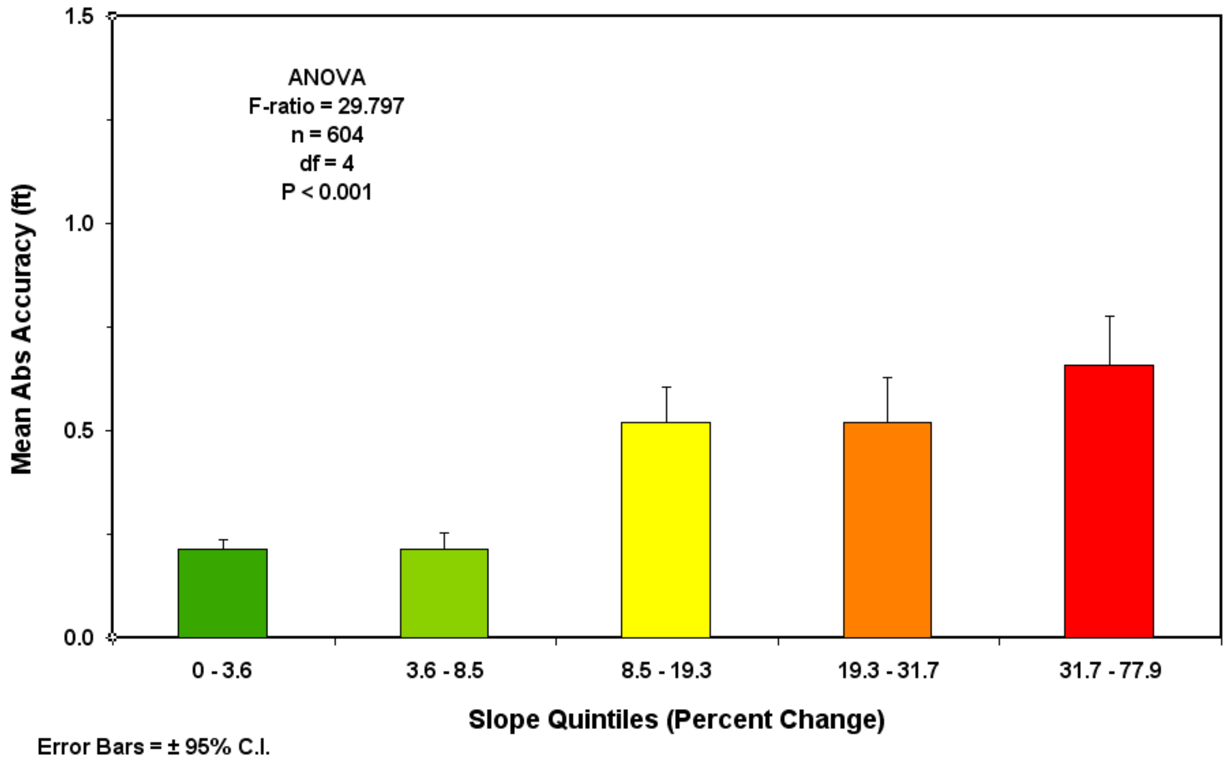


**2006 Mean Absolute Accuracy by Slope Quintile**

| Slope Quintiles | Mean 2006 Accuracy | n | stdev | ± 95% C.I. |
|---|---|---|---|---|
| **0 - 3.6** | **0.21** | **116** | **0.13** | **0.02** |
| **3.6 - 8.5** | **0.21** | **123** | **0.22** | **0.04** |
| **8.5 - 19.3** | **0.52** | **121** | **0.49** | **0.09** |
| **19.3 - 31.7** | **0.52** | **122** | **0.61** | **0.11** |
| **31.7 - 77.9** | **0.66** | **122** | **0.66** | **0.12** |

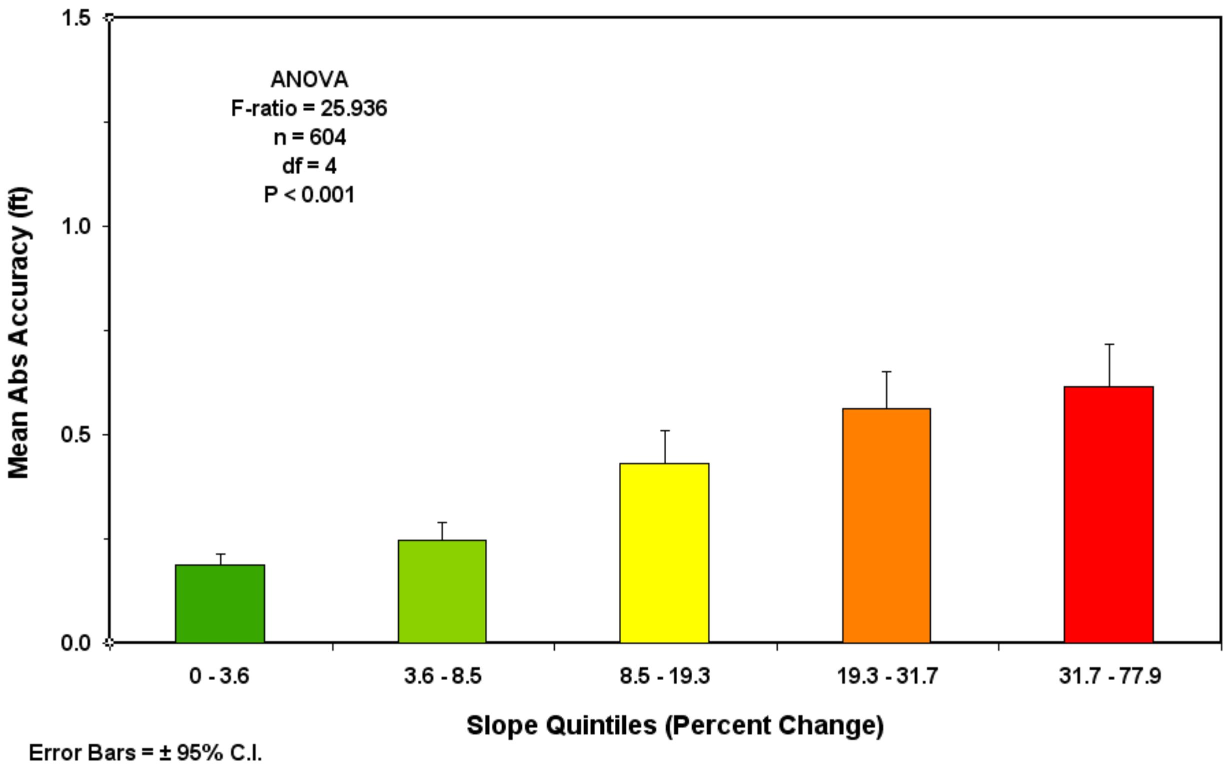


2007 Mean Absolute Accuracy by Slope Quintile

| Slope Quintiles | Mean 2007 Accuracy | n | stdev | ± 95% C.I. |
|---|---|---|---|---|
| 0 - 3.6 | 0.19 | 116 | 0.15 | 0.03 |
| 3.6 - 8.5 | 0.25 | 123 | 0.24 | 0.04 |
| 8.5 - 19.3 | 0.43 | 121 | 0.45 | 0.08 |
| 19.3 - 31.7 | 0.56 | 122 | 0.49 | 0.09 |
| 31.7 - 77.9 | 0.61 | 122 | 0.58 | 0.10 |

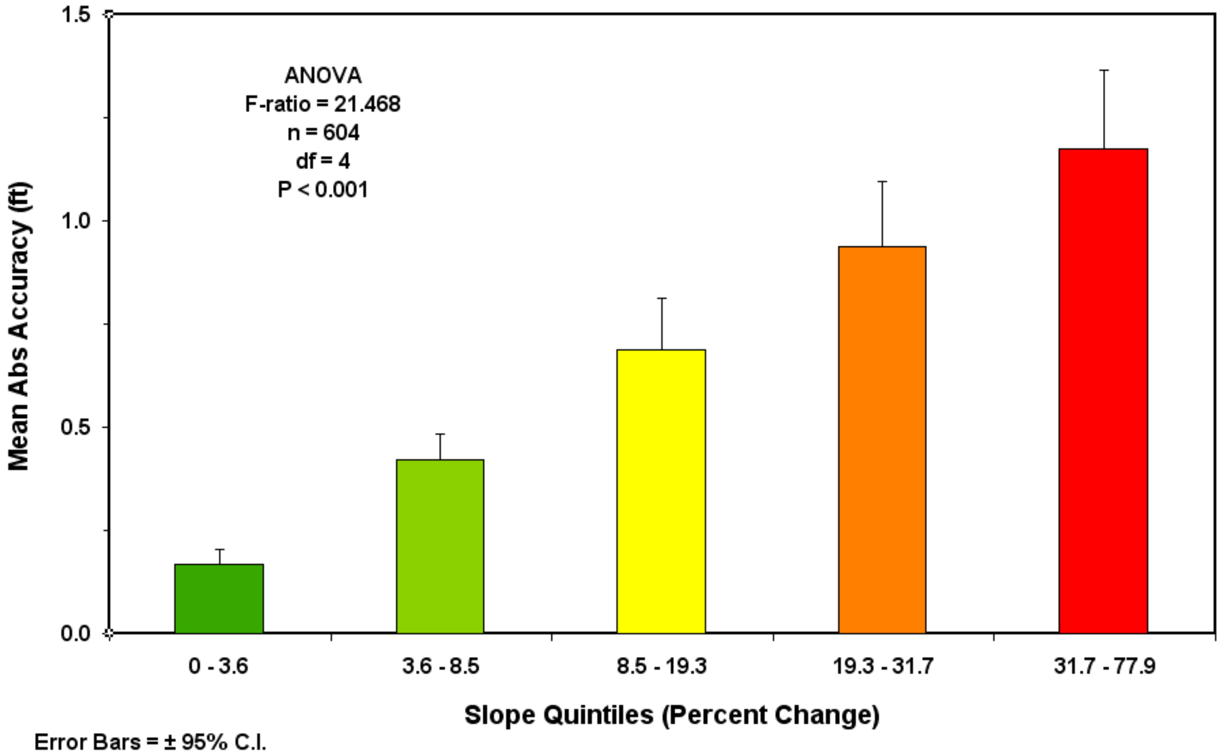


2008 Mean Absolute Accuracy by Slope Quintile

| Slope Quintiles | Mean 2008 Accuracy | n | stdev | ± 95% C.I. |
|---|---|---|---|---|
| 0 - 3.6 | 0.17 | 116 | 0.21 | 0.04 |
| 3.6 - 8.5 | 0.42 | 123 | 0.35 | 0.06 |
| 8.5 - 19.3 | 0.69 | 121 | 0.71 | 0.13 |
| 19.3 - 31.7 | 0.94 | 122 | 0.89 | 0.16 |
| 31.7 - 77.9 | 1.18 | 122 | 1.07 | 0.19 |

Appendix Two: Year-by-year mean absolute difference by slope quintile for ground control survey points (n = 604). These data are noisier than the sum of years but show the same general trend: increasing precision with lower slope.

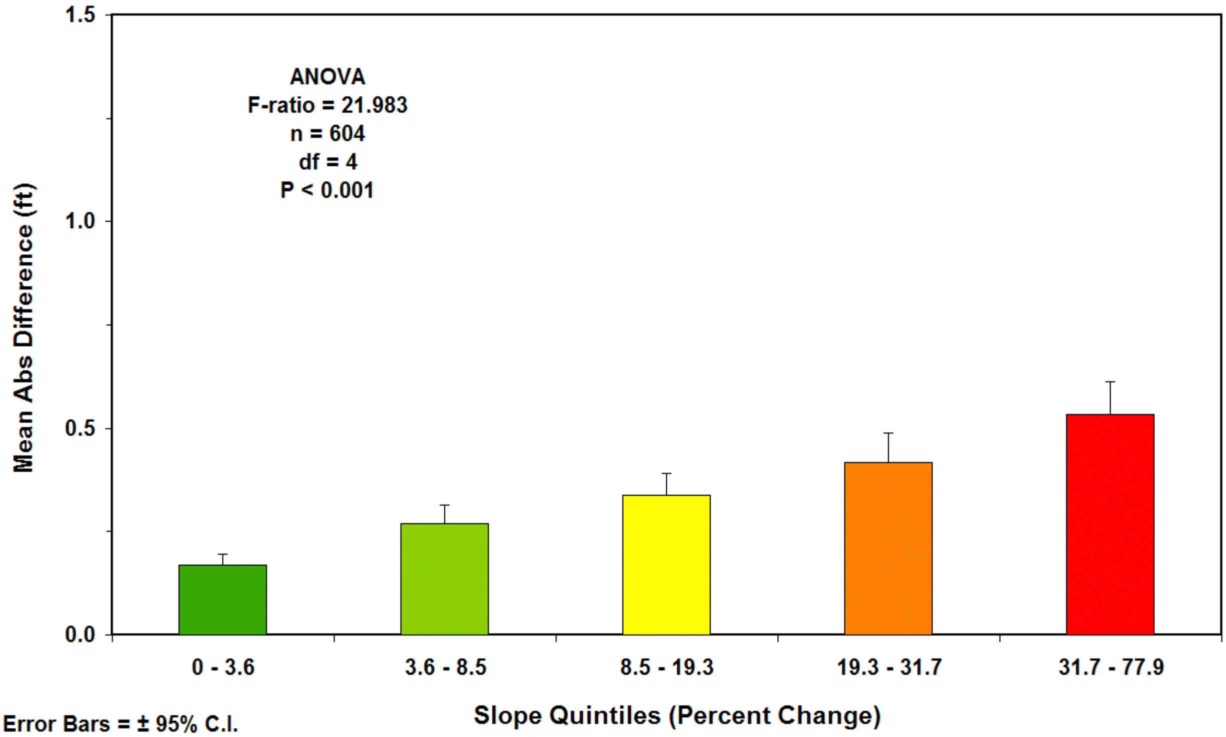


**2002-2004: Mean Absolute Difference by Slope Quintile**

| Slope Quintiles | MeanDiff 2002-04 | n | stdev | ± 95% C.I. |
|---|---|---|---|---|
| 0 - 3.6 | 0.17 | 116 | 0.14 | 0.03 |
| 3.6 - 8.5 | 0.27 | 123 | 0.25 | 0.04 |
| 8.5 - 19.3 | 0.34 | 121 | 0.29 | 0.05 |
| 19.3 - 31.7 | 0.42 | 122 | 0.39 | 0.07 |
| 31.7 - 77.9 | 0.53 | 122 | 0.45 | 0.08 |

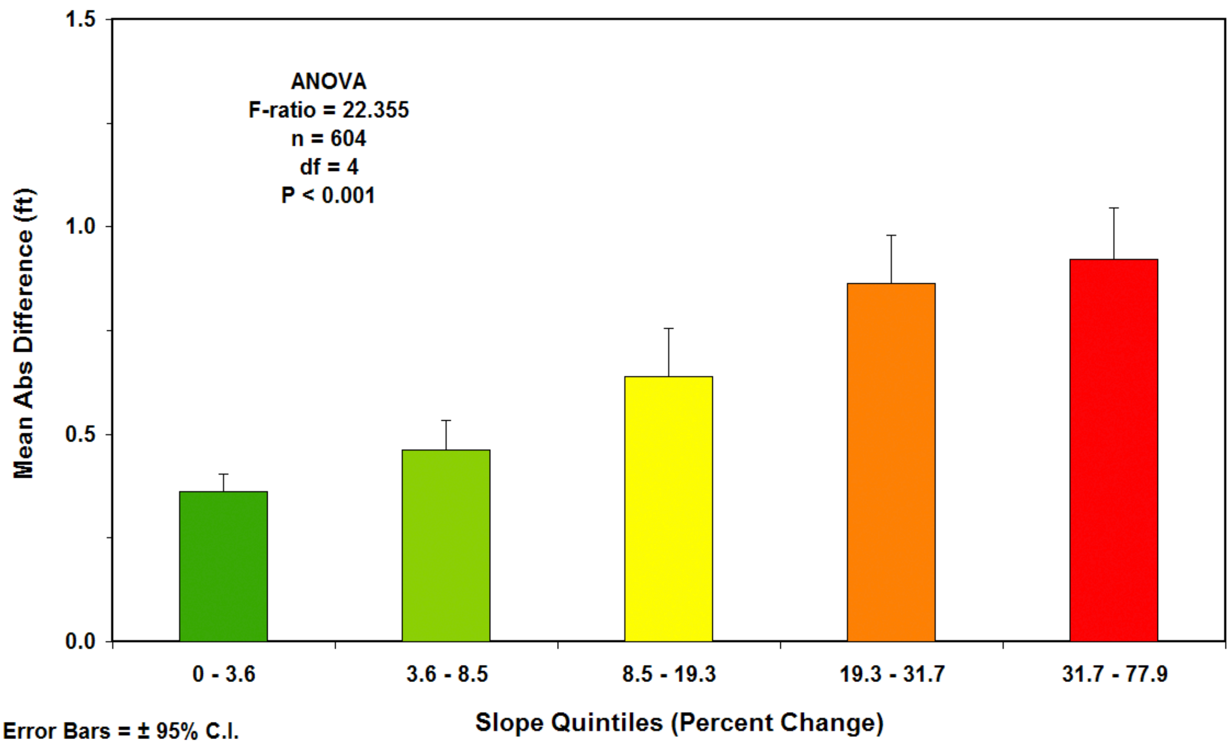


**2004-2006: Mean Absolute Difference by Slope Quintile**

| Slope Quintiles | MeanDiff 2004-06 | n | stdev | ± 95% C.I. |
|---|---|---|---|---|
| 0 - 3.6 | 0.36 | 116 | 0.24 | 0.04 |
| 3.6 - 8.5 | 0.46 | 123 | 0.40 | 0.07 |
| 8.5 - 19.3 | 0.64 | 121 | 0.64 | 0.11 |
| 19.3 - 31.7 | 0.86 | 122 | 0.67 | 0.12 |
| 31.7 - 77.9 | 0.92 | 122 | 0.70 | 0.12 |

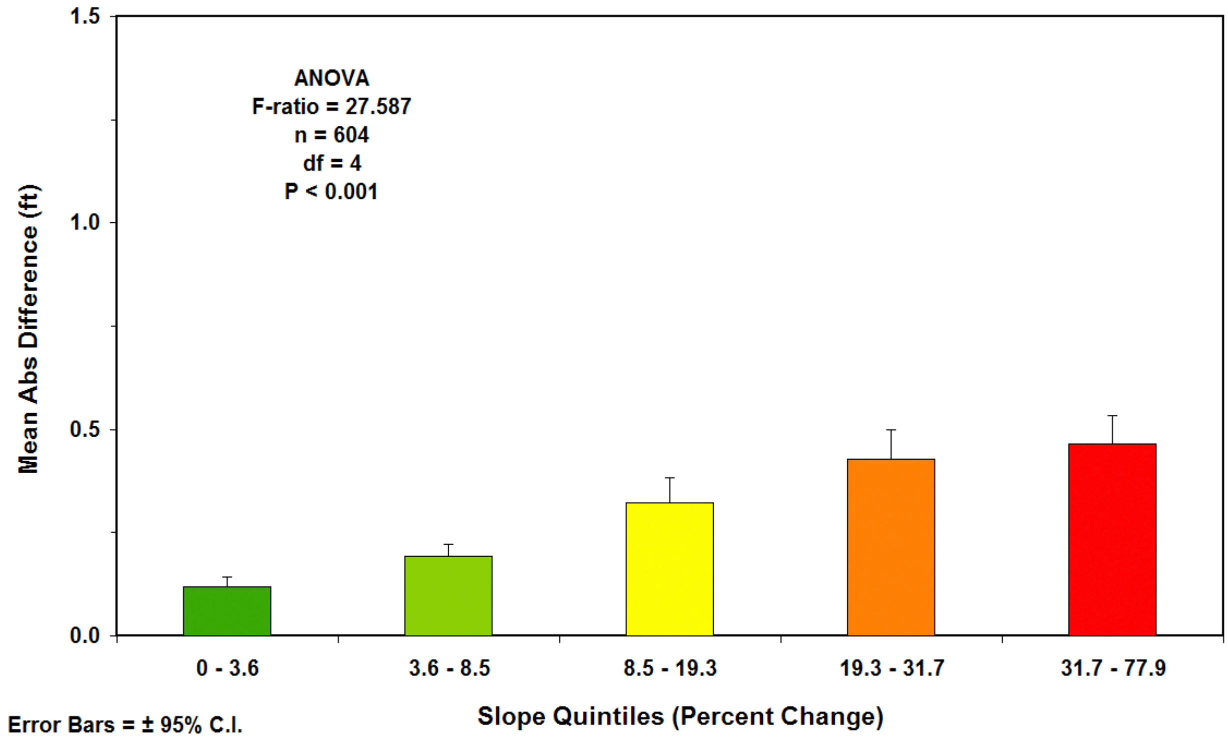


**2006-2007: Mean Absolute Difference by Slope Quintile**

| Slope Quintiles | MeanDiff 2006-07 | n | stdev | ± 95% C.I. |
|---|---|---|---|---|
| 0 - 3.6 | 0.12 | 116 | 0.14 | 0.03 |
| 3.6 - 8.5 | 0.19 | 123 | 0.17 | 0.03 |
| 8.5 - 19.3 | 0.32 | 121 | 0.34 | 0.06 |
| 19.3 - 31.7 | 0.43 | 122 | 0.41 | 0.07 |
| 31.7 - 77.9 | 0.47 | 122 | 0.38 | 0.07 |

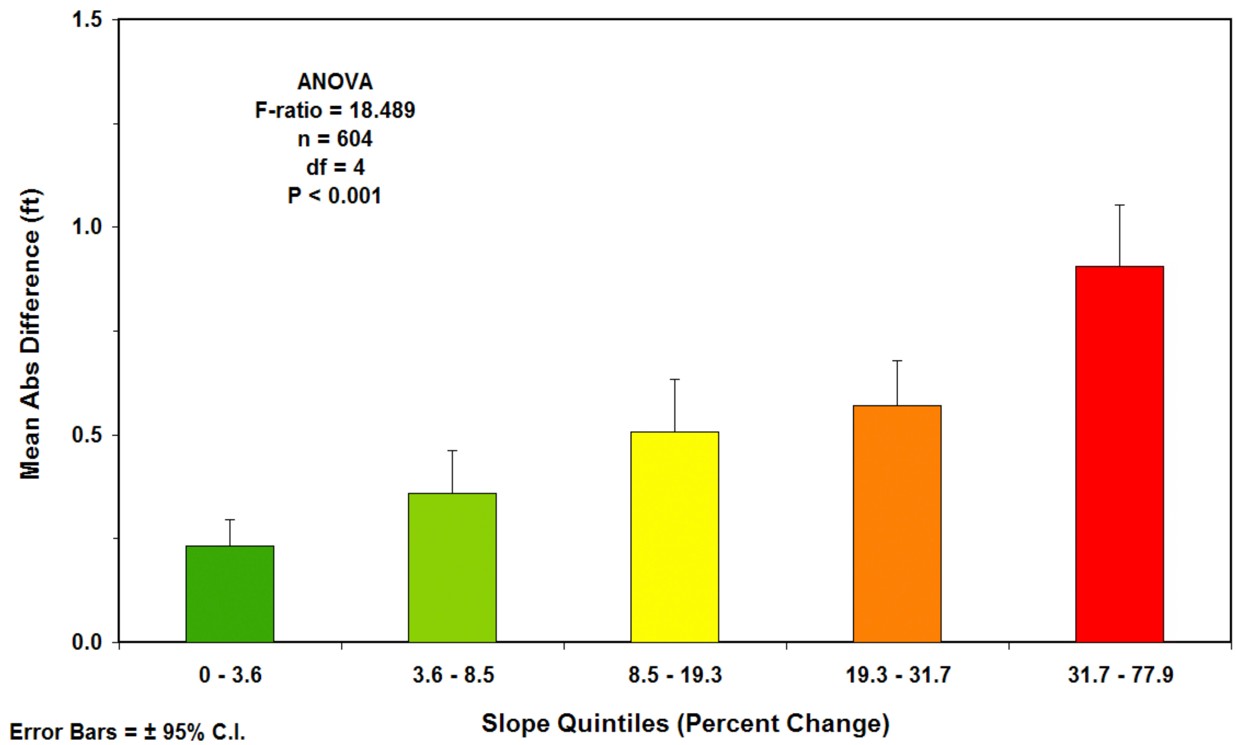


2007-2008: Mean Absolute Difference by Slope Quintile

| Slope Quintiles | MeanDiff 2007-08 | n | stdev | ± 95% C.I. |
|---|---|---|---|---|
| 0 - 3.6 | 0.23 | 116 | 0.34 | 0.06 |
| 3.6 - 8.5 | 0.36 | 123 | 0.57 | 0.10 |
| 8.5 - 19.3 | 0.51 | 121 | 0.72 | 0.13 |
| 19.3 - 31.7 | 0.57 | 122 | 0.60 | 0.11 |
| 31.7 - 77.9 | 0.91 | 122 | 0.84 | 0.15 |

Appendix Three: Sequence of modified Anderson Level One LULC classes mapped from 1-foot (or better) digital orthoimages (used as the ground-truth for LULC mapping) from the 1998, 2002, 2004, 2006, and 2008 aerial overflights by Montgomery County in the Clarksburg Special Protection Area. 1998 was used as the base year. LULC coverages were done for the Sopers Branch, Tributary 104 (T104), and Tributary 109 (T109) watershed areas, with the LULC mapped to a 500-foot buffer and the County-mapped stream channels overlaid.

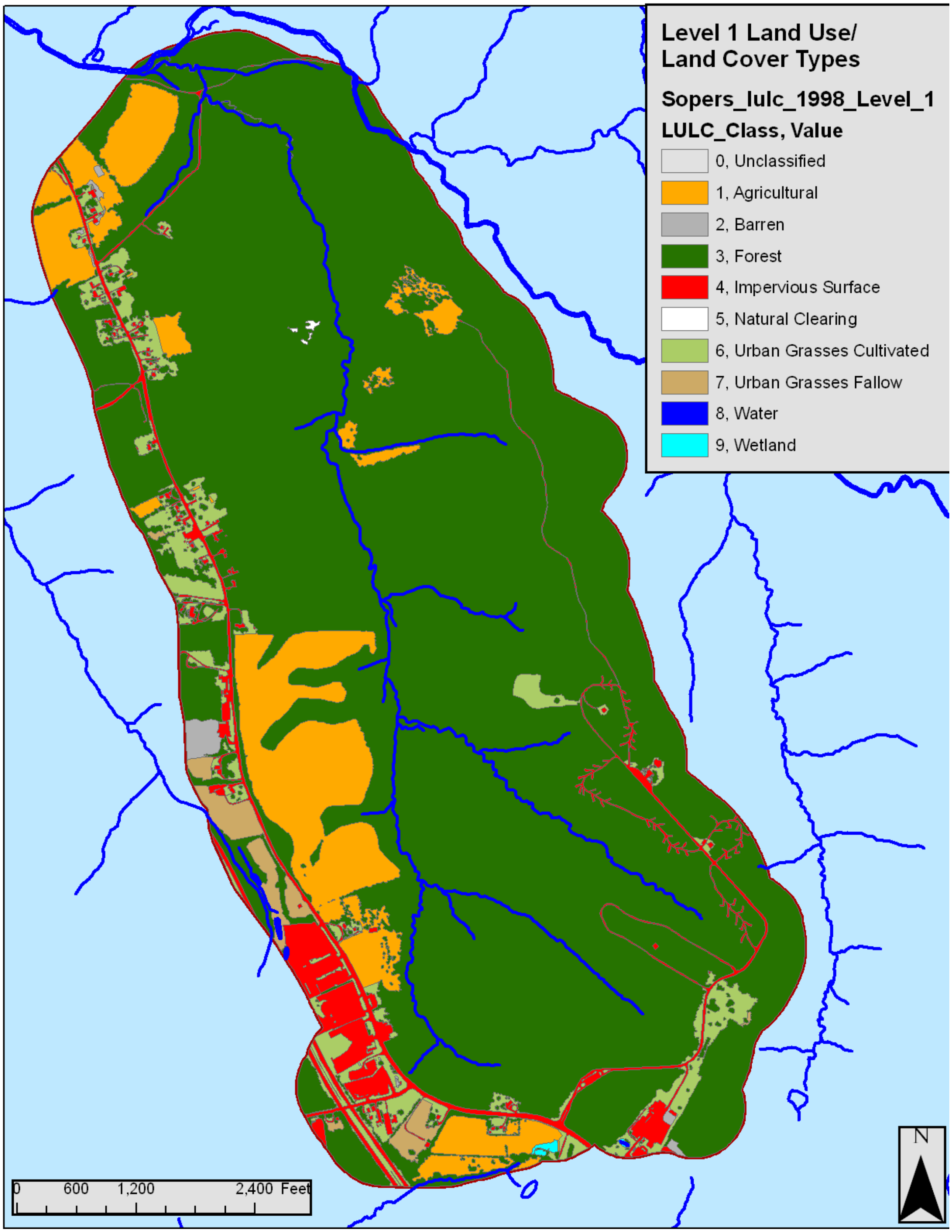

Sopers Branch - 1998 - Level 1 LULC

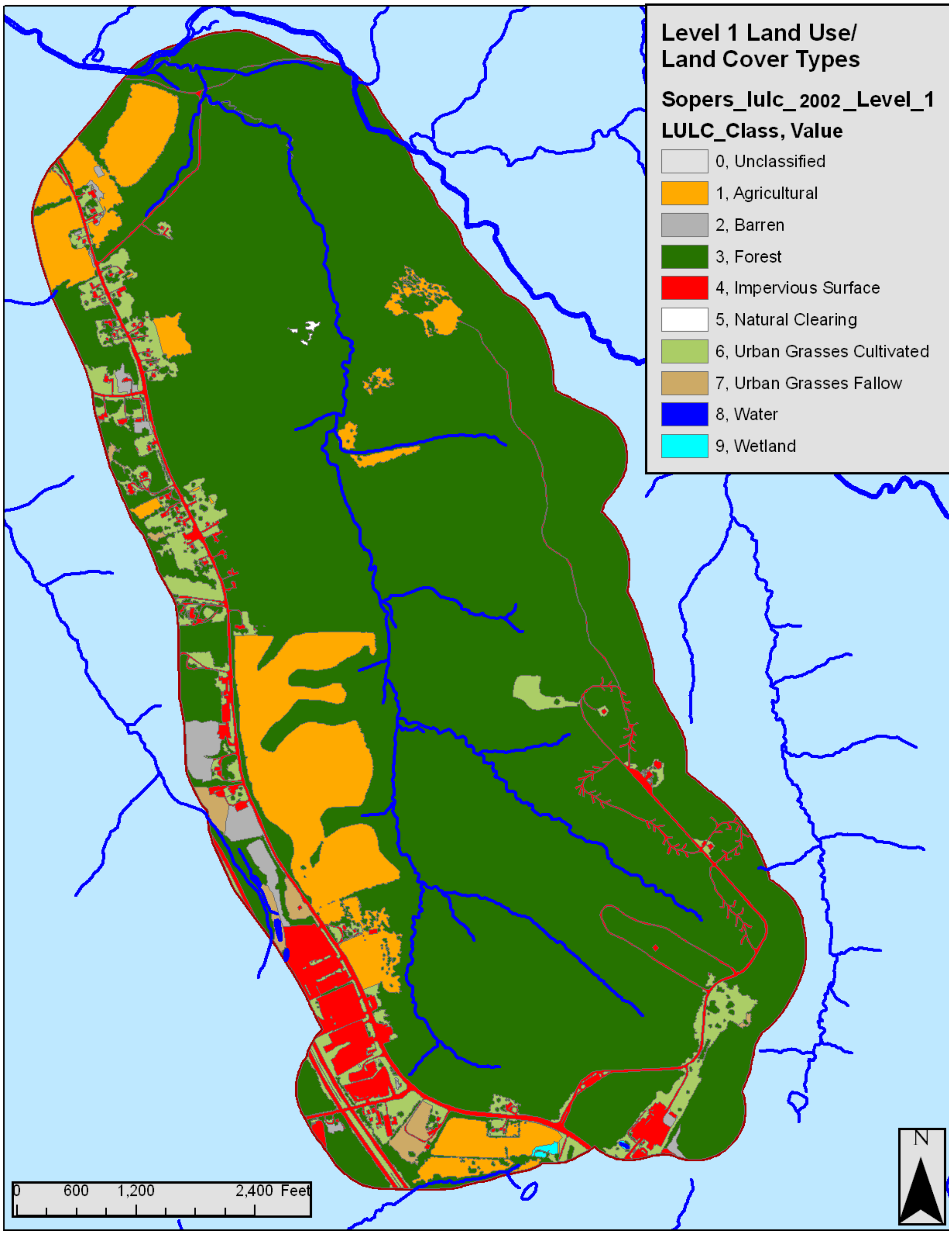


Sopers Branch - 2002 - Level 1 LULC

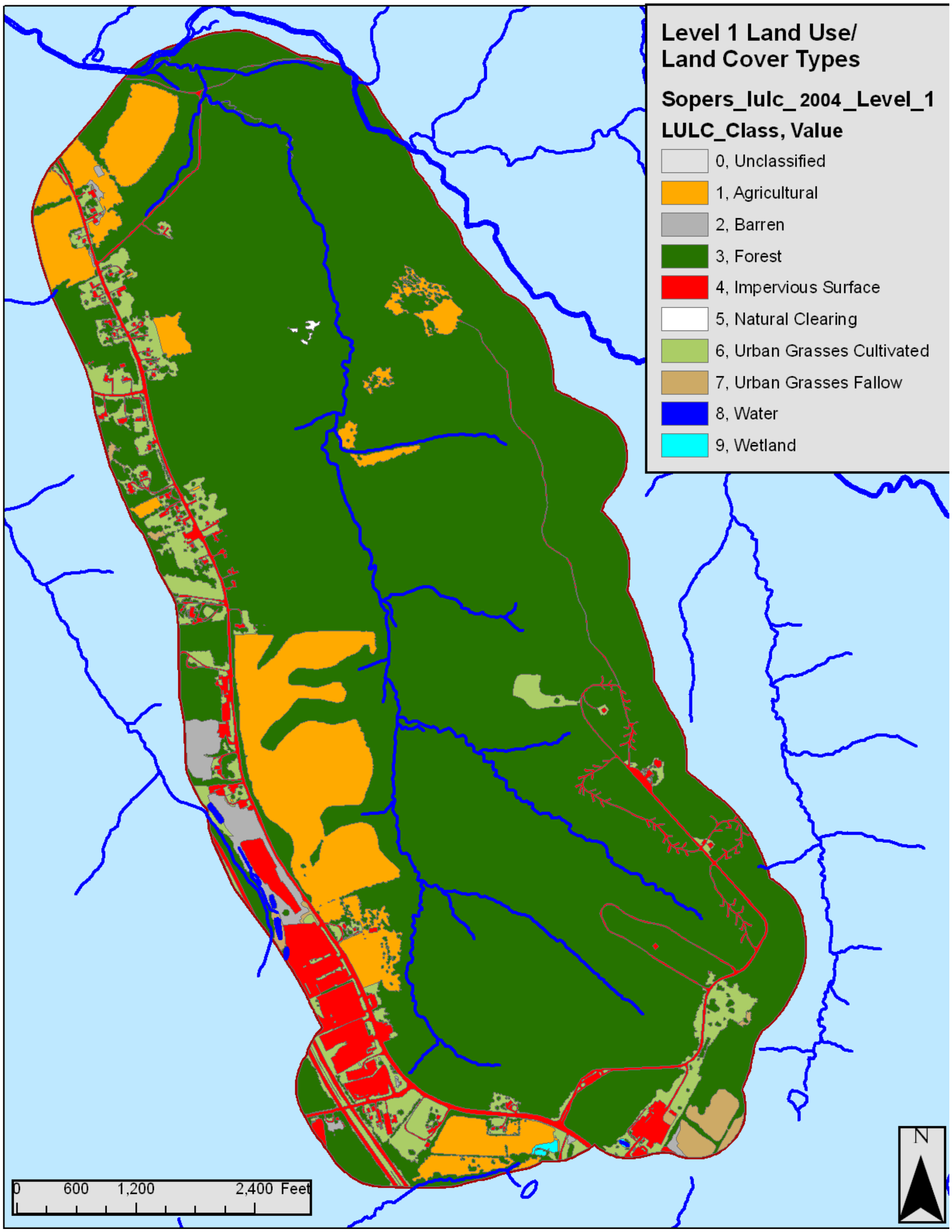


Sopers Branch - 2004 - Level 1 LULC

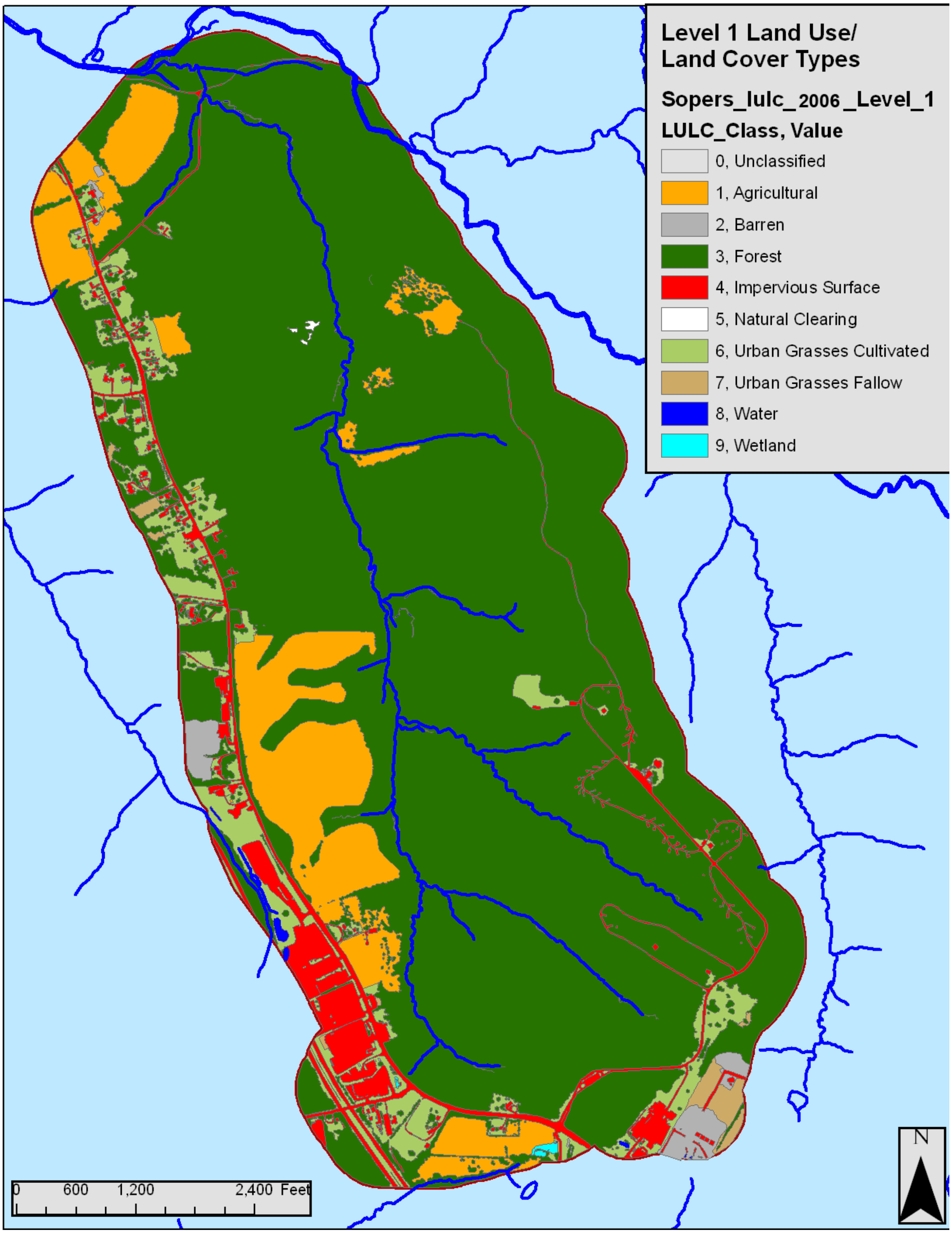


Sopers Branch - 2006 - Level 1 LULC

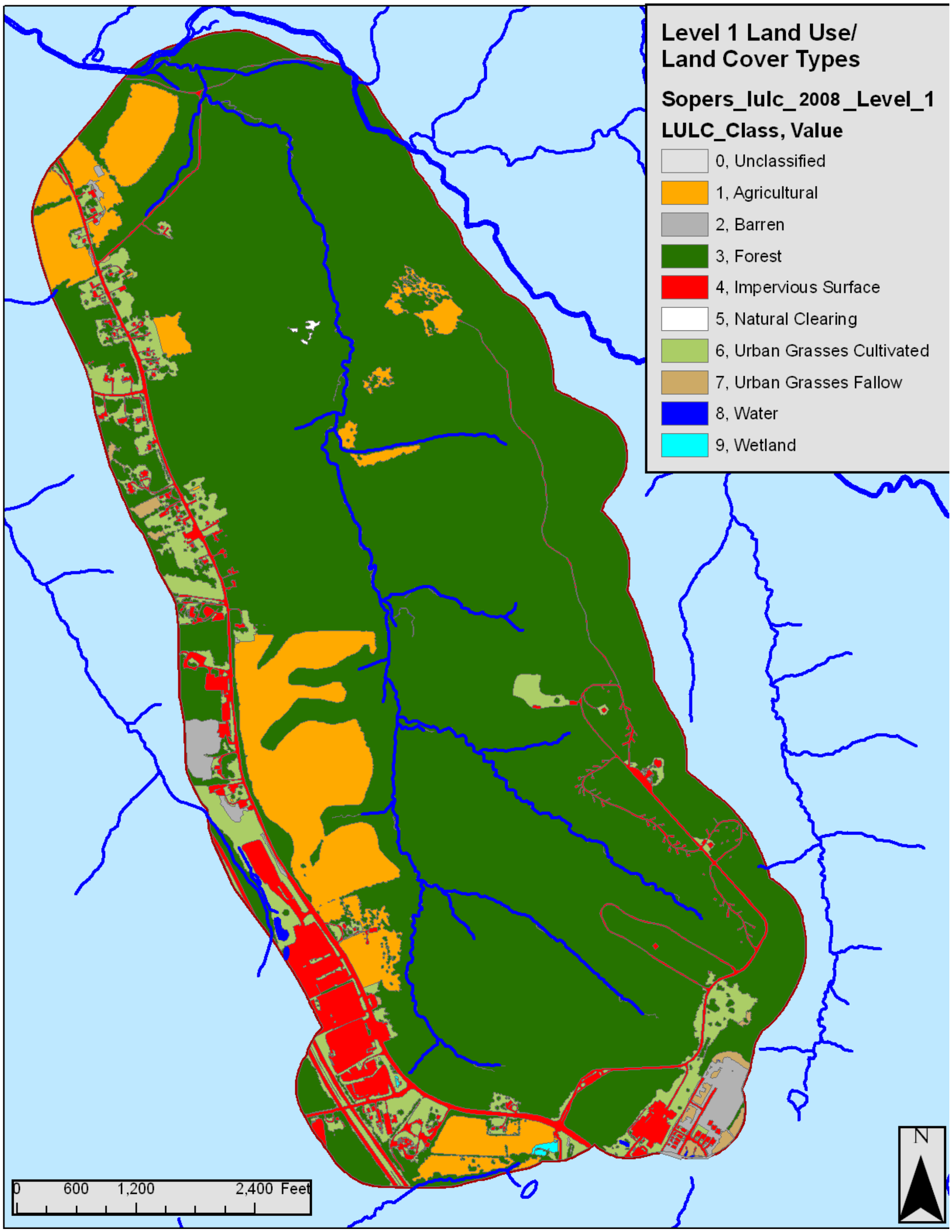


Sopers Branch - 2008 - Level 1 LULC

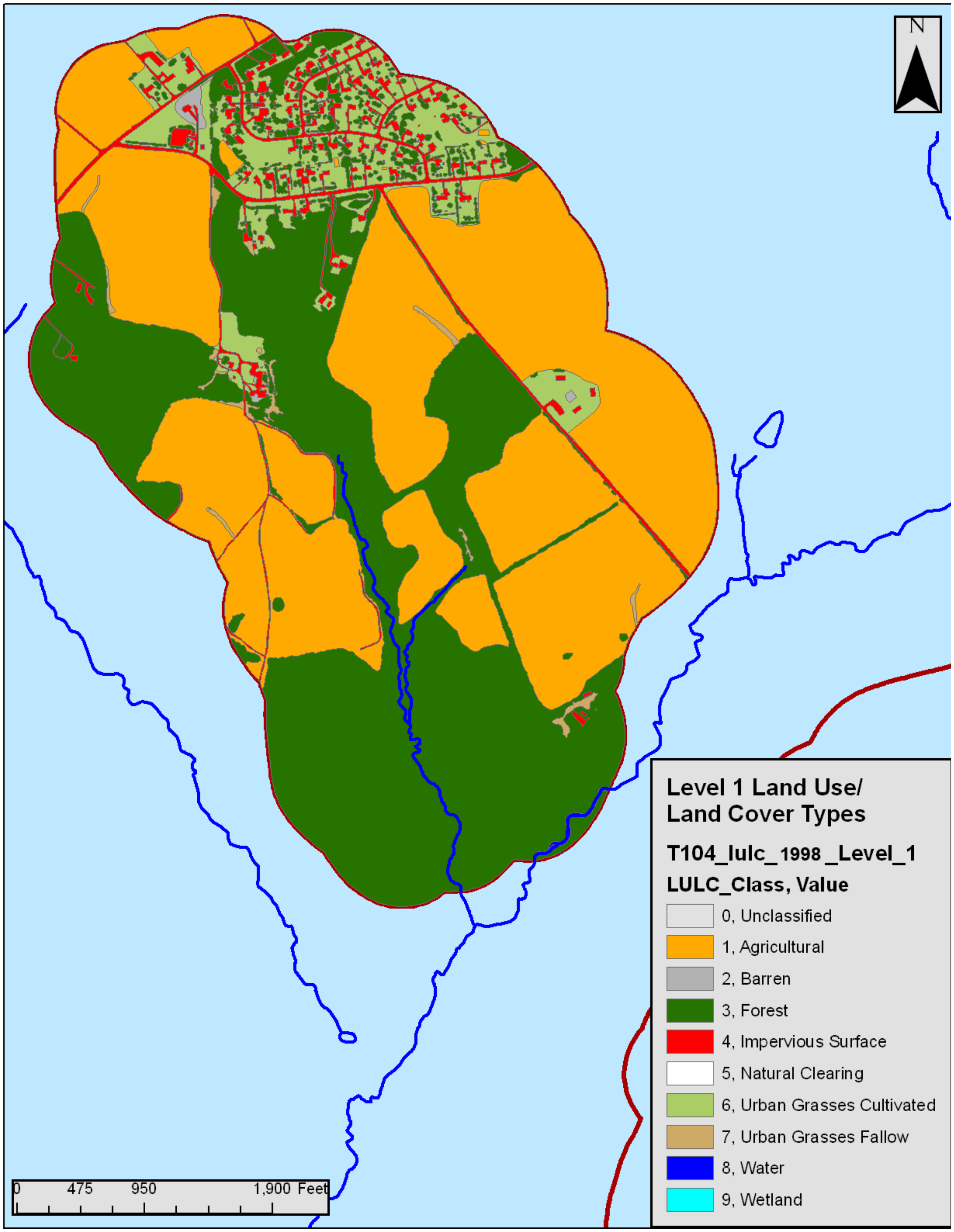

T104 - 1998 - Level 1 LULC

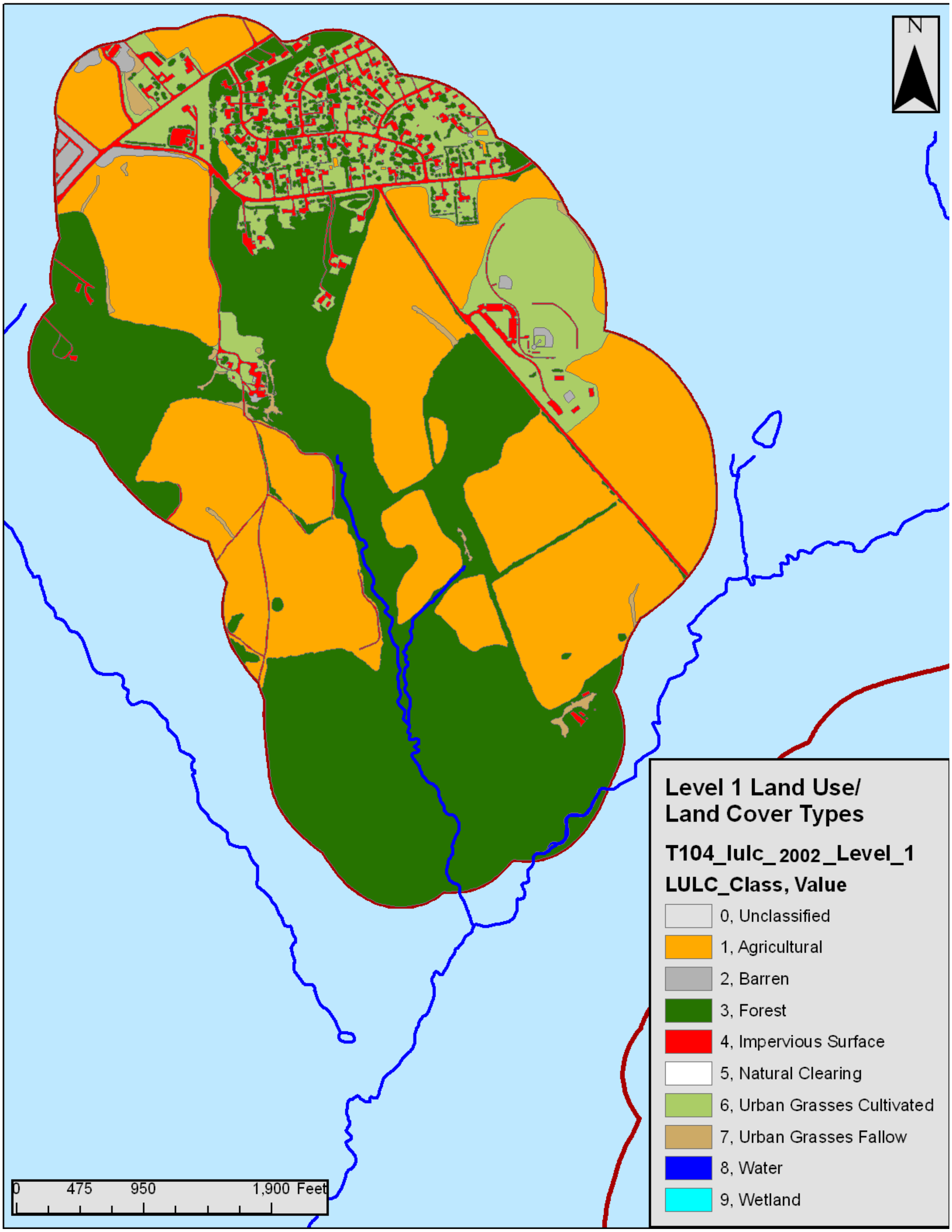


T104 - 2002 - Level 1 LULC

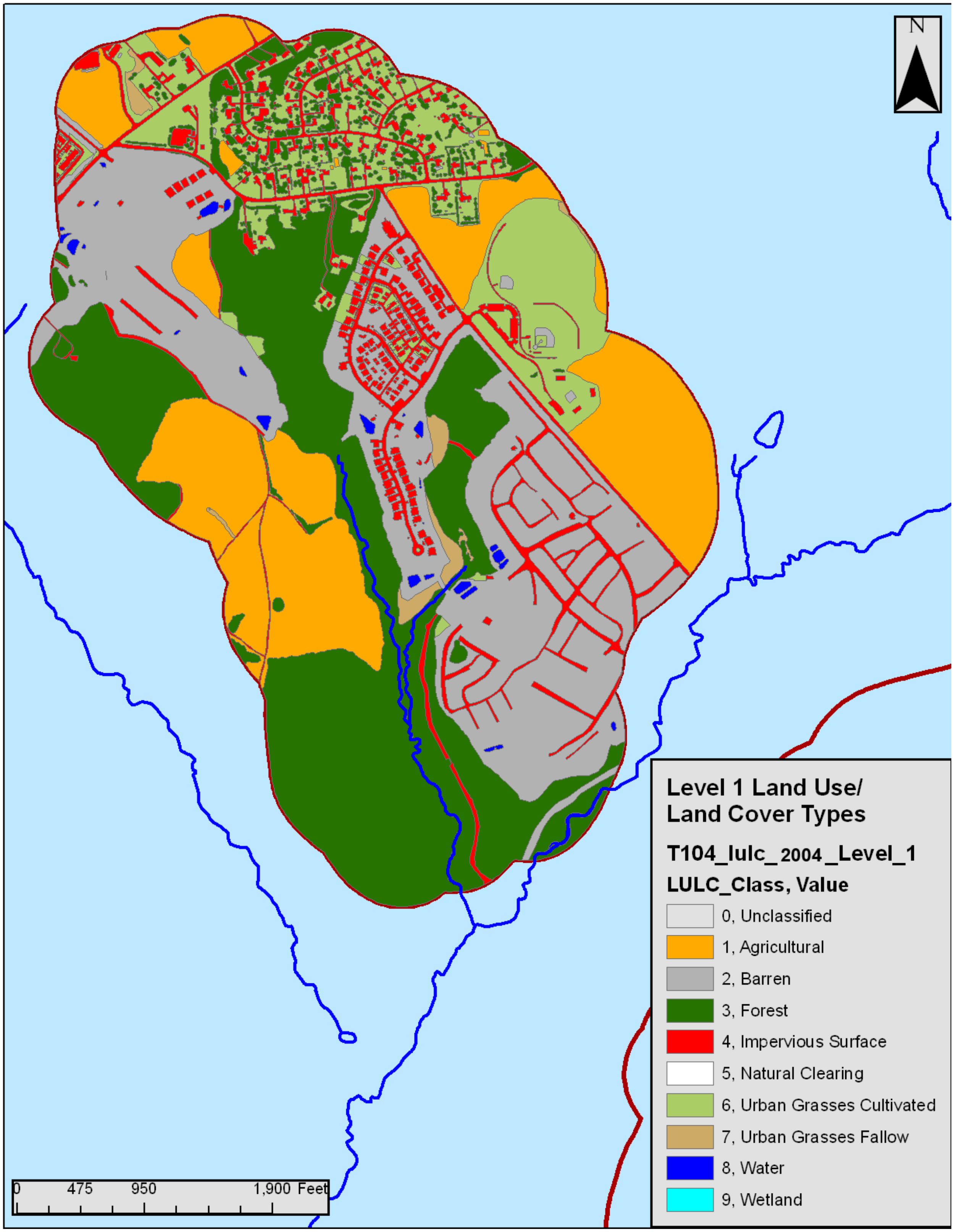


T104 - 2004 - Level 1 LULC


T104 - 2006 - Level 1 LULC

T104 - 2008 - Level 1 LULC

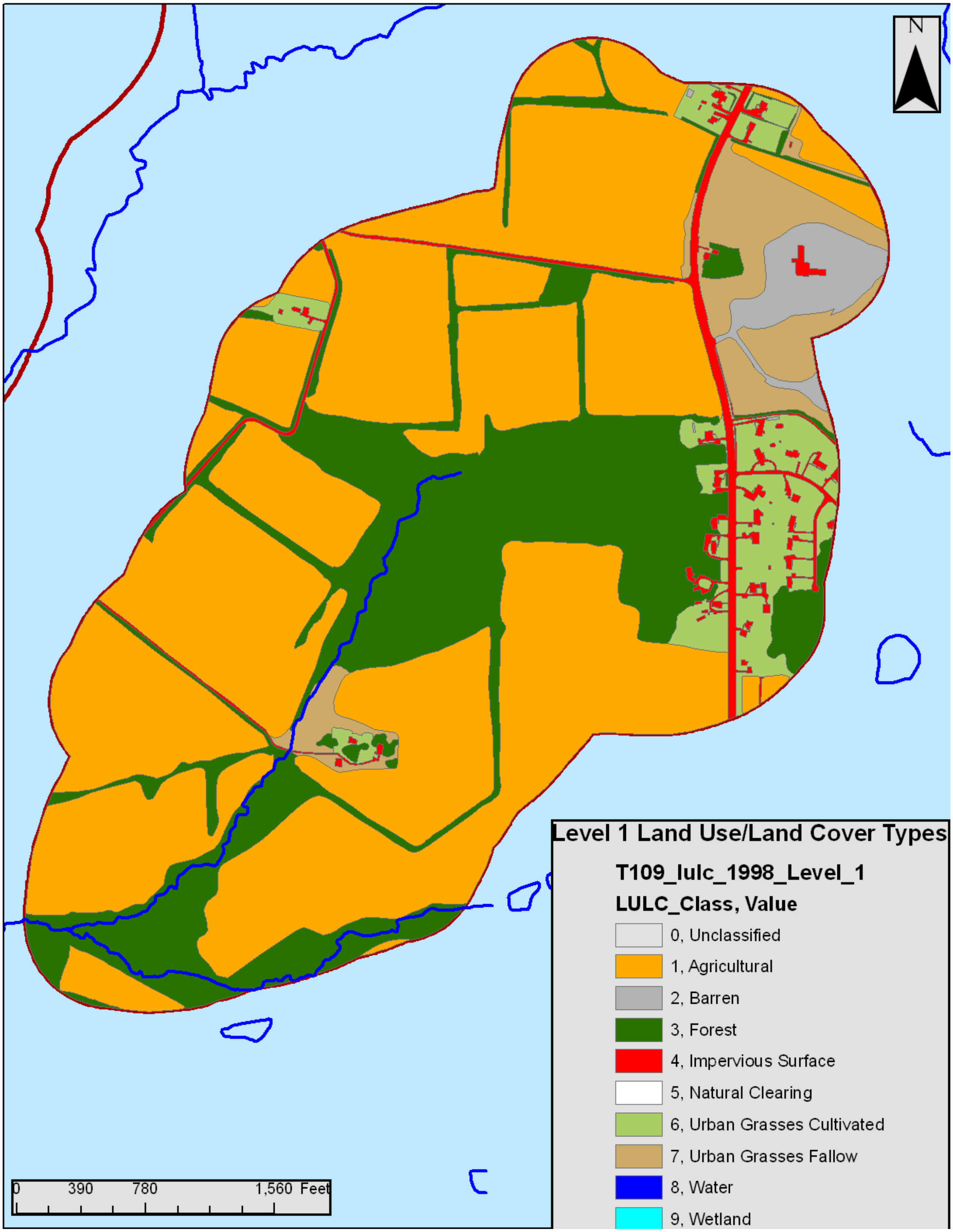


T109 - 1998 - Level 1 LULC

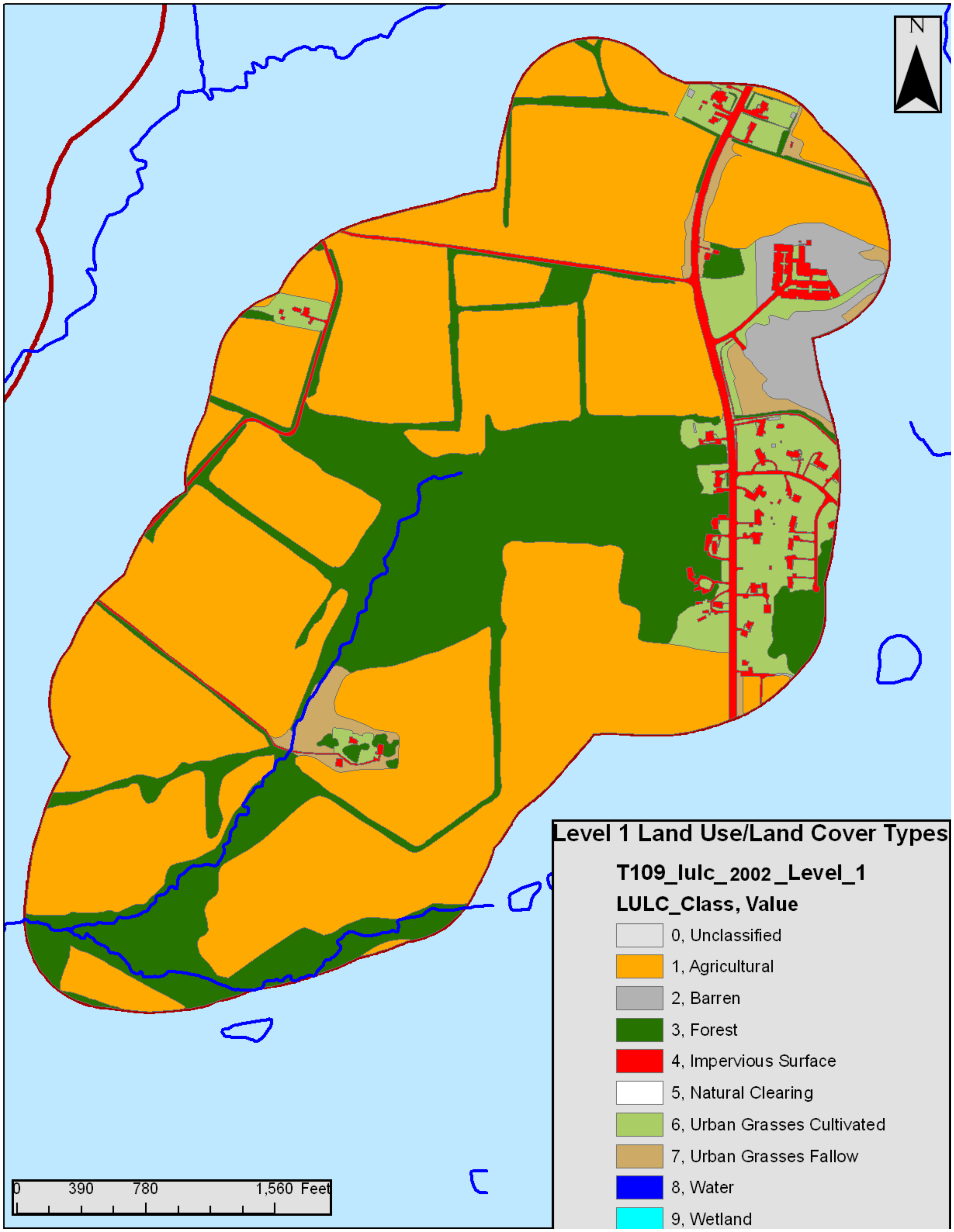


T109 - 2002 - Level 1 LULC

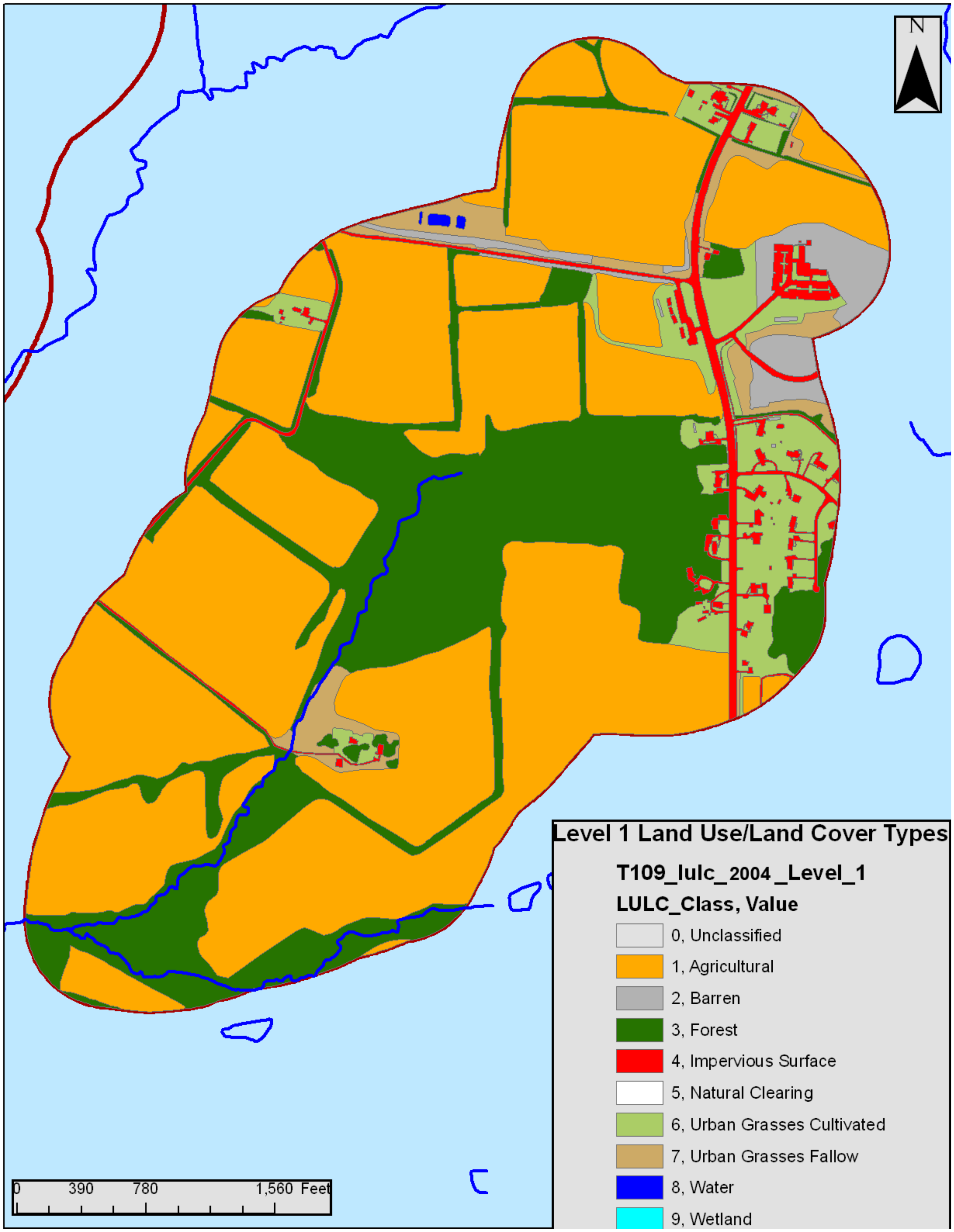


T109 - 2004 - Level 1 LULC

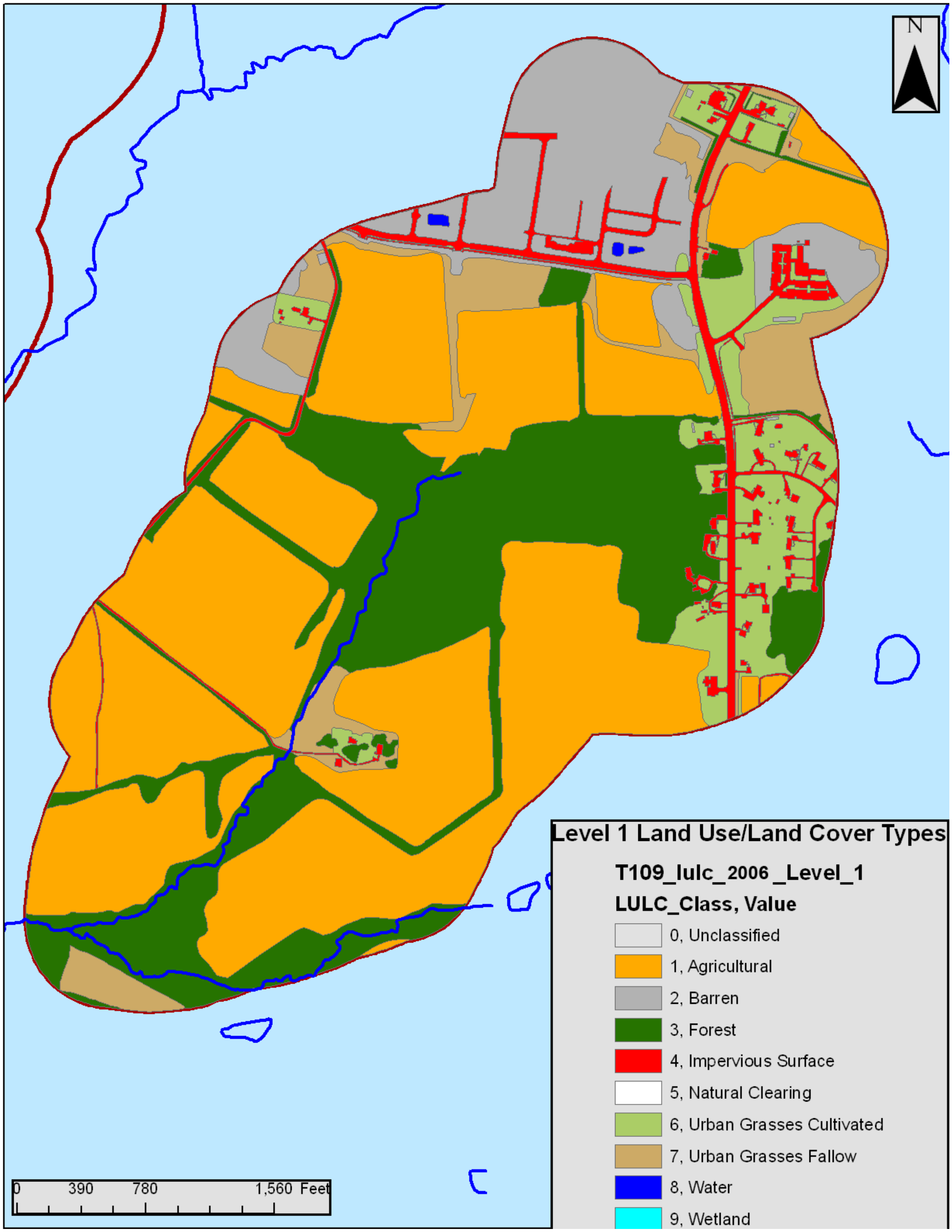


T109 - 2006 - Level 1 LULC

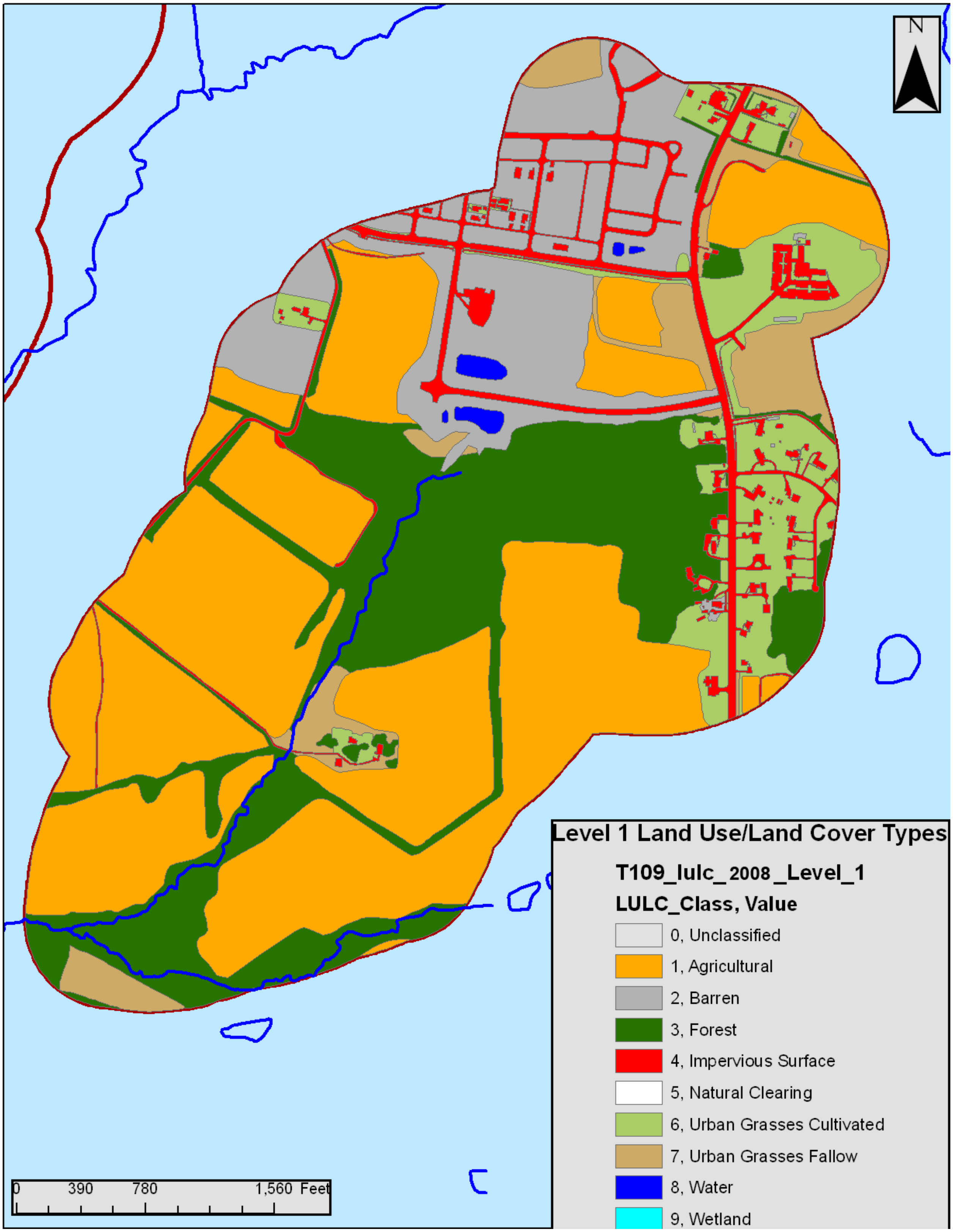


T109 - 2008 - Level 1 LULC

Appendix Four: Sequence of figures that display the ground-truth stream transect measurements and LiDAR-derived stream transect elevation values.

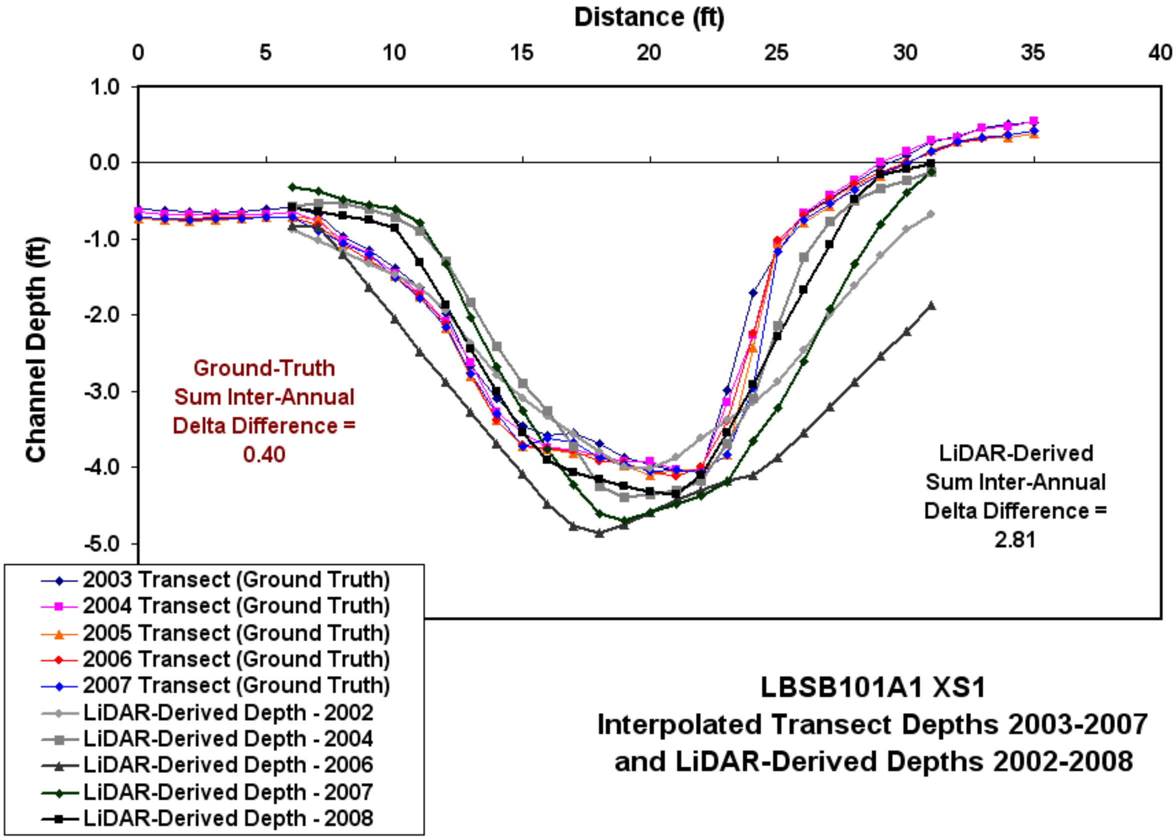


**LBSB101A1 XS1**
**Interpolated Transect Depths 2003-2007**
**and LiDAR-Derived Depths 2002-2008**

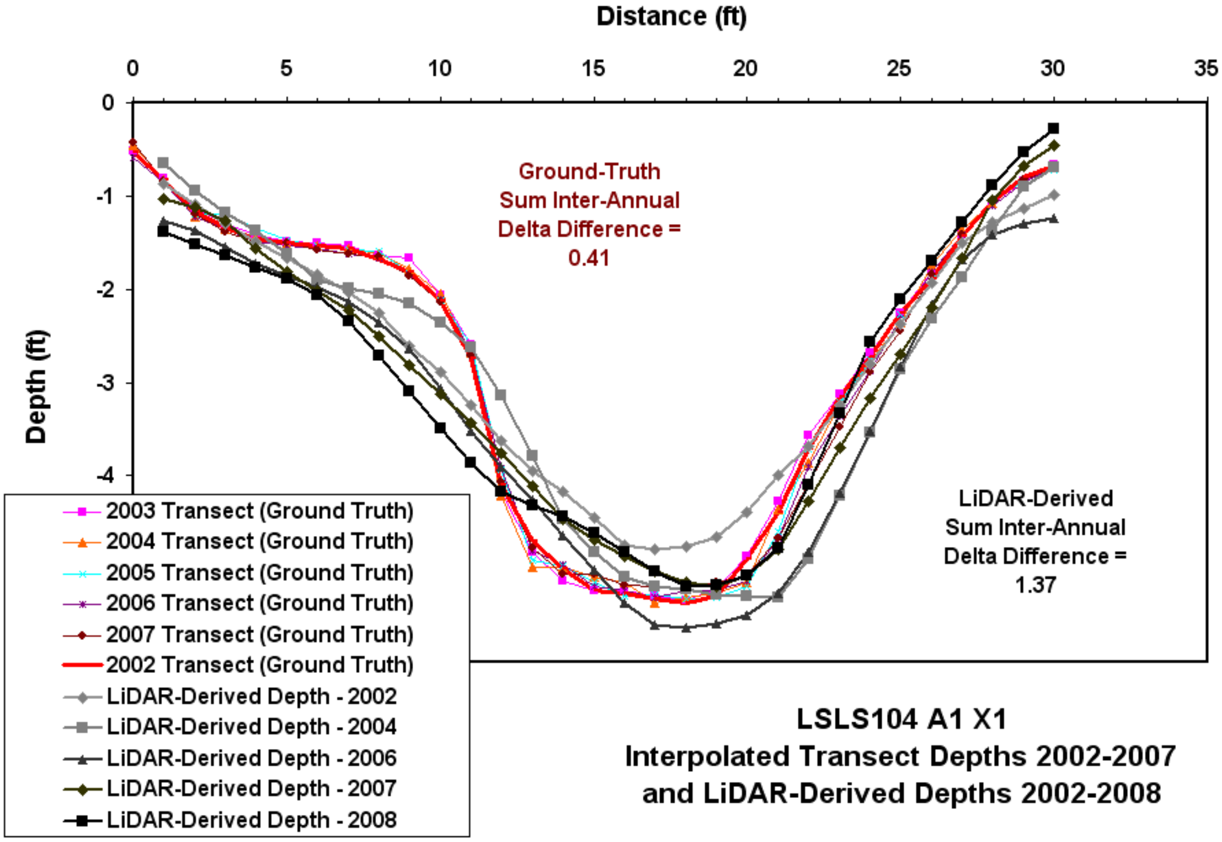


**LSLS104 A1 X1**
**Interpolated Transect Depths 2002-2007**
**and LiDAR-Derived Depths 2002-2008**

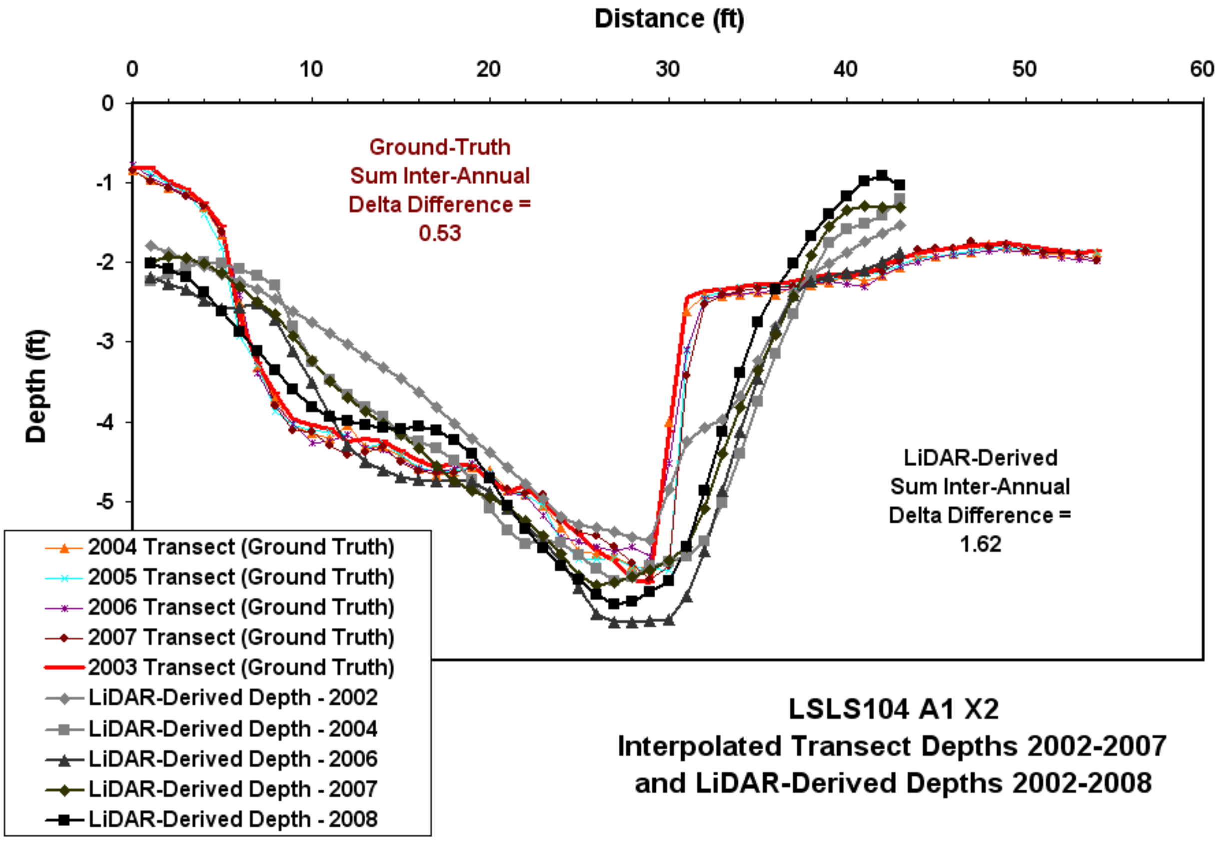


**LSLS104 A1 X2**
**Interpolated Transect Depths 2002-2007**
**and LiDAR-Derived Depths 2002-2008**

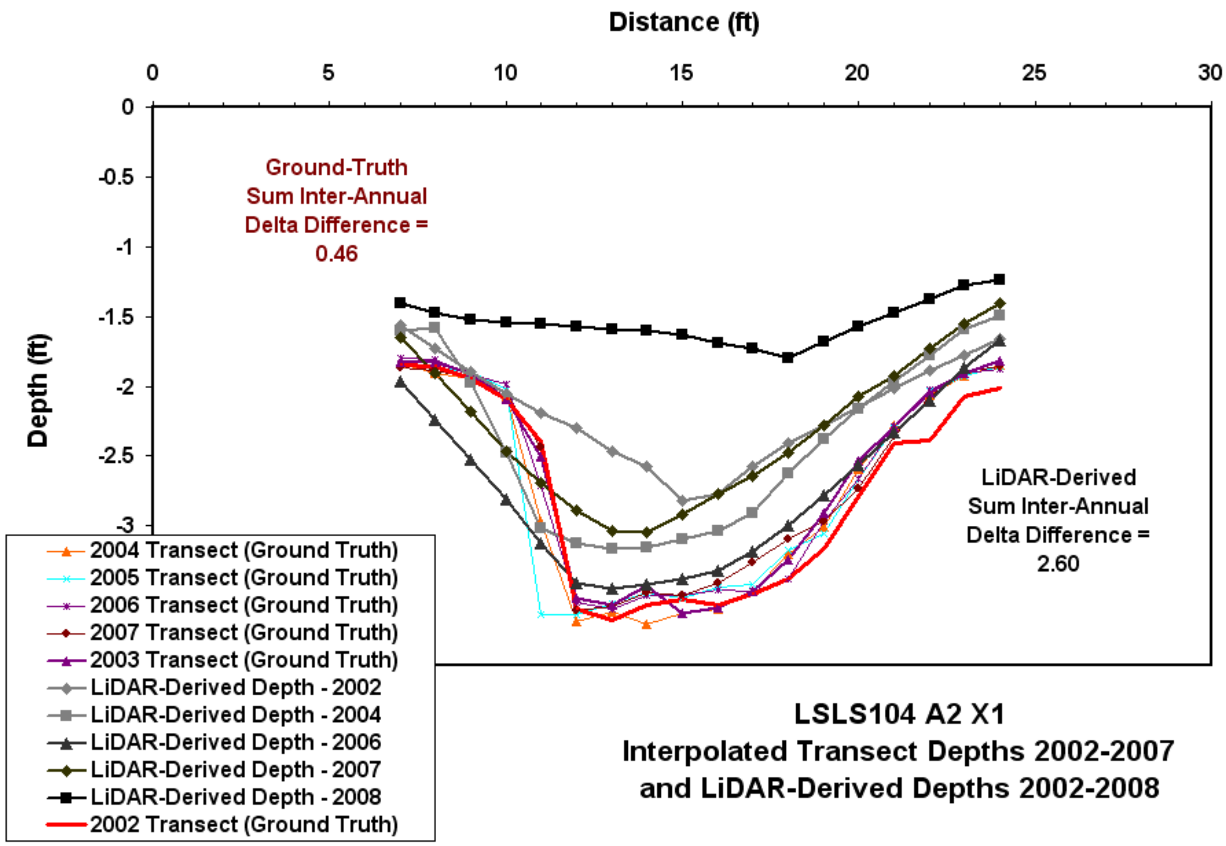
Distance (ft)
0
5
10
15
20
25
30
Depth (ft)
0
-0.5
-1
-1.5
-2
-2.5
-3
Ground-Truth
Sum Inter-Annual
Delta Difference =
0.46
LiDAR-Derived
Sum Inter-Annual
Delta Difference =
2.60
2004 Transect (Ground Truth)
2005 Transect (Ground Truth)
2006 Transect (Ground Truth)
2007 Transect (Ground Truth)
2003 Transect (Ground Truth)
LiDAR-Derived Depth - 2002
LiDAR-Derived Depth - 2004
LiDAR-Derived Depth - 2006
LiDAR-Derived Depth - 2007
LiDAR-Derived Depth - 2008
2002 Transect (Ground Truth)
LSLS104 A2 X1
Interpolated Transect Depths 2002-2007
and LiDAR-Derived Depths 2002-2008

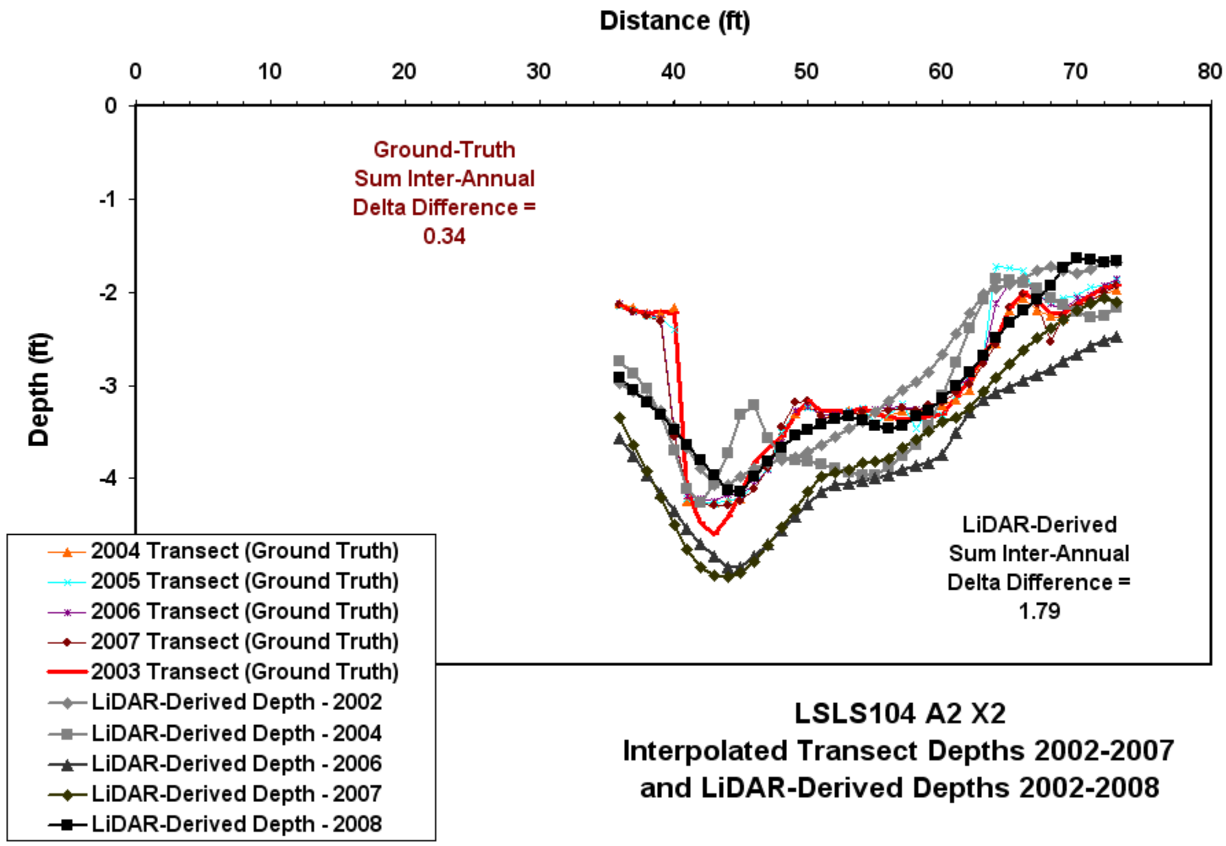


**LSLS104 A2 X2**
**Interpolated Transect Depths 2002-2007**
**and LiDAR-Derived Depths 2002-2008**

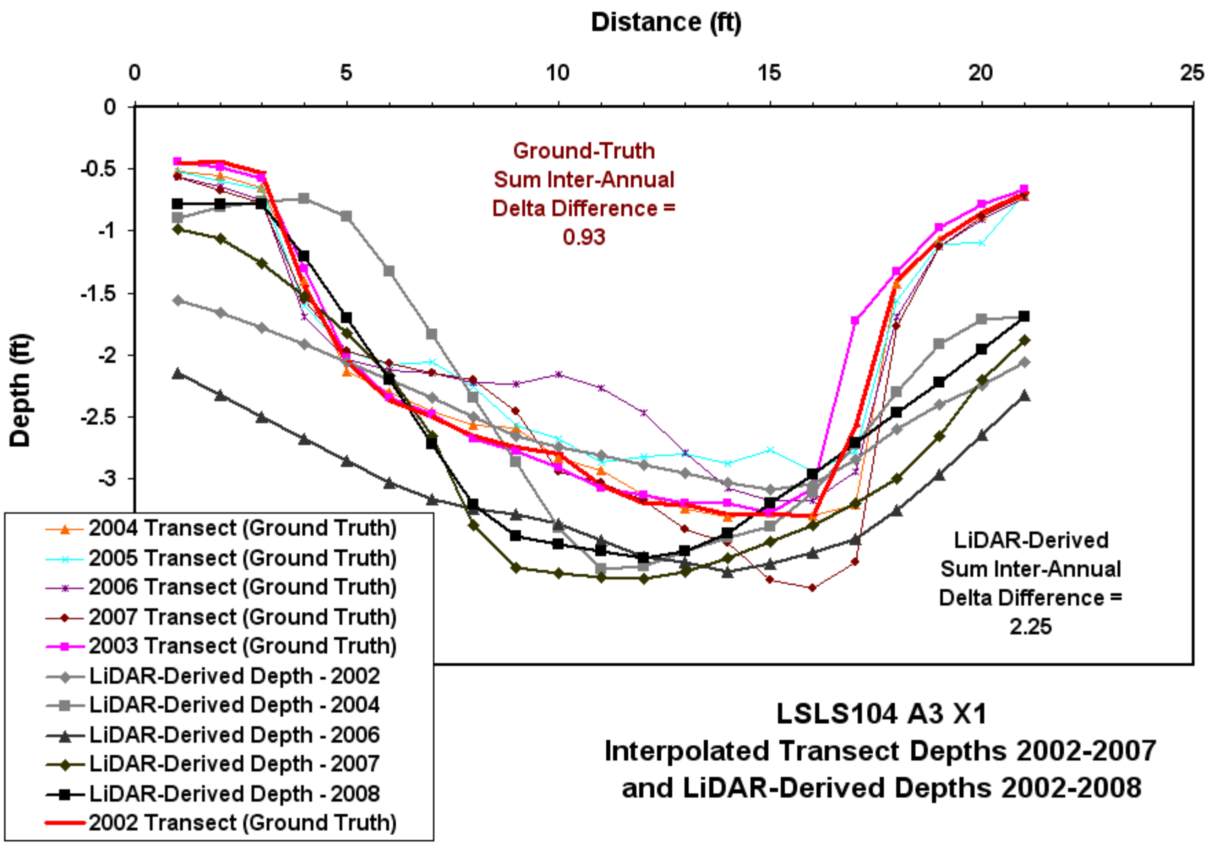


**LSLS104 A3 X1**
**Interpolated Transect Depths 2002-2007**
**and LiDAR-Derived Depths 2002-2008**

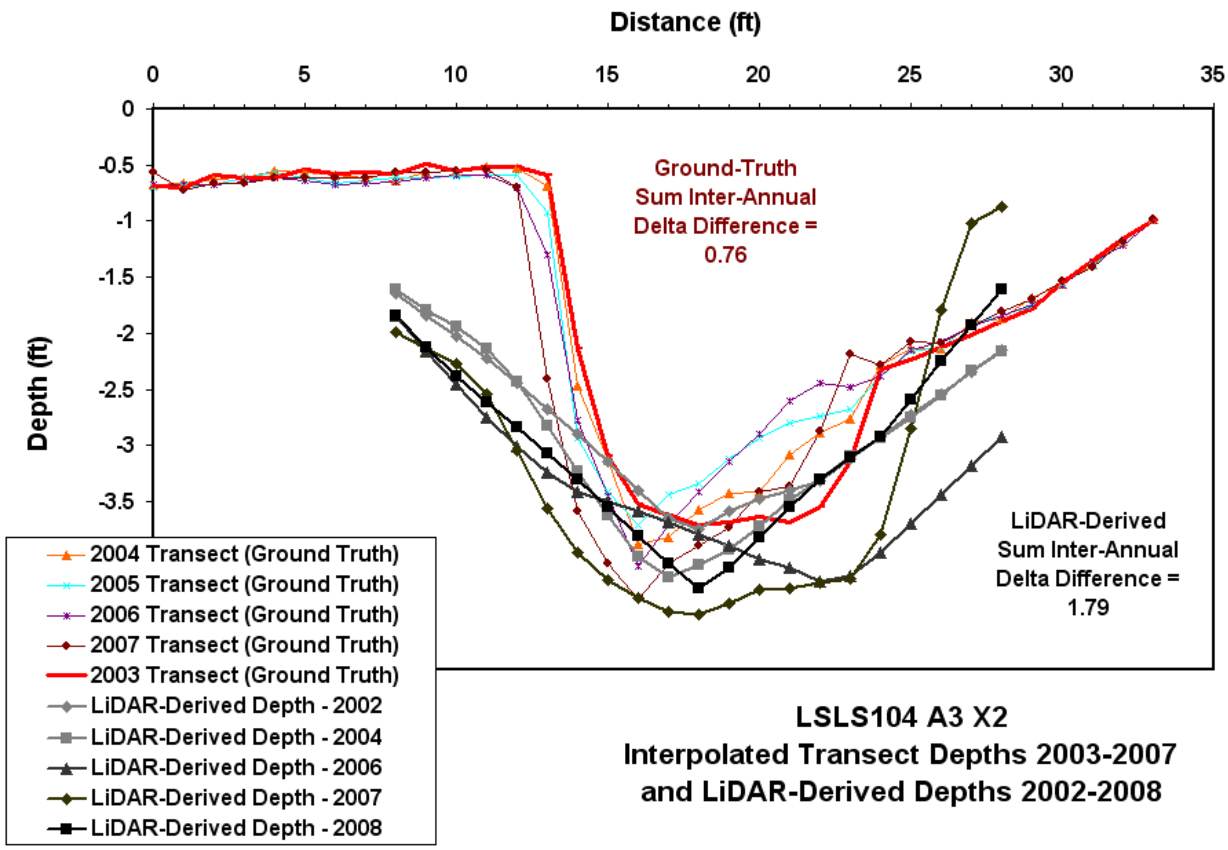


**LSLS104 A3 X2**
**Interpolated Transect Depths 2003-2007**
**and LiDAR-Derived Depths 2002-2008**

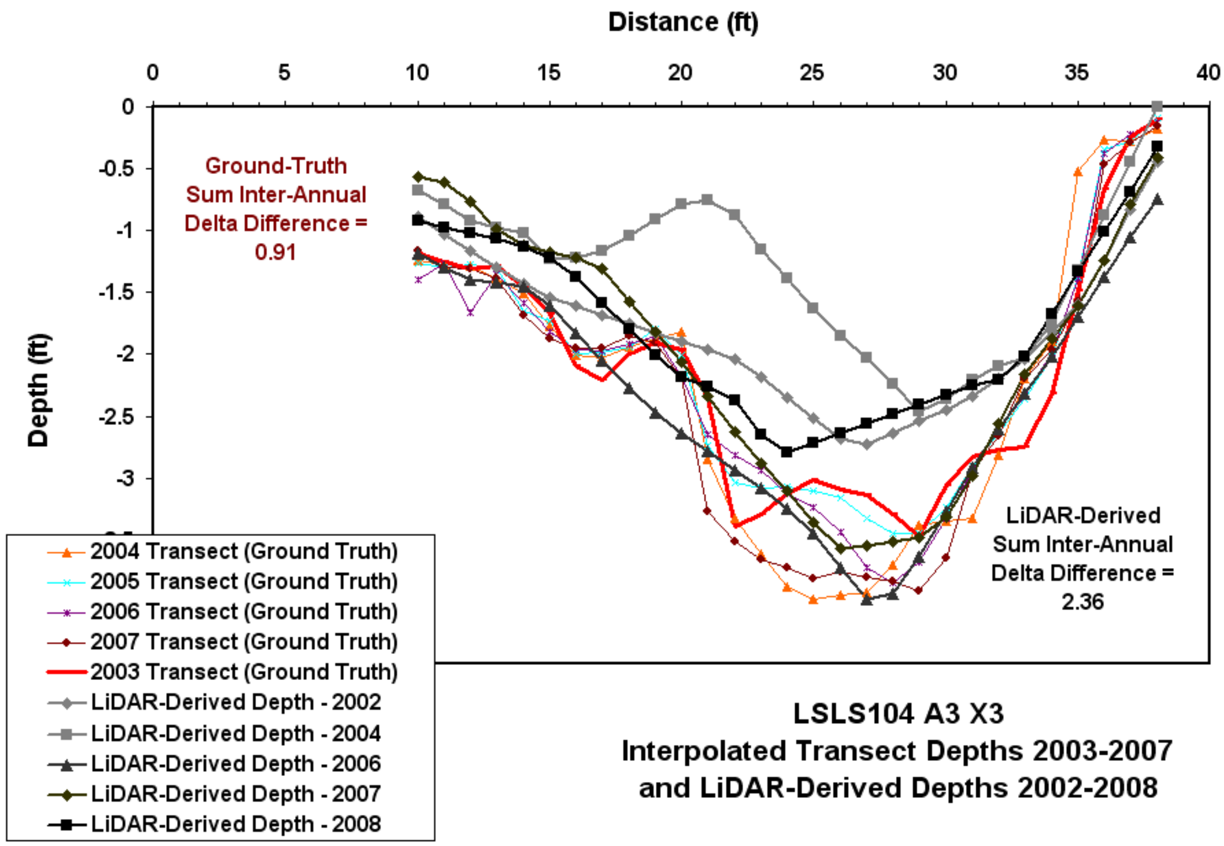


**LSLS104 A3 X3**
**Interpolated Transect Depths 2003-2007**
**and LiDAR-Derived Depths 2002-2008**

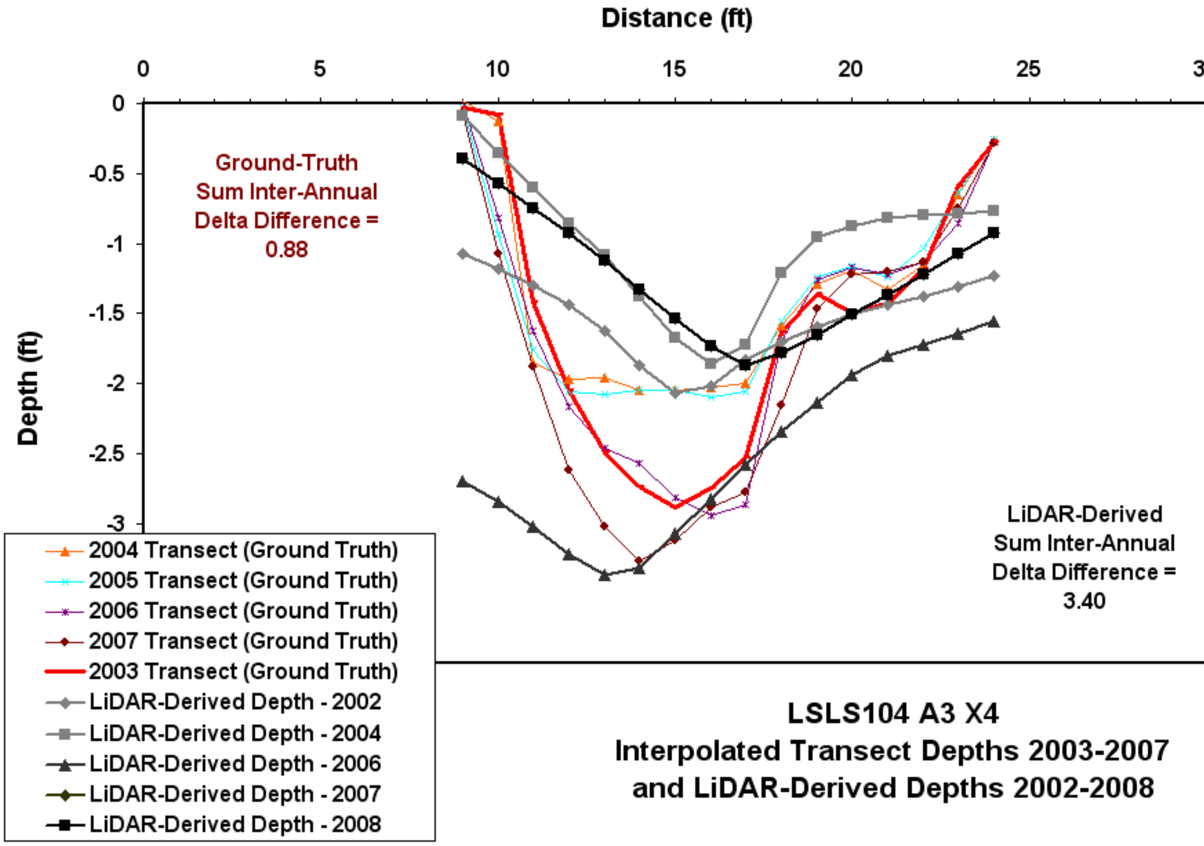


**LSLS104 A3 X4**
**Interpolated Transect Depths 2003-2007**
**and LiDAR-Derived Depths 2002-2008**

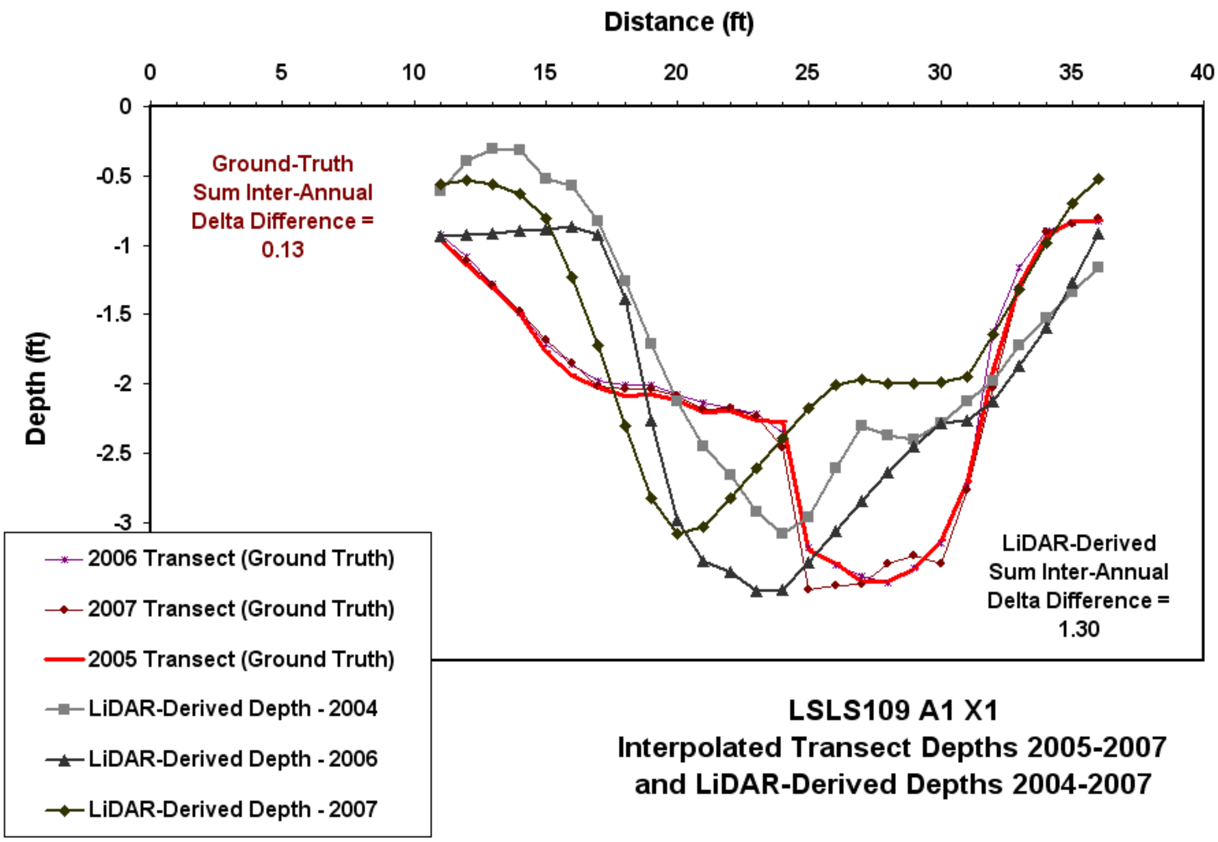


**LSLS109 A1 X1**
**Interpolated Transect Depths 2005-2007**
**and LiDAR-Derived Depths 2004-2007**

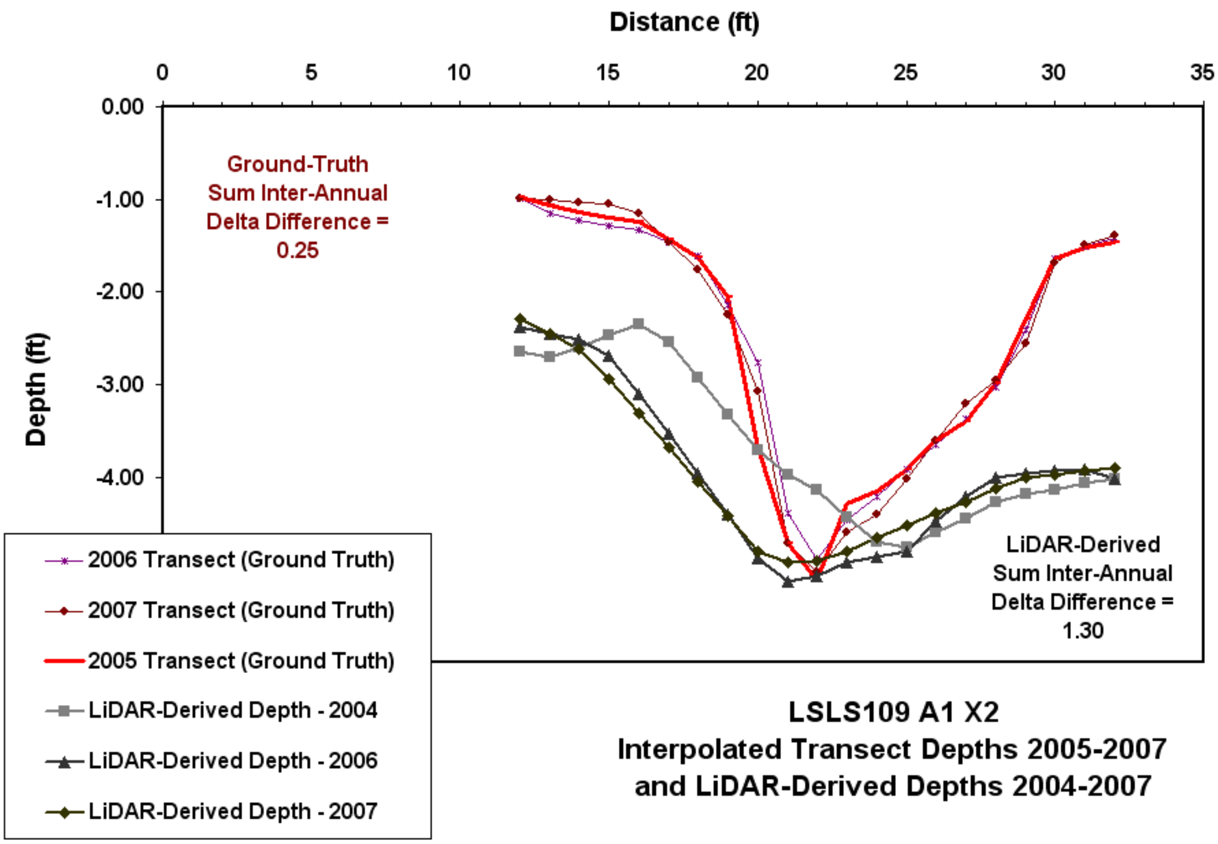


**LSLS109 A1 X2**
**Interpolated Transect Depths 2005-2007**
**and LiDAR-Derived Depths 2004-2007**

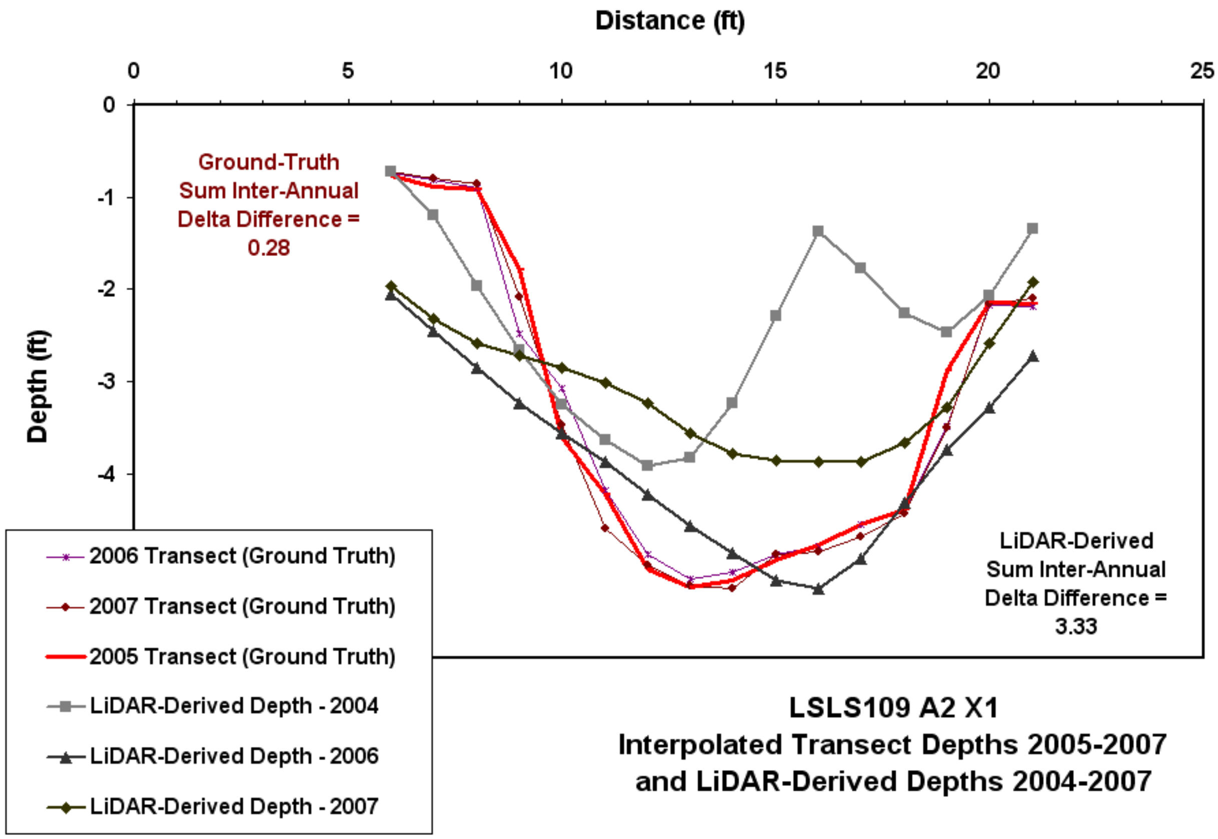


**LSLS109 A2 X1**
**Interpolated Transect Depths 2005-2007**
**and LiDAR-Derived Depths 2004-2007**

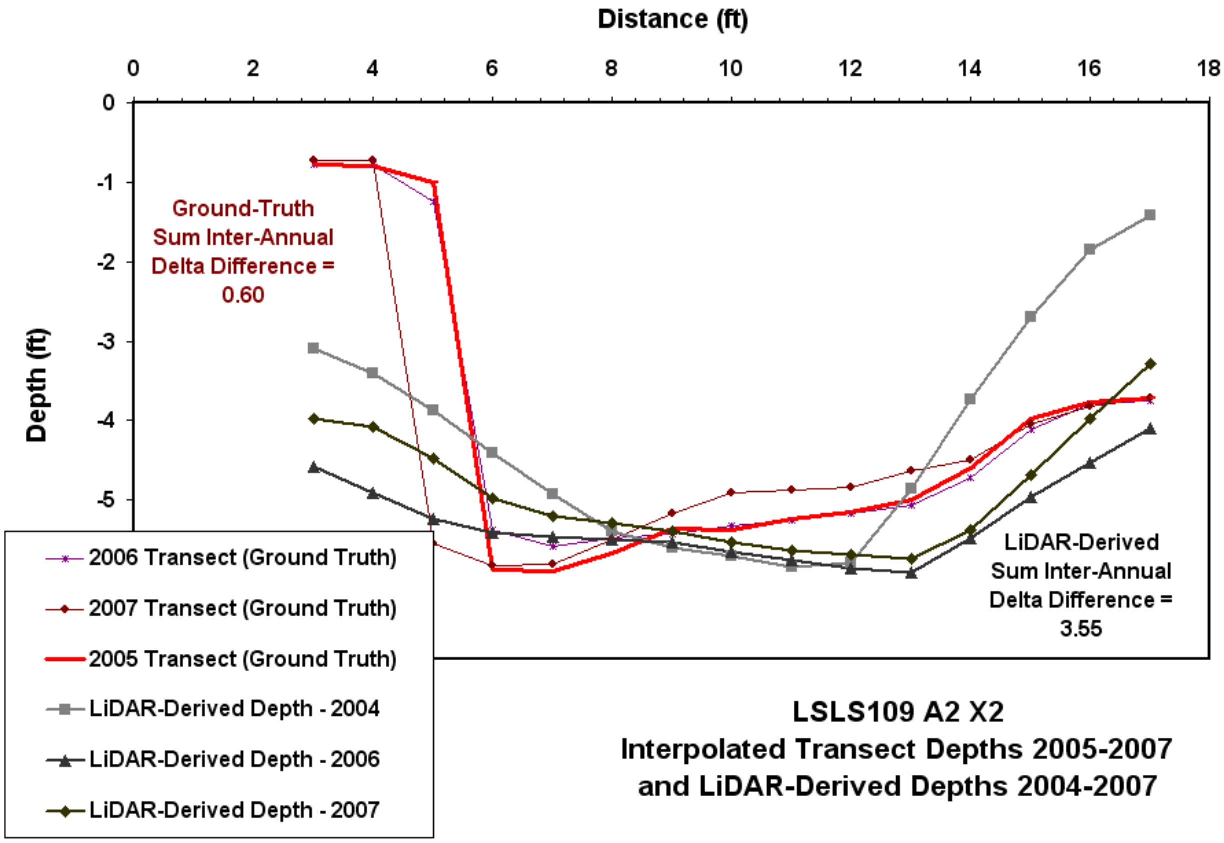


**LSLS109 A2 X2**
**Interpolated Transect Depths 2005-2007**
**and LiDAR-Derived Depths 2004-2007**

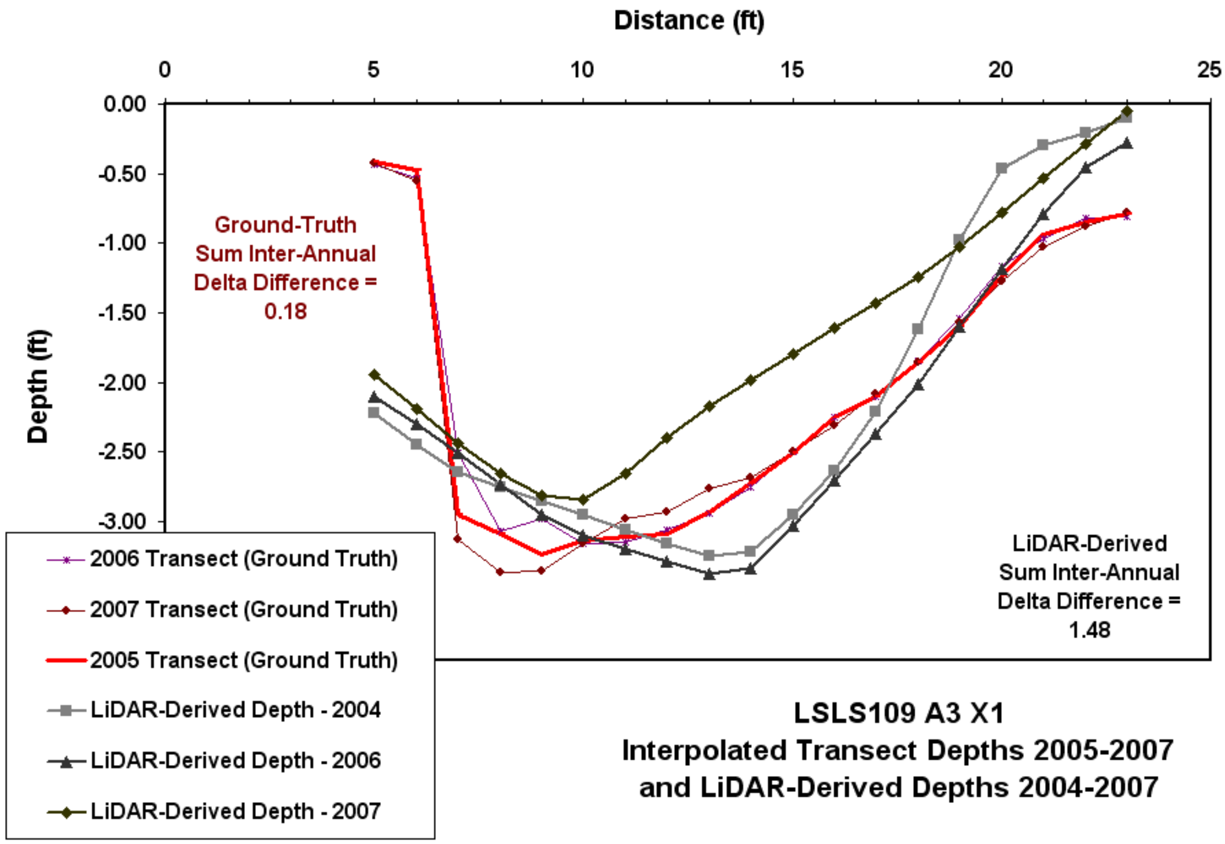


**LSLS109 A3 X1**
**Interpolated Transect Depths 2005-2007**
**and LiDAR-Derived Depths 2004-2007**

Appendix Five: Large-Scale Elevation Changes Shown in LiDAR. Year-to-year differences in 3-foot LiDAR-derived DEMs are shown for sequential years 2002-2004, 2004-2006, 2006-2007, and 2007-2008 for the Sopers Branch, T104, and T109 watersheds within the CSPA. All elevation differences have been scaled to the same metric, with the difference between the later year minus the earlier year shown; increasing red (negative) values indicate that the elevation was greater in the prior year (elevation has decreased over time) while increasing blue (positive) values indicate that the elevation was less in the prior year (elevation has increased over time).

-40.29556274 - -35.23375328
-35.23375327 - -24.09777246
-24.09777245 - -21.06068678
-21.06068677 - -19.03596299
-19.03596298 - -17.01123921
-17.0112392 - -13.97415353
-13.97415352 - -10.93706785
-10.93706784 - -7.899982168
-7.899982167 - -4.862896489
-4.862896488 - -2
-1.999999999 - -1
-0.999999999 - 0
0 - 1
1.000000001 - 2
2.000000001 - 3.742179601
3.742179602 - 7.285446227
7.285446228 - 10.82871285
10.82871286 - 13.86579853
13.86579854 - 16.90288421
16.90288422 - 19.93996989
19.9399699 - 22.47087462
22.47087463 - 24.49559841
24.49559842 - 26.52032219
26.5203222 - 28.54504598
28.54504599 - 30.56976977
30.56976978 - 32.59449355
32.59449356 - 37.65630302
37.65630303 - 47.273741
47.27374101 - 58.40972182
58.40972183 - 73.59515022
73.59515023 - 88.78057861

Legend for Large-Scale Elevation Changes

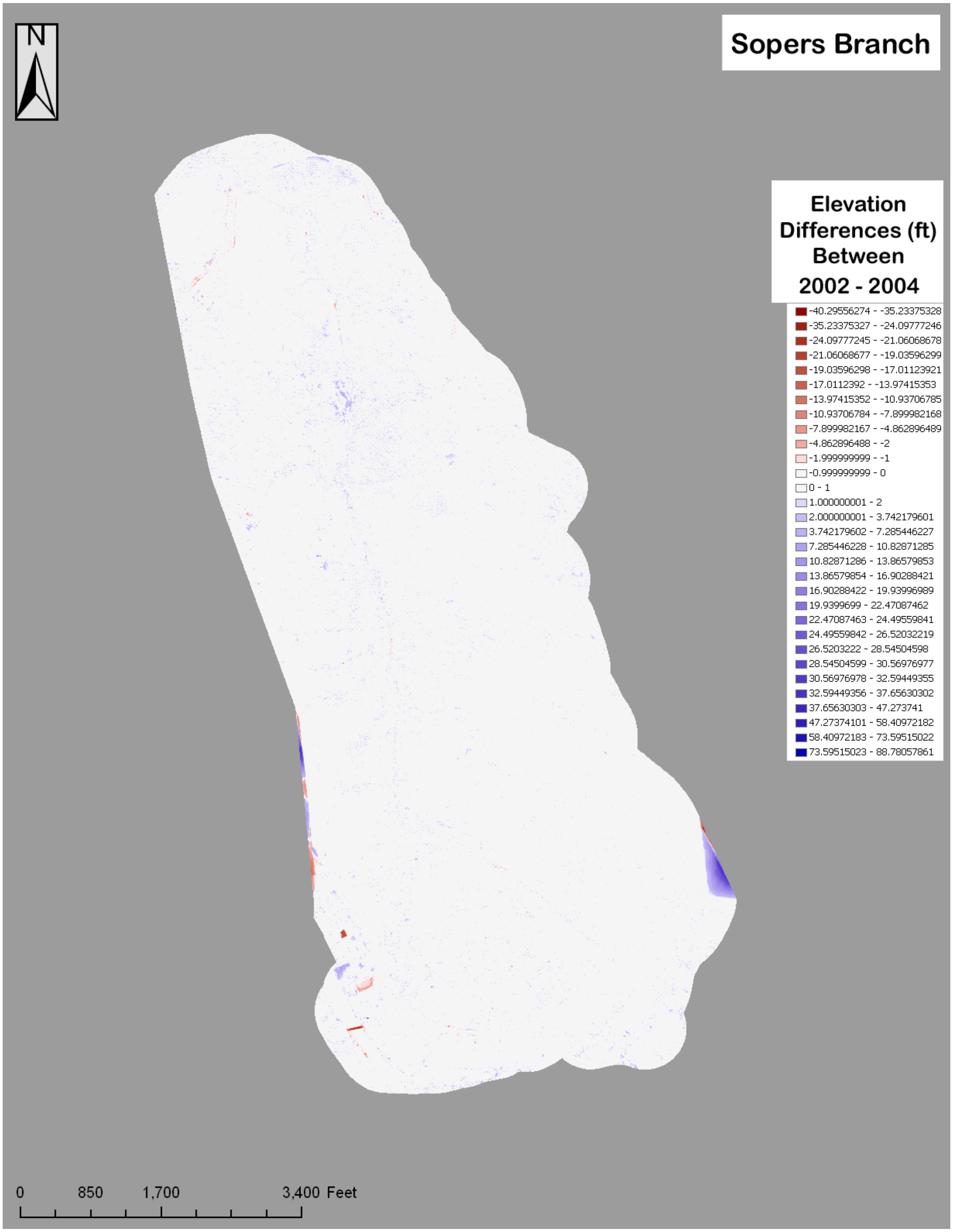


Sopers Branch 2002-2004

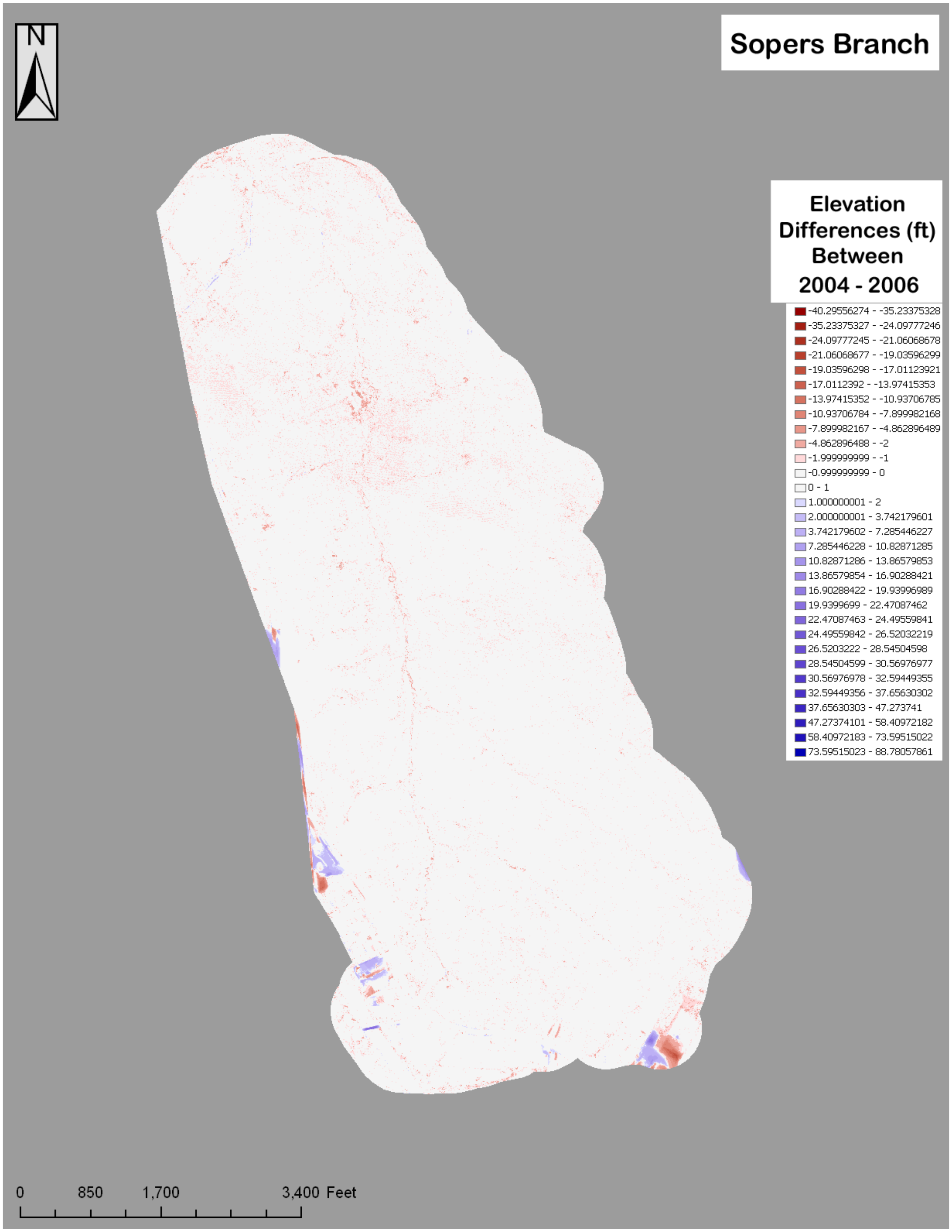


Sopers Branch 2004-2006


Sopers Branch 2006-2007

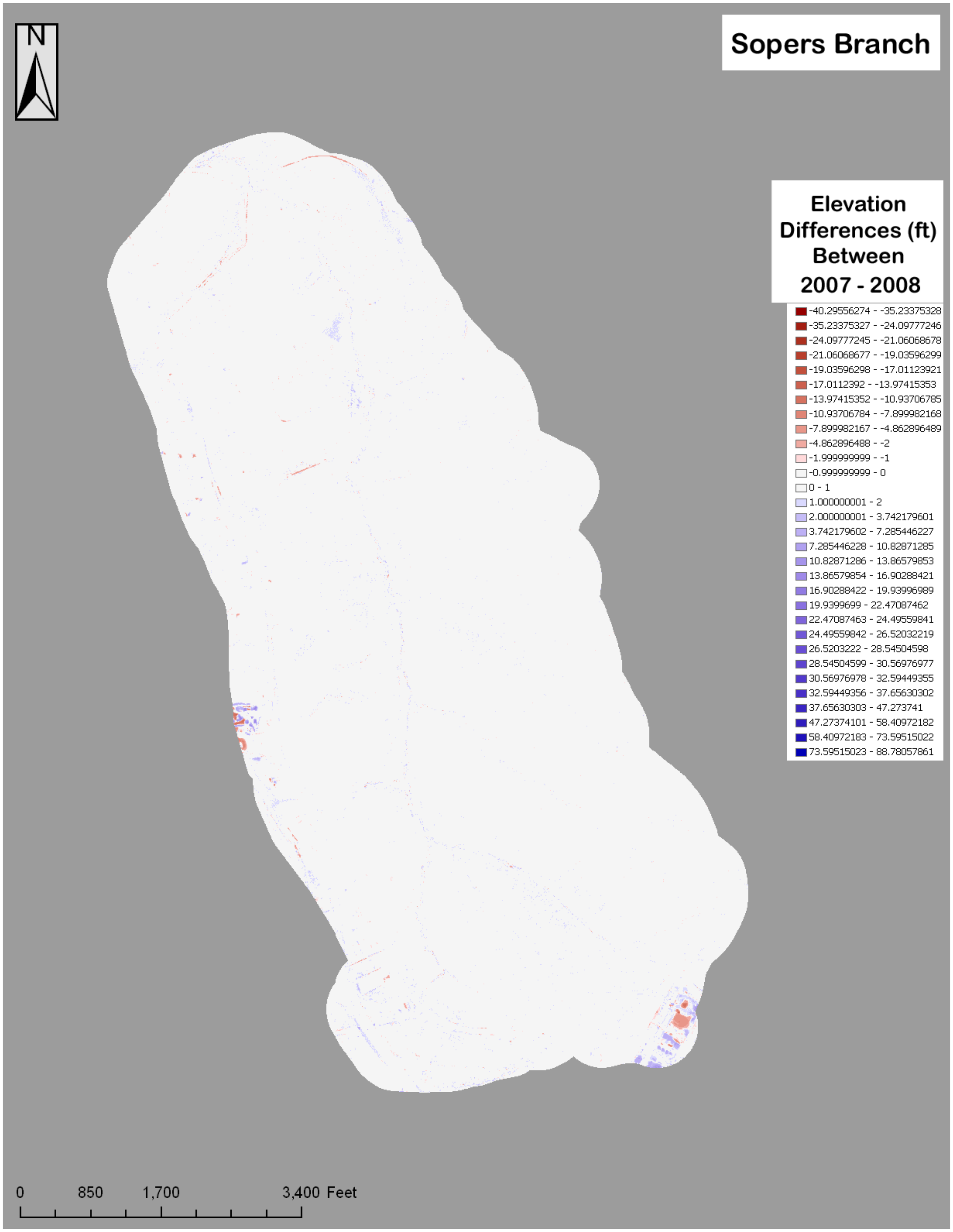


Sopers Branch 2007-2008

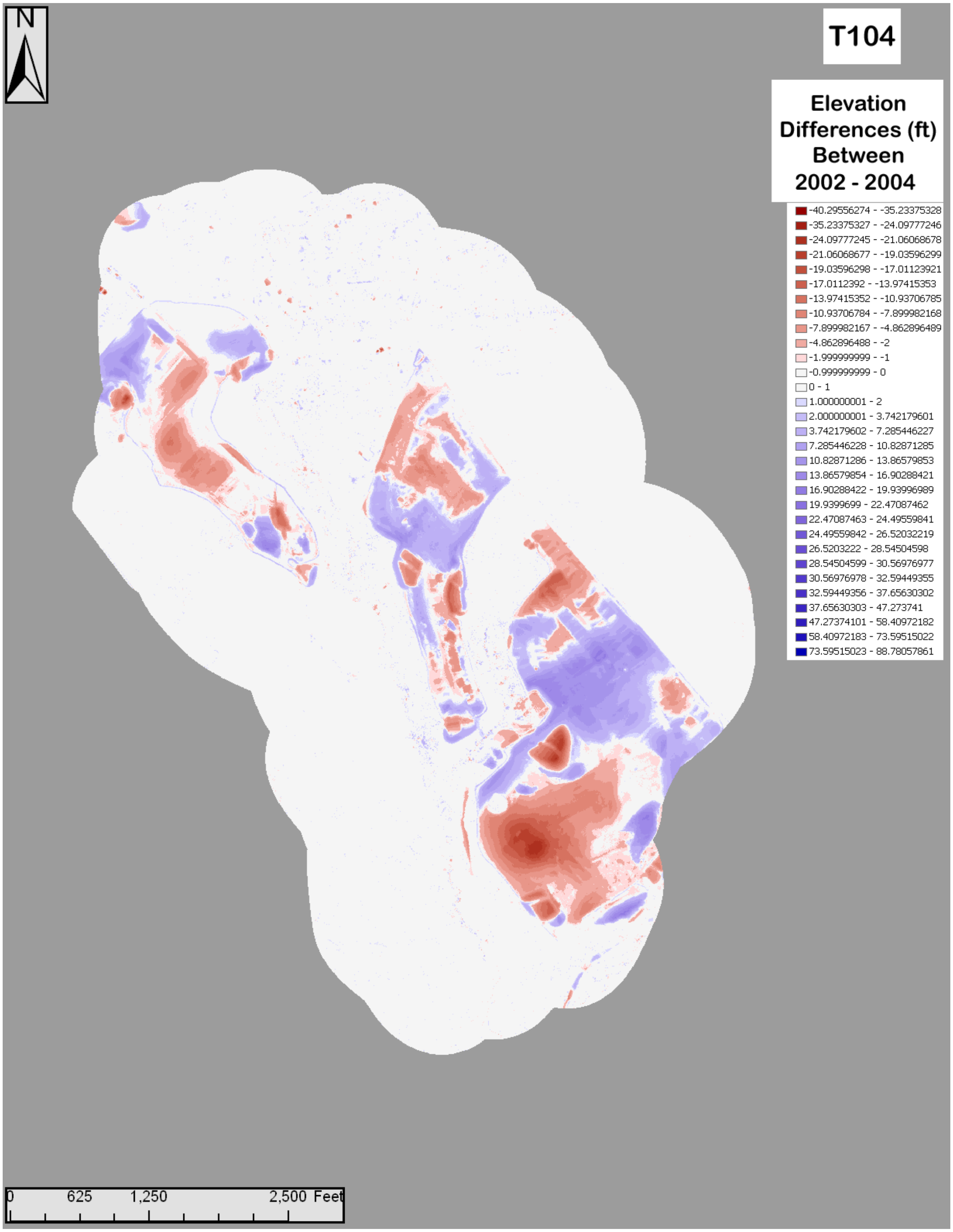


T104 2002-2004

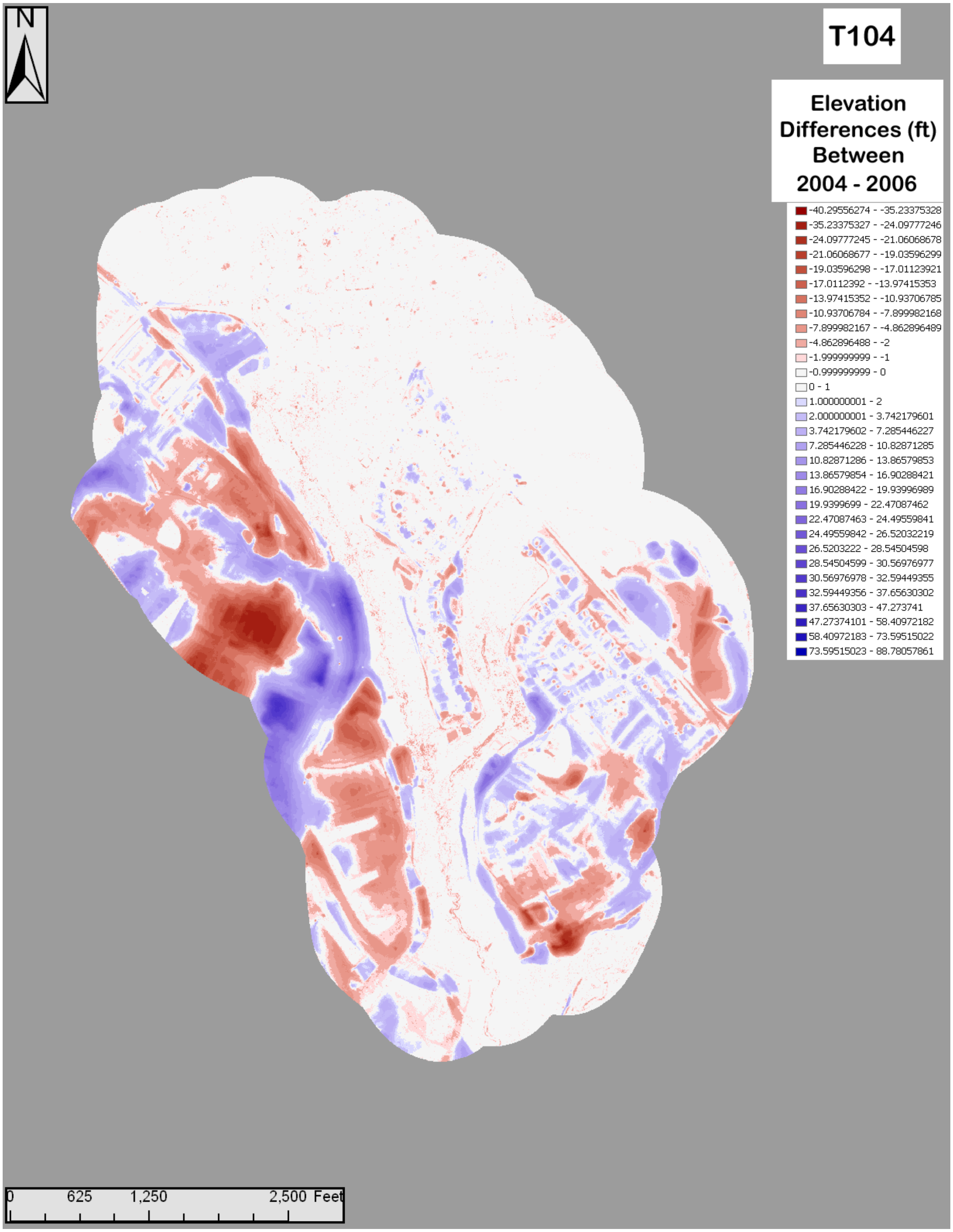


T104 2004-2006

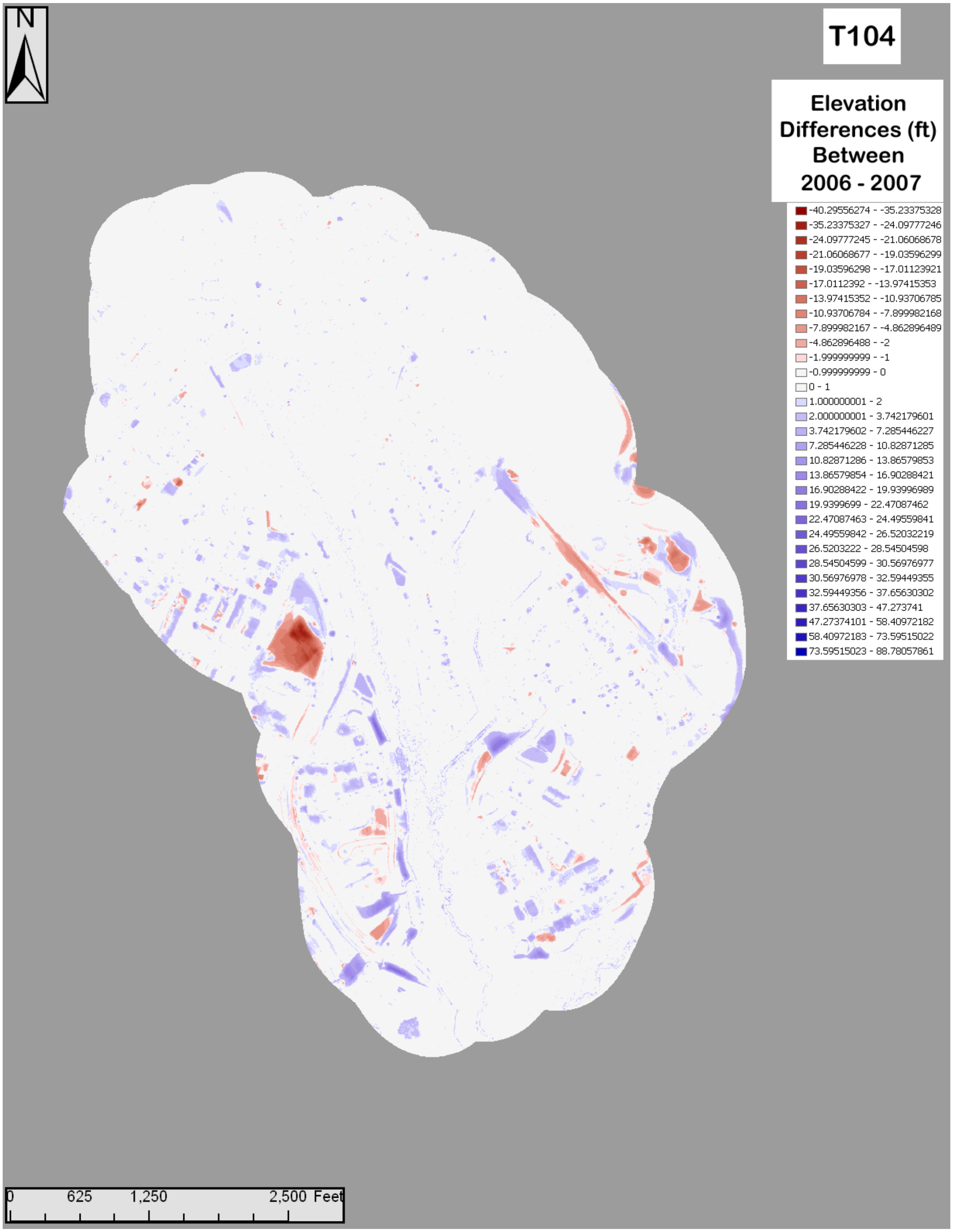


T104 2006-2007

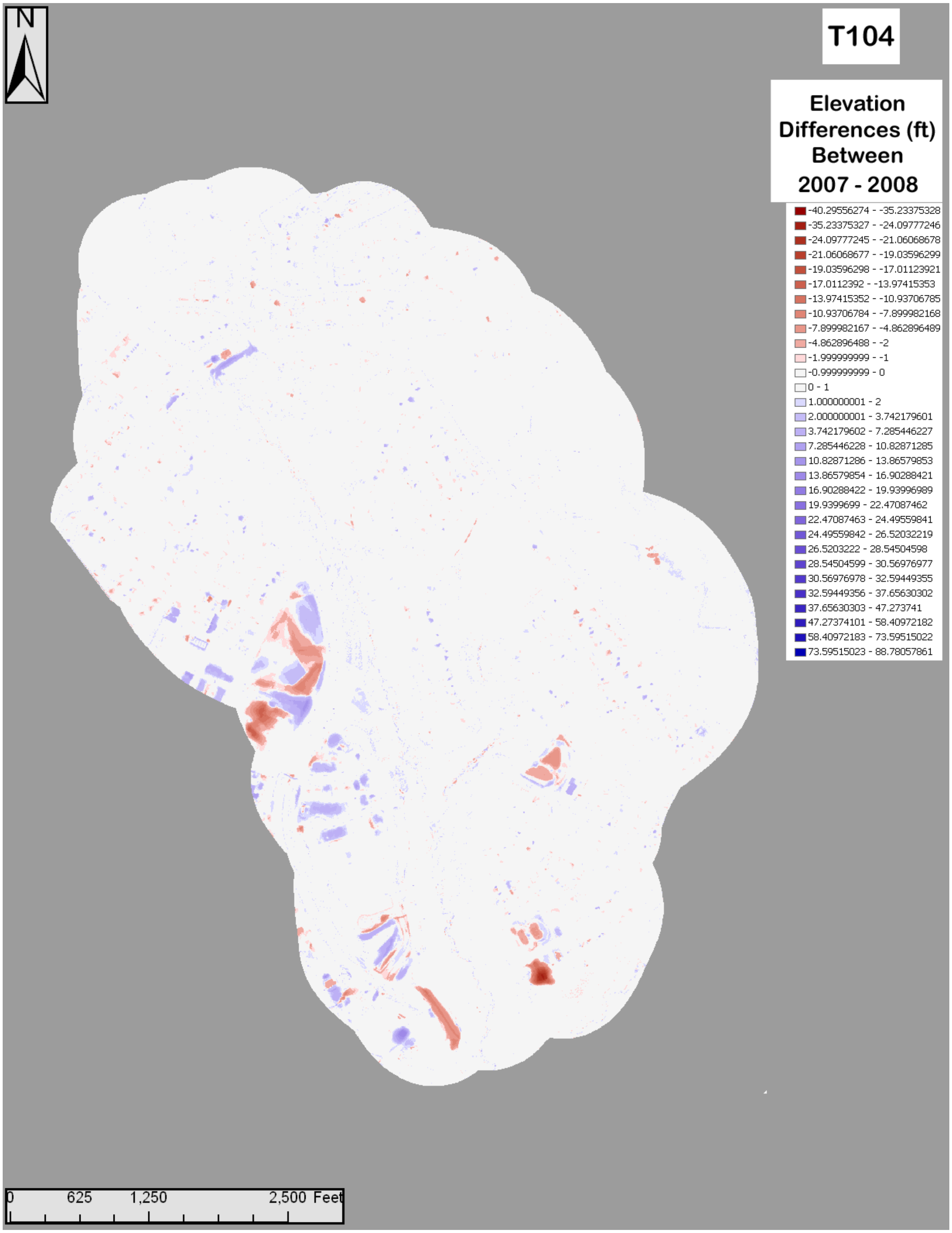


T104 2007-2008

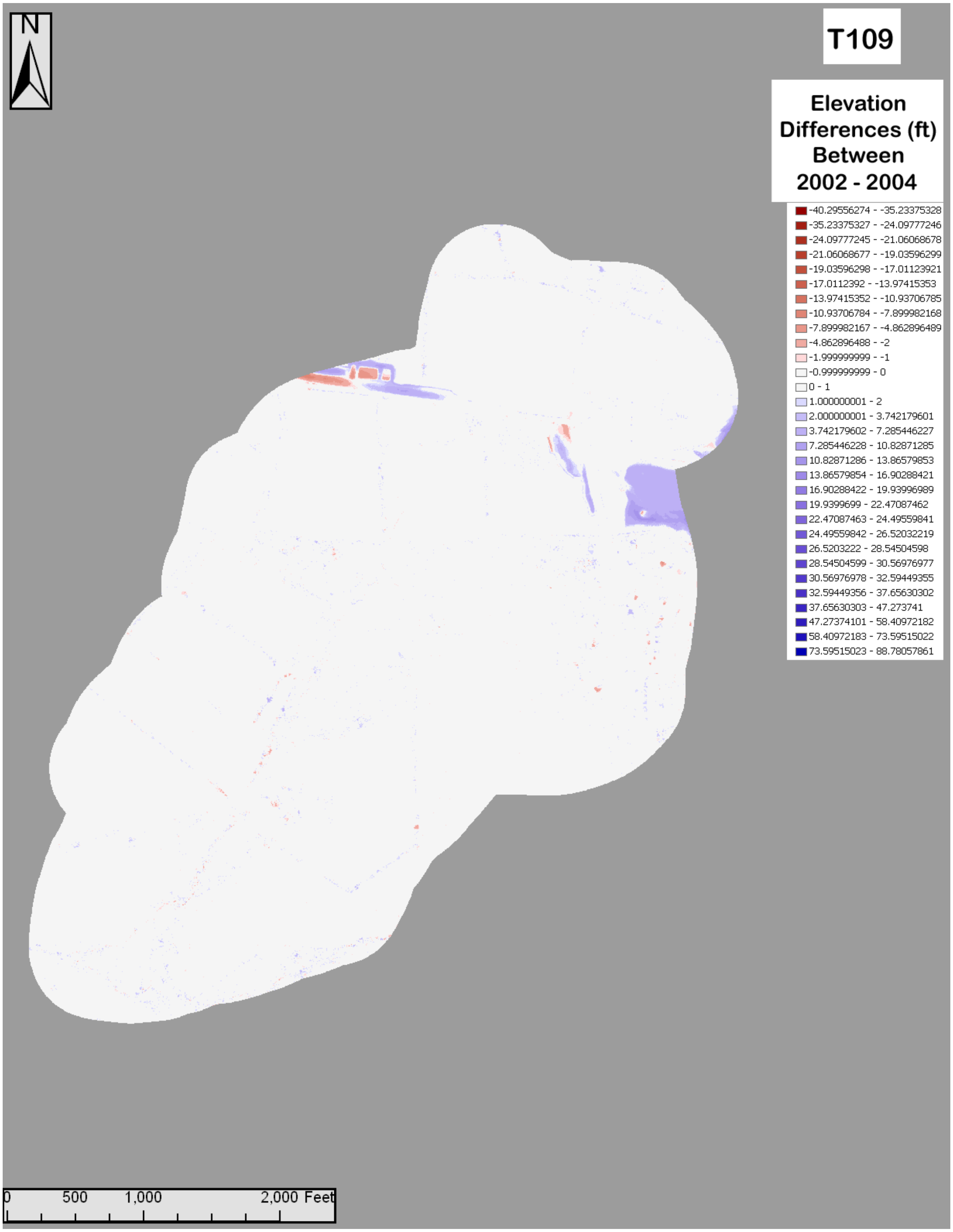


T109 2002-2004

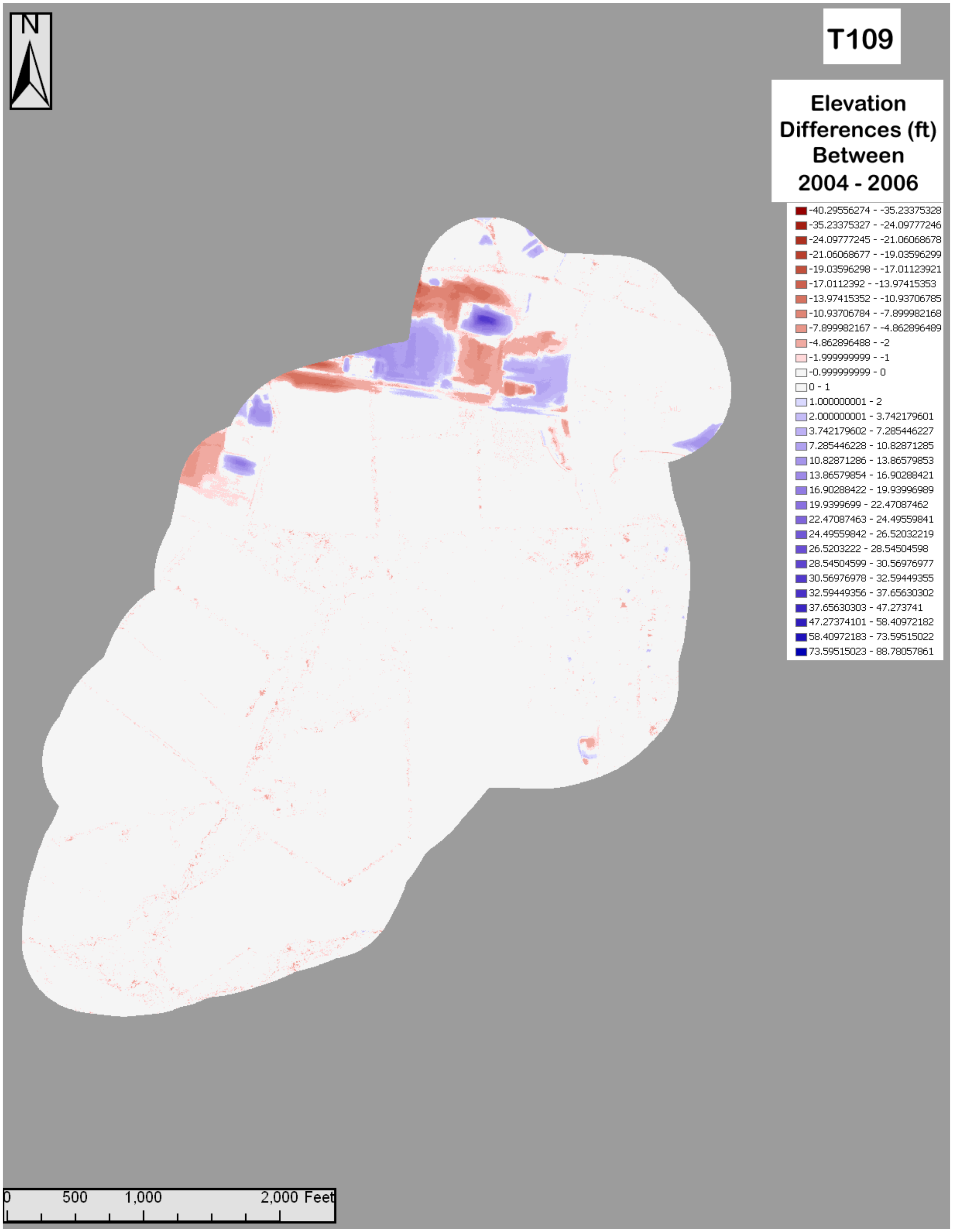


T109 2004-2006

L

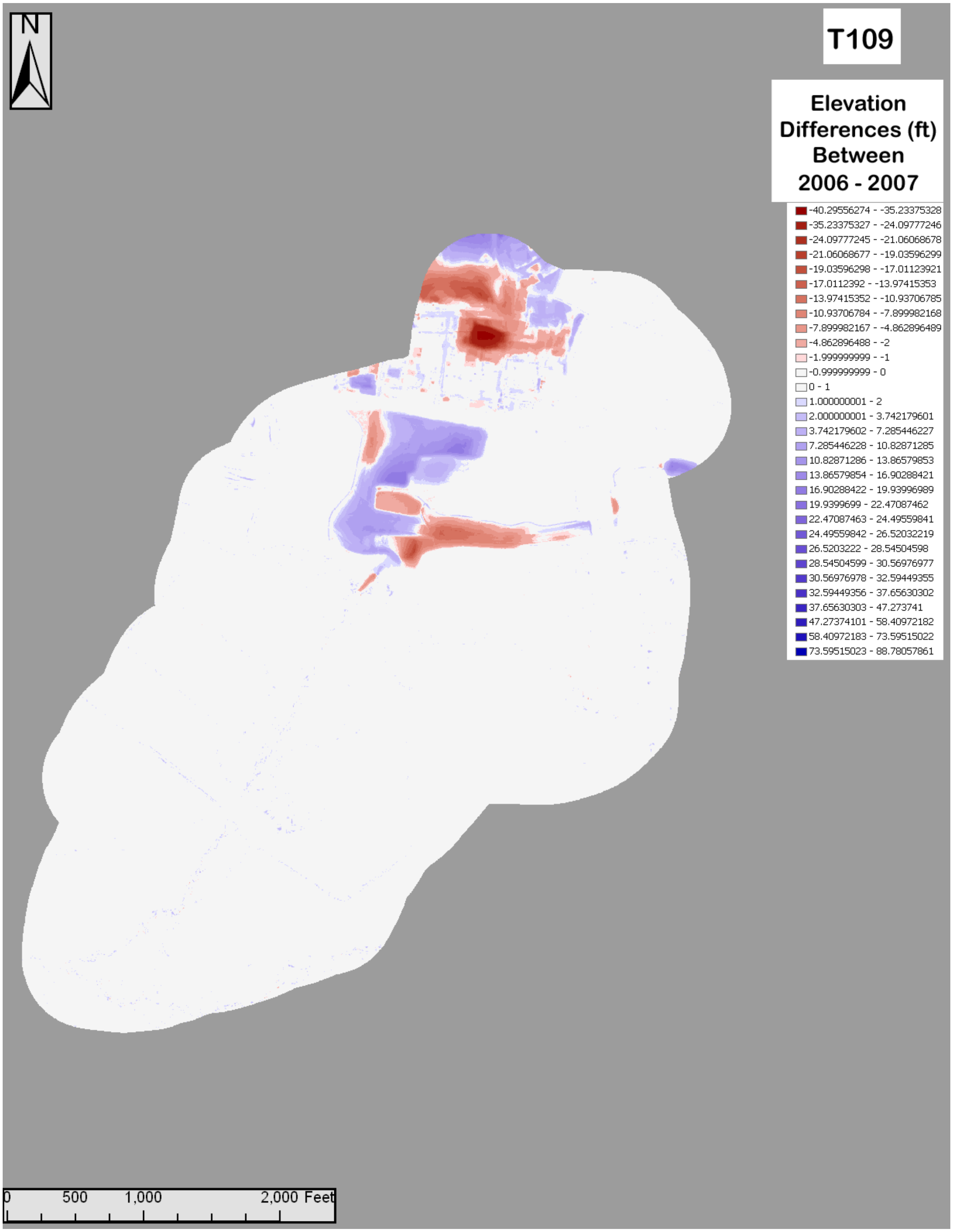


T109 2006-2007

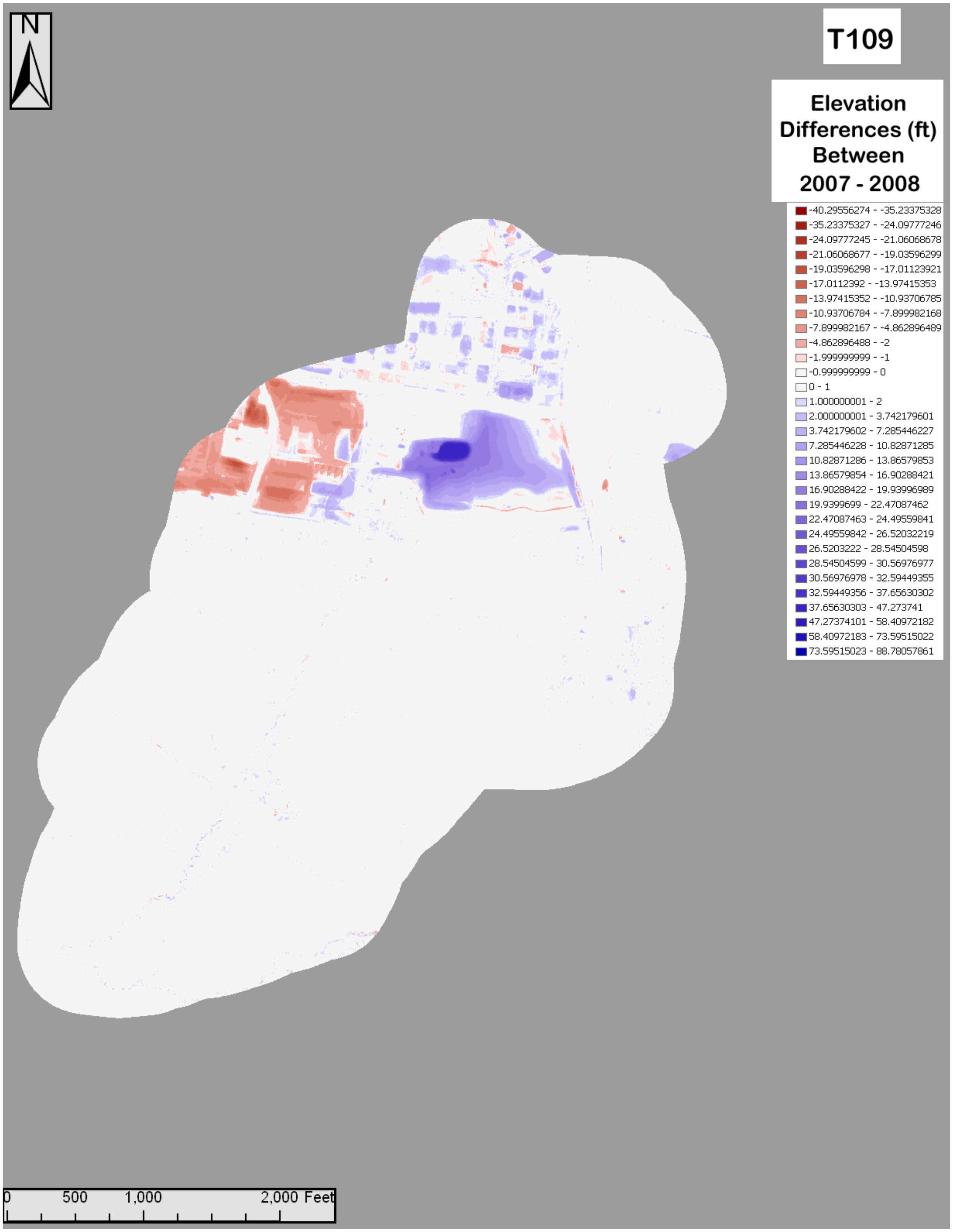


T109 2007-2008

Appendix Six: Individual Between-Year Differences in LiDAR-Derived DEM Precision by Slope Gradient by LULC

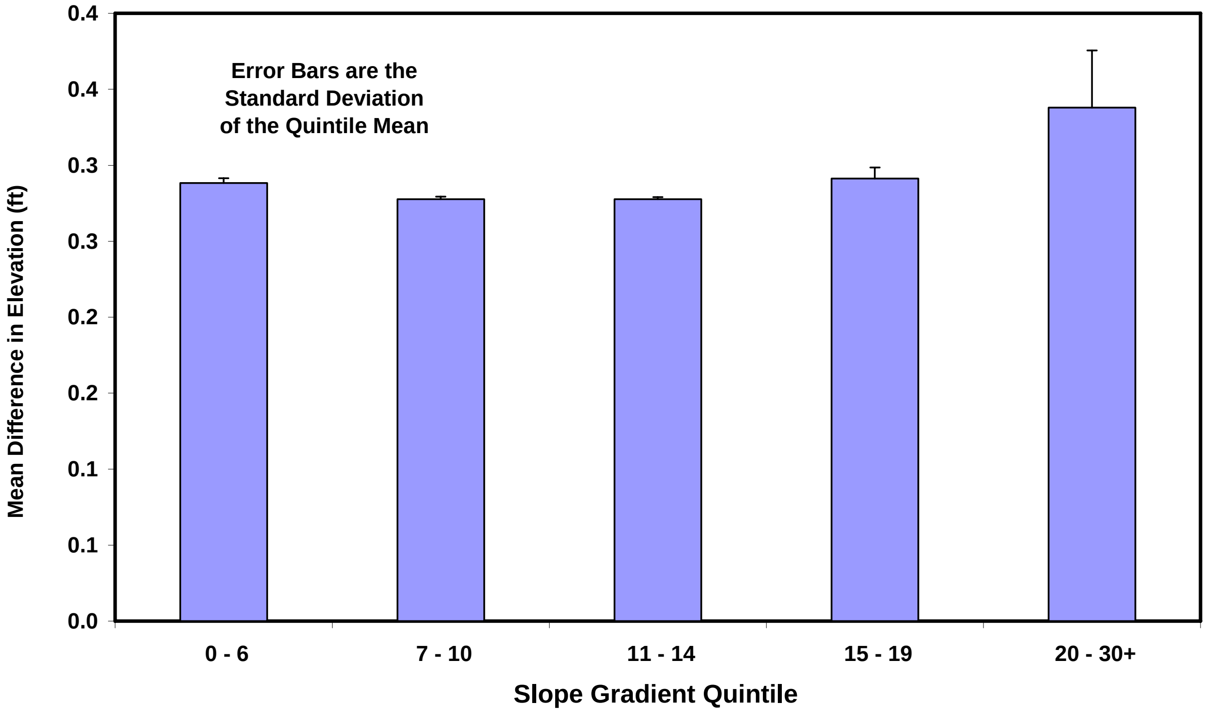


**2004-2002 Forest No-Change Land Cover, Sopers Branch: Mean Difference in Elevation by Slope Gradient Quintile**

| Quintile Slope Groups | Quintile n | Mean Diff 04 - 02 | Std Dev |
|---|---|---|---|
| 0 - 6 | 725651 | 0.288 | 0.003 |
| 7 - 10 | 870697 | 0.278 | 0.002 |
| 11 - 14 | 883311 | 0.278 | 0.001 |
| 15 - 19 | 811196 | 0.291 | 0.007 |
| 20 - 30+ | 856888 | 0.338 | 0.038 |

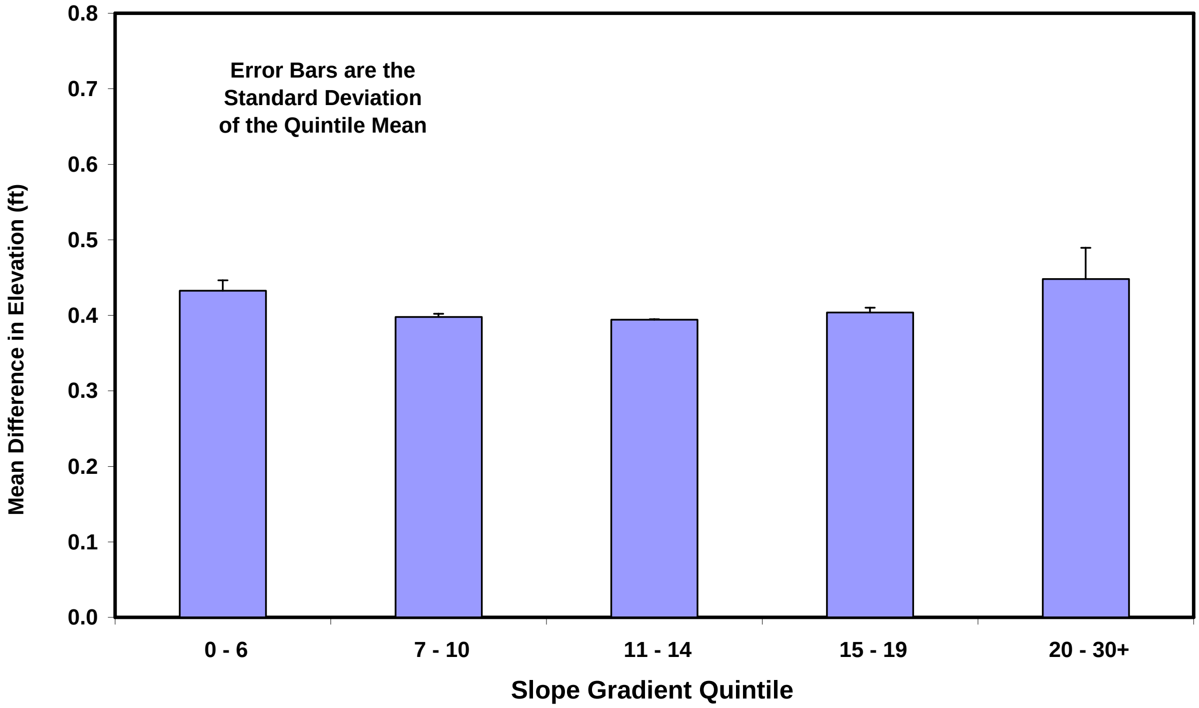


**2006-2004 Forest No-Change Land Cover, Sopers Branch:**
**Mean Difference in Elevation by Slope Gradient Quintile**

| Quintile Slope Groups | Quintile n | Mean Diff 06 - 04 | Std Dev |
|---|---|---|---|
| 0 - 6 | 725651 | 0.433 | 0.014 |
| 7 - 10 | 870697 | 0.398 | 0.004 |
| 11 - 14 | 883311 | 0.394 | 0.001 |
| 15 - 19 | 811196 | 0.404 | 0.006 |
| 20 - 30+ | 856888 | 0.448 | 0.041 |

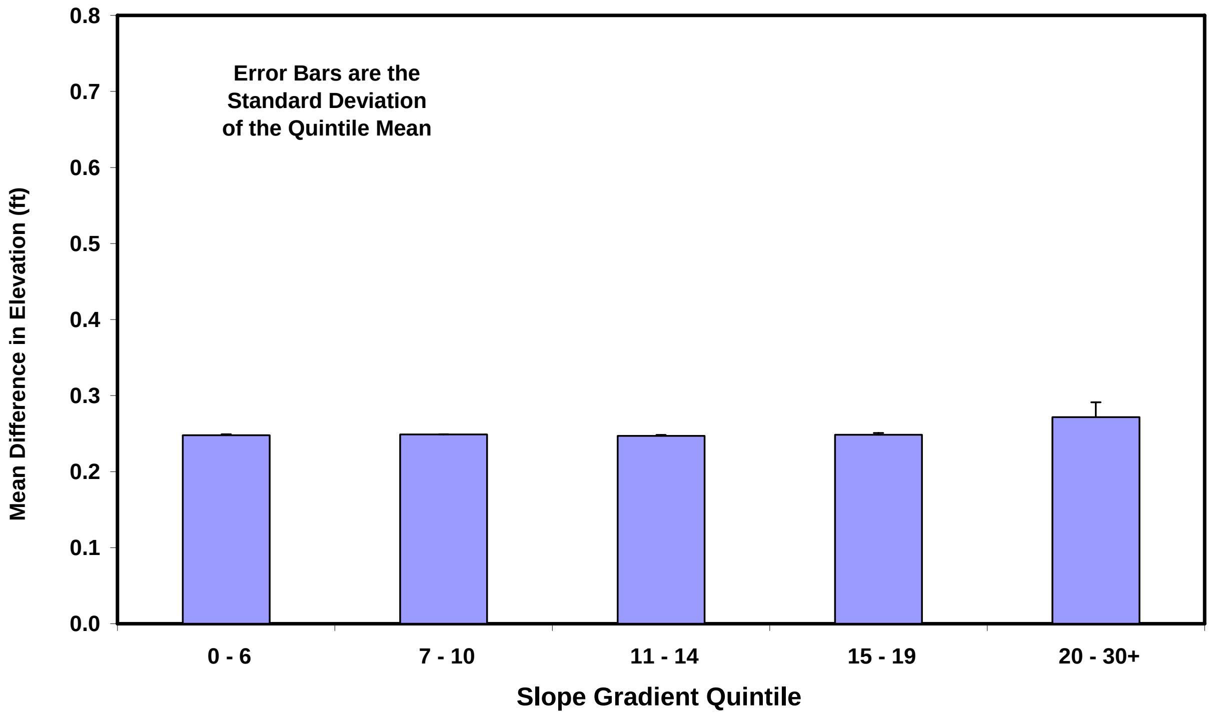


**2007-2006 Forest No-Change Land Cover, Sopers Branch:**
**Mean Difference in Elevation by Slope Gradient Quintile**

| Quintile Slope Groups | Quintile n | Mean Diff 07 - 06 | Std Dev |
|---|---|---|---|
| 0 - 6 | 725651 | 0.248 | 0.001 |
| 7 - 10 | 870697 | 0.249 | 0.000 |
| 11 - 14 | 883311 | 0.247 | 0.001 |
| 15 - 19 | 811196 | 0.249 | 0.002 |
| 20 - 30+ | 856888 | 0.272 | 0.020 |

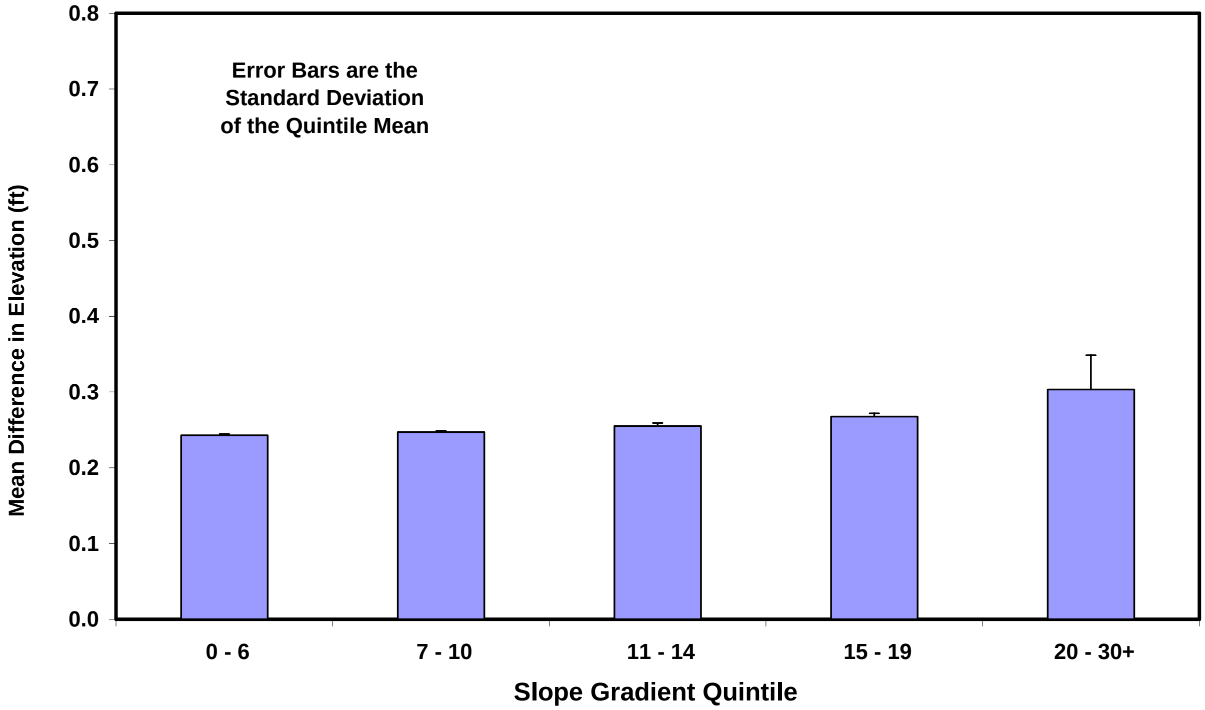


**2008-2007 Forest No-Change Land Cover, Sopers Branch:**
**Mean Difference in Elevation by Slope Gradient Quintile**

| Quintile Slope Groups | Quintile n | Mean Diff 08-07 | Std Dev |
|---|---|---|---|
| 0 - 6 | 725651 | 0.243 | 0.002 |
| 7 - 10 | 870697 | 0.247 | 0.002 |
| 11 - 14 | 883311 | 0.255 | 0.004 |
| 15 - 19 | 811196 | 0.268 | 0.004 |
| 20 - 30+ | 856888 | 0.303 | 0.045 |

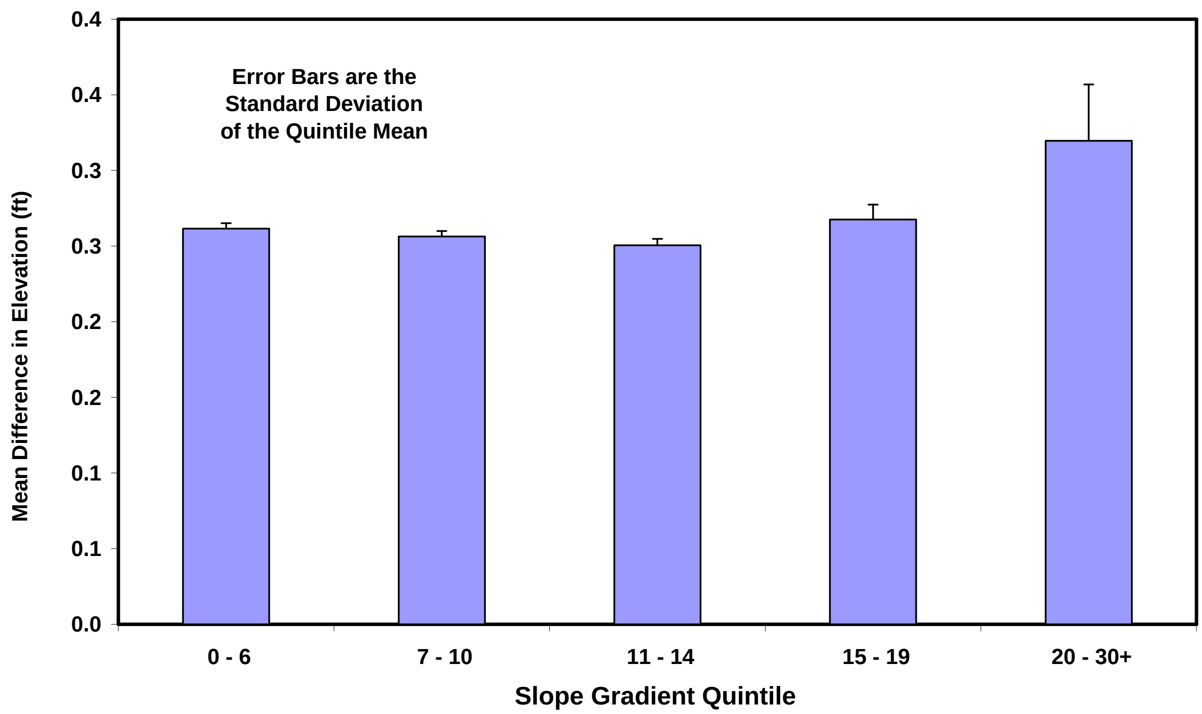


**2004-2002 Forest No-Change Land Cover, T104:**
**Mean Difference in Elevation by Slope Gradient Quintile**

| Quintile Slope Groups | Quintile n | Mean Diff 04 - 02 | Std Dev |
|---|---|---|---|
| 0 - 6 | 70616 | 0.262 | 0.004 |
| 7 - 10 | 68418 | 0.256 | 0.004 |
| 11 - 14 | 71703 | 0.251 | 0.004 |
| 15 - 19 | 71926 | 0.268 | 0.010 |
| 20 - 30+ | 99502 | 0.320 | 0.037 |

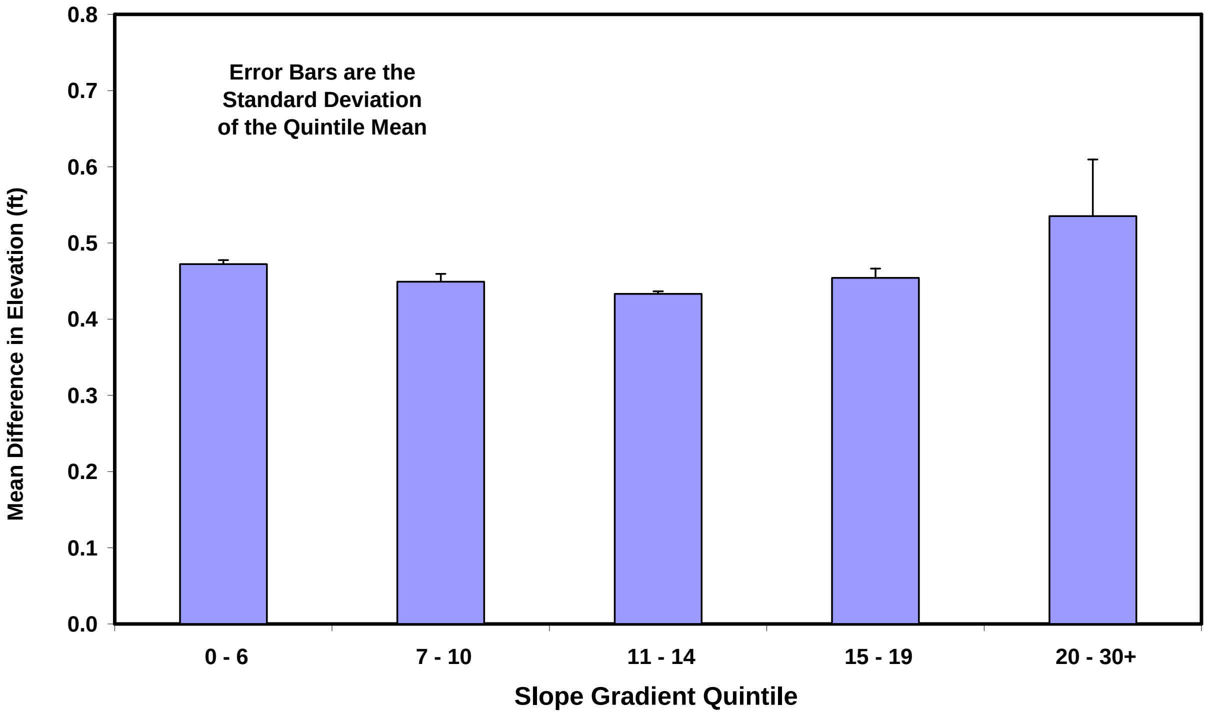


**2006-2004 Forest No-Change Land Cover, T104:**
**Mean Difference in Elevation by Slope Gradient Quintile**

| Quintile Slope Groups | Quintile n | Mean Diff 06 - 04 | Std Dev |
|---|---|---|---|
| 0 - 6 | 70616 | 0.472 | 0.005 |
| 7 - 10 | 68418 | 0.449 | 0.010 |
| 11 - 14 | 71703 | 0.433 | 0.003 |
| 15 - 19 | 71926 | 0.454 | 0.012 |
| 20 - 30+ | 99502 | 0.535 | 0.074 |

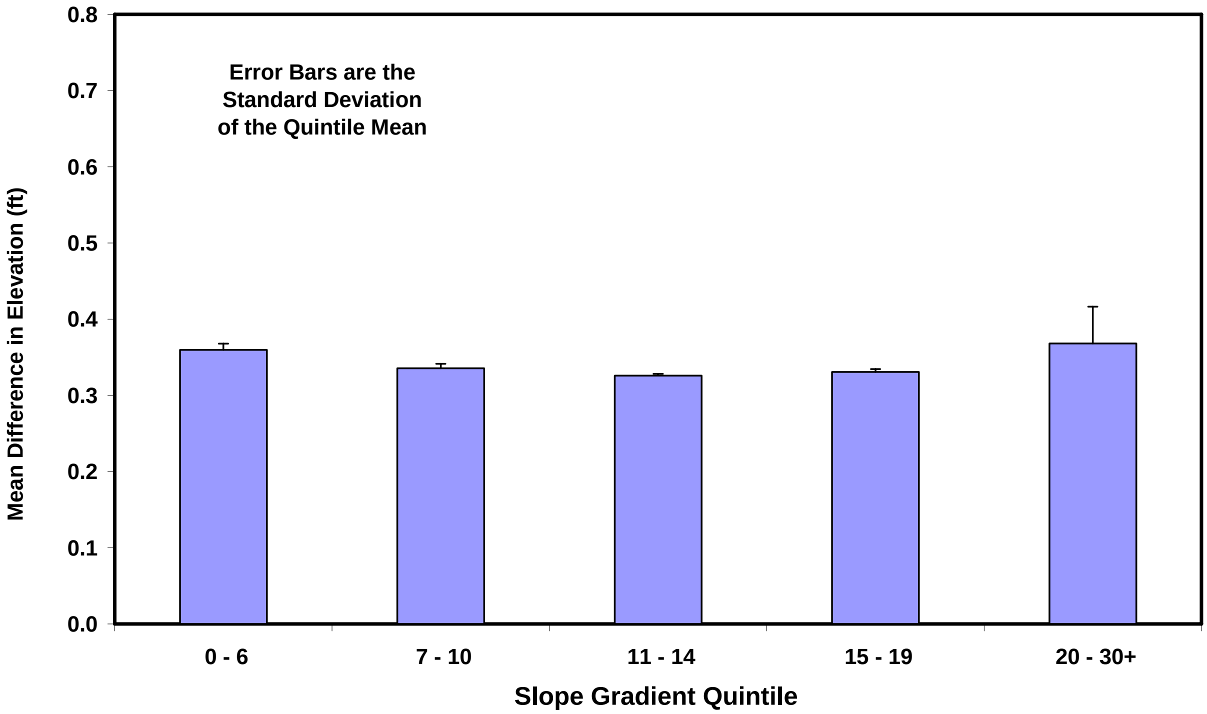


**2007-2006 Forest No-Change Land Cover, T104:**
**Mean Difference in Elevation by Slope Gradient Quintile**

| Quintile Slope Groups | Quintile n | Mean Diff 07 - 06 | Std Dev |
|---|---|---|---|
| 0 - 6 | 70616 | 0.360 | 0.008 |
| 7 - 10 | 68418 | 0.335 | 0.006 |
| 11 - 14 | 71703 | 0.326 | 0.002 |
| 15 - 19 | 71926 | 0.331 | 0.004 |
| 20 - 30+ | 99502 | 0.368 | 0.048 |

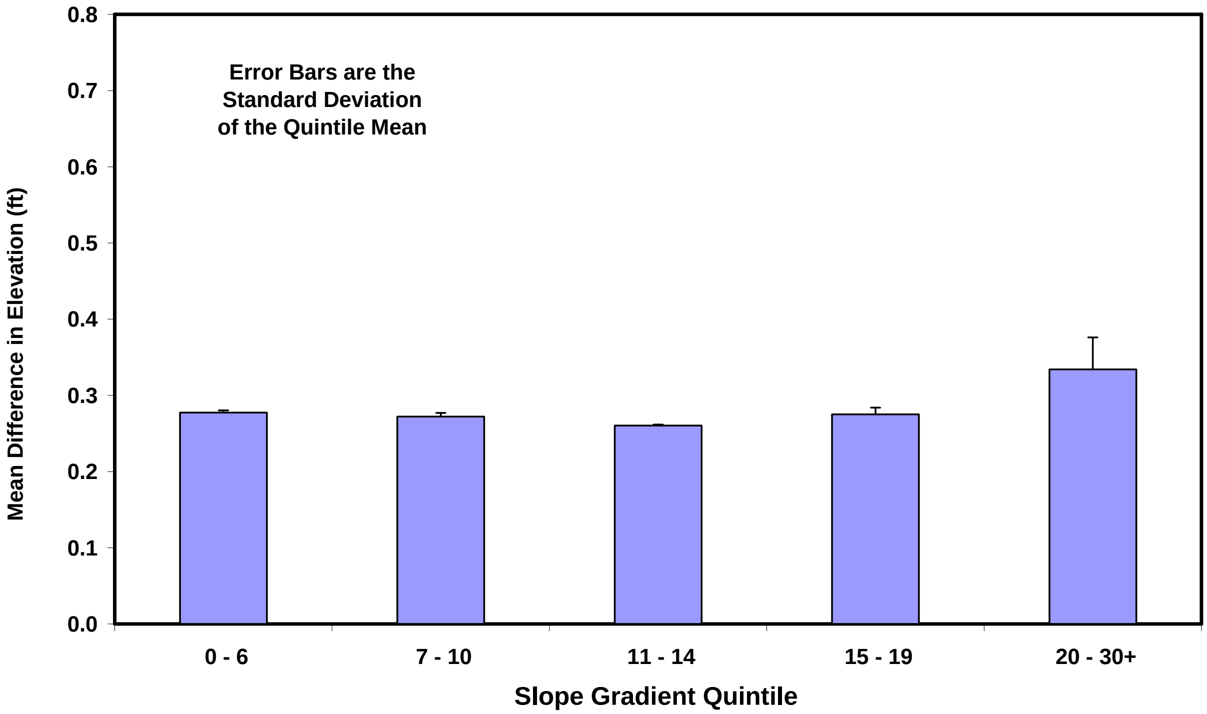


**2008-2007 Forest No-Change Land Cover, T104:**
**Mean Difference in Elevation by Slope Gradient Quintile**

| Quintile Slope Groups | Quintile n | Mean Diff 08-07 | Std Dev |
|---|---|---|---|
| 0 - 6 | 70616 | 0.277 | 0.003 |
| 7 - 10 | 68418 | 0.272 | 0.005 |
| 11 - 14 | 71703 | 0.260 | 0.001 |
| 15 - 19 | 71926 | 0.275 | 0.009 |
| 20 - 30+ | 99502 | 0.334 | 0.042 |

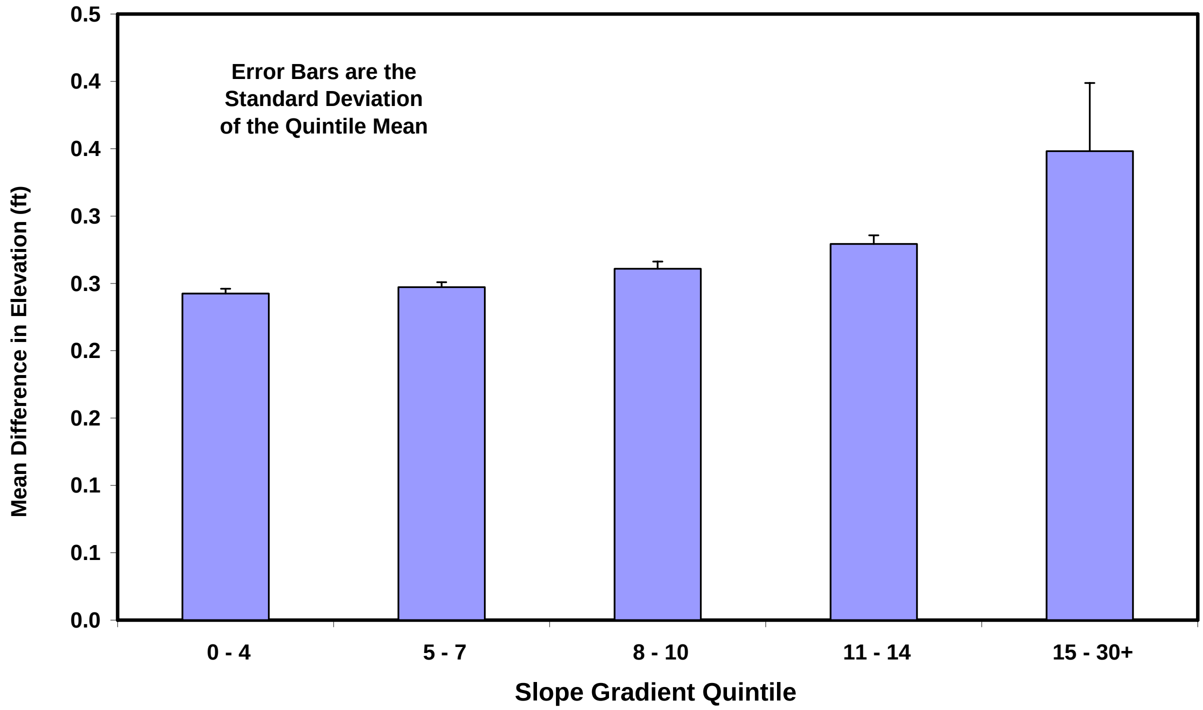


**2004-2002 Forest No-Change Land Cover, T109:**
**Mean Difference in Elevation by Slope Gradient Quintile**

| Quintile Slope Groups | Quintile n | Mean Diff 04 - 02 | Std Dev |
|---|---|---|---|
| 0 - 4 | 80026 | 0.242 | 0.004 |
| 5 - 7 | 106454 | 0.247 | 0.004 |
| 8 - 10 | 98950 | 0.261 | 0.005 |
| 11 - 14 | 87391 | 0.279 | 0.006 |
| 15 - 30+ | 88943 | 0.348 | 0.051 |

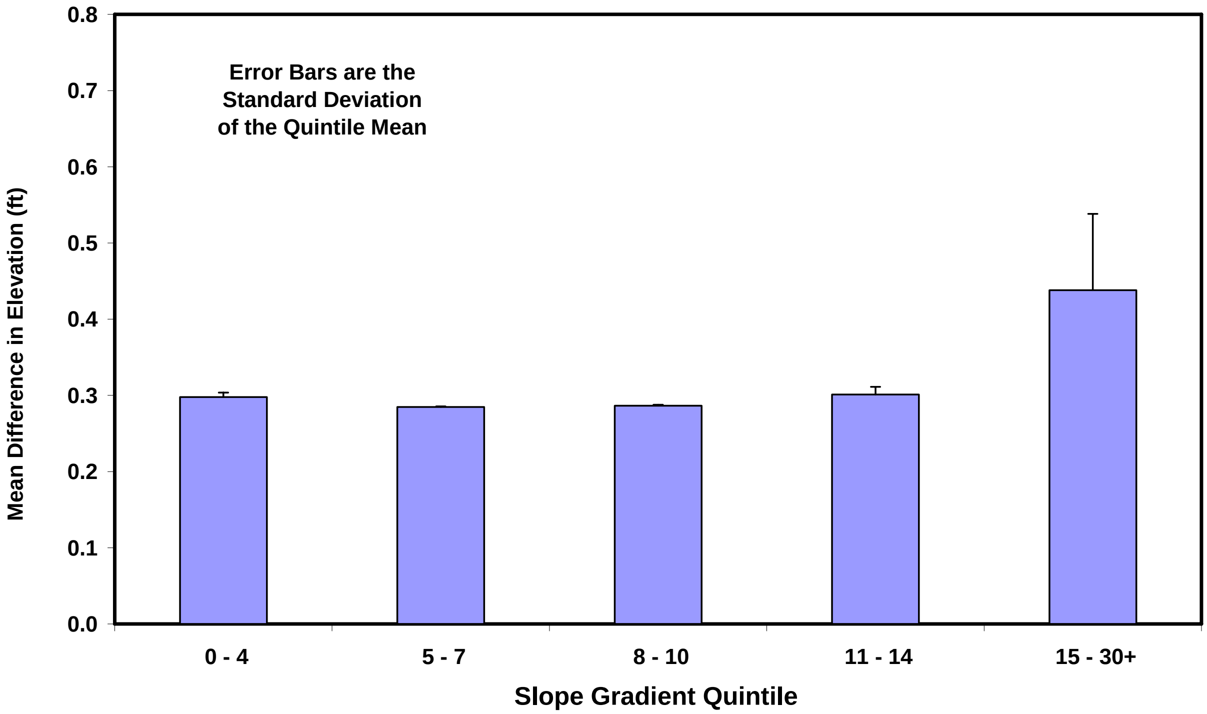


**2006-2004 Forest No-Change Land Cover, T109:**
**Mean Difference in Elevation by Slope Gradient Quintile**

| Quintile Slope Groups | Quintile n | Mean Diff 06 - 04 | Std Dev |
|---|---|---|---|
| 0 - 4 | 80026 | 0.298 | 0.006 |
| 5 - 7 | 106454 | 0.285 | 0.001 |
| 8 - 10 | 98950 | 0.286 | 0.002 |
| 11 - 14 | 87391 | 0.301 | 0.010 |
| 15 - 30+ | 88943 | 0.438 | 0.100 |

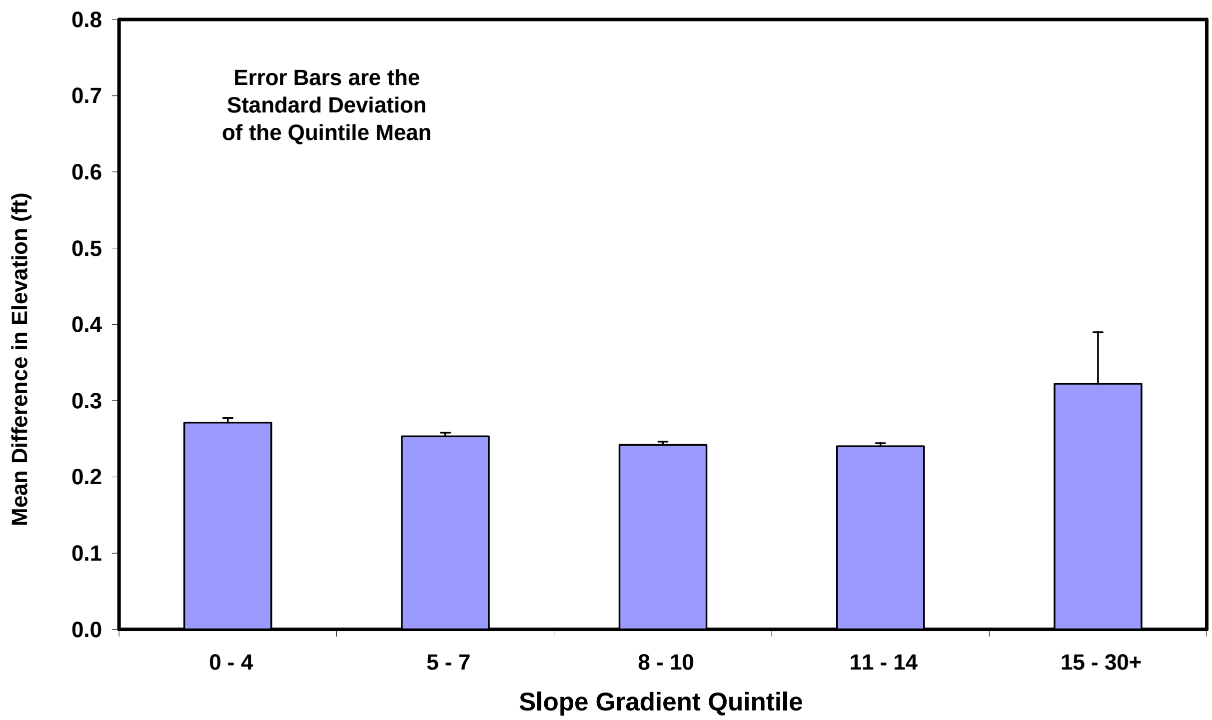


**2007-2006 Forest No-Change Land Cover, T109:
Mean Difference in Elevation by Slope Gradient Quintile**

| Quintile Slope Groups | Quintile n | Mean Diff 07 - 06 | Std Dev |
|---|---|---|---|
| 0 - 4 | 80026 | 0.271 | 0.006 |
| 5 - 7 | 106454 | 0.253 | 0.005 |
| 8 - 10 | 98950 | 0.242 | 0.004 |
| 11 - 14 | 87391 | 0.240 | 0.004 |
| 15 - 30+ | 88943 | 0.322 | 0.068 |

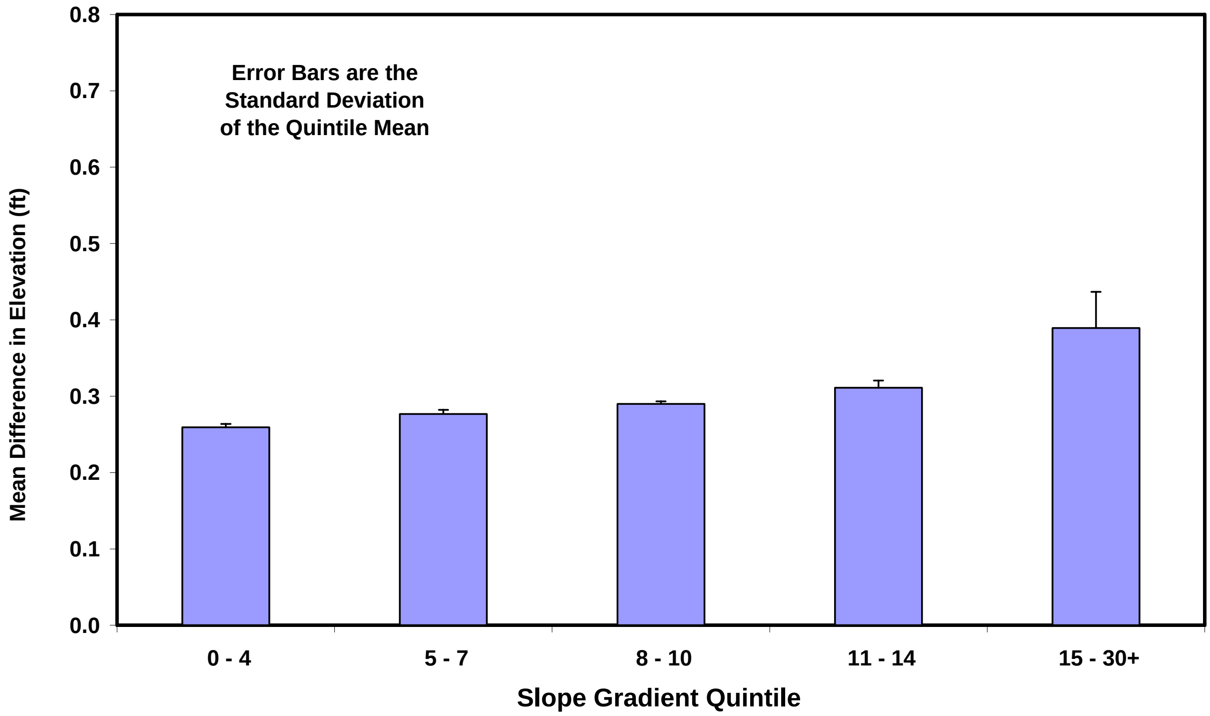


**2008-2007 Forest No-Change Land Cover, T109:**
**Mean Difference in Elevation by Slope Gradient Quintile**

| Quintile Slope Groups | Quintile n | Mean Diff 08-07 | Std Dev |
|---|---|---|---|
| 0 - 4 | 80026 | 0.259 | 0.004 |
| 5 - 7 | 106454 | 0.277 | 0.006 |
| 8 - 10 | 98950 | 0.290 | 0.003 |
| 11 - 14 | 87391 | 0.311 | 0.009 |
| 15 - 30+ | 88943 | 0.389 | 0.048 |

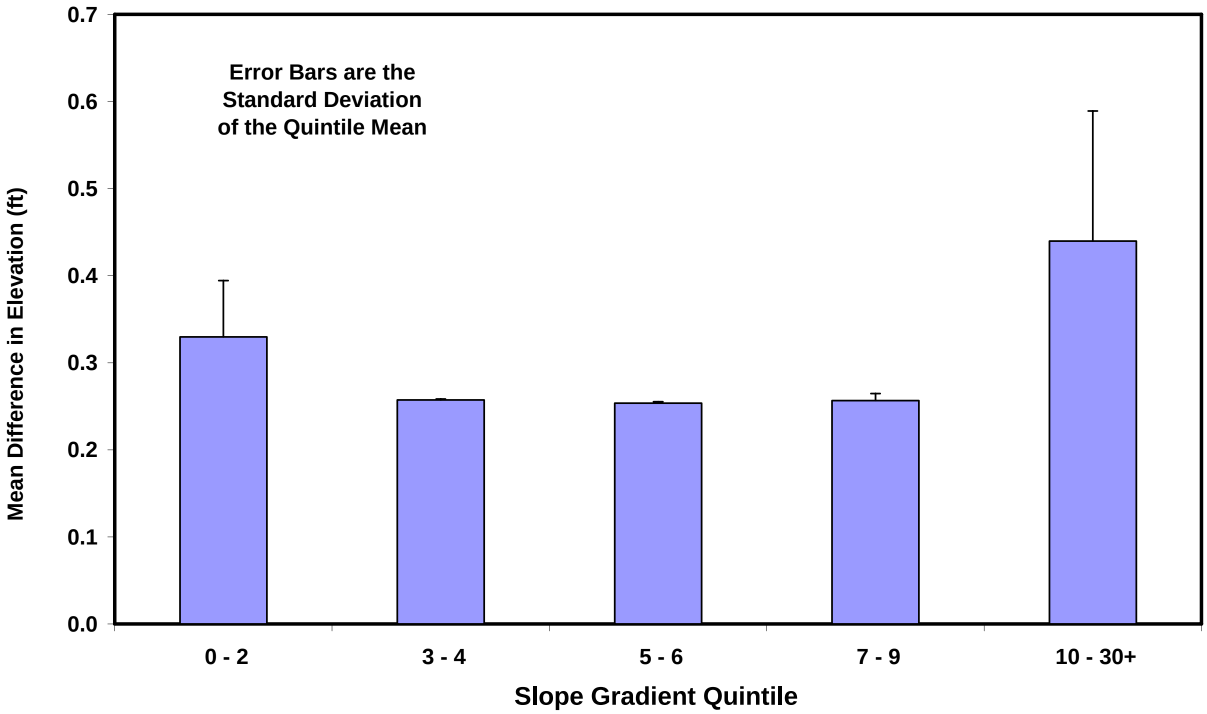


**2004-2002 Impervious Surface No-Change Land Cover, Sopers Branch: Mean Difference in Elevation by Slope Gradient Quintile**

| Quintile Slope Groups | Quintile n | Mean Diff 04 - 02 | Std Dev |
|---|---|---|---|
| 0 - 2 | 36243 | 0.330 | 0.065 |
| 3 - 4 | 54216 | 0.257 | 0.001 |
| 5 - 6 | 45313 | 0.254 | 0.002 |
| 7 - 9 | 36238 | 0.257 | 0.008 |
| 10 - 30+ | 26169 | 0.440 | 0.149 |

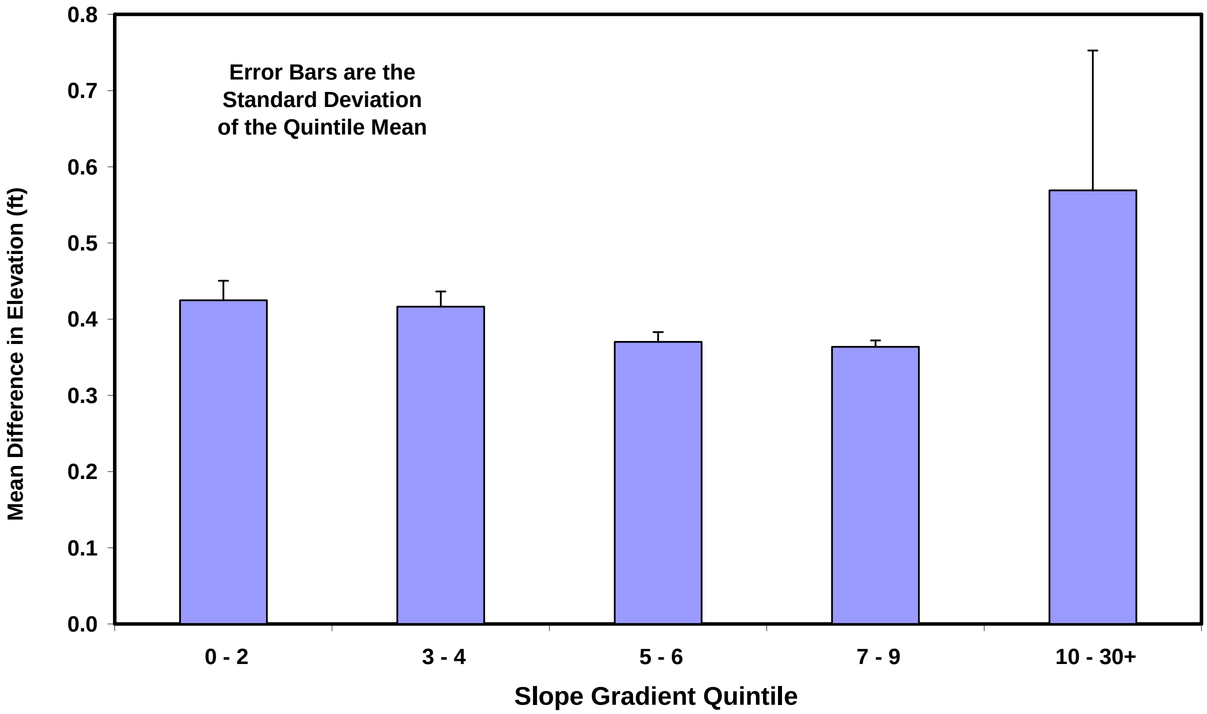


**2006-2004 Impervious Surface No-Change Land Cover, Sopers Branch:**
**Mean Difference in Elevation by Slope Gradient Quintile**

| Quintile Slope Groups | Quintile n | Mean Diff 06 - 04 | Std Dev |
|---|---|---|---|
| 0 - 2 | 36243 | 0.425 | 0.026 |
| 3 - 4 | 54216 | 0.416 | 0.020 |
| 5 - 6 | 45313 | 0.370 | 0.013 |
| 7 - 9 | 36238 | 0.364 | 0.009 |
| 10 - 30+ | 26169 | 0.569 | 0.184 |

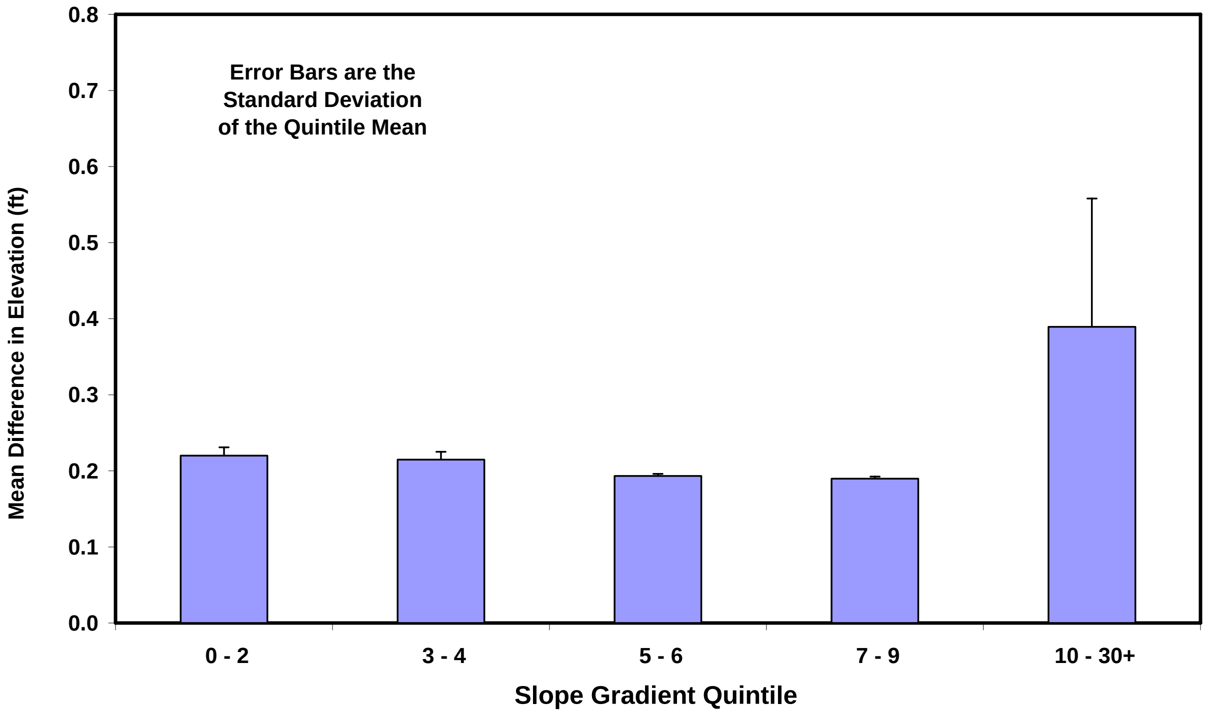


**2007-2006 Impervious Surface No-Change Land Cover, Sopers Branch: Mean Difference in Elevation by Slope Gradient Quintile**

| Quintile Slope Groups | Quintile n | Mean Diff 07 - 06 | Std Dev |
|---|---|---|---|
| 0 - 2 | 36243 | 0.220 | 0.011 |
| 3 - 4 | 54216 | 0.215 | 0.011 |
| 5 - 6 | 45313 | 0.193 | 0.003 |
| 7 - 9 | 36238 | 0.190 | 0.003 |
| 10 - 30+ | 26169 | 0.389 | 0.169 |

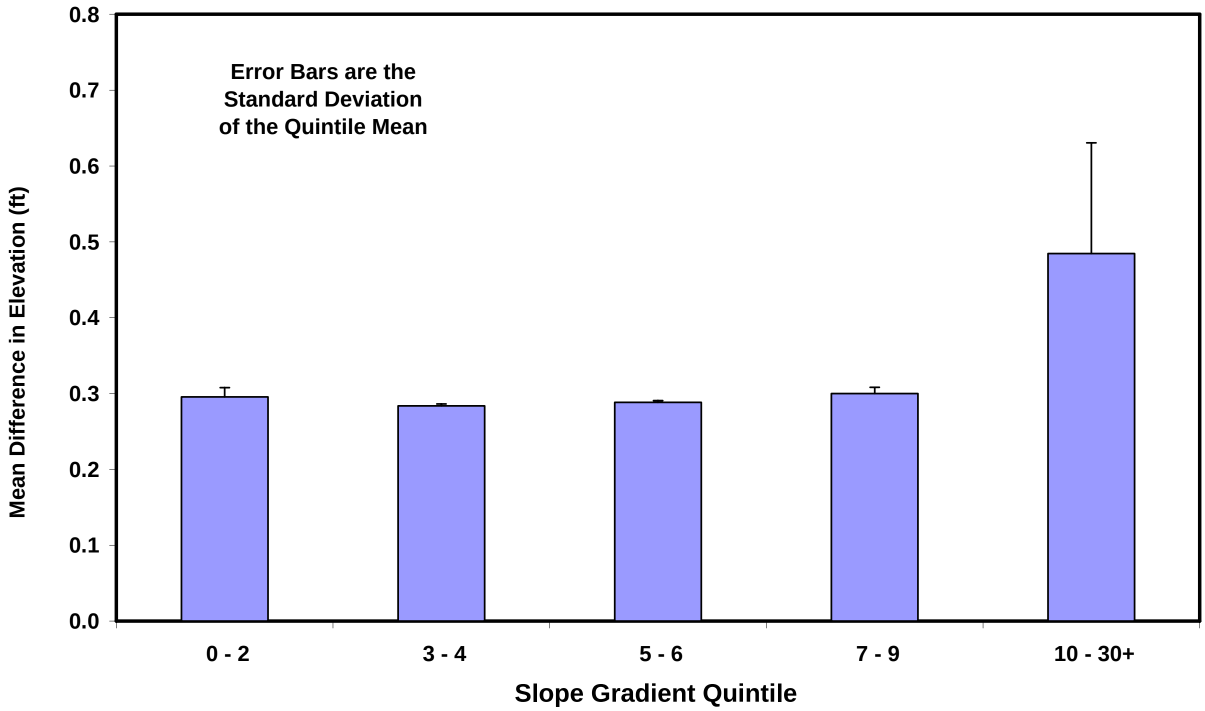


**2008-2007 Impervious Surface No-Change Land Cover, Sopers Branch:**
**Mean Difference in Elevation by Slope Gradient Quintile**

| Quintile Slope Groups | Quintile n | Mean Diff 08-07 | Std Dev |
|---|---|---|---|
| 0 - 2 | 36243 | 0.296 | 0.012 |
| 3 - 4 | 54216 | 0.284 | 0.003 |
| 5 - 6 | 45313 | 0.288 | 0.002 |
| 7 - 9 | 36238 | 0.300 | 0.008 |
| 10 - 30+ | 26169 | 0.485 | 0.146 |

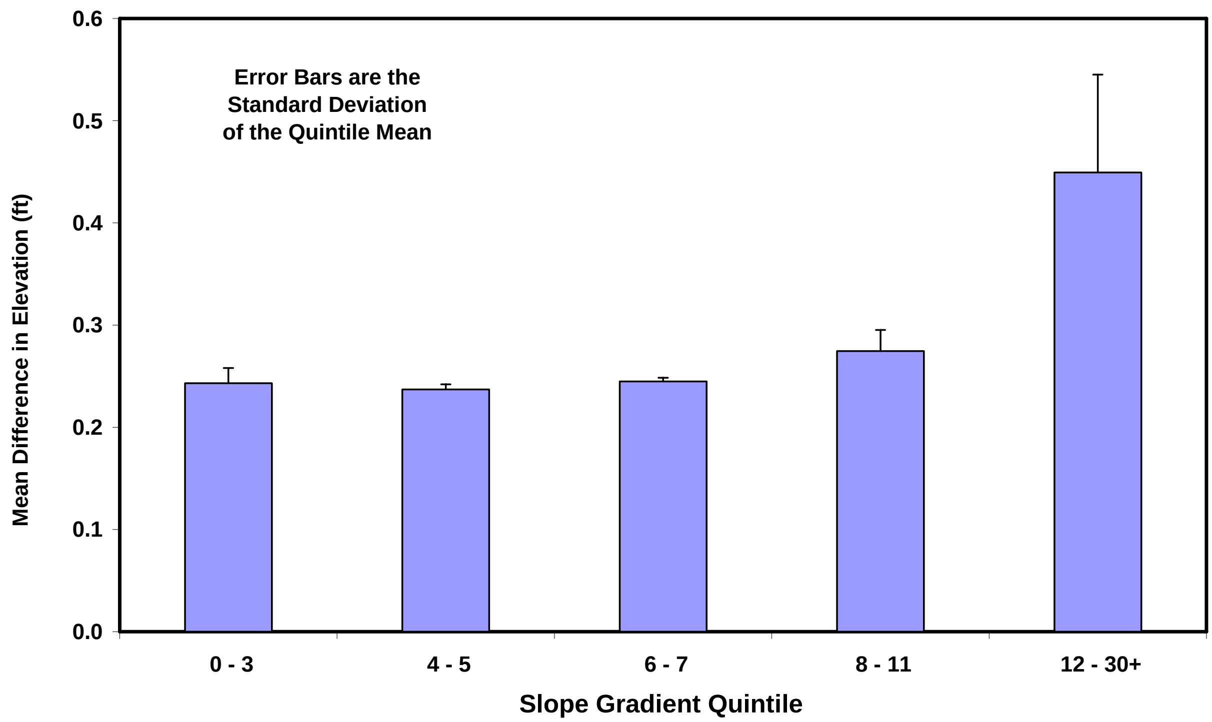


**2004-2002 Impervious Surface No-Change Land Cover, T104: Mean Difference in Elevation by Slope Gradient Quintile**

| Quintile Slope Groups | Quintile n | Mean Diff 04 - 02 | Std Dev |
|---|---|---|---|
| 0 - 3 | 17047 | 0.243 | 0.015 |
| 4 - 5 | 17231 | 0.237 | 0.005 |
| 6 - 7 | 15674 | 0.245 | 0.004 |
| 8 - 11 | 18996 | 0.275 | 0.021 |
| 12 - 30+ | 22870 | 0.449 | 0.096 |

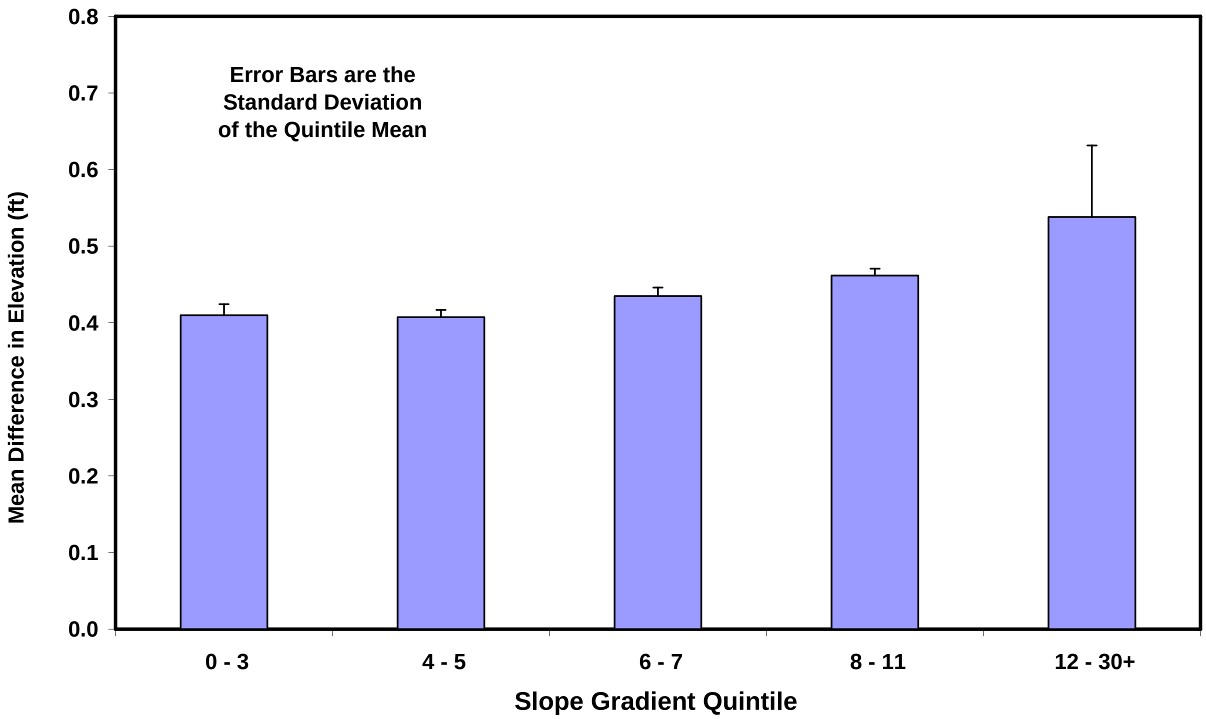


**2006-2004 Impervious Surface No-Change Land Cover, T104:**
**Mean Difference in Elevation by Slope Gradient Quintile**

| Quintile Slope Groups | Quintile n | Mean Diff 06 - 04 | Std Dev |
|---|---|---|---|
| 0 - 3 | 17047 | 0.410 | 0.014 |
| 4 - 5 | 17231 | 0.407 | 0.009 |
| 6 - 7 | 15674 | 0.435 | 0.011 |
| 8 - 11 | 18996 | 0.462 | 0.009 |
| 12 - 30+ | 22870 | 0.538 | 0.094 |

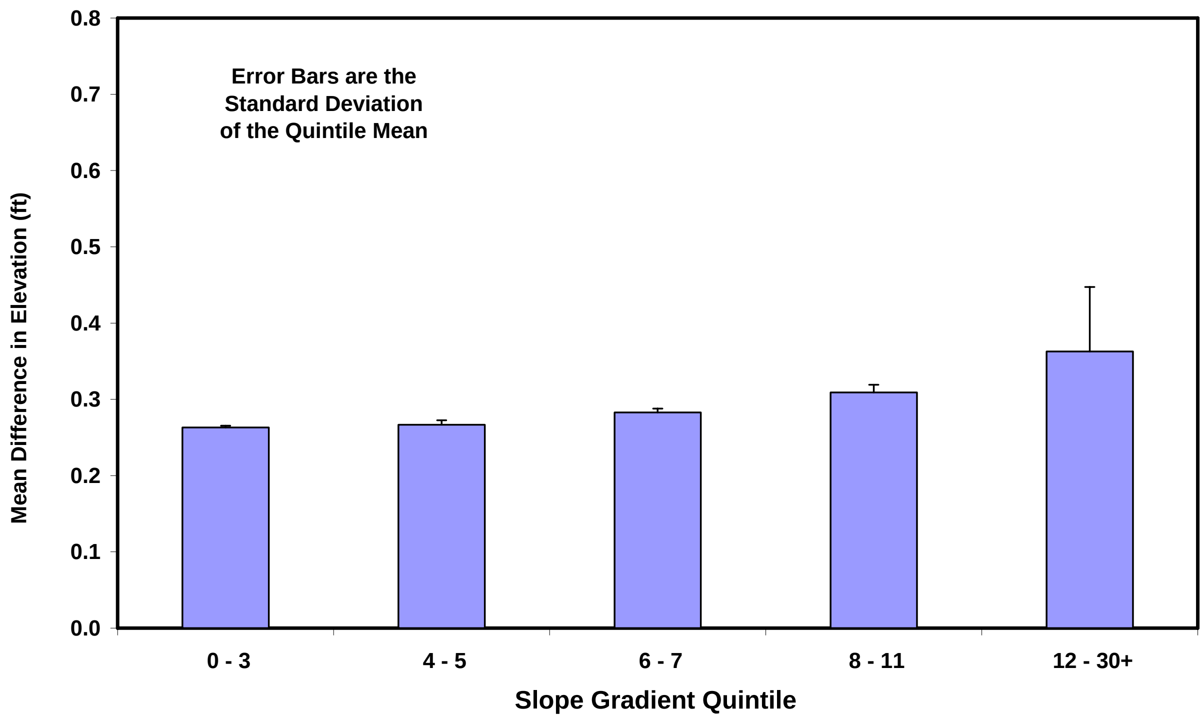


**2007-2006 Impervious Surface No-Change Land Cover, T104:**
**Mean Difference in Elevation by Slope Gradient Quintile**

| Quintile Slope Groups | Quintile n | Mean Diff 07 - 06 | Std Dev |
|---|---|---|---|
| 0 - 3 | 17047 | 0.263 | 0.002 |
| 4 - 5 | 17231 | 0.267 | 0.006 |
| 6 - 7 | 15674 | 0.283 | 0.005 |
| 8 - 11 | 18996 | 0.309 | 0.010 |
| 12 - 30+ | 22870 | 0.363 | 0.084 |

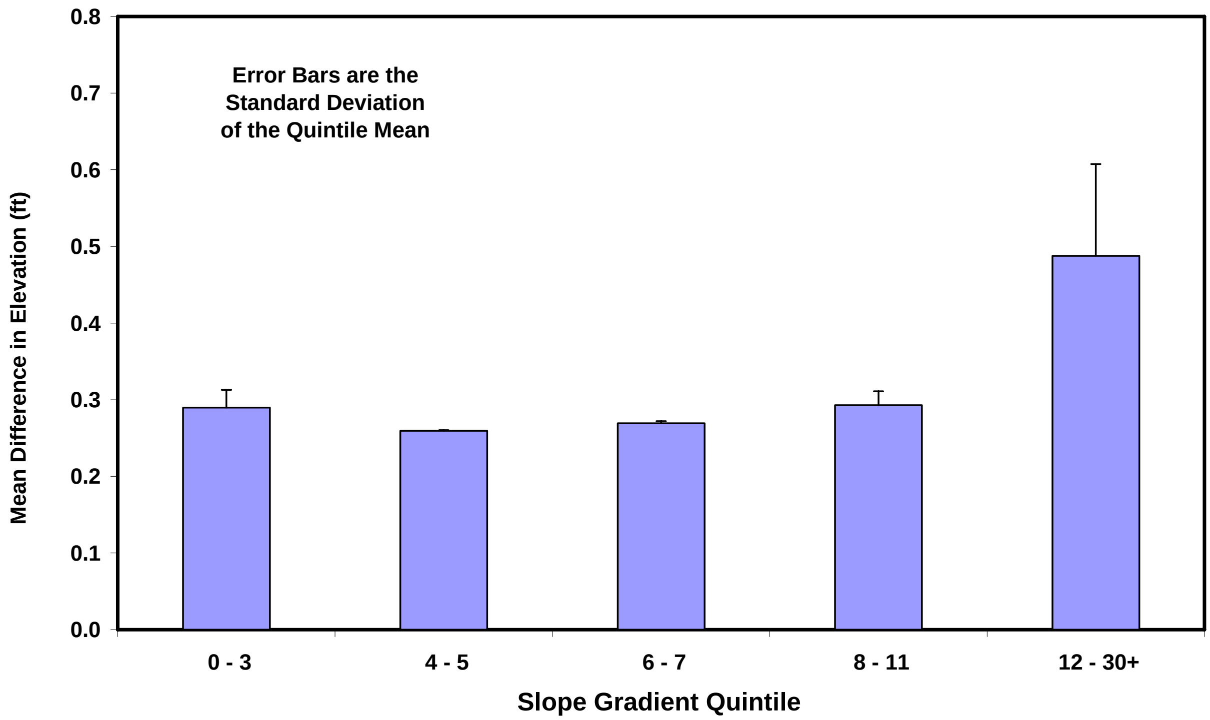


**2008-2007 Impervious Surface No-Change Land Cover, T104:**
**Mean Difference in Elevation by Slope Gradient Quintile**

| Quintile Slope Groups | Quintile n | Mean Diff 08-07 | Std Dev |
|---|---|---|---|
| 0 - 3 | 17047 | 0.290 | 0.023 |
| 4 - 5 | 17231 | 0.260 | 0.001 |
| 6 - 7 | 15674 | 0.269 | 0.003 |
| 8 - 11 | 18996 | 0.293 | 0.018 |
| 12 - 30+ | 22870 | 0.488 | 0.120 |

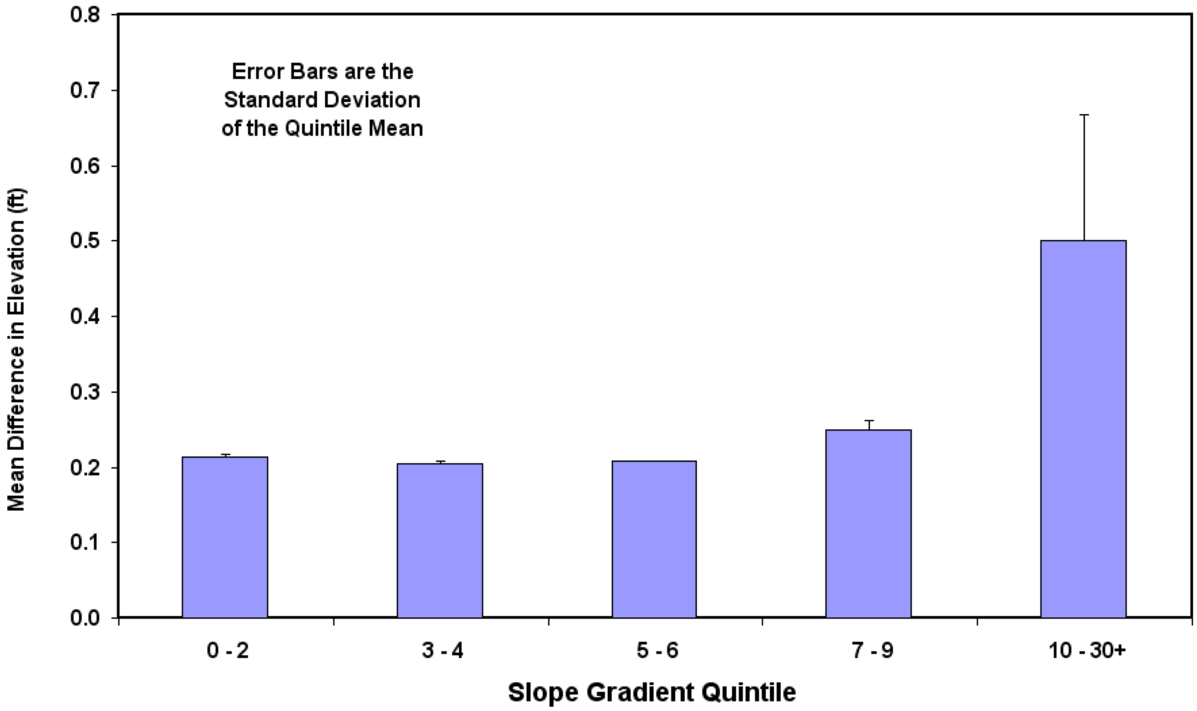


2004-2002 Impervious Surface No-Change Land Cover, T109:
Mean Difference in Elevation by Slope Gradient Quintile

| Quintile Slope Groups | Quintile n | Mean Diff 04 - 02 | Std Dev |
|---|---|---|---|
| 0 - 2 | 10299 | 0.213 | 0.004 |
| 3 - 4 | 15552 | 0.205 | 0.004 |
| 5 - 6 | 13947 | 0.208 | 0.001 |
| 7 - 9 | 12007 | 0.250 | 0.012 |
| 10 - 30+ | 12662 | 0.501 | 0.166 |

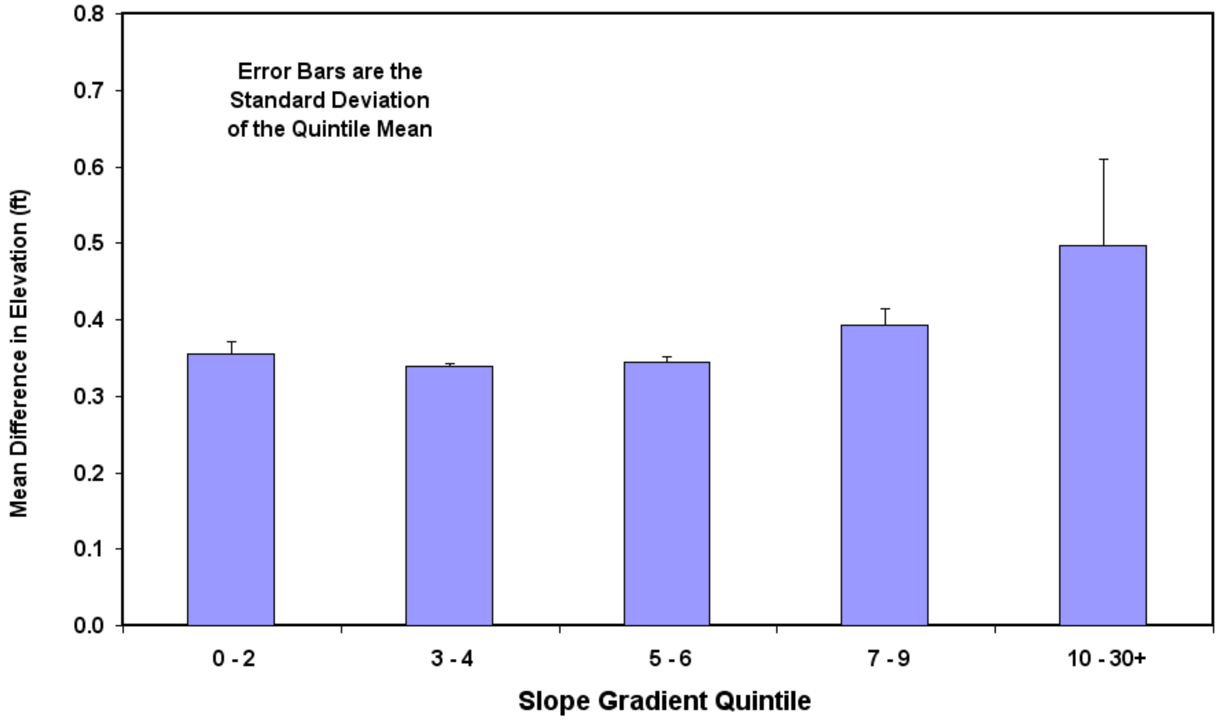


**2006-2004 Impervious Surface No-Change Land Cover, T109:**
**Mean Difference in Elevation by Slope Gradient Quintile**

| Quintile Slope Groups | Quintile n | Mean Diff 06 - 04 | Std Dev |
|---|---|---|---|
| 0 - 2 | 10299 | 0.356 | 0.016 |
| 3 - 4 | 15552 | 0.340 | 0.004 |
| 5 - 6 | 13947 | 0.344 | 0.008 |
| 7 - 9 | 12007 | 0.393 | 0.021 |
| 10 - 30+ | 12662 | 0.498 | 0.112 |


**2007-2006 Impervious Surface No-Change Land Cover, T109:**
**Mean Difference in Elevation by Slope Gradient Quintile**

| Quintile Slope Groups | Quintile n | Mean Diff 07 - 06 | Std Dev |
|---|---|---|---|
| 0 - 2 | 10299 | 0.188 | 0.009 |
| 3 - 4 | 15552 | 0.200 | 0.001 |
| 5 - 6 | 13947 | 0.204 | 0.001 |
| 7 - 9 | 12007 | 0.225 | 0.014 |
| 10 - 30+ | 12662 | 0.345 | 0.104 |

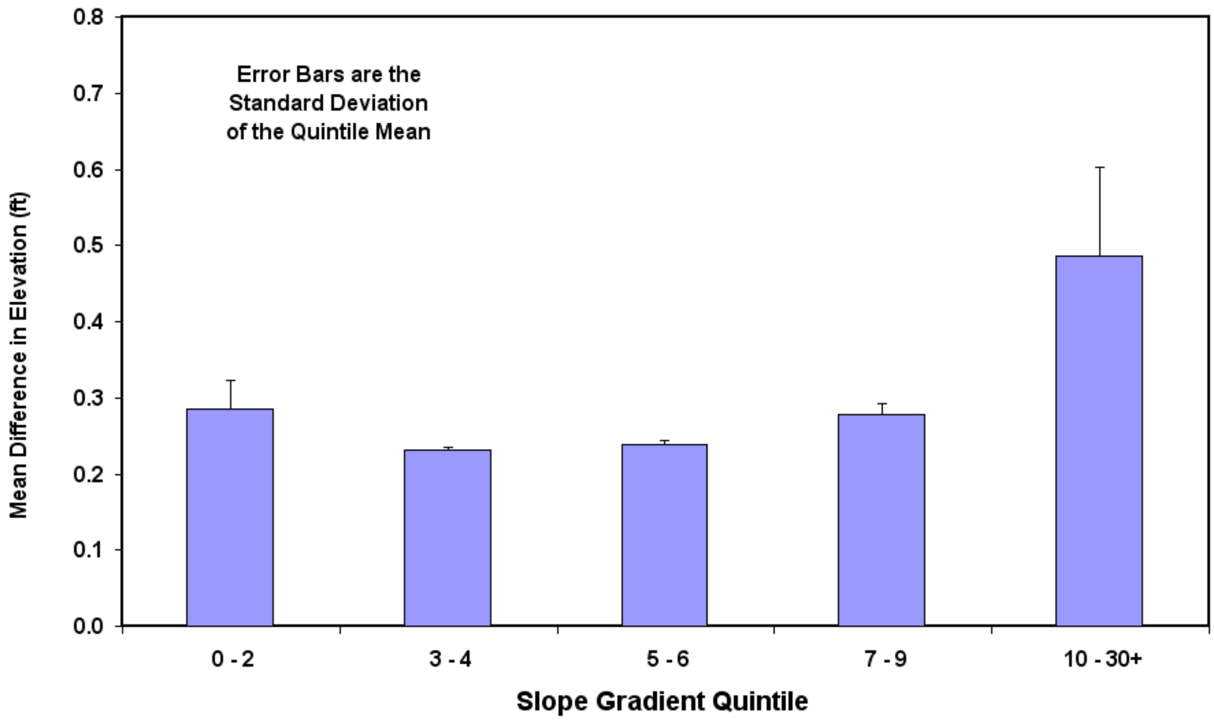


**2008-2007 Impervious Surface No-Change Land Cover, T109:
Mean Difference in Elevation by Slope Gradient Quintile**

| Quintile Slope Groups | Quintile n | Mean Diff 08-07 | Std Dev |
|---|---|---|---|
| 0 - 2 | 10299 | 0.285 | 0.039 |
| 3 - 4 | 15552 | 0.231 | 0.004 |
| 5 - 6 | 13947 | 0.238 | 0.006 |
| 7 - 9 | 12007 | 0.279 | 0.013 |
| 10 - 30+ | 12662 | 0.485 | 0.118 |

Appendix Seven: Metrics calculated for stream buffer High vs. Low-Variance Stream Channel Areas.

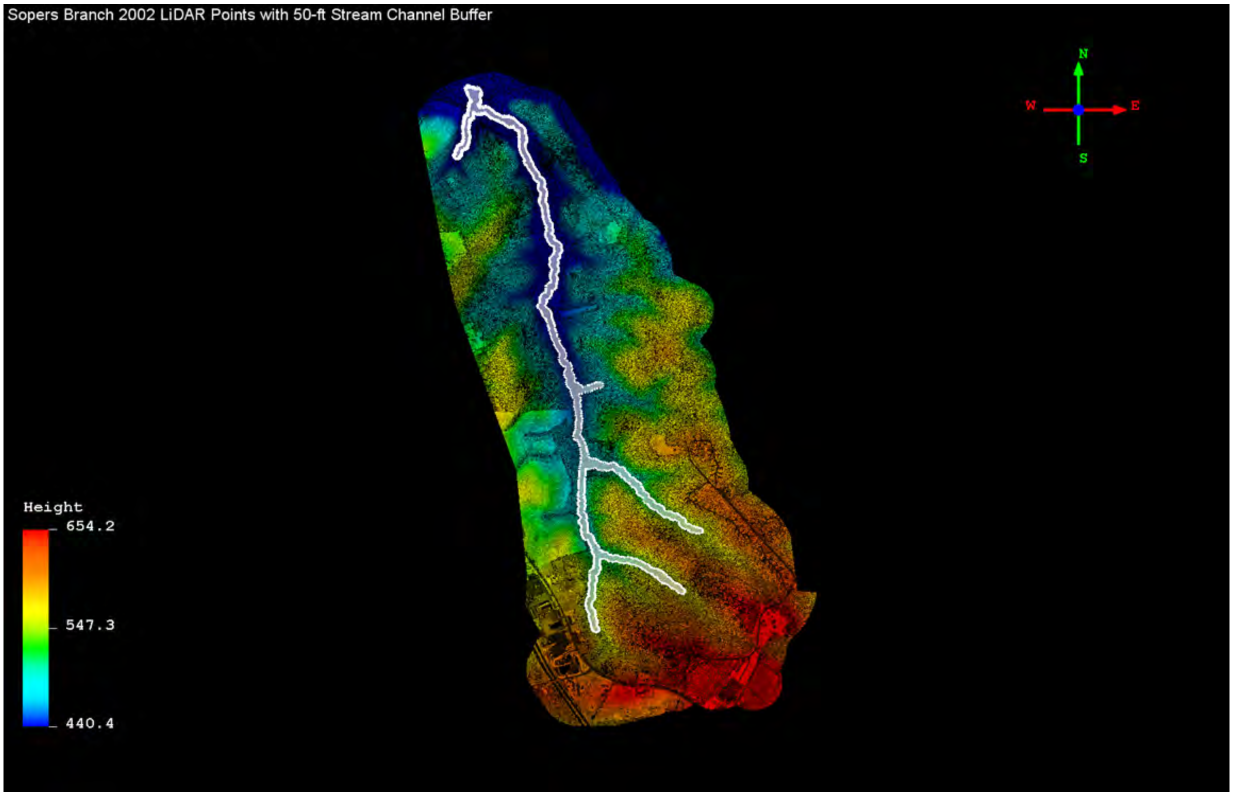

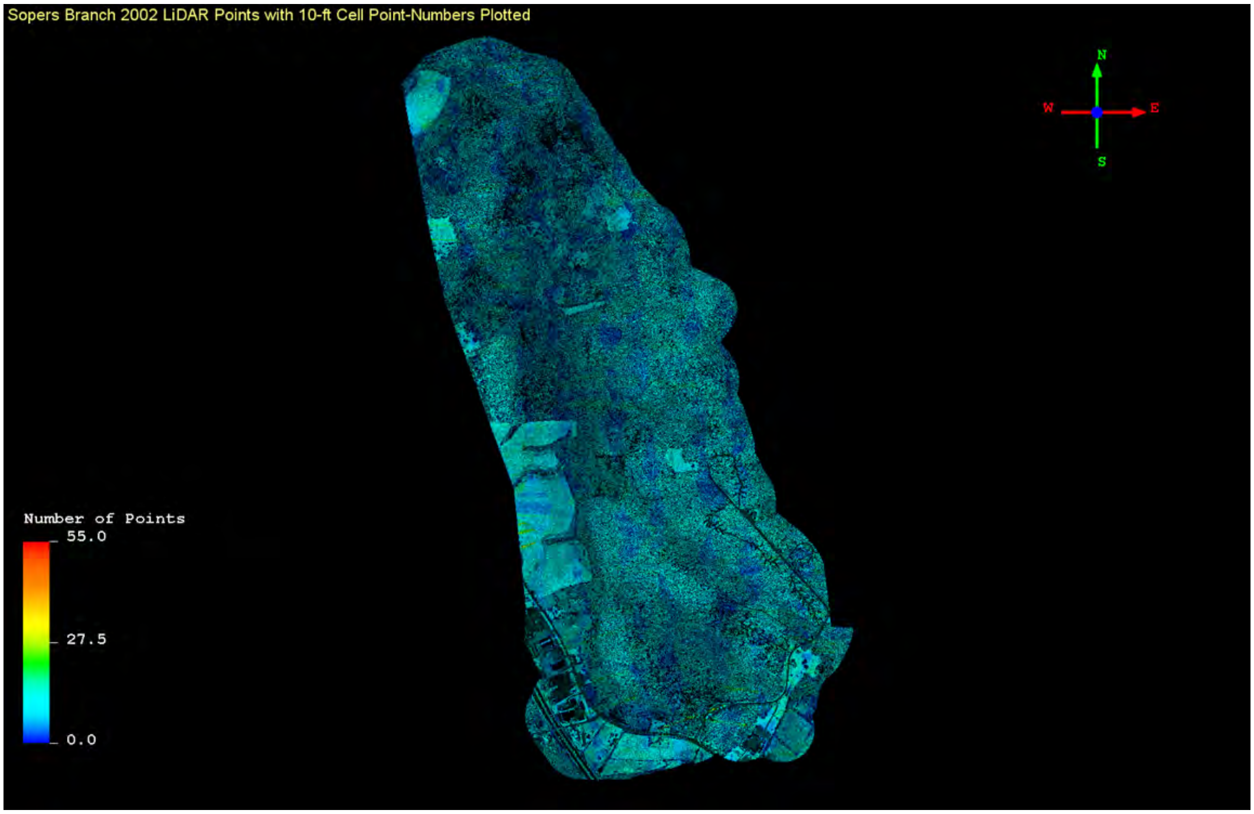
Sopers Branch 2002 LiDAR Points with 10-ft Cell Point-Numbers Plotted
N
W
E
S
Number of Points
55.0
27.5
0.0

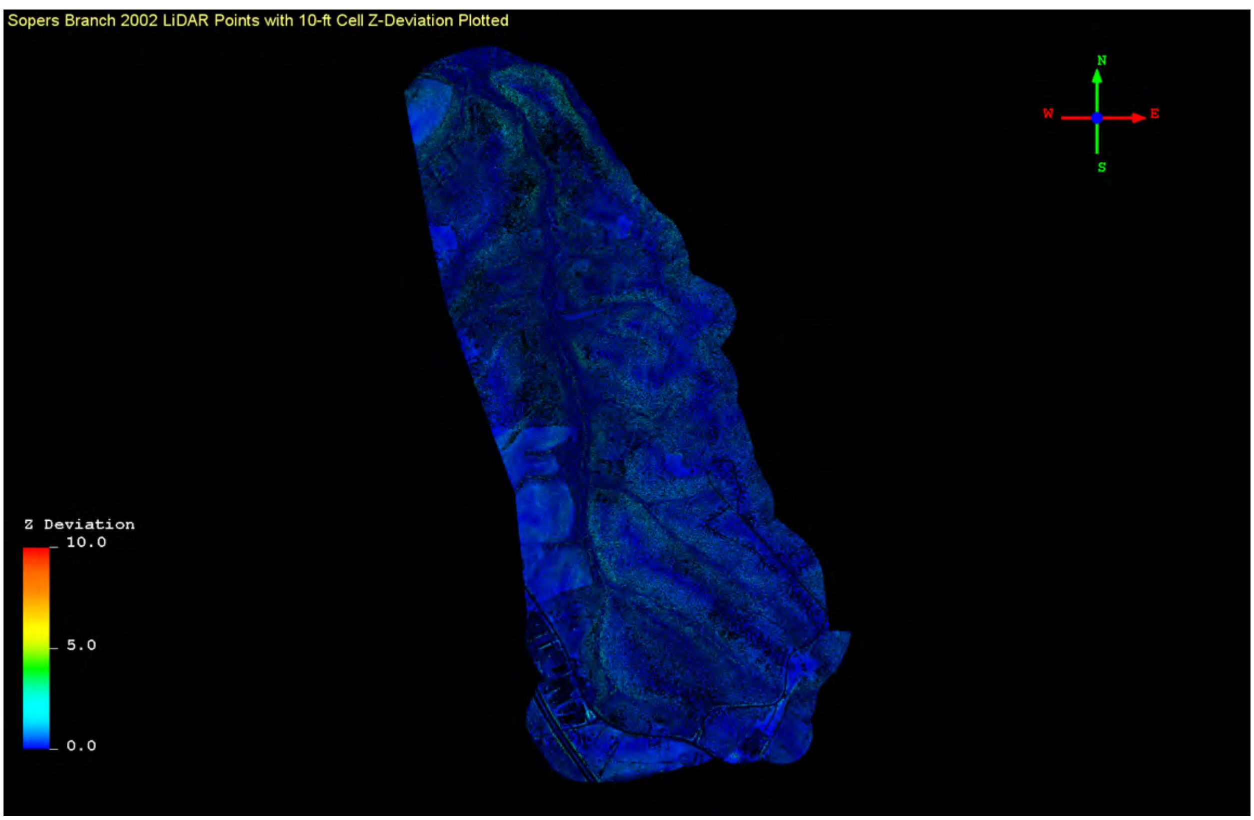
Sopers Branch 2002 LiDAR Points with 10-ft Cell Z-Deviation Plotted
N
W
E
S
Z Deviation
10.0
5.0
0.0

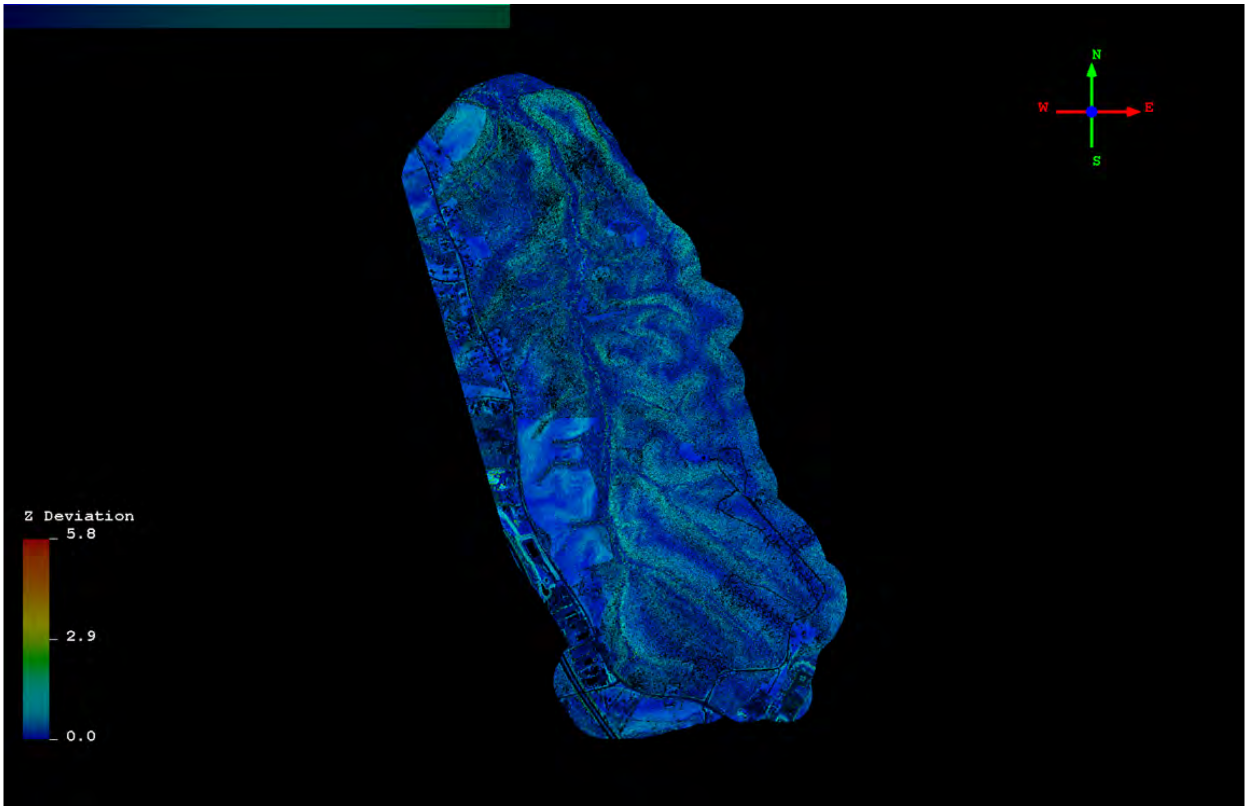
N
W
E
S
Z Deviation
5.8
2.9
0.0

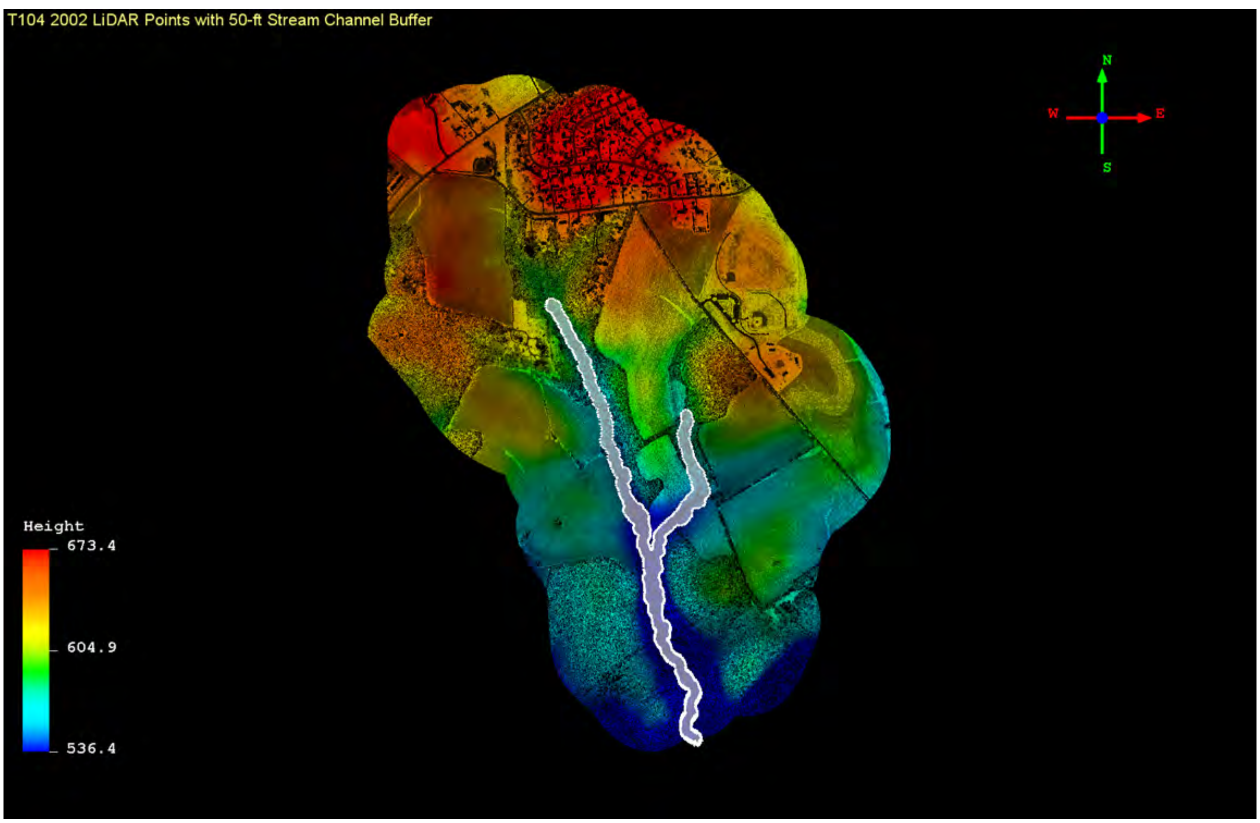
T104 2002 LiDAR Points with 50-ft Stream Channel Buffer
N
W
E
S
Height
673.4
604.9
536.4

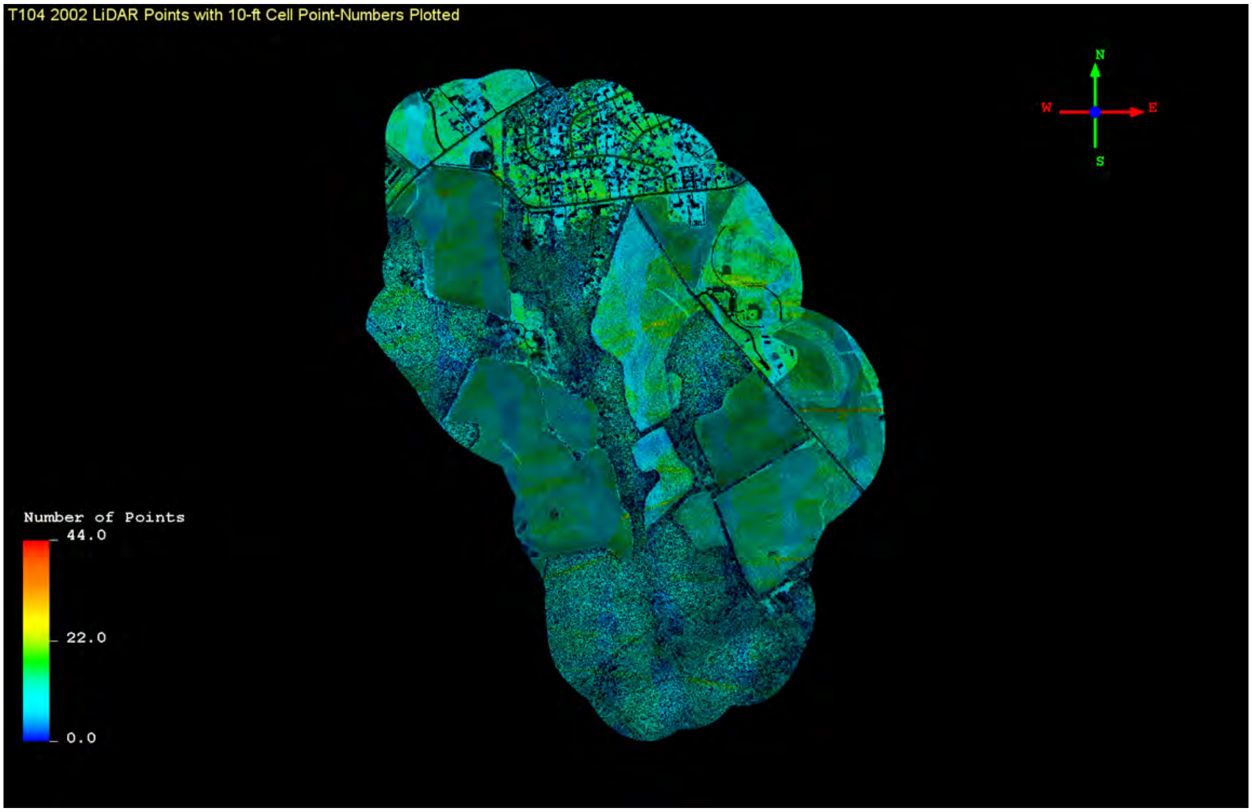
T104 2002 LiDAR Points with 10-ft Cell Point-Numbers Plotted
N
W
E
S
Number of Points
44.0
22.0
0.0

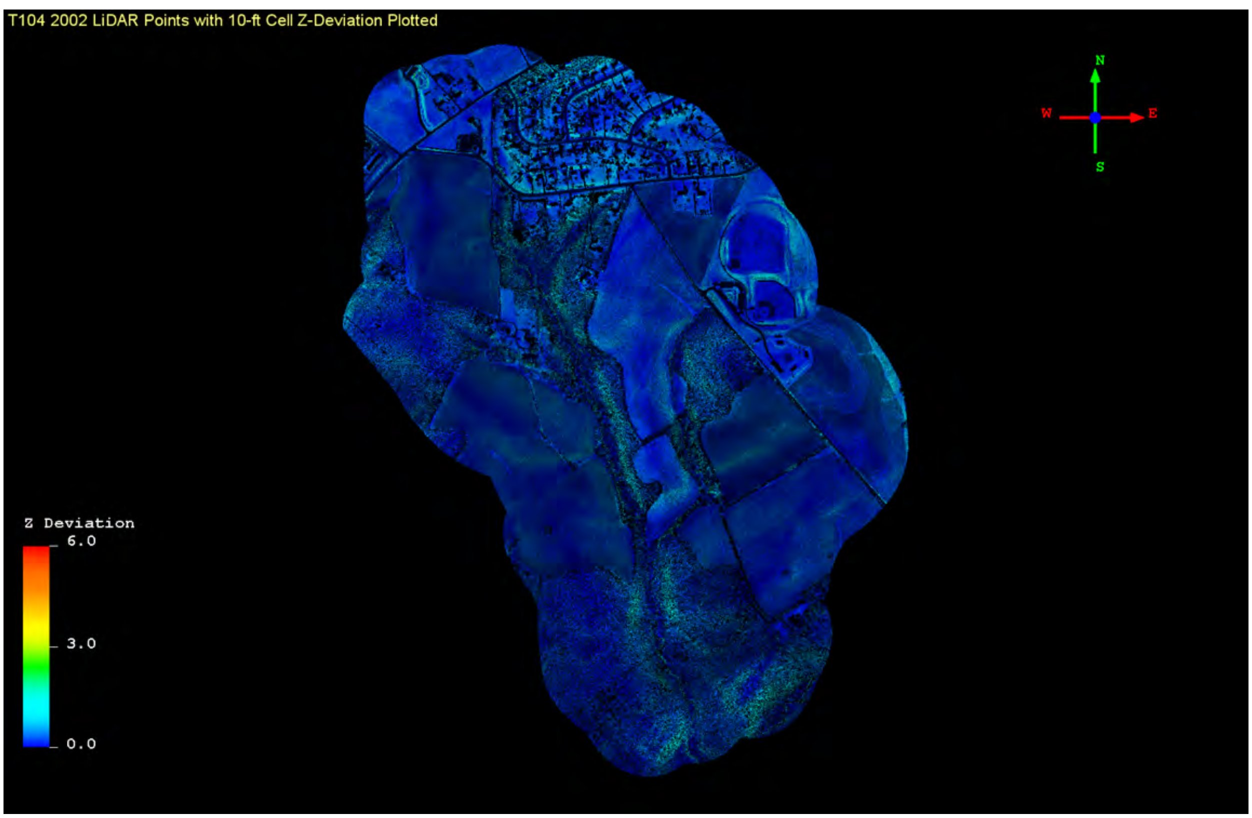
T104 2002 LiDAR Points with 10-ft Cell Z-Deviation Plotted
N
W
E
S
Z Deviation
6.0
3.0
0.0

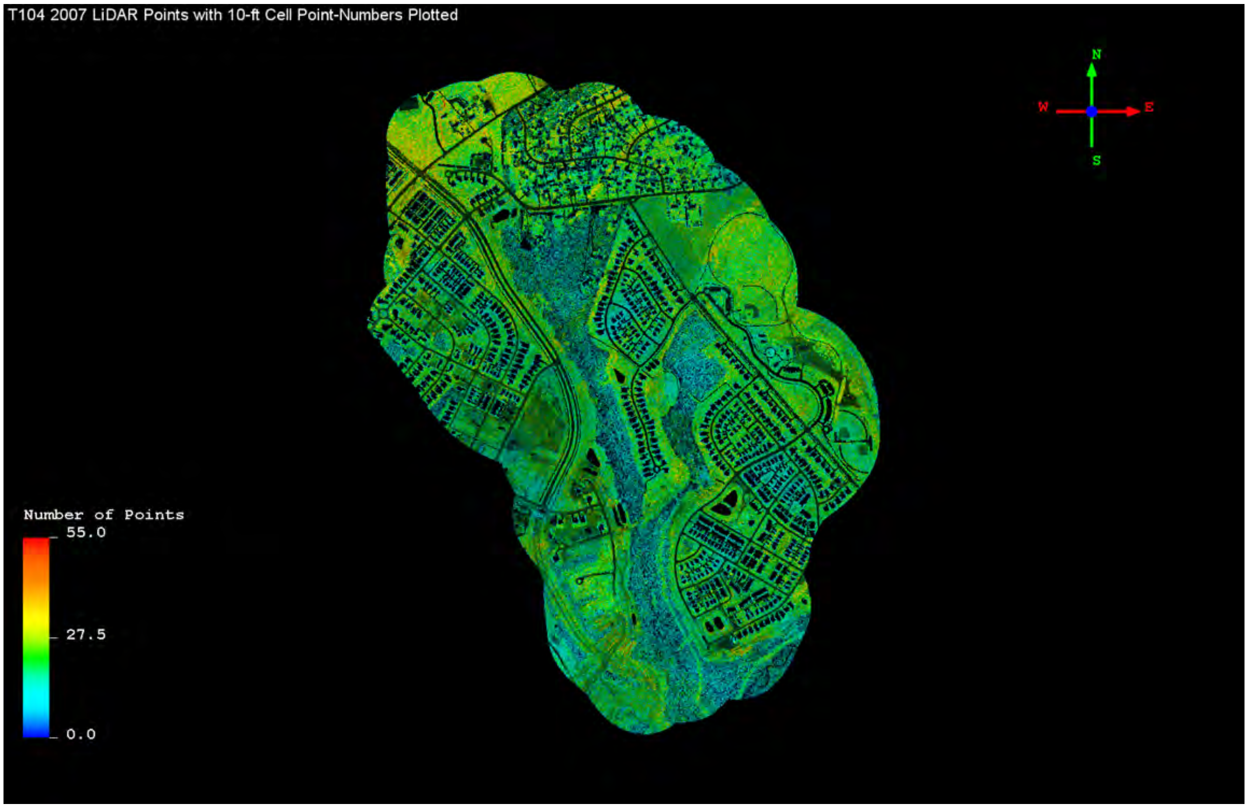
T104 2007 LiDAR Points with 10-ft Cell Point-Numbers Plotted
N
W
E
S
Number of Points
55.0
27.5
0.0

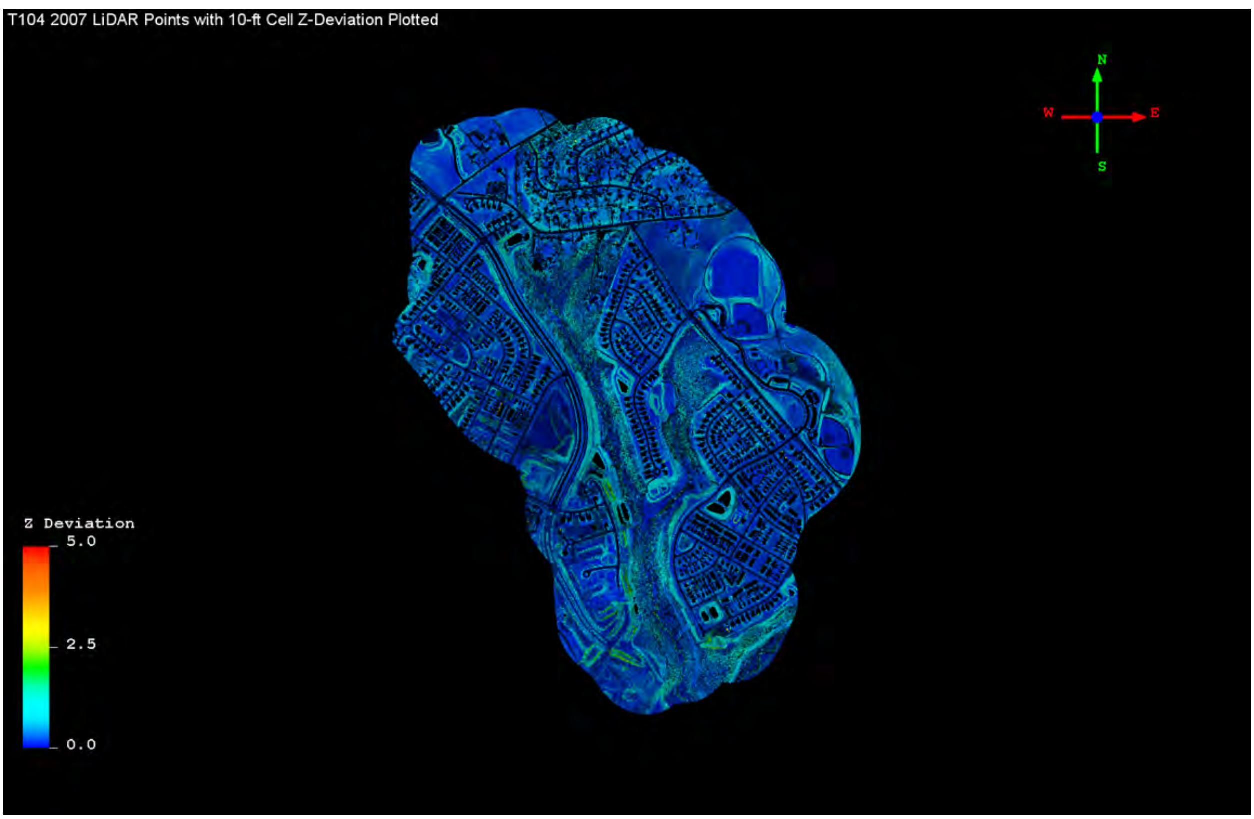
T104 2007 LiDAR Points with 10-ft Cell Z-Deviation Plotted
N
W
E
S
Z Deviation
5.0
2.5
0.0

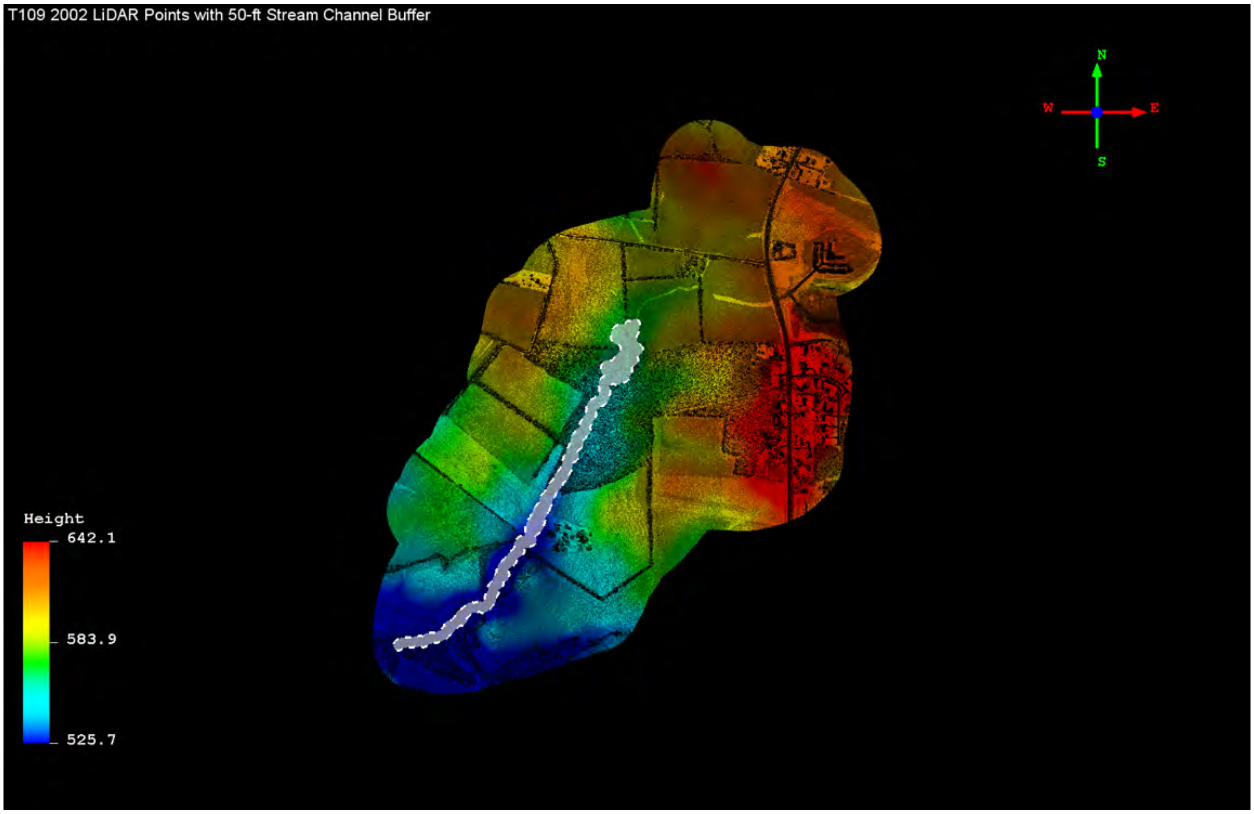
T109 2002 LiDAR Points with 50-ft Stream Channel Buffer
N
W
E
S
Height
642.1
583.9
525.7

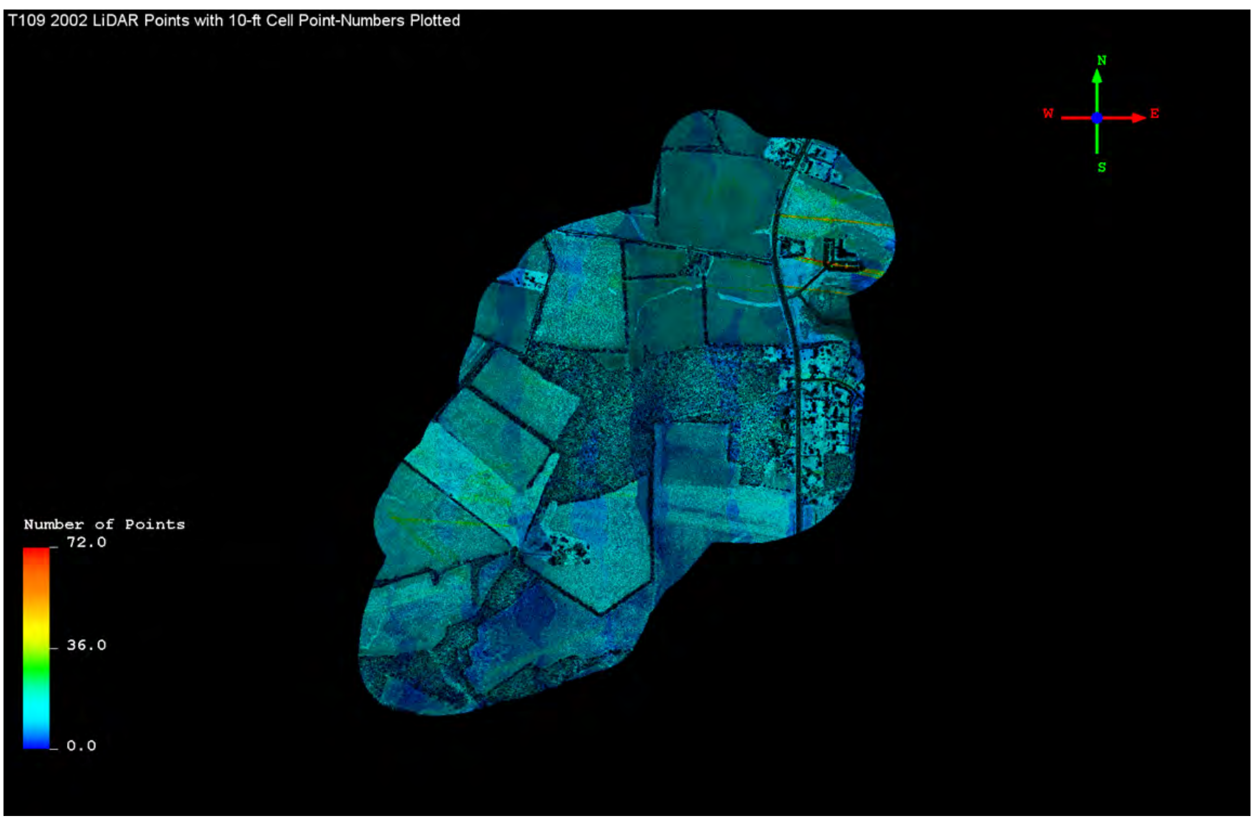
T109 2002 LiDAR Points with 10-ft Cell Point-Numbers Plotted
N
W
E
S
Number of Points
72.0
36.0
0.0

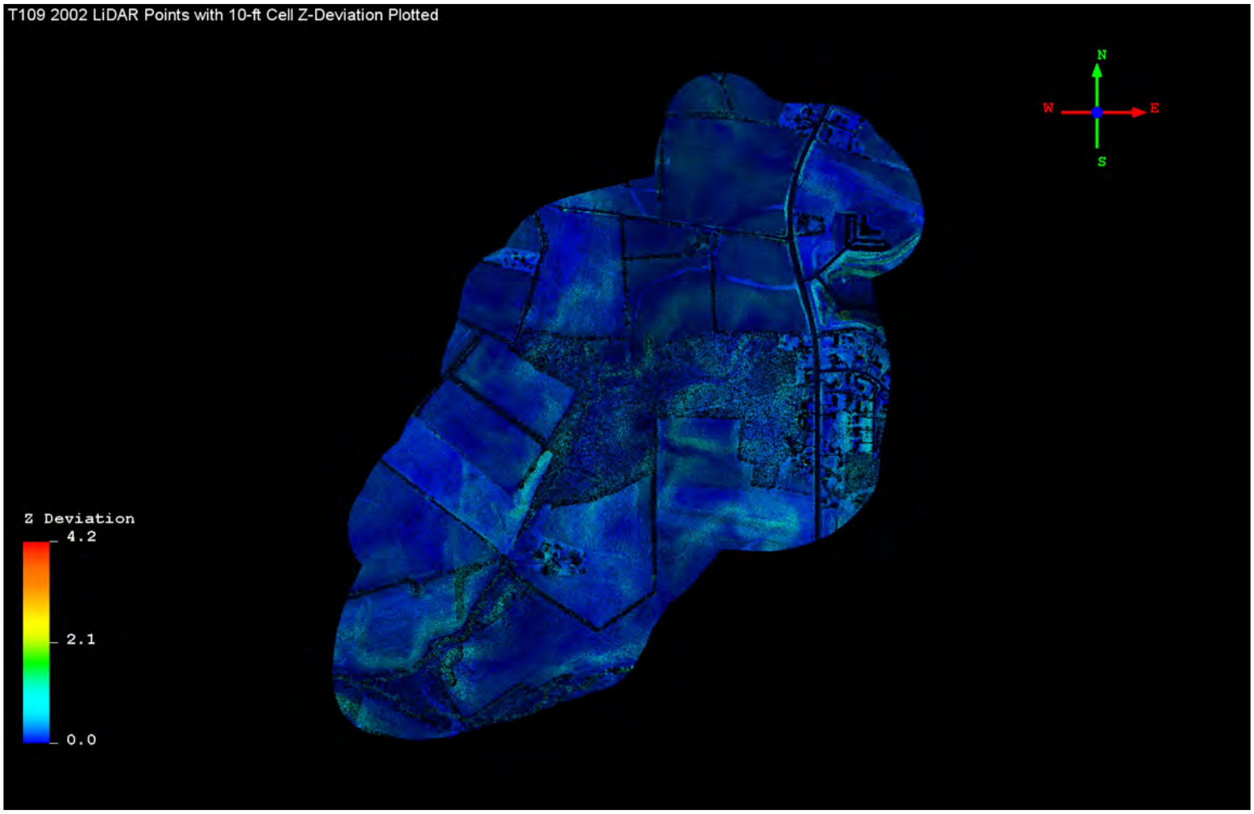
T109 2002 LiDAR Points with 10-ft Cell Z-Deviation Plotted
N
W
E
S
Z Deviation
4.2
2.1
0.0

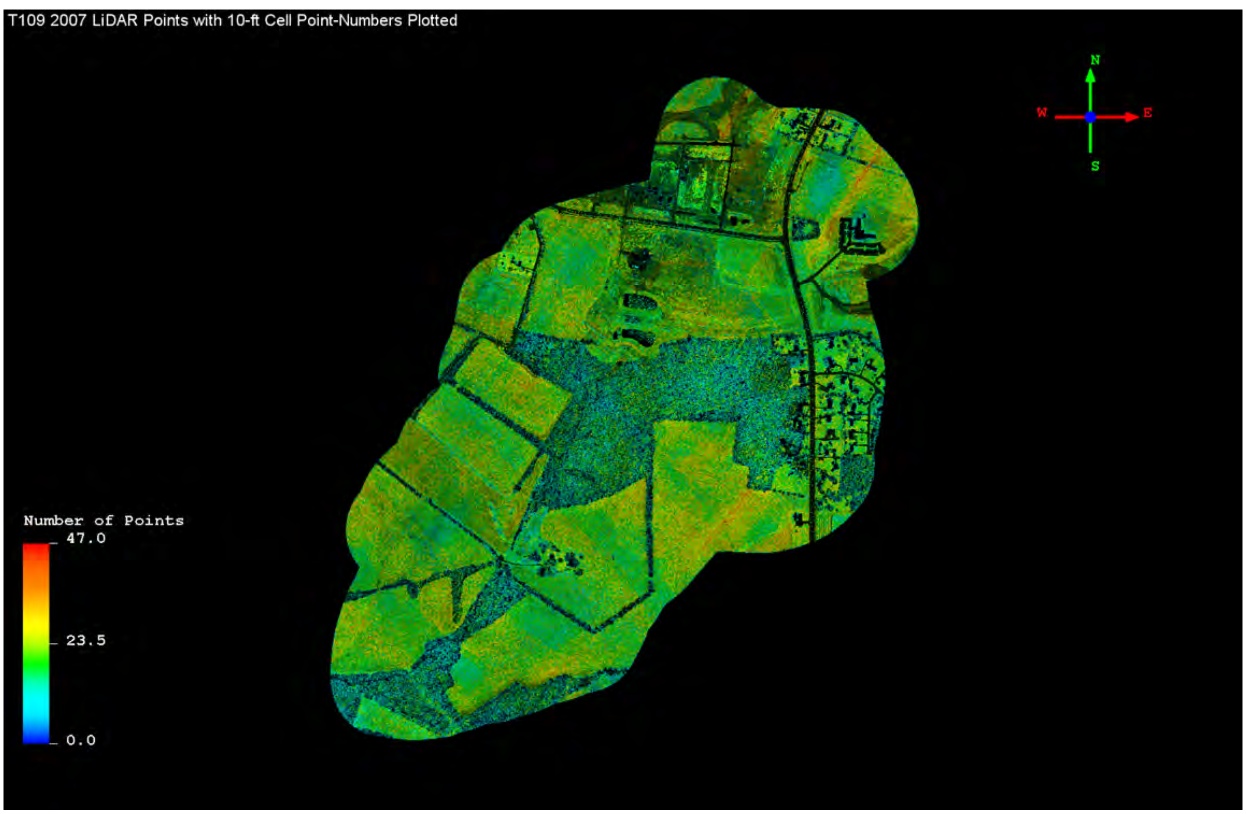
T109 2007 LiDAR Points with 10-ft Cell Point-Numbers Plotted
N
W
E
S
Number of Points
47.0
23.5
0.0

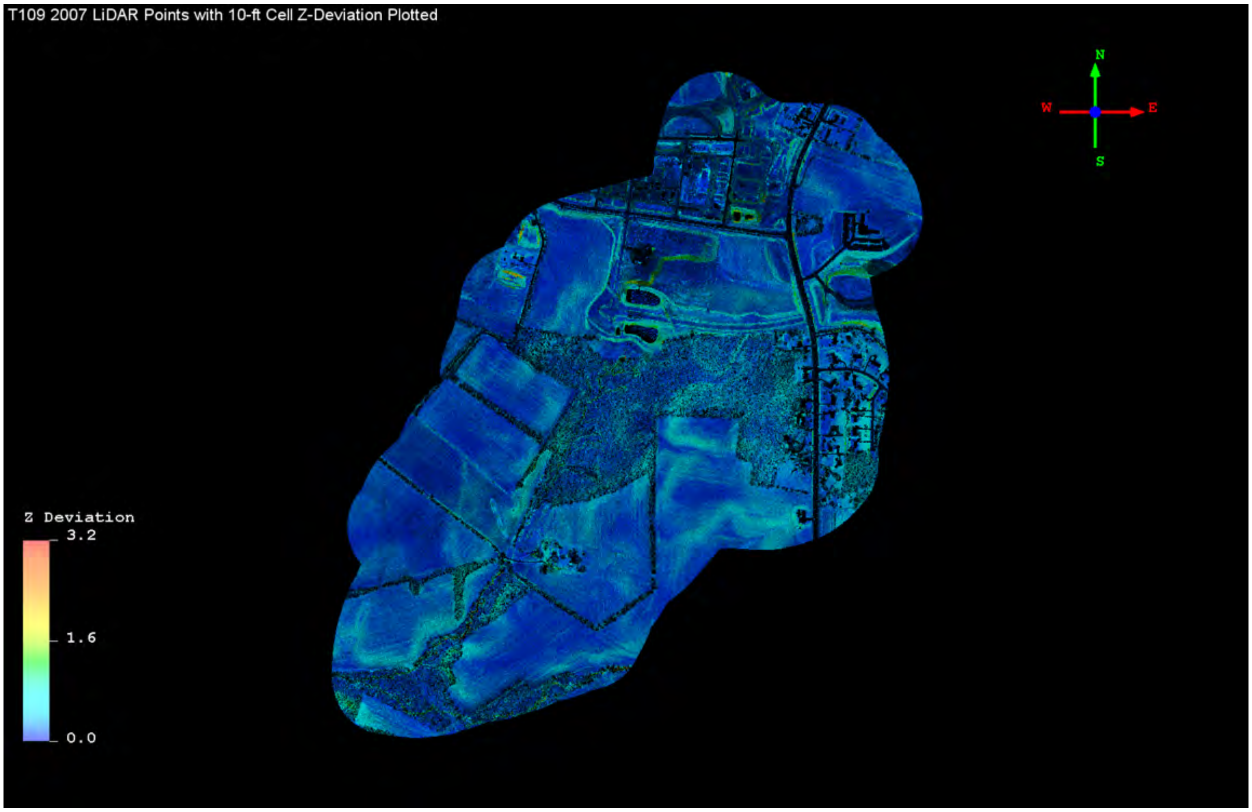
T109 2007 LiDAR Points with 10-ft Cell Z-Deviation Plotted
N
W
E
S
Z Deviation
3.2
1.6
0.0

Appendix Eight: Year-to-year differences in watersheds calculated from subsequent years of LiDAR coverages. Gray = Area Present in both coverages; Red = Area Present in Year 1 but not Year 2; Blue = Area Present in Year 2 but not Year 1.

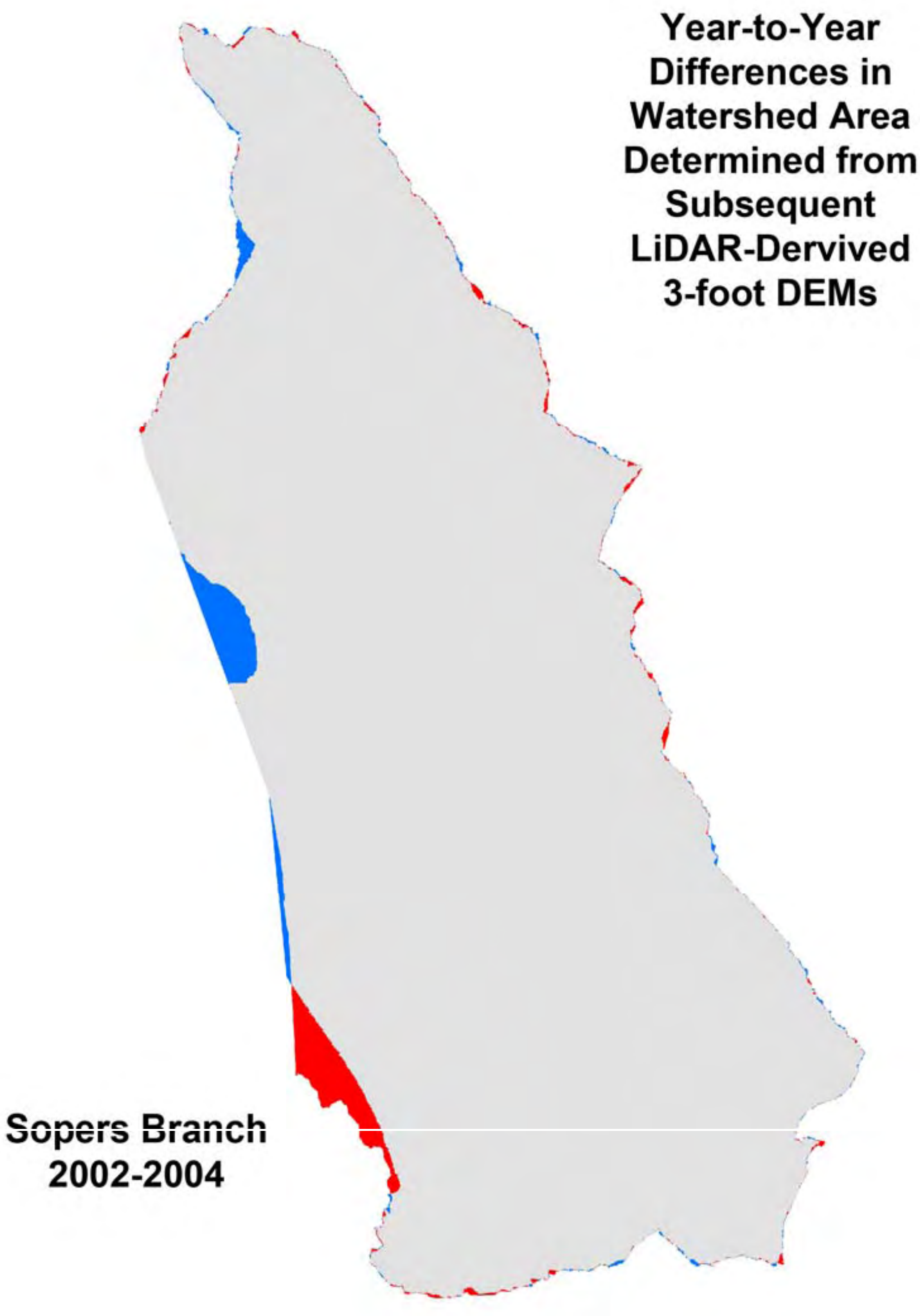


Gray = Area Present in both coverages; Red = Area Present in Year 1 but not Year 2; Blue = Area Present in Year 2 but not Year 1.

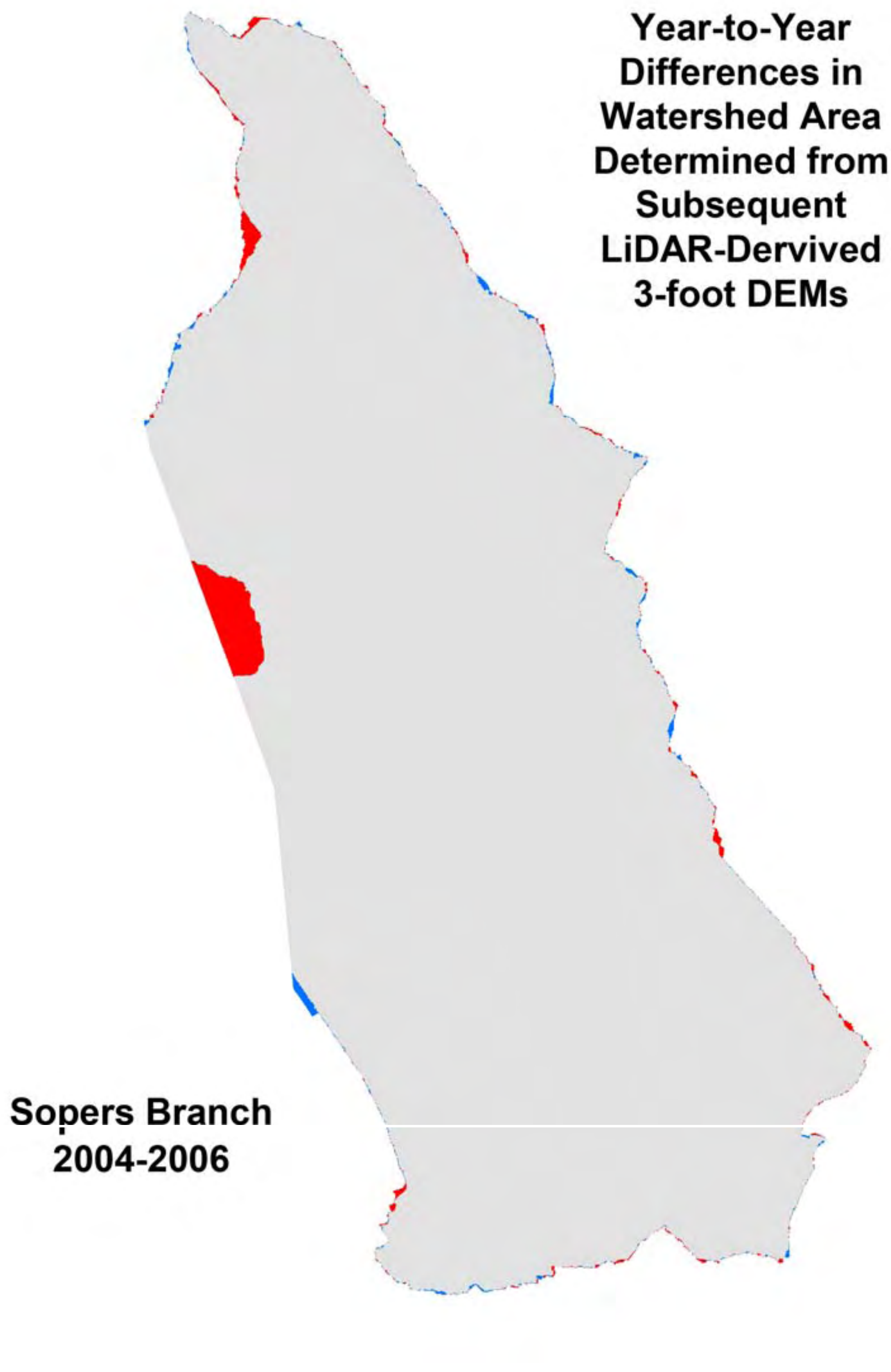


Gray = Area Present in both coverages; Red = Area Present in Year 1 but not Year 2; Blue = Area Present in Year 2 but not Year 1.

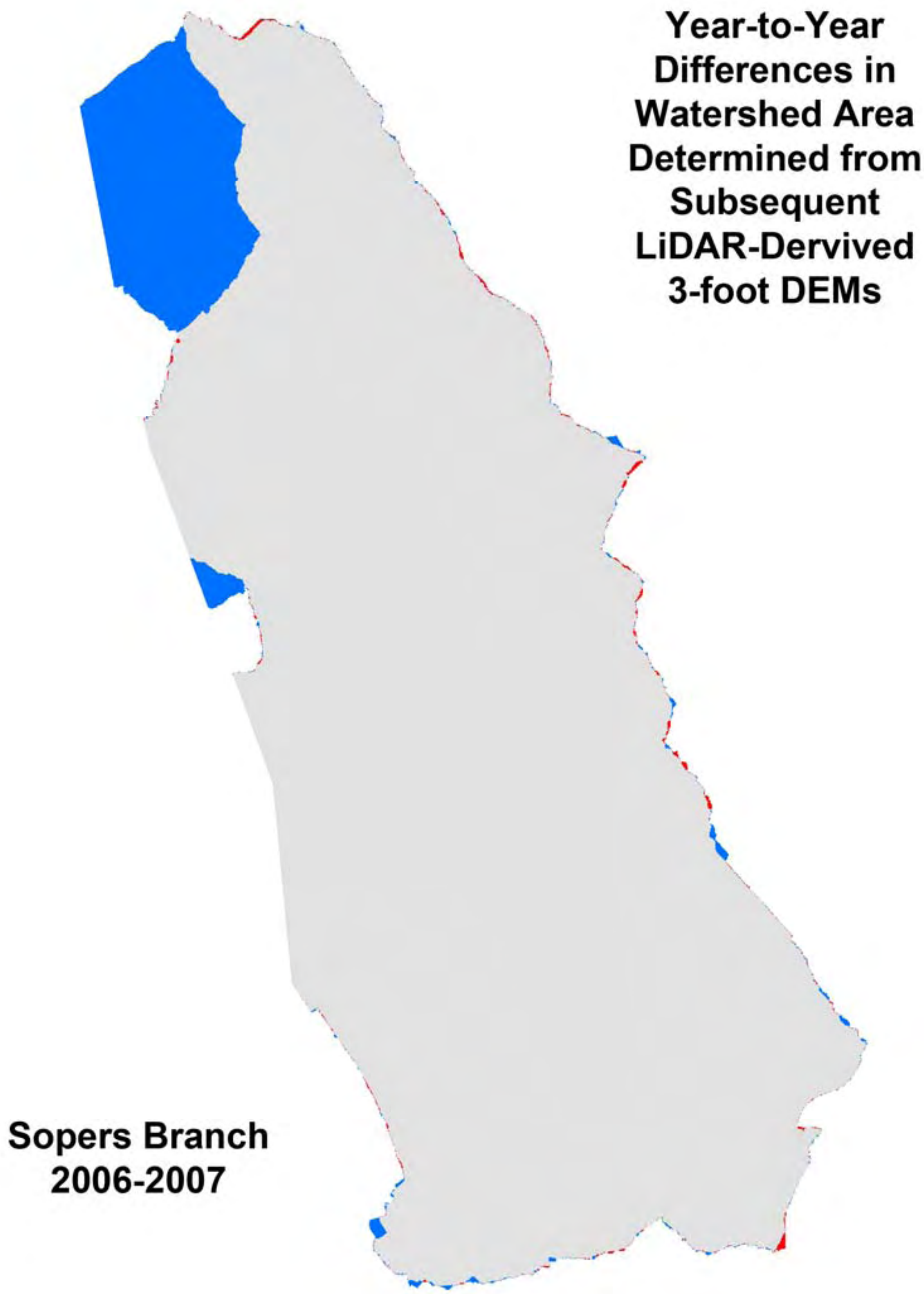


Gray = Area Present in both coverages; Red = Area Present in Year 1 but not Year 2; Blue = Area Present in Year 2 but not Year 1.

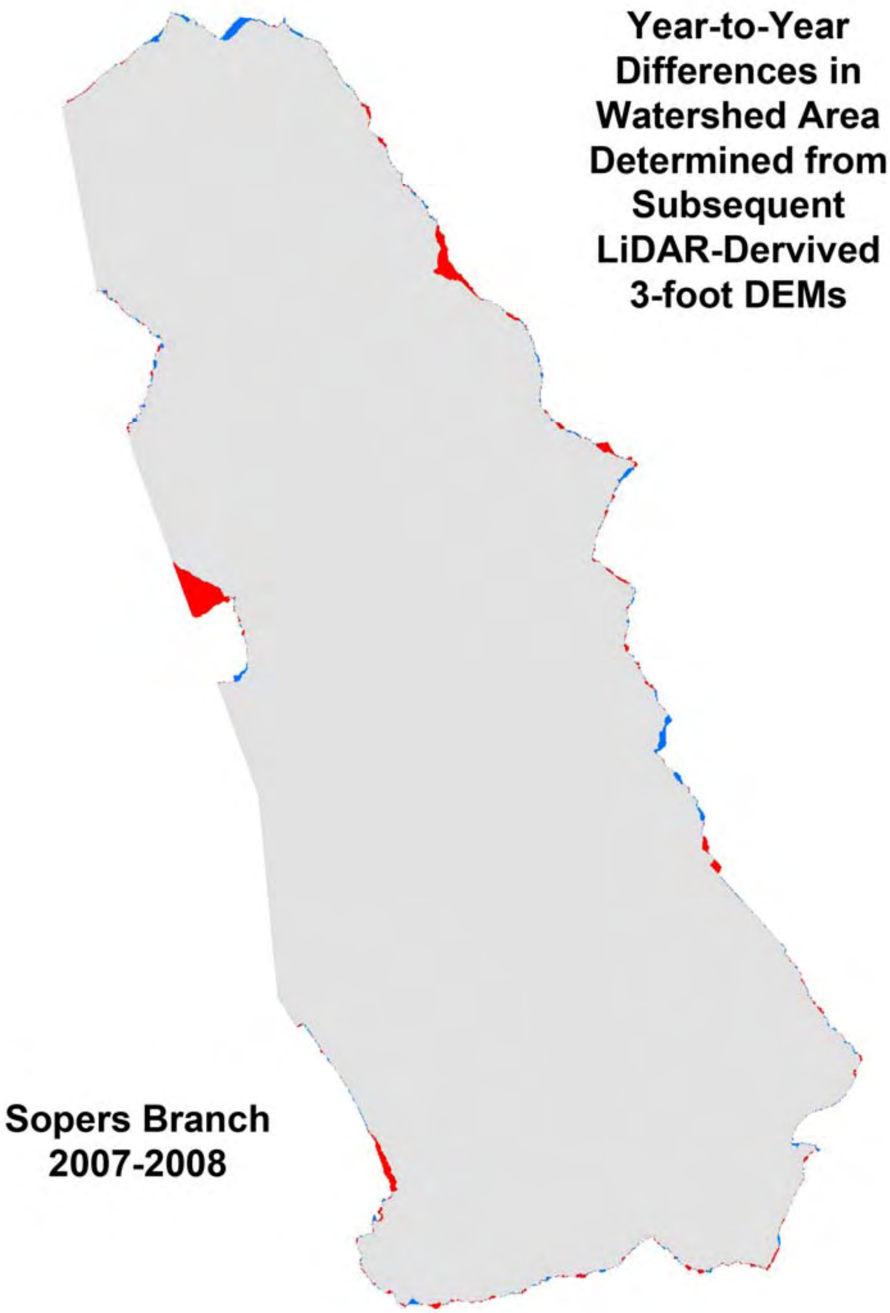


Gray = Area Present in both coverages; Red = Area Present in Year 1 but not Year 2; Blue = Area Present in Year 2 but not Year 1.

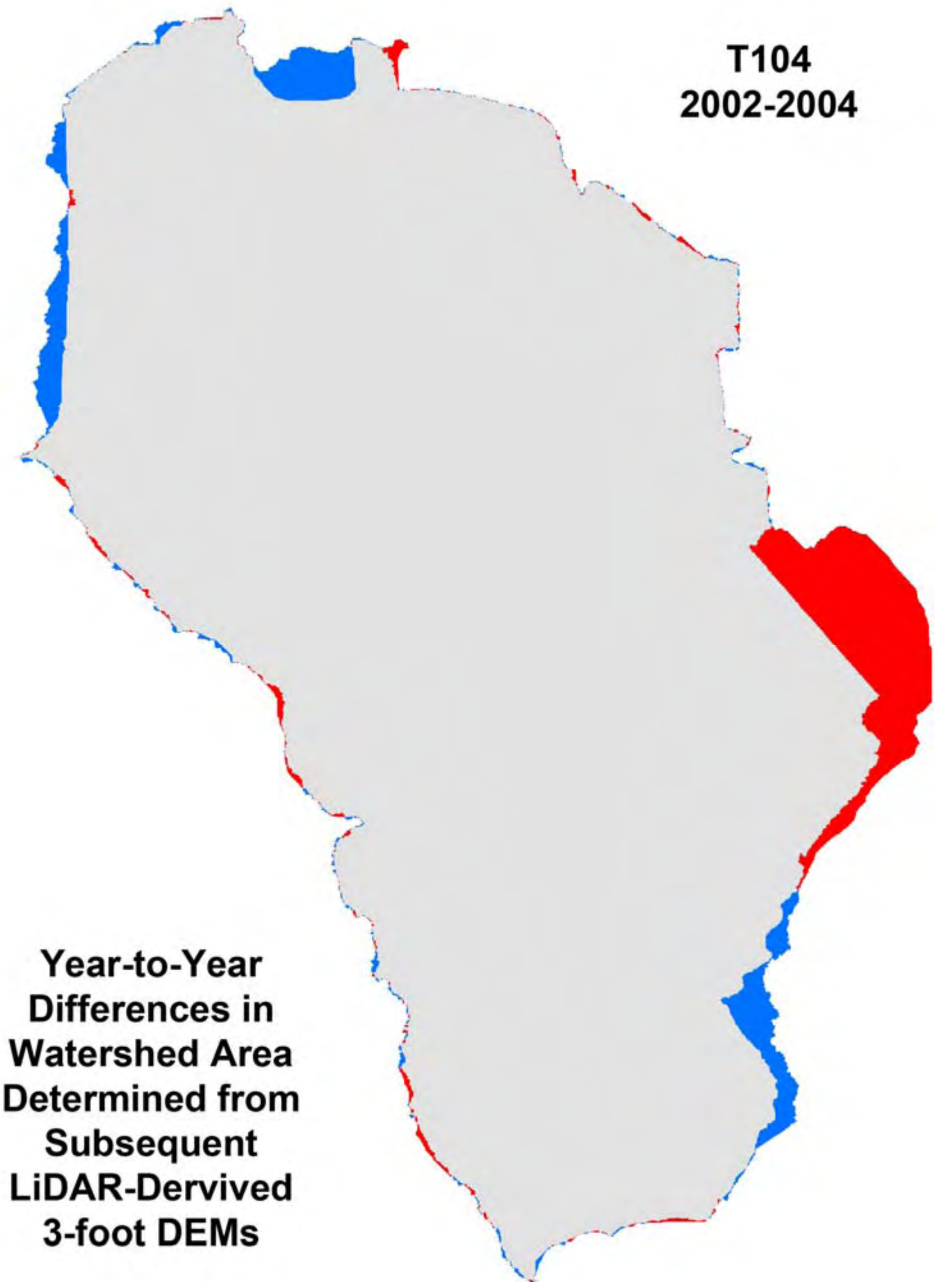


Gray = Area Present in both coverages; Red = Area Present in Year 1 but not Year 2; Blue = Area Present in Year 2 but not Year 1.


Gray = Area Present in both coverages; Red = Area Present in Year 1 but not Year 2; Blue = Area Present in Year 2 but not Year 1.

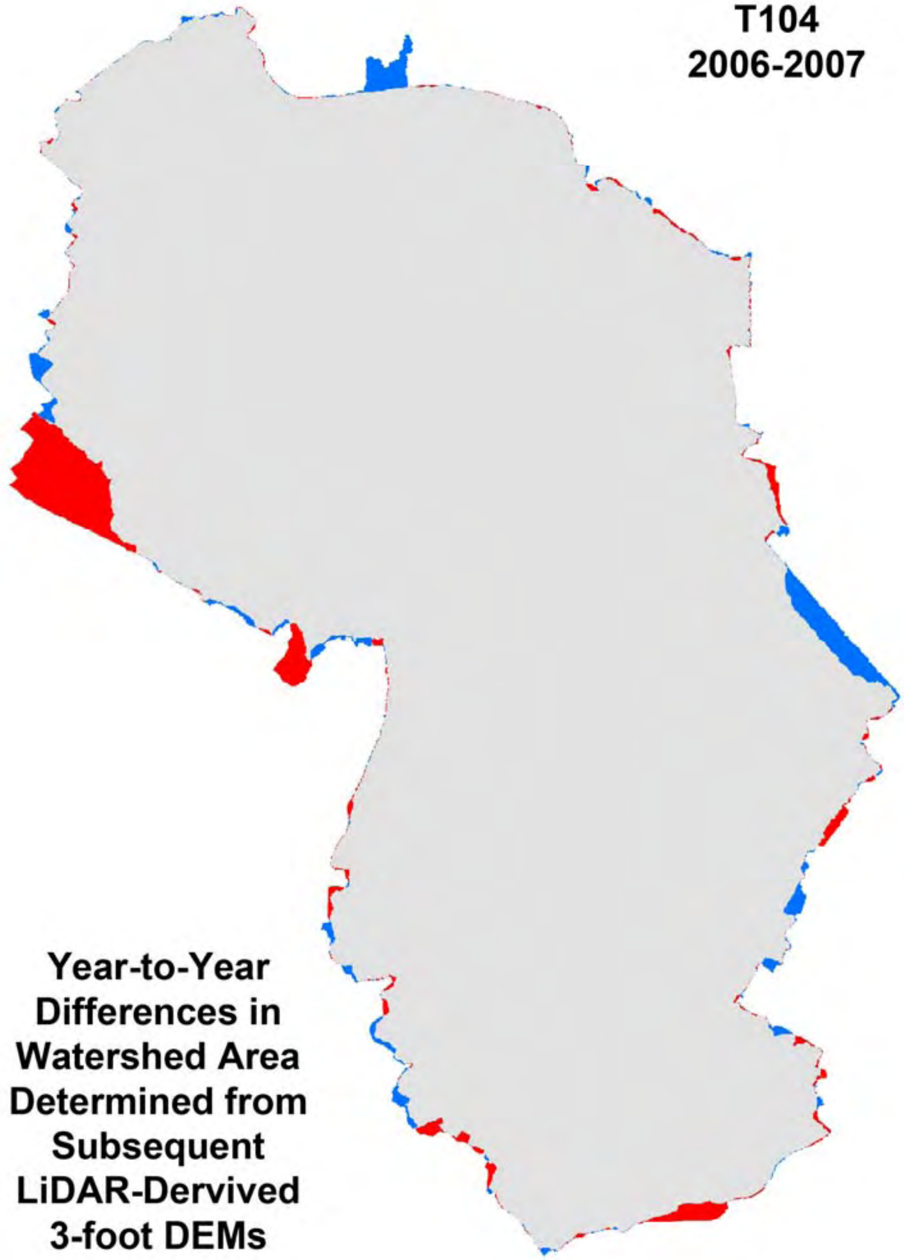


Gray = Area Present in both coverages; Red = Area Present in Year 1 but not Year 2; Blue = Area Present in Year 2 but not Year 1.


Gray = Area Present in both coverages; Red = Area Present in Year 1 but not Year 2; Blue = Area Present in Year 2 but not Year 1.

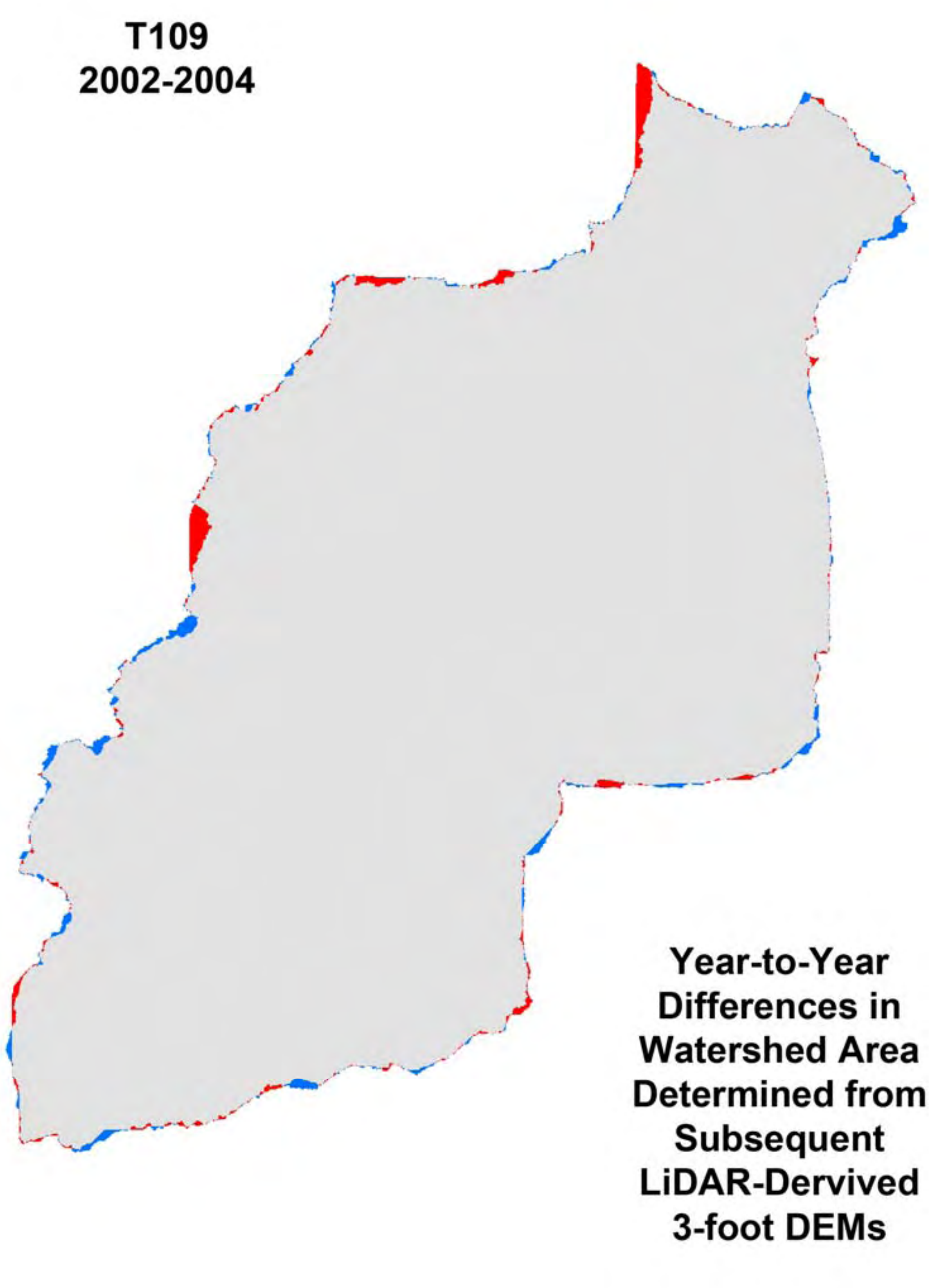


Gray = Area Present in both coverages; Red = Area Present in Year 1 but not Year 2; Blue = Area Present in Year 2 but not Year 1.

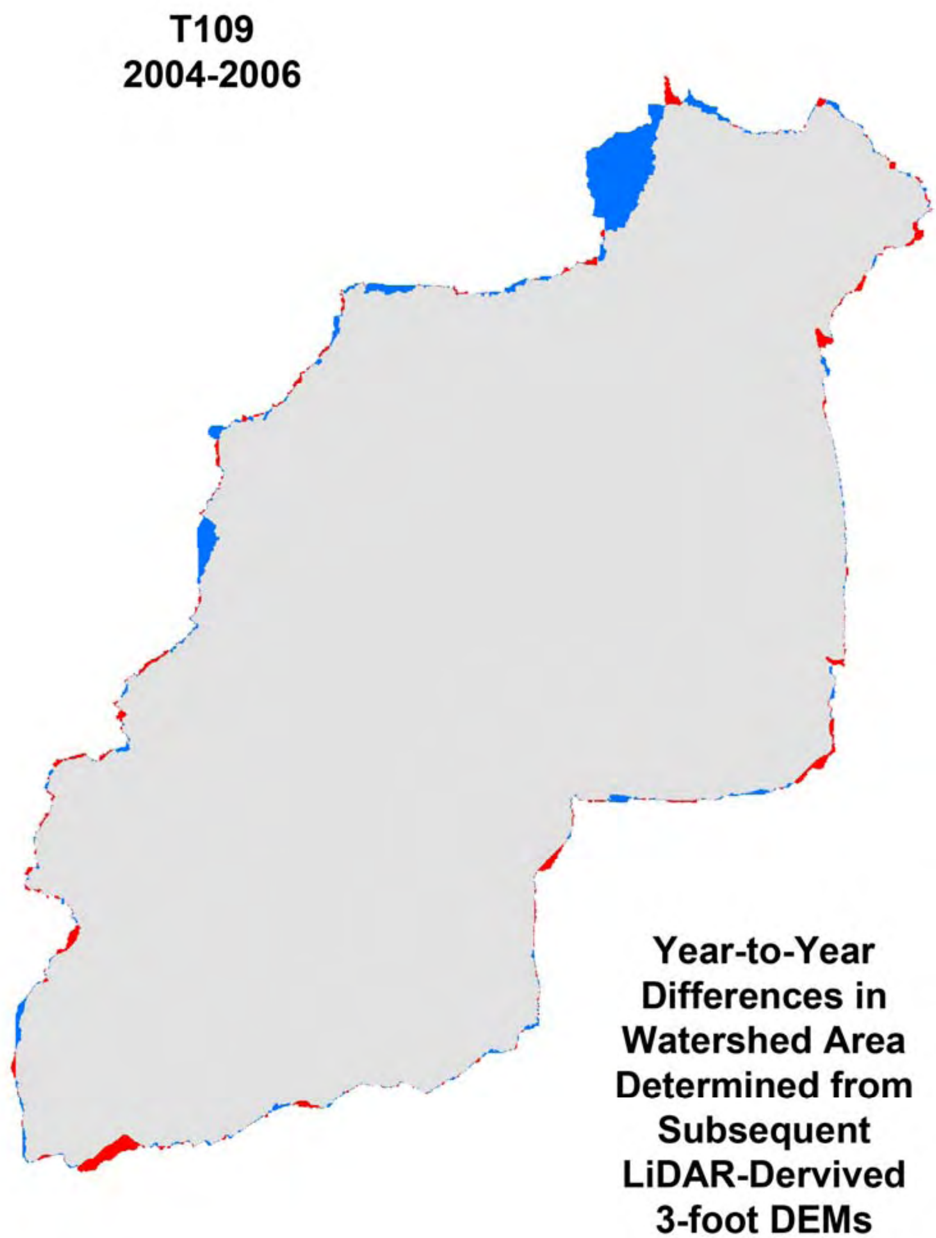


Gray = Area Present in both coverages; Red = Area Present in Year 1 but not Year 2; Blue = Area Present in Year 2 but not Year 1.

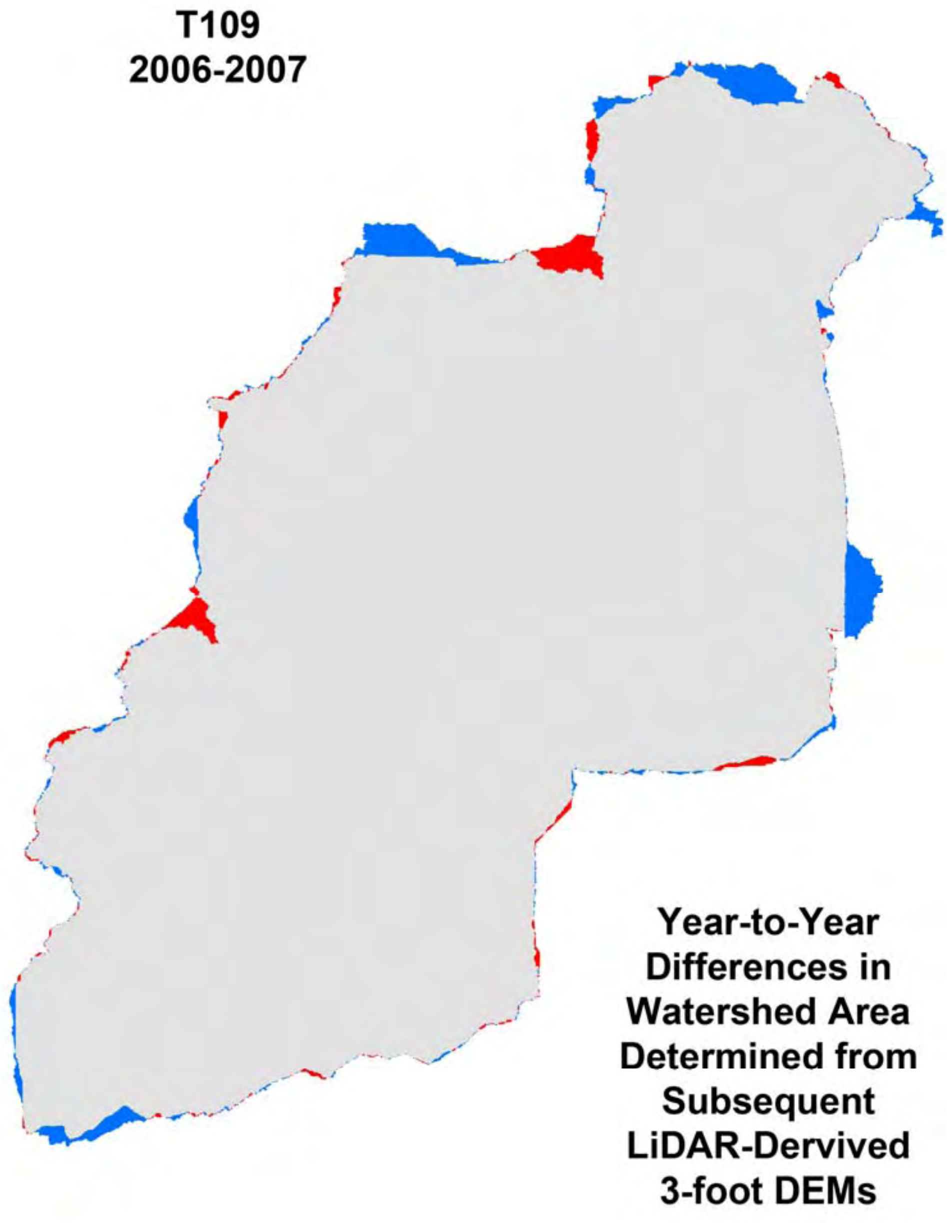


Gray = Area Present in both coverages; Red = Area Present in Year 1 but not Year 2; Blue = Area Present in Year 2 but not Year 1.

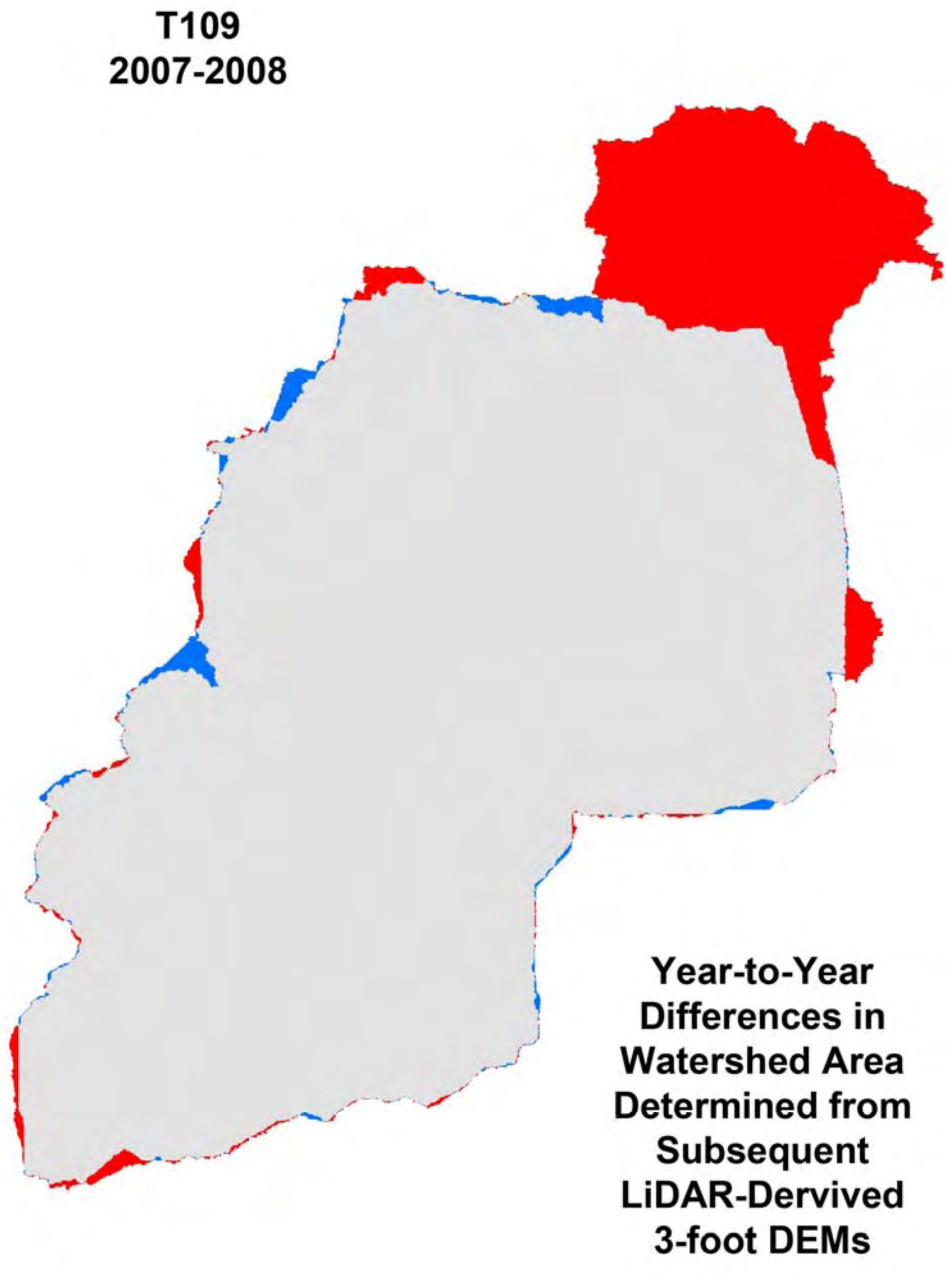


Gray = Area Present in both coverages; Red = Area Present in Year 1 but not Year 2; Blue = Area Present in Year 2 but not Year 1.

Appendix Nine: Examples of Vegetation Classes used in the LiDAR Accuracy Assessment Ground Truth Survey Area.



"OK" near-stream vegetative conditions have
relatively little ground vegetation:
Jarnagin 2009 EPA LEB
photo by K. Brubaker - UMD - Mar-2006


"OK" near-stream vegetative conditions have
relatively more overhanging branches:
Jarnagin 2009 EPA LEB
photo by K. Brubaker - UMD - Mar-2006


"OK" near-stream vegetative conditions have more irregular and softer ground conditions:
Jarnagin 2009 EPA LEB
photo by K. Brubaker - UMD - Mar-2006


"Bad" near-stream vegetative conditions have dense underbrush:
Jarnagin 2009 EPA LEB

C


"Bad" near-stream vegetative conditions have a relatively dense overhanging branches:
Jarnagin 2009 EPA LEB
photo by K. Brubaker - UMD - Mar-2006

United States Environmental Protection Agency

Office of Research
and Development (8101R)
Washington, DC 20460

Official Business
Penalty for Private Use
$300

EPA/600/R-10/120
October 2010
www.epa.gov

Please make all necessary changes on the below label, detach or copy, and return to the address in the upper left-hand corner.

If you do not wish to receive these reports CHECK HERE ☐; detach, or copy this cover, and return to the address in the upper left-hand corner.

PRESORTED STANDARD
POSTAGE & FEES PAID
EPA PERMIT No. G-35